Tar Formation and Transformation in Steam Gasification of Biomass in a Dual Fluidised Bed Gasifier

A thesis submitted in partial fulfilment
of the requirements for the
Degree of Doctor of Philosophy
in
Chemical and Process Engineering
of University of Canterbury
by

Ziyin Zhang

August 2017

Summary

Gasification is a promising thermos-chemical process that converts biomass into syngas (producer gas). However, the generation of tar compounds during the gasification process limit the subsequent syngas application, since it causes operational problems by blocking downstream equipment. Furthermore, tar removal is one of the main challenges for the commercialisation of the biomass gasification technology. Since 2007, a 100kW dual fluidised bed (DFB) gasifier is under development by the Bioenergy Research Group at the University of Canterbury to assess the performance of syngas. But there is an apparent knowledge gap in understanding tar formation and conversion in the DFB gasifier, especially for the transformation of gas and tar production from initial devolatilization to subsequent gasification. This thesis aims to fundamentally understand and establish the tar formation and conversion during biomass gasification, with the objective of determining the operating parameters and selection of feedstocks and bed materials for reduction of the tar content in the producer gas.

To achieve the objective, the evolution of gas and tar compounds produced from initial devolatilization stage to subsequent gasification stage have been experimentally investigated in the 100kW DFB gasifier. N_2 and steam were respectively introduced into the DFB gasifier as fluidisation agent for devolatilization and gasification process. The producer gas composition was analysed by a micro-gas chromatography (GC), while the tar compounds were identified and quantified by the GC analysis.

The first part of the thesis deals with the effect of operating parameters on tar conversion and reduction. The operating parameters included the gasification temperature (in the range of 700-800°C), mean gas residence time (from 0.19 to 0.25 s) and steam to biomass ratio (from 0.63 to 1.51). Pellets of radiata pine wood were used as the feedstock, and silica sand was used as the bed material.

The results demonstrated the correlations between tar and light gas from initial devolatilization to final gasification. During devolatilization, linear relations on the mass production between of light poly-aromatic hydrocarbon (PAH) tar compounds and CH_4, and between heavy PAH tar compounds and C_2 gas (C_2H_2+C_2H_4) were obtained. In the subsequent gasification, a linear relation between heavy PAH tar compounds and C_2H_2+C_2H_4 were also presented. Consequently, CH_4, C_2H_2 and C_2H_4 could be used as indicators of tar production and speciation.

These results provided an understanding of the tar conversion and transformation is taking place in the DFB gasifier, the correlation between tar and light gas could be used to estimate the PAH tar compounds during biomass gasification.

Besides, it was found that the total tar concentration in the producer gas was reduced by 34%, 36% and 46%, respectively, by changing the operating parameters (1) the elevating gasification temperature, (2) longer the residence time, and (3) increasing steam to biomass (S/B) ratio. Interestingly, within the testing range, the proportion of heavy PAH tar in the total tar production was increased from 30% to 48%, and from 33% to 42%, respectively, by changing the temperature and S/B ratio. However, the residence time had very few effects on the proportion of heavy PAH tar.

In the second part, the tar formation and conversion during the steam gasification of various biomass species at 700 and 800°C were studied. Radiata pine wood, corn stover and rice husk were selected as the biomass feedstock. Cellulose, hemicellulose and lignin are three main components in the biomass, whose chemical structure, composition and thermal decomposition properties are different. It was found that corn stove was rich in cellulose, rice husk had a high content of hemicellulose and pine had a high content of lignin.

In devolatilization process, the experimental results demonstrated that radiata pine generated a high proportion of toluene, while corn stover exhibited a high proportion of phenols, while in the subsequent gasification process, radiata pine wood produced a high proportion of naphthalene, while corn stover gave a large proportion of biphenyl. The results allow understanding of the main conversion mechanisms taking place in the gasifier. Consequently, two simplified chemical pathways of secondary tar conversion (phenols and toluene were used as the precursor, respectively) were proposed. In addition, the proportion of total PAH tar compounds in the producer gas from gasification of pine wood was the highest followed by gasification of rice husk and then corn stover, because lignin represents a potential precursor for PAH tar formation.

In the last part, the effects of bed material on tar reduction in the steam gasification were experimentally investigated. The selected catalytic bed materials were calcined olivine sand, Woodhill sand and limestone-silica blends (50-50 wt.%) while silica sand was used as control. The experimental results have demonstrated that catalytic bed materials effectively reduce the

tar concentration. It was found that, in comparison with silica sand, the tar concentration was reduced by 24%, 28% and 43%, respectively, with calcined olivine, Woodhill sand and limestone-silica blends. In the meantime, H_2 production was promoted by using catalytic bed material, since the effect on the equilibrium of water-gas shift reaction.

This research demonstrated the influence of operating parameter and selection of feedstock and bed material on the tar reduction in the DFB gasifier, providing the information for the further development on the downstream tar removal system and syngas application.

Acknowledgements

There are many people whose provided support and generous help with my completion of this PhD thesis. To all these people, I would like to say, ‘thank you’.

First of all, I would like to express my special gratitude to Professor Shusheng Pang, who is my principal supervisor and the leader of the ‘BTSL’ program in Department of Chemical and Process Engineering (CAPE). In 2013, Professor Pang provided me with the golden opportunity to do this project with a scholarship. Many thanks for his enthusiastic encouragement and critical suggestion through the five-year PhD journey, making me understand how to be a qualified researcher and engineer.

I would also like to thank Dr Woei Saw for his advice and assistance in keeping my progress on schedule at the early stage of PhD study. Special appreciation goes to Dr Woei Saw who shared his knowledge and experience on the gasification and guided me to operate the pilot scale gasifier. Without him, I could not imagine how to complete my experiments.

Thanks to my co-supervisor Dr Chris Williamson, and all CAPE academic staff, for offering me with help on solving some technical issues of my project. My sincere thanks also go to all CAPE technical staff, who contributed their experience and support for me to complete my experiments. Many appreciations to Mr Leigh Richardson for his brilliant efforts in modification and maintaining the CAPE gasifier in normal operation.

I am also indebted to the departmental administrators and postgraduate mates for their help, support and making me feel in a home environment. I would like to give thanks to the colleagues in this BTSL research team particularly, Dr Qixiang Xu, Mr Cheng Li and Miss Yanjie Wang, who are also my good friends and helped in my project at the different stage.

Last but not least, I would like to give my special gratitude to the support and love of my family – my parents; my wife, Lorraine Liu; and my lovely little princess, Annabel Zhang, who just arrived in the world before my thesis submission. They all helped me going through difficult times; I presume this thesis is impossible to be completed without their love and supports.

Contents

List of Figures

Lists of Tables

Nomenclatures

A	cross section area
Ar	Archimedes number
g	gravity (9.81 m/s^2)
d_p	diameter of particle, m
C_D	drag coefficient
d_{bv}	effective bubble diameter, m
ε_b	voidage of the bubble phase
ε_f	Voidage of BFB
ε_{mf}	voidage at minimum fluidisation
L_{mf}	bed height at the minimum fluidisation
L_f	expansion bed height
M	mass, kg
N	number of holes per unit area in the distributor (1/m^2)
ρ_p	density of particle, kg/m^3
ρ_f	density of fluid, kg/m^3
Q_b	volumetric flow rate, m^3/s
Re	Reynolds number
U	Superficial velocity, m/s
U_b	rise velocity of a bubble, m/s
U_{mf}	minimum fluidisation velocity, m/s
U_{pg}	superficial velocity of producer gas, m/s
U_t	terminal velocity, m/s
μ	viscosity of fluid, Pa·s
τ_f	mean gas residence time of producer gas, s
Y	correction factor for two phase theories

Abbreviations

ASTM	American Society for Testing and Materials
BTSL	biomass to syngas and liquid fuels
BFB	bubbling fluidised bed
daf	dry and ash free
DCM	dichloromethane
DFB	dual fluidised bed
FB	fluidised bed
FFB	fast fluidised bed
GC–FID	gas chromatography – flame ionization detector
HACA	hydrogen abstraction acetylene addition
IPA	isopropanol
IS	internal standard
Micro-GC	micro-gas chromatography
PAH	poly-aromatic hydrocarbons
S/B	steam to biomass ratio
SPE	solid phase extraction
TCD	thermal conductivity detector

Chapter 1. Introduction

In this chapter, the biomass resource and biomass conversion technologies are briefly introduced. The program of Biomass to Syngas and Liquid Fuels (BTSL) at the University of Canterbury are then presented. Finally, the objectives of this research and thesis structures are outlined.

1.1. Background

1.1.1. Global energy issues

Due to the industrialization, high growth rates of population and urbanization, and the developments in transportation, the world is currently faced with a series of issues involving extensive use of fossil fuels including resource depletion and negative impacts on the environment (air pollution and climate change due to greenhouse gas emissions). Therefore, renewable and sustainable energy is becoming more and more attractive, which is expected to play an important role in future energy supply to substitute fossil fuels. According to International Energy Outlook 2016 by U.S energy information administration, although fossil fuels still account for more than three-quarters of world energy consumption through 2040, renewable energy is the world's fastest-growing energy contributor increasing by 2.6% per year through to 2040 [1], as shown in Fig. 1-1.

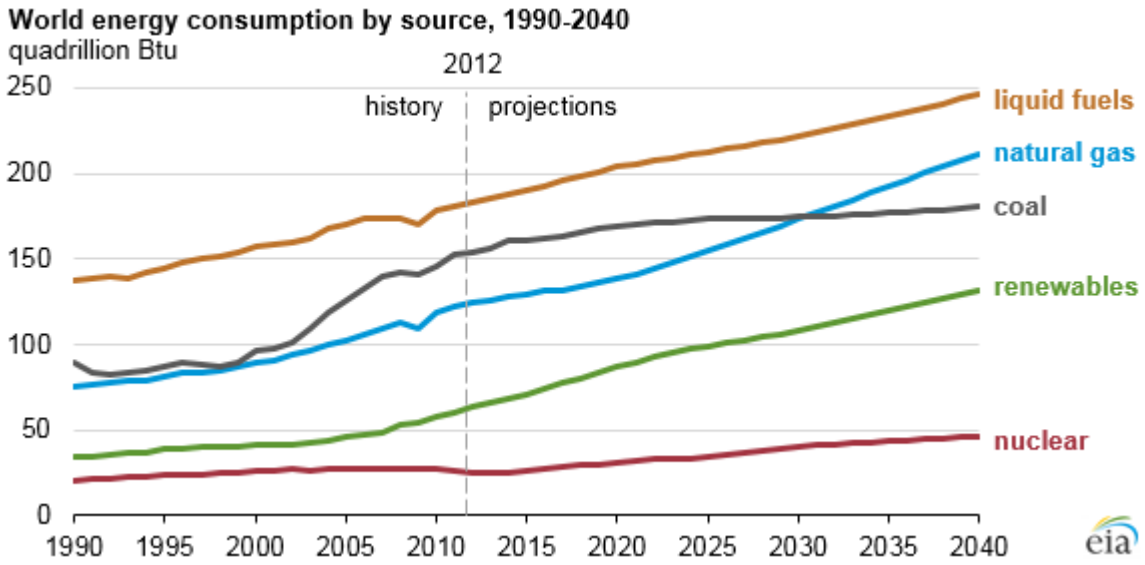

Fig. 1-1. World energy consumption by source [1].

1.1.2. Biomass and biomass energy

Biomass as a renewable and environmentally friendly energy source [2, 3] is estimated to contribute a significant share (approximately 14%) in the worldwide energy consumption, while it is also likely to remain the main source of primary energy feedstock for the developing countries [4].

Biomass, including all land and water based vegetation, is produced by green plants and may also include all organic solid wastes [5]. It is available in different forms, for example, agricultural and forestry residues, biological materials by-products, wood, organic parts of municipal and sludge wastes having variable moisture content and chemical compositions [6]. From a view of chemistry, biomass stores chemical energy in the form of carbohydrates by combining solar energy and carbon dioxide through photosynthesis process [7]. Biomass has been identified as a carbon neutral energy source since the carbon dioxide captured during photosynthesis is released when the biomass or biomass fuels are combusted in use [8].

Biomass can be transformed to solid, liquid and gaseous fuels or heat and power. The key drivers for the growing interests in using biomass are: (1) Biomass can substitute fossil fuels thus can reduce dependency on fossil fuel. (2) Biomass energy processing industry generates employment in rural areas [9]. (3) Biomass energy can help to deal with environmental problems by decreasing CO_2 and other pollutant gas emissions [10]. Therefore, it is critically important to develop clean and efficient biomass energy conversion technologies for commercialisation.

1.1.3. Biomass conversion technologies

There are several routes to convert biomass into useful energy products depending on the biomass characteristics and the requirement of the end product and its applications [11]. The most promising conversion technologies which are commercialised either at present or in next 5 to 10 years are in the category of thermochemical conversion route [12]. Thermochemical conversion processes including combustion, gasification, pyrolysis and hydrothermal liquefaction, are flexibility in accepting the various biomass feedstock and also producing a wide range of energy products [13-15]. In the thermochemical conversion, heat is applied to break biomass down into smaller, constituent units, which are then combusted or further

processed into useful compounds [16]. The major thermochemical conversion routes of biomass are shown in Fig. 1-2.

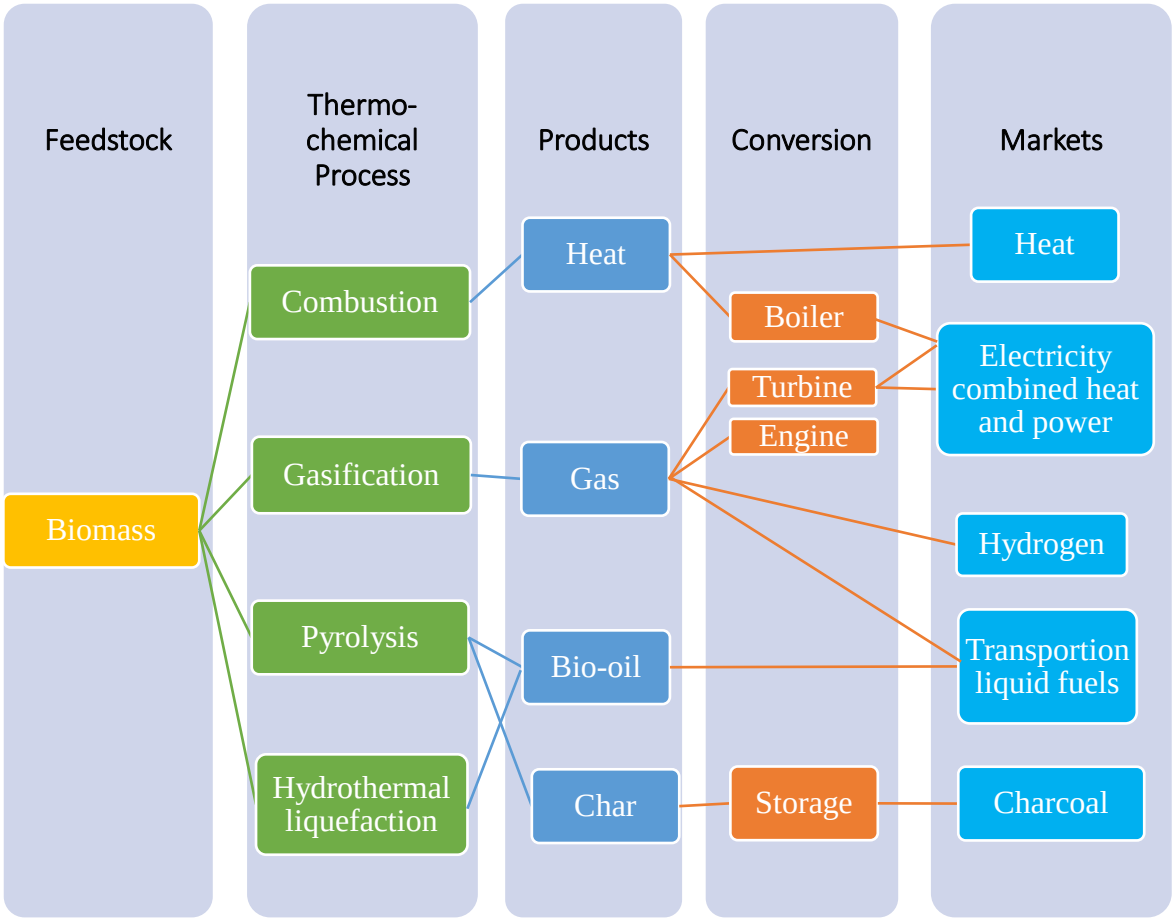

Fig. 1-2. Thermochemical conversion of biomass [17].

Among the three main thermochemical process as shown in Fig. 1-2, gasification has been considered to be a more attractive process [18, 19], which converts solid biomass into a combustible gas mixture in the presence of gasification agents (air or steam) [20-22]. The gas mixture produced (which is also called producer gas or product gas) can be utilized directly as fuels for power generation or for the synthesis of liquid fuel and chemicals, such as Fischer-Tropsch for manufacturing diesel [23]. The key advantage of gasification is high conversion efficiency, which a value of 70-80% being reported [24, 25], and flexibility for the producer gas use.

The use of steam as the gasification agent generates the producer gas which can have a higher calorific value, approaching 20MJ/Nm^3, and a higher hydrogen content than that from air

gasification [26]. The steam gasification process can be divided into two main stages after a short period of biomass drying: biomass devolatilization and subsequent gasification reactions between char and gases (heterogeneous) and among gases (homogeneous).

1.1.4. Tar issues in biomass gasification

During biomass gasification, many undesirable compounds are generated such as tar and other gaseous contaminants (NH_3, HCl and H_2S). Tar is a complex mixture of condensable hydrocarbons comprising single-ring to 5-ring aromatic compounds plus other oxygen-containing hydrocarbons and complex polyaromatic hydrocarbons (PAHs) [27]. The presence of tar in the producer gas can cause operational problems in the downstream applications. For example, the condensable heavy tar compounds may lead to blockage of the downstream equipment – filters, valve and pipelines where the temperature is below the dew points of these compounds. Therefore, tar formation and condensation at reduced temperatures are the major issues which need to be effectively removed from the producer gas in the commercialisation of the biomass gasification technology [28].

It has been found that the higher volatile matter in the biomass makes it more susceptible to tar formation [29]. In the initial devolatilization stage, the molecular structure of biomass is first decomposed into char, tar, and vapours gases when the temperature is increased to 300-500°C. [30]. As the temperature is further increased, tar is further subject to decomposition, oxidation, reforming, and depolymerisation reactions, which change the compound composition [31]. It can be classified into several classes according to formation temperature and composition [32]. Fig. 1-3 presents the tar formation process with temperature.

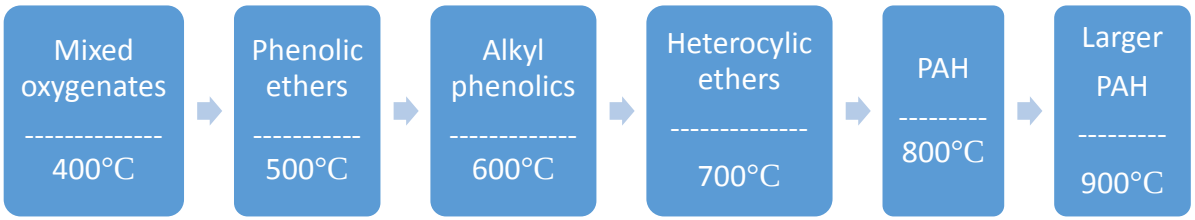

Fig. 1-3. Tar maturation scheme proposed by Elliott [33].

Methods to control tar formation and for tar removal during biomass gasification can be categorized into two types depending on the location where the tar is removed: “Primary”

measures reduce tar within the gasifier itself through optimization of design/operating conditions and the addition of catalytic bed materials [34, 35], whereas “secondary” measures remove the tar from in the producer gas by filtration, scrubbing, or catalysis in a separate step after gasification [36, 37].

1.2. BTSL program

In past ten years, the Bioenergy Research Group in the Department of Chemical and Process Engineering, University of Canterbury, has been conducting a research programme, Biomass to Hydrogen-Rich Syngas and Liquid Fuel (BTSL), whose focus is on adapting and developing the thermos-chemical process technologies for biomass conversion.

There are four primary objectives in this programme:

- To produce hydrogen-rich syngas from advanced biomass gasification technology;
- To produce liquid fuel using the hydrogen-rich syngas through Fischer-Tropsch (FT) synthesis;
- To produce the liquid fuel from biomass pyrolysis technology; and
- To establish and develop new biomass resources.

Since 2007, a 100kW dual fluidised bed (DFB) gasifier has been designed, constructed and commissioned [38, 39]. The advantage of this gasifier is its ability to produce a syngas with a high calorific value and a high hydrogen content. The configurations of the DFB gasifier will be introduced in Chapter 3. A large number of experiments have been conducted on the DFB gasifier. Different feedstock, such as woody and herbaceous species, biosolid wastes [26] and biomass-coal blends [40] have been tested in the DFB gasifier. In addition, the impacts of operation conditions [41] and bed materials [42] were also investigated to provide flexibility for syngas applications such as hydrogen production, heat and power generation, or Fischer-Tropsch (FT) synthesis.

At the same time, some fundamental studies including gasification kinetics studies, hydrodynamics studies and mathematic modelling were undertaken for the optimisation of scale-up design and operation of the DFB gasifier. Dr Mook Tzeng Lim [43] had simulated the

hydrodynamics of a cold model of a dual fluidised bed gasification plant Lim. Dr Prasanth Gopalakrishnan [44] and Dr Qixiang Xu [45] had developed a mathematical modelling of biomass gasification and co-gasification of coal-biomass blends, respectively, to predict the syngas quality (gas composition and yield).

As one of the main challenges for the successful development of commercial gasification technologies. Removal of the impurities in gasification syngas is essential to meet the stringent requirement of the FT synthesis process and other downstream application. Tar and other gaseous contaminants, such as NH_3 and H_2S, are the unavoidable contamination produced during biomass gasification. Dr Janjira Hongrapipat [46] had developed the gas cleaning technology for removal of NH_3 and H_2S with low construction and operating cost.

However, there is still knowledge gap on the tar formation and reduction in a DFB gasifier. This thesis will focus on the tar formation and transformation during the biomass gasification process. Meanwhile, the optimisation of operation conditions, biomass selection and catalytic bed material addition for tar reduction in the DFB gasifier will be investigated.

1.3. Objectives of studies

The objectives of this project are: (1) to investigate mechanism of tar formation during the gasification processes and to examine effects of the operation conditions, such as gasification temperature, steam to biomass ratio and gas residence time; (2) to investigate the influences of biomass species on the tar formation; (3) to investigate the effect of catalytic bed materials in the DFB gasification process on tar content in the producer gas. The results from this study will be used to in practical gasification operation to optimize the operational conditions for production of a syngas with low tar concentrations.

1.4. Thesis outline

Chapter 2 will present a comprehensive literature review in which biomass characteristics, properties and biomass conversion technologies are described. Following this, the tar properties and classification, tar formation reactions and kinetics models are presented. Finally, the reported studies on the tar removal method are reviewed.

In order to investigate the tar formation and destruction during the steam gasification process, a series of experiments were conducted on the 100kW dual fluidised bed steam gasifier. The details of this gasifier are described in Chapter 3. In addition, development of producer gas and tar sampling system are presented, and chemical analysis methods are described.

Chapter 4 presents the experimental investigation on the yields and quality of intermediate products (gas and tar) from the devolatilization and those from steam gasification of woody biomass in the DFB gasifier. Based on the experimental results, correlations between products from the initial devolatilization and those of final producer gas from the biomass gasification are established. The work in this chapter has recently been published in Fuel journal [47]. In addition, the influences of operation conditions (temperature, residence time and steam to biomass ratio) on the tar yield and concentration in the producer gas are also studied in Chapter 5. Based on the results from Chapter 4 and 5, the gasification operation conditions are optimised to achieve low tar content and high gas yield.

In Chapter 6, the gasification performances of various biomass species are experimentally investigated, and components (cellulose, hemicellulose and lignin) in each biomass species are determined. Different biomass component decomposes at different temperatures and produces different products with heating. Therefore, biomass gasification yields a complex mixture of vapour and gaseous compounds including tar compounds. In this chapter, the effects of the primary components of the biomass on the tar formation are analysed, and linkage of tar formation from the initial devolatilization to final steam gasification is also studied. A journal paper on this study has been submitted to 'Renewable Energy'.

In Chapter 7, the effects of four types of bed materials (silica sand, calcined olivine, Woodhill sand and limestone) on the tar content and gas composition in steam gasification of woody biomass in a dual fluidised bed gasifier are experimentally investigated. The catalytic effects of bed material on the tar productions were compared are analysed.

Finally, the conclusion of this research and recommendations for the future work are given in Chapter 8.

1.5. Reference

[1] L. Doman, "EIA projects 48% increase in world energy consumption by 2040," EIA, 2016.

[2] A. V. Bridgwater, "The technical and economic feasibility of biomass gasification for power generation," *Fuel*, vol. 74, pp. 631-653, 1995.

[3] A. V. Bridgwater, "Renewable fuels and chemicals by thermal processing of biomass," *Chemical Engineering Journal*, vol. 91, pp. 87-102, 2003.

[4] S. K. Sansaniwal, K. Pal, M. A. Rosen, and S. K. Tyagi, "Recent advances in the development of biomass gasification technology: A comprehensive review," *Renewable and Sustainable Energy Reviews*, vol. 72, pp. 363-384, 2017.

[5] P. McKendry, "Energy production from biomass Part 1: overview of biomass," *Bioresource Technology*, vol. 83, pp. 37-46, 2002.

[6] F. Bilgili, E. Koçak, Ü. Bulut, and S. Kuşkaya, "Can biomass energy be an efficient policy tool for sustainable development?," *Renewable and Sustainable Energy Reviews*, vol. 71, pp. 830-845, 2017.

[7] D. L. Klass, *Biomass for renewable energy, fuels, and chemicals*. San Diego: Academic Press, 1998.

[8] H. Suopajärvi, A. Kemppainen, J. Haapakangas, and T. Fabritius, "Extensive review of the opportunities to use biomass-based fuels in iron and steelmaking processes," *Journal of Cleaner Production*, vol. 148, pp. 709-734, 2017.

[9] M. F. Demirbas, M. Balat, and H. Balat, "Potential contribution of biomass to the sustainable energy development," *Energy Conversion and Management*, vol. 50, pp. 1746-1760, 2009.

[10] J. Hill, E. Nelson, D. Tilman, S. Polasky, and D. Tiffany, "Environmental, economic, and energetic costs and benefits of biodiesel and ethanol biofuels," *Proceedings of the National Academy of Sciences*, vol. 103, pp. 11206-11210, 2006.

[11] R. C. Saxena, D. Seal, S. Kumar, and H. B. Goyal, "Thermo-chemical routes for hydrogen rich gas from biomass: A review," *Renewable and Sustainable Energy Reviews*, vol. 12, pp. 1909-1927, 2008.

[12] H. B. Goyal, D. Seal, and R. C. Saxena, "Bio-fuels from thermochemical conversion of renewable resources: A review," *Renewable and Sustainable Energy Reviews*, vol. 12, pp. 504-517, 2008.

[13] A. Demirbas, "Biomass resource facilities and biomass conversion processing for fuels and chemicals," *Energy Conversion and Management,* vol. 42, pp. 1357-1378, 2001.

[14] P. McKendry, "Energy production from biomass Part 2: conversion technologies," *Bioresource Technology,* vol. 83, pp. 47-54, 2002.

[15] A. Bridgwater, A. Toft, and J. Brammer, "A techno-economic comparison of power production by biomass fast pyrolysis with gasification and combustion," *Renewable and Sustainable Energy Reviews,* vol. 6, pp. 181-246, 2002.

[16] A. V. Bridgwater and D. G. B. Boocock, *Developments in thermochemical biomass conversion*, 1st ed. London ; New York: Blackie Academic & Professional, 1997.

[17] M. Crocker, *Thermochemical conversion of biomass to liquid fuels and chemicals*. Cambridge: RSC Publishing, 2010.

[18] C. Higman and M. v. d. Burgt, *Gasification*. Boston: Gulf Professional Pub., 2003.

[19] V. Kirubakaran, V. Sivaramakrishnan, R. Nalini, T. Sekar, M. Premalatha, and P. Subramanian, "A review on gasification of biomass," *Renewable and Sustainable Energy Reviews,* vol. 13, pp. 179-186, 2009.

[20] P. McKendry, "Energy production from biomass Part 3: gasification technologies," *Bioresource Technology,* vol. 83, pp. 55-63, 2002.

[21] A. Kumar, D. D. Jones, and M. A. Hanna, "Thermochemical biomass gasification: a review of the current status of the technology," *Energies,* vol. 2, pp. 556-581, 2009.

[22] A. C. Chang, H.-F. Chang, F.-J. Lin, K.-H. Lin, and C.-H. Chen, "Biomass gasification for hydrogen production," *International Journal of Hydrogen Energy,* vol. 36, pp. 14252-14260, 2011.

[23] T. Chmielniak and M. Sciazko, "Co-gasification of biomass and coal for methanol synthesis," *Applied Energy,* vol. 74, pp. 393-403, 2003.

[24] S. Lee, J. G. Speight, and S. K. Loyalka, *Handbook of alternative fuel technologies*. Boca Raton: CRC Press, 2007.

[25] J. J. Hernández, R. Ballesteros, and G. Aranda, "Characterisation of tars from biomass gasification: Effect of the operating conditions," *Energy,* vol. 50, pp. 333-342, 2013.

[26] W. Saw, H. McKinnon, I. Gilmour, and S. Pang, "Production of hydrogen-rich syngas from steam gasification of blend of biosolids and wood using a dual fluidised bed gasifier," *Fuel,* vol. 93, pp. 473-478, 2012.

[27] S. Van Paasen, J. Kiel, and H. Veringa, "Tar formation in a fluidised bed gasifier," Energy research Centre of the Netherlands (ECN) Report, The Netherlands, ECN-C-04-013, 2004.

[28] B. Vreugdenhil, R. Zwart, and J. P. A. Neeft, "Tar formation in pyrolysis and gasification," Energy research Centre of the Netherlands (ECN) Report, The Netherlands, ECN-E--08-087, 2009.

[29] H. Yu, Z. Zhang, Z. Li, and D. Chen, "Characteristics of tar formation during cellulose, hemicellulose and lignin gasification," *Fuel*, vol. 118, pp. 250-256, 2014.

[30] C. Kinoshita, Y. Wang, and J. Zhou, "Tar formation under different biomass gasification conditions," *Journal of Analytical and Applied Pyrolysis*, vol. 29, pp. 169-181, 1994.

[31] C. Font Palma, "Modelling of tar formation and evolution for biomass gasification: A review," *Applied Energy*, vol. 111, pp. 129-141, 2013.

[32] T. A. Milne, N. Abatzoglou, and R. J. Evans, "Biomass gasifier" tars": their nature, formation, and conversion," National Renewable Energy Laboratory, Golden, Colorado, USA, 1998.

[33] D. C. Elliott, "Relation of Reaction Time and Temperature to Chemical Composition of Pyrolysis Oils," in *Pyrolysis Oils from Biomass*. vol. 376: American Chemical Society, 1988, pp. 55-65.

[34] S. Anis and Z. A. Zainal, "Tar reduction in biomass producer gas via mechanical, catalytic and thermal methods: A review," *Renewable and Sustainable Energy Reviews*, vol. 15, pp. 2355-2377, 2011.

[35] L. Devi, K. J. Ptasinski, and F. J. J. G. Janssen, "A review of the primary measures for tar elimination in biomass gasification processes," *Biomass and Bioenergy*, vol. 24, pp. 125-140, 2003.

[36] J. Han and H. Kim, "The reduction and control technology of tar during biomass gasification/pyrolysis: An overview," *Renewable and Sustainable Energy Reviews*, vol. 12, pp. 397-416, 2008.

[37] A. Paethanom, S. Nakahara, M. Kobayashi, P. Prawisudha, and K. Yoshikawa, "Performance of tar removal by absorption and adsorption for biomass gasification," *Fuel Processing Technology*, vol. 104, pp. 144-154, 2012.

[38] D. R. Bull, "Performance Improvements to a Fast Internally Circulating Fluidised Bed (FICFB) Biomass Gasifier for Combined Heat and Power Plants," in *Department of Chemical and Process Engineering*: University of Canterbury, 2008.

[39] J. Rutherford, "Heat and power applications of advanced biomass gasifiers in New Zealand's wood industry : a chemical equilibrium model and economic feasibility assessment " in *Department of Chemical and Process Engineering*: University of Canterbury, 2006.

[40] W. L. Saw and S. Pang, "Co-gasification of blended lignite and wood pellets in a 100kW dual fluidised bed steam gasifier: The influence of lignite ratio on producer gas composition and tar content," *Fuel,* vol. 112, pp. 117-124, 2013.

[41] W. L. Saw and S. Pang, "Influence of mean gas residence time in the bubbling fluidised bed on the performance of a 100-kW dual fluidised bed steam gasifier," *Biomass Conversion and Biorefinery,* vol. 2, pp. 197-205, 2012.

[42] W. L. Saw and S. Pang, "The influence of calcite loading on producer gas composition and tar concentration of radiata pine pellets in a dual fluidised bed steam gasifier," *Fuel,* vol. 102, pp. 445-452, 2012.

[43] M. T. Lim, "Hydrodynamics of a Cold Model of a Dual Fluidized Bed Gasification Plant," in *Department of Chemical and Process Engineering*: University of Canterbury, 2012.

[44] P. Gopalakrishnan, "Modelling of Biomass Steam Gasification in a Bubbling Fluidized Bed Gasifier," in *Department of Chemical and Process Engineering*: University of Canterbury, 2013.

[45] Q. Xu, "Investigation of Co-Gasification Characteristics of Biomass and Coal in Fluidized Bed Gasifiers," in *Department of Chemical and Process Engineering*: University of Canterbury, 2013.

[46] J. Hongrapipat, "Removal of NH3 and H2S from Biomass Gasification Producer Gas," in *Department of Chemical and Process Engineering*: University of Canterbury, 2014.

[47] Z. Zhang and S. Pang, "Experimental investigation of biomass devolatilization in steam gasification in a dual fluidised bed gasifier," *Fuel,* vol. 188, pp. 628-635, 2017.

Chapter 2. Tar Formation and Transformation in Steam Gasification of Biomass in a DFB Gasifier: Literature Review

In this chapter, biomass resources and characteristics are introduced firstly. After this, dual fluidised bed (DFB) gasification technology and gasification process are described. Issues in the DFB, steam gasification of biomass are identified with a focus on tar composition and classification. Finally, mechanisms of the tar formation during the gasification are examined, and various tar removal technologies are assessed.

2.1. Biomass

Biomass as a renewable and environmentally friendly energy source has been considered to play an important role for future generation heat, power, and gaseous and liquid fuels [1]. Biomass can broadly be defined as organic matters grown in plants through photosynthesis in which carbon dioxide and light (solar energy) are converted to organic compounds (chemical energy) [2]. Hence, among all of the renewable resources, biomass is the only renewable source as a sustainable carbon carrier for energy utilisation [3]. In this way, the biomass is considered to be largely carbon-neutral, since CO_2 emitted during the biomass energy utilisation can be balanced by the CO_2 absorbed by growing plants through photosynthesis [4].

2.1.1. Biomass resource and variability

Biomass resources can be sourced from forest sector, agriculture sector and bio-solid wastes (animal wastes, waste from food processing, aquatic plants, algae and so on) [5]. Biomass resources can be divided into different groups, according to their distinct biological diversity and similar source and origin, as listed in Table 2-1.

Table 2-1. General classification of biomass resources [6].

Biomass group	Example and species
Woody biomass	Stems, branches, bark, chips sawdust, sawmill and others from various wood species [7, 8]
Herbaceous and agricultural biomass	Grasses and flowers – switchgrass [9, 10], Miscanthus
	Straws from rice [11], wheat, corn crops
	Other residues – shells, husks, bagasse [12], cobs
Aquatic biomass	Macro-algae, microalgae
Animal and human bio-solid wastes	Bones, chicken litter [13]
Contaminated biomass	Used fiberboard, waste paper
Biomass mixture	Blends from the above varieties

2.1.2. Biomass properties

The inherent properties of the biomass source determine both the choice of the conversion process and any subsequent processing related issues that may arise. For that purpose, physical and chemical characterizations of various biomass resources have been conducted in literature. Two methods, proximate analysis and ultimate analysis, are commonly used to quantify the properties of biomass as shown in Fig. 2-1 [14].

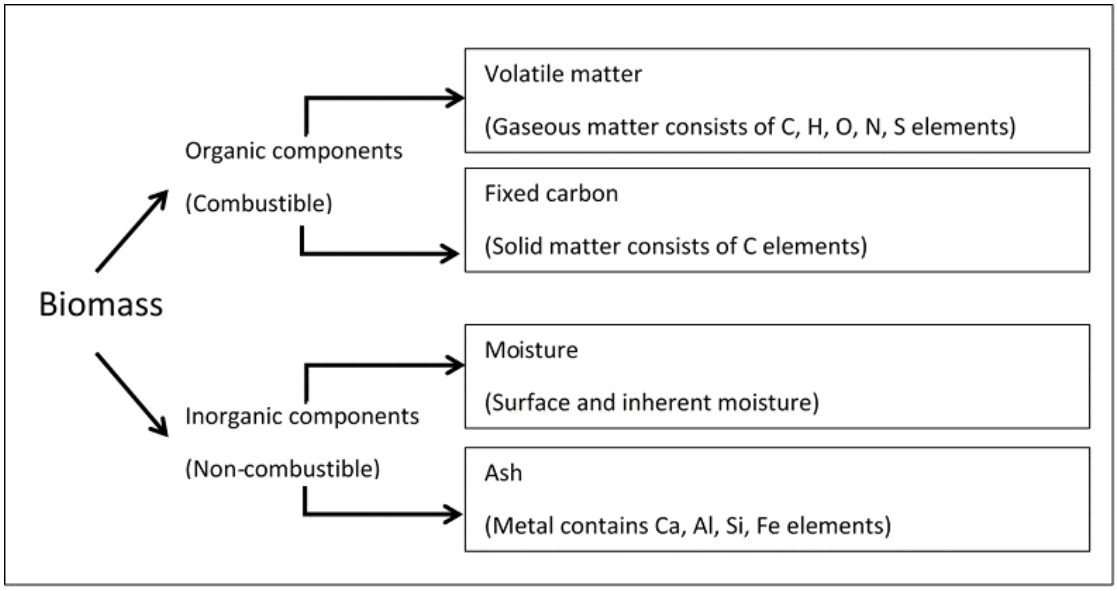

Fig. 2-1. Biomass component present in the proximate analysis [15].

Table 2-2. Proximate analysis and ultimate analysis of several types of common biomass and coal.

		Biomass				Coal
		Corn cobs [16]	Switch grass [17]	Pine [18]	Rice Straw [11]	Lignite [19]
Proximate analysis (wt.% in air dry basis)	Moisture	9.7	20	8.0	5.6	7.4
	Ash	3.0	4.6	0.4	12.7	6.8
	Volatiles	71.2	58.4	77.4	62.2	8.3
	Fixed carbon	16.1	17.1	14.2	16.6	47.4
Ultimate analysis (wt.% in dry ash free basis)	C	40.2	47.0	51.6	38.6	81.5
	H	4.1	5.3	5.9	4.3	4.0
	O	42.6	41.4	42.3	37.2	3.3
	N	0.4	0.5	0.2	1.1	1.2
	S	0.04	0.1	0.1	0.65	3.0

The compositions of several types of biomass and coal are listed in Table 2-2 from which it can be seen that the biomass contain more oxygen and less carbon compared to the coal. The high oxygen content in the biomass is due to the acid alcoholic groups in the cellulose, hemicelluloses and lignin [19]. However, the coals contain higher contents of sulphur and nitrogen. Biomass has a relatively high reactivity as it contains

high atomic H/C ratio and has a high content of volatile matters. In addition, the high reactivity of biomass is also a consequence of the large surface area of biomass and the inherent alkali metals [20]. For example, agricultural residues contain abundant calcium and potassium species [21]. The high reactivity of biomass can enhance the thermochemical conversion reactions [22].

Cellulose, hemicellulose and lignin are found to be the major components of woody biomass and biomass from other crops [23]. In general, biomass is typically composed of 65-85 wt.% polymers including cellulose and hemicelluloses (both combinations is also termed as holocellulose), with another 15-30 wt.% corresponding to lignin [24]. Different kinds of biomass have different contents of holocellulose and lignin. Agricultural and herbaceous biomass (grasses and straw) generally contain less lignin, but more holocellulose as compared to woody biomass [25]. Table 2-4 presents the reported results of holocellulose and lignin contents of some types of biomass.

Table 2-3. Cellulose/hemicellulose/lignin content of some types of biomass (wt.%) [26, 27].

Types of biomass	Cellulose (%)	Hemicellulose (%)	Lignin (%)	Other (%)
Softwood	41	24	28	7
Hardwood	39	35	20	7
Wheat straw	40	28	17	15
Rice husk	47	25	26	2
Pine wood	46	22	31	1
Bagasse	38	39	20	3

Cellulose is a high molecular weight linear polymer of glucopyranose units [28]. It has a chemical formula as $(C_6H_{10}O_5)_n$, where n is the number of monomer units, from 200 to 10,000. Hemicellulose is a mixture of polysaccharides present in the cell wall, being composed of various monosaccharides, including glucose, hexoses, xylose and glucose [29]. Lignin is an organic substance binding the cells, fibres and vessels which constitute wood and the lignified elements of plant [30, 31], as in straw. It is a generic

term for a large group of aromatic polymers and is composed of p-hydroxyphenyl, guaiacyl and syringyl units [32].

Figs. 2-2 to 2-4 illustrate the structures of cellulose, hemicellulose and lignin, respectively. From these figures, it can be seen that the monomer of cellulose and hemicellulose is a saccharide, and does not contain an aromatic functional group. On the contrary, the lignin fraction of the biomass is aromatic. Therefore, lignin represents a potential precursor for poly aromatic hydrocarbon formation [33].

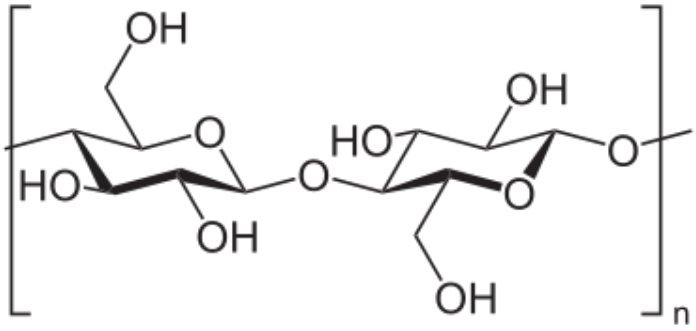

Fig. 2-2. Building units of cellulose [34].

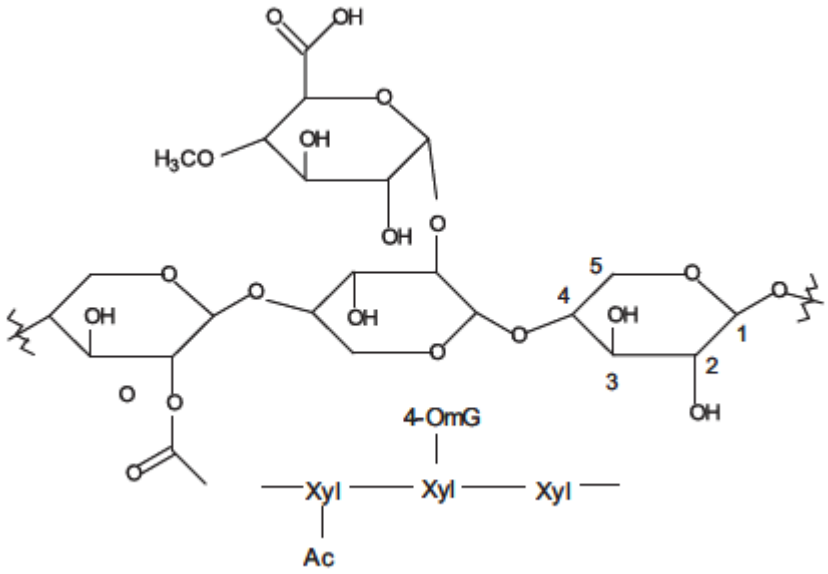

Fig. 2-3. Partial structure of hemicellulose [35].

(Xyl: xylopyranose, Ac: acetyl, 4-OmG: 4-O-methylgucuronic acid)

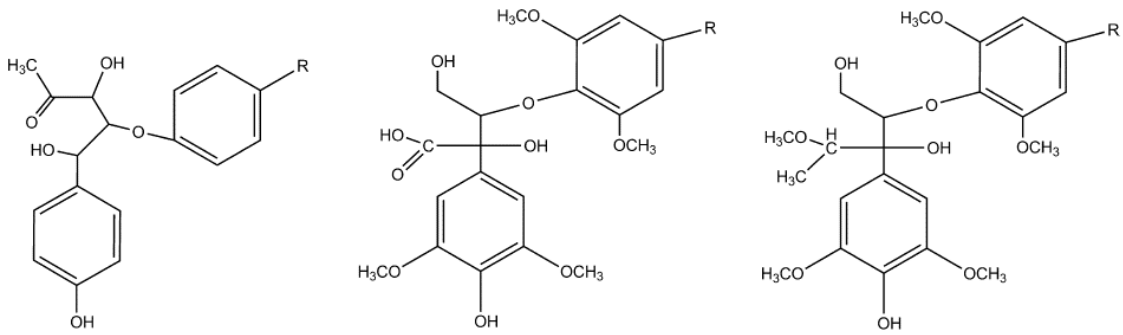

Fig. 2-4. Building units in lignin [36].

During the thermochemical conversion, cellulose and hemicellulose and lignin behave very differently in terms of their thermal stability. Cellulose starts to decompose between 300°C and 400°C. Hemicellulose is decomposed in a way similar to cellulose. However, the hemicellulose has a lower thermal stability than cellulose; it decomposes between 220°C and 320°C. Cellulose and hemicellulose compounds have the structure of branching chain of polysaccharides, which consist more C=O, OH and C-O functional group. Therefore, both cellulose and hemicellulose are easily volatilized [37]. However, lignin is thermally more stable than cellulose and hemicellulose, due to the strong stretching of functional groups, such as C-O-C, methoxyl-O-CH_3, and aromatic structural units in lignin [38]. Consequently, lignin is the most difficult to decompose among the three biomass components. Lignin does not decompose completely even temperatures above 700°C [39].

In summary, different types of biomass have different elemental and chemical compositions, and molecular structures, therefore, behave differently upon heating. It is important to understand the mechanisms and pathways in thermochemical conversion, which significantly affect product yields and compositions.

2.2. Biomass steam gasification in a dual fluidised bed gasifier

Biomass can be converted into useful energy products including heat, power, and gaseous and liquid fuels using the thermochemical conversion technologies. These technologies include gasification, pyrolysis, liquefaction and combustion. However,

biomass feedstock often contains 40 wt.% oxygen which is much higher than that of fossil crude oil, coal and natural gas which only have an oxygen content of less than 5 wt.%. Hence, biomass has a low heating value and low energy density which contributes to low efficiency in thermochemical conversion.

Biomass gasification is believed to one of the most promising technologies in which oxygen hetero-atom removal occurs most readily by dehydration and decarboxylation by heat [40]. In this way, oxygen is removed while gaseous product, producer gas, is generated which consists of hydrogen (H_2), carbon monoxide (CO), carbon dioxide (CO_2) and methane (CH_4).

2.2.1. Gasification agent

Gasification is a complex thermochemical process in which a carbonaceous solid fuel (coal, biomass) is converted into a gaseous product (producer gas) at high temperatures, typically in the range 700-1100°C and in the presence of a gasification agent (air or steam) [41]. The key advantage of gasification is the high energy efficiency of 70-80% [42]. Moreover, producer gas from gasification has flexibility for applications: production of heat and power, and as feedstock for synthesis of fuels and chemicals.

When steam is used as the gasification agent, biomass gasification can generate a hydrogen-rich (up to 60 vol.%) producer gas with higher calorific values of 13-20 MJ/Nm^3 than the producer gases using air as gasification agents [43]. Moreover, a nitrogen-free syngas can be generated with steam as gasification agent [44]. In comparison with oxygen as gasification agent, the steam is much cheaper. However, unlike air-blown or oxygen-blown gasification (heat is generated directly by partial oxidation in the gasifier itself); steam-blown gasification reaction in overall are endothermic, and thus the steam gasification requires an external heat [45].

2.2.2. Fluidised bed gasifier

The fluidised bed (FB) gasifier is an alternative biomass gasification technology. FB gasifiers provide excellent mixing and gas-solid contact which enhance the reaction rate and conversion efficiencies. In the FB gasifier, gas (gasification agent) is blown through a bed of solid particles at a sufficient velocity to keep the particles suspended.

The fluidisation regimes vary with gas velocity and properties of the solid particle (such as density and particle size) as illustrated in Fig. 2-5 [46]. As given solid particles, with an increase in gas velocity, the fluidisation regime changes from fixed bed, through bubbling fluidisation, turbulent fluidisation to fast circulating fluidisation and eventually pneumatic transportation.

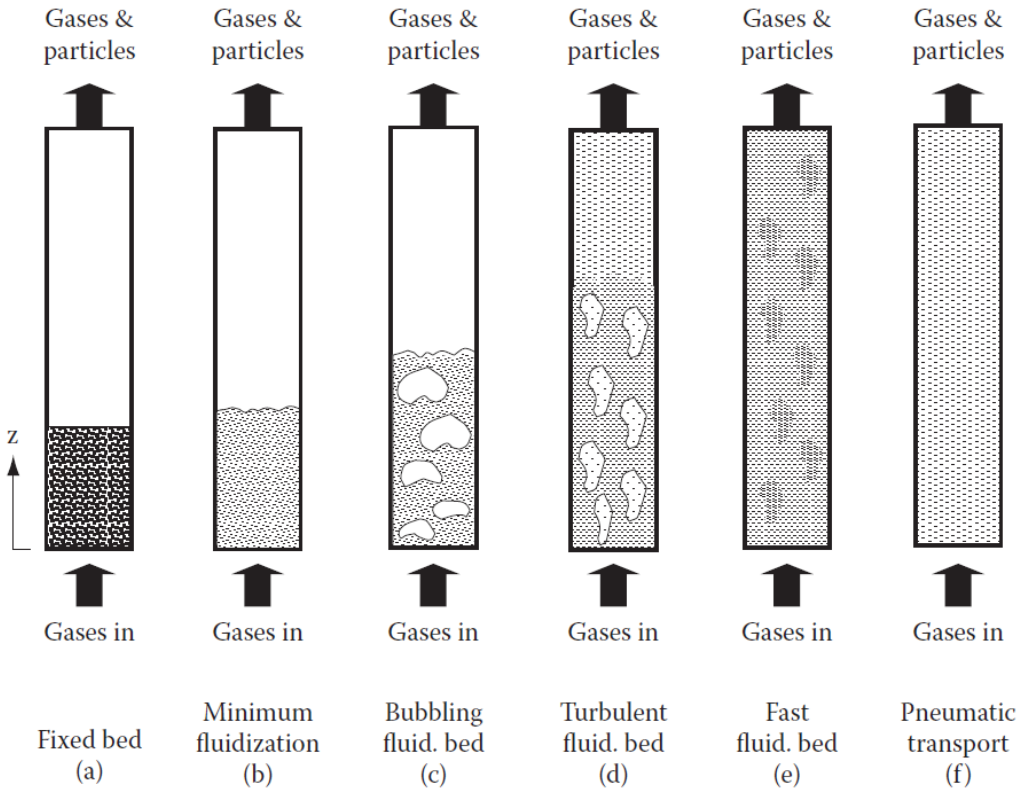

Fig. 2-5. Flow regime map for gas-solids fluidisation [47].

The DFB gasification with steam as the gasification agent is believed to be a promising conversion technology [48]. This system consists of two separate reactors: one for steam biomass gasification to generate a producer gas, and the other for char combustion with air to external heat for the endothermic steam gasification. By application of the fluidisation knowledge, the bubbling fluidised bed (BFB) can be used as a gasifier to provide a high rate of heat transfer between bed materials and biomass, resulting in a nearly uniform temperature distribution throughout the reactor [49]. The other reactor, termed as fast fluidised bed (FFB), used as a combustor, in which the injected air and the flue gas at sufficiently high velocity carry the solid particles (bed material) upward to the top of the reactor. Then the hot bed materials are flown out of

the FFB reactor and separated from the flue gas in a cyclone before being delivered back to the BFB reactor for heat supply [50, 51]. Therefore, DFB steam gasifier has the advantages for producing a nitrogen-free producer gas and low-temperature operation [52].

2.2.3. Mechanisms of steam gasification

As feedstock proceeds through a DFB gasifier, the gasification reactions that may occur sequentially or simultaneously can be considered as a three-stage process in BFB. The gasification reaction formulae in every stage are listed in Table 2-5. In these reactions, the standard enthalpies for the reaction are all at the standard temperature of 298K.

Three stages of steam gasification of biomass

- Initial drying: drying occurs at about 100-200°C when moisture in the biomass is removed by vaporisation.
- Devolatilization: it occurs at 300-500°C. In this stage, biomass is decomposed into solid char, volatiles and a few unsaturated hydrocarbons, e.g., tar. The volatiles contains a mixture gas of H_2, CO, CO_2, CH_4 and other longer molecular weight hydrocarbons. The char is the residual solids mainly comprised of solid carbon [53].
- Steam Gasification at a temperature above 500°C: it consists of the homogeneous reactions (among gases and steam) and heterogeneous reactions (among char and gases as well as steam). The heterogeneous reactions include steam-char gasification, Boudouard reaction and Methanation reaction. The homogeneous reactions include water gas shift reaction and steam methane reforming reaction.

Table 2-4. A list of gasification reactions and the reaction enthalpies [54].

Reaction names	Reaction formulae
Drying	Moist feedstock + Heat $\rightarrow$ Dry feedstock + H_2O (vapour)
Devolatilization	Biomass $\rightarrow$ Gas (H_2, CH_4, CO_2, CO) + char + tar (2-1)
Gasification reactions	
Steam char reaction	$C + H_2O \rightarrow CO + H_2 - 131.4kJ/mol$ (2-2) $C + 2H_2O \rightarrow CO_2 + H_2 - 90.2kJ/mol$ (2-3)
Boudouard reaction	$C + CO_2 \rightarrow 2CO - 172.6kJ/mol$ (2-4)
Methanation reaction	$C + 2H_2 \rightarrow CH_4 + 75kJ/mol$ (2-5)
Water-gas shift reaction	$CO + H_2O \leftrightarrow CO_2 + H_2 + 41.2kJ/mol$ (2-6)
Steam methane reforming reaction	$CH_4 + H_2O \leftrightarrow CO + 3H_2 - 206kJ/mol$ (2-7)

2.3. Fundamental of tar formation and removal

In biomass gasification, tar formation and presence in the producer gas are the major technical problem. Tar is a highly viscous liquid mixture with a dark colour which is an unavoidable by-product of the biomass gasification. Tar condenses or polymerises into more complex structures with time and with cooling down, which causes operational problems by blocking equipment, such as, pump, filter and engine. In order to develop efficient and low cost technologies to remove tar from the producer gas, fundamental understanding of the tar formation during biomass gasification is important. Accordingly, optimum operation conditions can be proposed both for gasification process and downstream gas cleaning process to reduce and eliminate the tar in the producer gas.

2.3.1. Tar definition and classification

Tar can be described a mixture of a number of organic compounds. Due to the complexity of tar compounds, various definitions have been reported. A study by Milne et al. [55] reported that tar is the aromatic organics in the producer gas from gasification. Other authors described that tar is a complex mixture of condensable hydrocarbons [56]. While in the meeting of the IEA Bioenergy Gasification Task in 1998, tar is defined as hydrocarbons with molecular weight higher than benzene [57]. In order to study the tar conversion process and formation mechanisms, classification of tar compounds have been proposed depending on the chemical structure, molecular weight and condensation behaviour. There are two types of tar classifications in the literature which have been widely cited.

The first classification was reported by Evans and Milne [58] who classified tar into four groups as given in Table 2-5. Class 1 is the primary tar which is directly from the decomposition of cellulose, hemicellulose and lignin. Class 2 is the secondary tar which is marked by phenolics and olefins. Class 3 is the tertiary tar which is methyl derivatives of aromatic compounds. Class 4 is the condensed tertiary tar which is poly aromatic hydrocarbon without a substituent.

A more commonly accepted classification of tar was proposed by Energy Research Center of The Netherlands (ECN) [59]. In this report, tar compounds can be classified

into five classes based on the molecular weight which is also described in Table 2-6. Class 1 tar refers to GC-undetectable compounds. However, its impact is insignificant due to the low concentrations. Therefore, in virtually all reports. Class 1 tar compounds are ignored. Class 2 tar refers to heterocyclic compounds (containing N and O atoms) that generally have high water solubility, such as phenol and cresol as shown in Table 2-7. Class 3 tar includes 1-ring aromatic compounds, e.g. xylene and toluene. Table 2-8 lists class 3 tar compounds. Class 4 tar refers to 2-3 ring PAH compounds, such as naphthalene and phenanthrene as shown in Table 2-9. Class 5 includes higher PAH compounds, that is, 4-7 ring aromatic compounds. Table 2-10 presents the chemical structure and molecular formulae of class 5 tar compound.

Table 2-5. Description of tar compounds and their classification.

Classification 1 [58]	
Primary	Products derived from the fuel thermal cleavage; levoglucosan, furfurals, guaiacols
Secondary	Phenols and olefins
Tertiary	Alkyl-aromatics
Condensed-tertiary	Poly-aromatic hydrocarbons (PAH)
Classification 2 [59]	
Class-1 tar	GC no detectable
Class-2 tar - Heterocyclic	Tar containing hetero atoms: highly water soluble compounds
Class-3 tar - Light aromatic (1 ring)	do not pose a problem regarding condensability and solubility
Class-4 - Light PAH compounds (2-3 rings)	condense at low temperature even at very low concentration
Class-5 - Heavy PAH compounds (4-7 rings)	condense at high-temperature at low concentrations

Table 2-6. Class 2 tar compounds based on ECN classification method.

Name	Tar class	Structure	Elementary
Pyridine	2	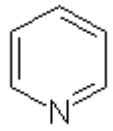	C_5H_5N
Phenol	2	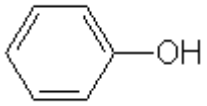	C_6H_6O
O,m,p-Cresol	2	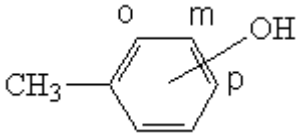	C_7H_8O
Quinoline	2	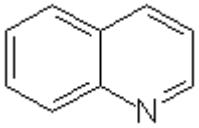	C_9H_7N
Isoquinoline	2	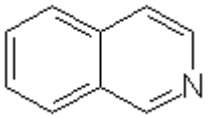	C_9H_7N

Table 2-7. Class 3 tar compounds based on ECN classification method.

Name	Tar class	Structure	Elementary
Toluene	3	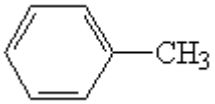	C_7H_8
O, m, p-xylene	3	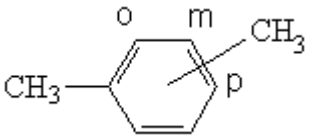	C_8H_{10}
Styrene	3	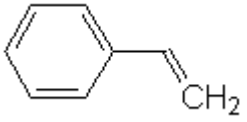	C_8H_8

Table 2-8. Class 4 tar compounds based on ECN classification method.

Name	Tar class	Structure	Elementary
Indene	4	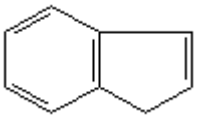	C_9H_8
Naphthalene	4	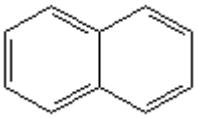	$C_{10}H_8$
2-Methylnaphthalene	4	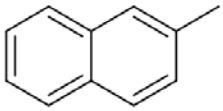	$C_{11}H_{10}$
1-Methylnaphthalene	4	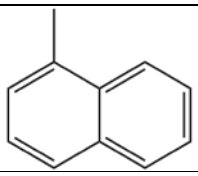	$C_{11}H_{10}$
Biphenyl	4	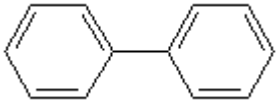	$C_{12}H_{10}$
Acenaphthylene	4	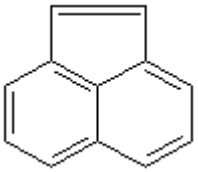	$C_{12}H_8$
Acenaphtene	4	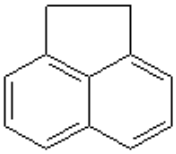	$C_{12}H_{10}$
Fluorene	4	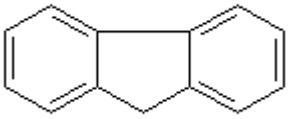	$C_{13}H_{10}$
Phenanthrene	4	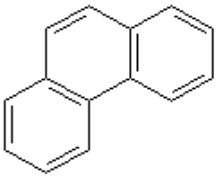	$C_{14}H_{10}$
Anthracene	4	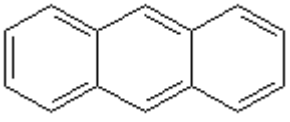	$C_{14}H_{10}$

Table 2-9. Class 5 tar compounds based on ECN classification method.

Name	Tar class	Structure	Elementary
Fluoranthene	5	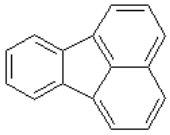	$C_{16}H_{10}$
Pyrene	5	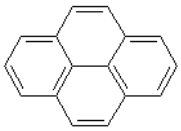	$C_{16}H_{10}$
Bens(a)anthracene	5	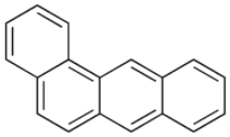	$C_{18}H_{12}$
Chrysene	5	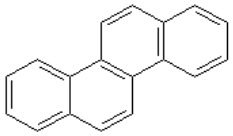	$C_{18}H_{12}$
Benzo(b)fluoranthene	5	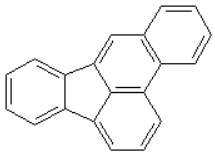	$C_{20}H_{12}$
Benzo(k)fluoranthene	5	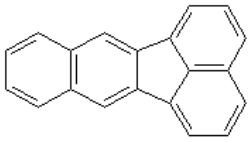	$C_{20}H_{12}$
Benzo(a)Pyrene	5	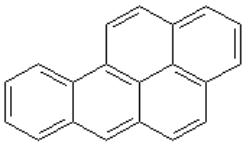	$C_{20}H_{12}$
Indeno(1,2,3-cd) pyrene	5	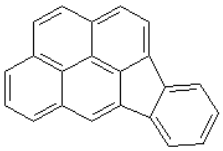	$C_{22}H_{12}$
Benzo(g,h,i)perylene	5	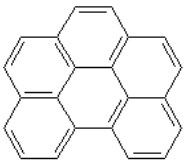	$C_{22}H_{12}$
Dibenzo(a,h)anthracene	5	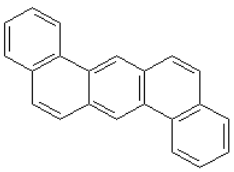	$C_{22}H_{14}$

Dew point of tar compounds is an important thermodynamic property which indicates when tar starts to condense and may become problematic [60]. For the operational purpose, it is useful to know the tar dew point to prevent potential fouling. ECN developed a model for calculation of tar dew points of various tar compounds based on their concentrations in the producer gas [61]. From the simulation results as shown in Fig. 2-6, it is found that the dew points of most tar compounds in the producer gas are between 150 and 250°C. From Fig. 2-6, it can be seen that the tar compounds with 1 or 2 aromatic rings like phenol or naphthalene have lower tar dew points, whereas the compounds with 3 and more aromatic rings have higher dew point [62] which are more important for consideration. Therefore, the tar issue is mainly determined by the heavy PAHs and their concentration [63].

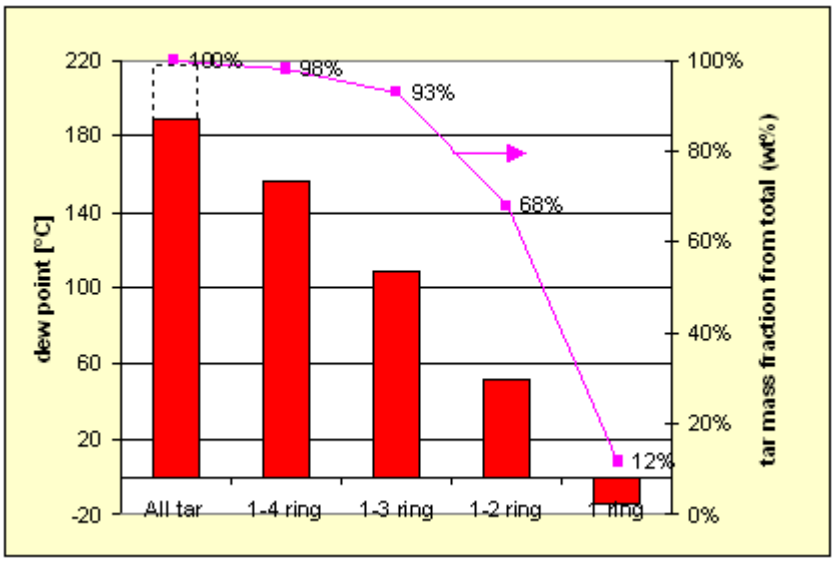

Fig. 2-6. Dew points of various tar compounds [62].

2.3.2. Tar formation and conversion during biomass gasification

Tar is formed during biomass gasification with a series of complex reactions. It is also highly dependent on the reaction conditions, especially reaction temperature, residence time and gasification agent. Therefore, a number of studies have been reported on tar formation and evolution.

Based on the present literature reviews, it is found that in the temperature range from 200°C to 500°C, the biomass breaks down through depolymerisation, which consists of various bond breaking between the monomer units in cellulose, hemicellulose and lignin, into primary tar [64]. This primary tar formation is not avoidable. Evans and Milne [65] described the distribution of four tar classes which are formed at a different temperature from 500 – 1000 °C as shown in Fig. 2-7. At 500°C, the primary tar compounds formed at a lower temperature start to decompose into smaller, lighter non-condensable gases and a series of secondary tar compounds. When temperature increased above 500°C, the formation of secondary tar increases significantly until 750°C. With further increase in temperature, the secondary tar concentration is decreased indicating decomposition of the secondary tar compounds. The formation of secondary tar proceeds through breakage and decarboxylation of the primary tar compounds. The subsequent decomposition of the secondary tar compounds above 750°C is explained by (1) direct combination of two aromatic species producing a dimer; and (2) addition of light unsaturated hydrocarbon to aromatic rings for PAH formation and growth. Therefore, tertiary tar compounds consisting of aromatics are formed at temperatures of around 750°C and their concentrations increase with temperature up to 1000°C [66].

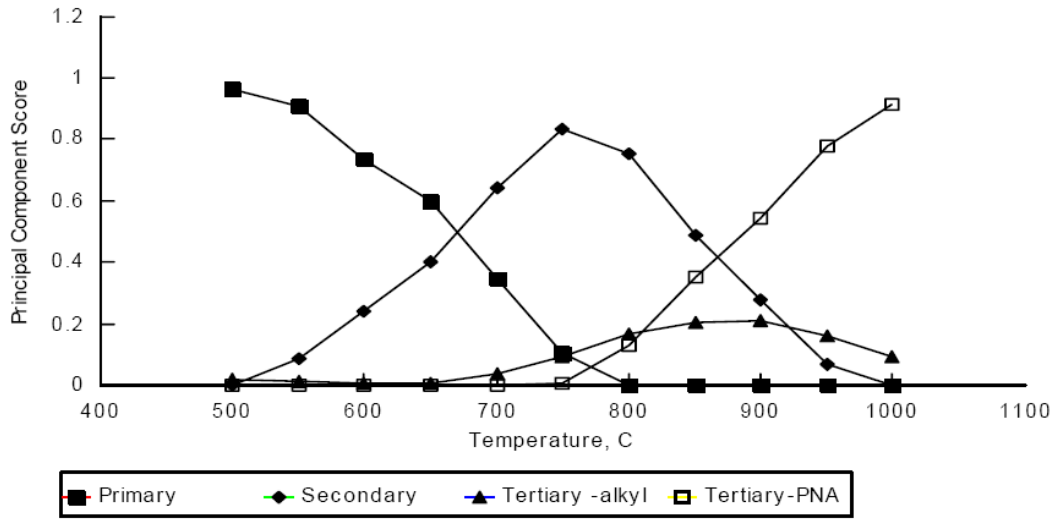

Fig. 2-7. The distribution of four tar class compounds as a function of temperature from 500 to 1000°C [65].

Elliott [67] also proposed a concept on the evolution of tar compounds from primary tar to phenolic compounds and then to poly-aromatic hydrocarbons (PAH) with increasing temperature. Fig. 2-8 presents the tar evolution scheme with temperatures increase from 400 to 900°C. From the figure, it is observed that at a temperature less than 400°C, the main tar compounds are oxygenated hydrocarbon from biomass decomposition. With temperatures increase, the oxygenated hydrocarbons are converted into phenolic containing hydrocarbon. Finally, higher hydrocarbons and larger PAHs in tertiary are formed at 900°C. It is also seen from the figure that more stable aromatic hydrocarbons are formed with the increase in temperature to above 800°C. Therefore, the temperature is the key factor for tar distribution.

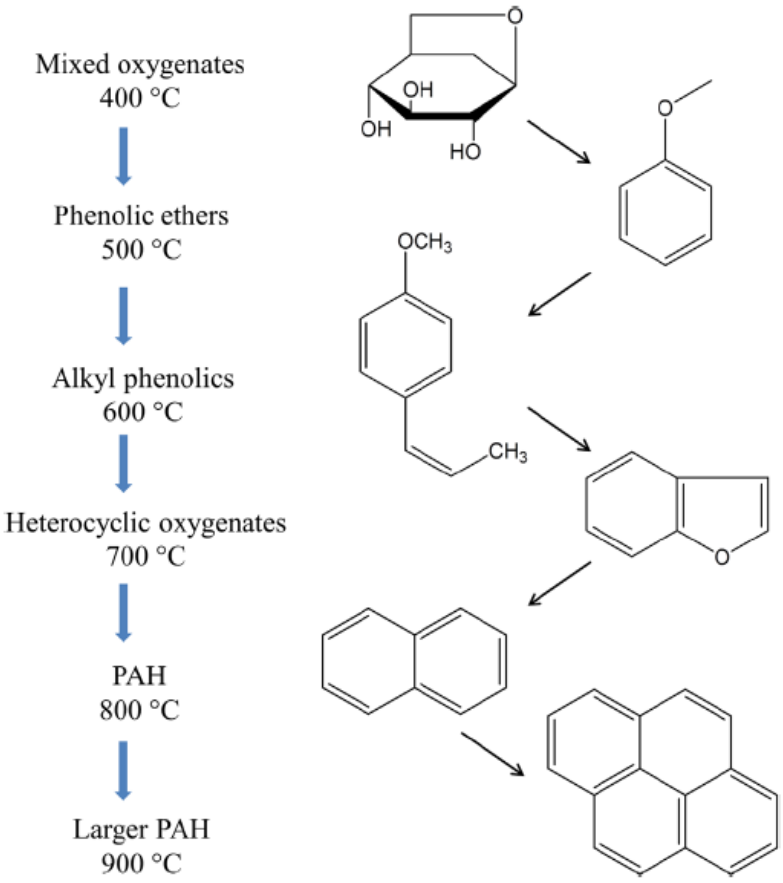

Fig. 2-8. Evolution scheme of tar compounds proposed by Elliott [68].

In a separate study, Font Palma [69] proposed the mechanism for tar formation in which lignin units in the biomass, namely vanillin ($C_8H_8O_3$), guaiacol ($C_7H_8O_2$), and catechol ($C_6H_6O_2$), are assumed to be precursors for the formation of various tar compounds. This mechanism is illustrated in Fig. 2-9 from which it can be seen that the lignin units

are firstly decomposed into primary tar compounds containing a large number of oxygen-containing hydrocarbons. After this, the secondary tar compounds consisting of the single aromatic ring, such as benzene and phenol, are formed through the dealkylation and decarboxylation reactions. Finally, the tertiary tar compounds with 2 to 4 aromatic rings are produced.

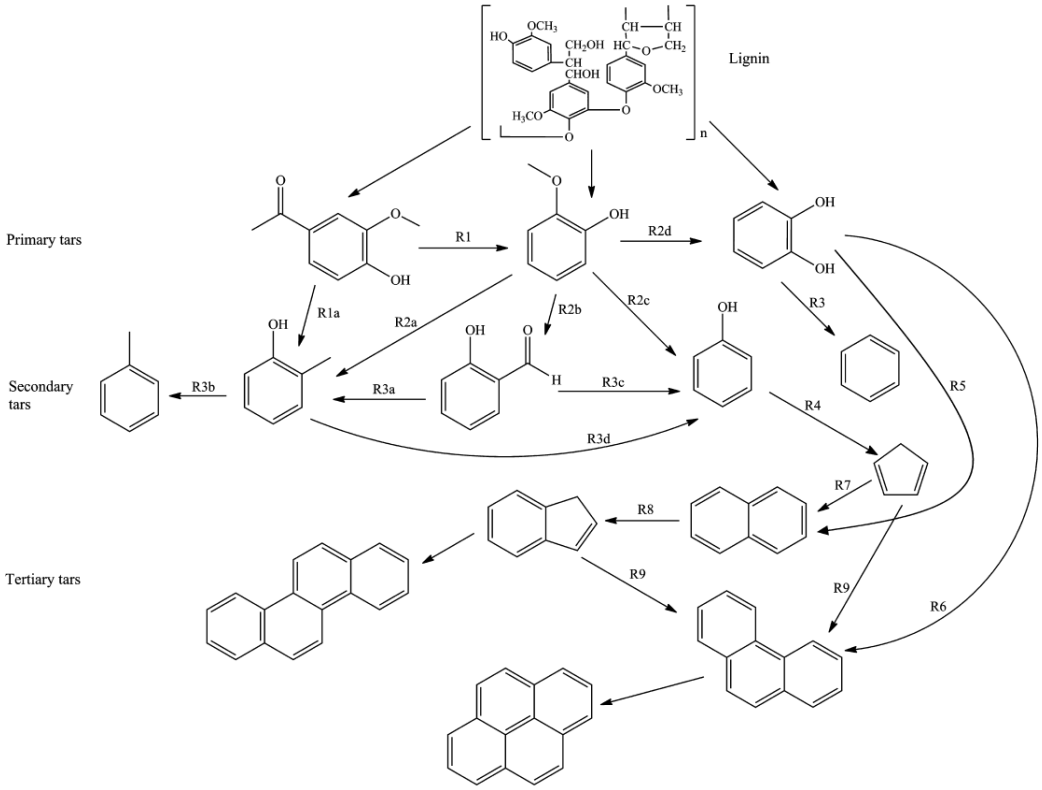

Fig. 2-9. Proposed mechanism for formation of primary, secondary and tertiary tar compounds by Font Palma [69].

From above discussion, tar formation during biomass gasification comprises sequential steps. In the initial devolatilization or pyrolysis process, biomass components (largely lignin units) are decomposed to produce oxygen-containing compounds which are termed as primary tar such as acetaldehyde, hydroxypropanone and acetic acid [70]. With increases in temperature, the oxygen-containing compounds (for example phenol) are converted to aromatic compounds (benzene and toluene) and then higher molecular weight compounds, such as naphthalene in steam gasification [71]. Finally, at temperatures of 900°C or above, most oxygen-containing tar compounds were cracked, and only stable aromatics (naphthalene and PAH) remain [72].

In order to verify the above proposed mechanisms of tar formation and conversion, experiments have been carried out to build a reaction pathway and to explore the thermal cracking of tar compounds [63]. In these experimental studies, model tar compounds are commonly selected. For example, toluene [73-75] and naphthalene [71, 76, 77] were chosen, respectively, as the secondary and tertiary tar compounds. Toluene is a good representative tar compound because it represents a stable aromatic structure found in tars formed during high temperature biomass gasification. Naphthalene is a 2-ring PAH that is very difficult to crack in comparison to other tertiary tar compounds and is the main species found in tertiary tar. In the study of Zhao et al. [78], steam reforming of toluene was used in experiments with a fixed bed reactor from 750°C to 900°C. It was found that the toluene was effectively reformed to form benzene and naphthalene. However, the concentration of naphthalene decreased while that of benzene increased with increase in temperatures.

In a sperate study, Zhou et al. [79] conducted experiments on pyrolysis of xylan (commonly representative of hemicellulose) and lignin in a fixed bed furnace at 800 °C. They found that lignin generated more PAH in which naphthalene was the most abundant although 1-methylnaphthalene and 2-methylnaphthalene were also detected.

Zhai et al.[80] conducted experiments on high temperature (700 - 1300°C) pyrolysis of rice husk and tar cracking in a two-stage pyrolysis system. It was found that the content of oxy-organics in the pyrolysis gas reached 24.5% for pyrolysis temperature of 700 °C, and these compounds were almost completely cracked at 1100°C. However, the content of naphthalene was significantly low at 700 °C, but reached to the maximum of 26.4% at 800 °C. With further increase in temperature, The content of naphthalene decreased and virtually disappeared at 1200 °C. The content of fluorene is was non-detectable at 700 °C, and then increased gradually with temperature until 1000 °C from which its content increased significantly.

Yu et al. [81] compared the tar formation in gasification of individual biomass component, cellulose, hemicellulose and lignin in an entrained flow gasifier. The results from this study indicated that the tar yields of the three components all decreased with increasing temperature. Lignin had a significantly higher tar yield than cellulose and hemicellulose.

2.3.3. Reactions of tar formation and decomposition

From the above discussion, tar compounds are formed through a series of complex thermochemical reactions such as depolymerisation, oxidation, repolymerisation, and cycloaddition. These reactions may be divided into two groups of "tar cracking" and "PAH tar polymerisation" [82].

- *Tar cracking reactions*

Some tar compounds can be cracked at high temperatures, or reformed in reaction with gaseous species including gasification agent during gasification. With the thermal cracking of tar compounds, the tar compounds are converted or cracked into lighter gaseous species [83]. Li and Suzuki [84] and Devi and Janssen [76] have listed possible reactions for tar cracking and reforming

Thermal cracking $pC_mH_n \leftrightarrow qC_xH_y + rH_2$

Steam reforming $C_mH_n + mH_2O \leftrightarrow mCO + (m + \frac{n}{2})H_2$

Dry reforming $C_mH_n + mCO_2 \leftrightarrow 2mCO + (\frac{n}{2})H_2$

Carbon formation $C_mH_n \leftrightarrow mC + (\frac{n}{2})H_2$

Partial oxidation $C_mH_n + \frac{m}{2}O_2 \leftrightarrow mCO + (\frac{n}{2})H_2$

Where C_mH_n represents tar which can be a mixture of several individual tar compounds and C_xH_y represents hydrocarbons with carbon number less than C_mH_n.

In a separate study, Jess [85] presented a simple reaction scheme of thermal decomposition of aromatic hydrocarbon (naphthalene and toluene were used as tar samples) as shown in Fig. 2-10. Based on this scheme, naphthalene and toluene are firstly transformed to benzene with the presence of hydrogen and steam. Then the benzene is transformed to lighter molecules gas (CO, H_2, and CH_4). In the meantime, the carbonaceous residue (soot) reacts with steam to form CO and H_2.

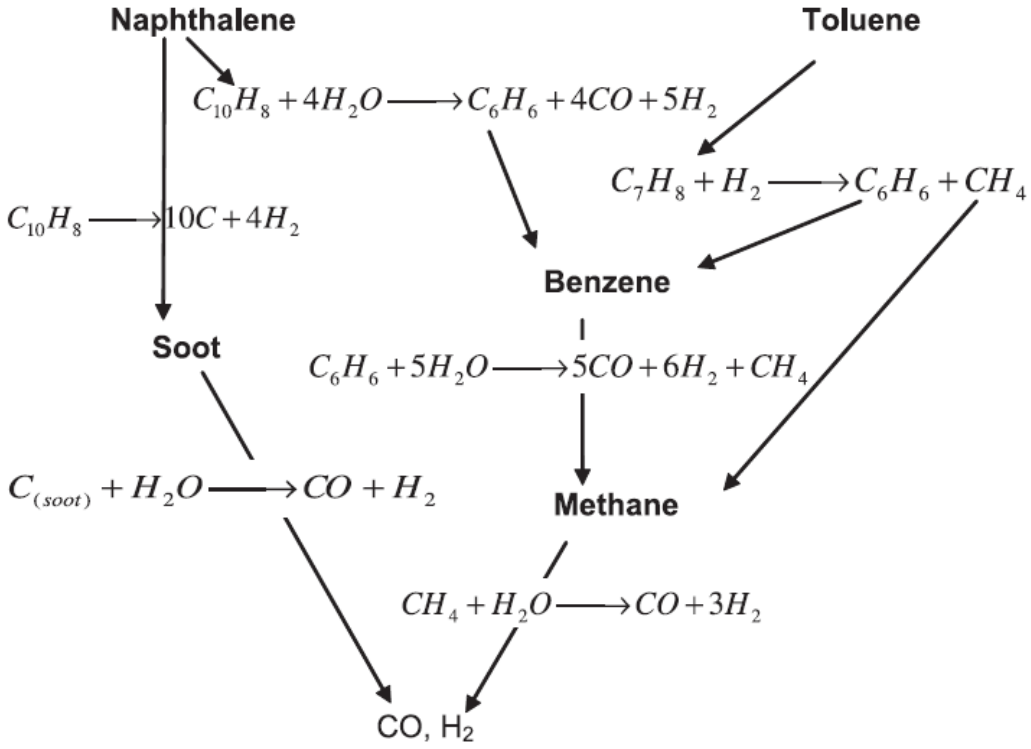

Fig. 2-10. Reaction scheme of thermal conversion of PAH (naphthalene and toluene) in the presence of hydrogen and steam [86].

- *Mechanism of PAH tar formation*

During biomass gasification, a series of tar cracking reaction as described above lead to decreasing concentration of the primary and secondary tar compounds, which are decomposed into light gas components (such as CO, H_2 and CH_4) and small hydrocarbons (benzene). Although the total tar concentration in the producer gas decreases with increasing gasification temperature, the radicals from the tar decomposition contribute to ring-growth reactions, leading to the formation of larger PAH tar compounds. The PAH tar compounds have relatively high tar dew points even at low concentrations, resulting in condensation at relatively high temperatures. Therefore, it is important to understand the mechanisms of PAH tar formation and thus to find effective gas cleaning method. Based on previous studies [87, 88], the growth of aromatics to higher molecular PAH compounds can be explained by three pathways:

1. Dealkylation and decarboxylation: It states that the aromaticity of the tar mixture is promoted by the cleavage of alkyl groups attached to the aromatic rings from which the

intact aromatic ring is formed. Fig. 2-11 illustrates the cleavage of methyl from toluene and of hydroxyl from phenol, to form benzene and cyclopentadiene.

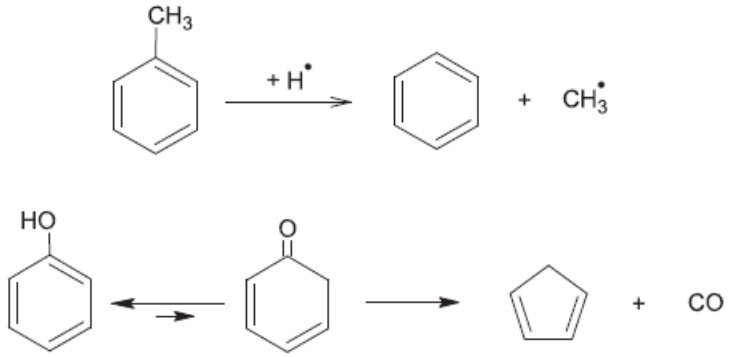

Fig. 2-11. Reactions of Dealkylation and decarboxylation.

2. Dimerization reactions of two PAH compounds: This mechanism is a direct combination of intact aromatic rings, resulting in the large PAH tar compounds, for example, three different reactions on dimerization as shown in Fig. 2-12. There are three possible combination reactions: (1) the biphenyl formation by the combination of two benzene ring, (2) the naphthalene formation from two cyclopentadienyl radicals; and (3) the combination of indenyl and cyclopentadienyl to form phenanthrene.

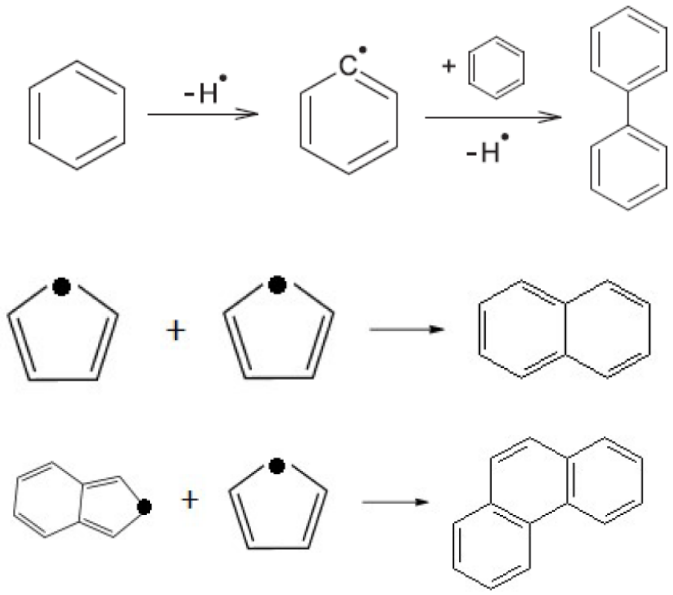

Fig. 2-12. Combination reactions of dimerization.

3. Cyclisation or hydrogen abstraction acetylene addition (HACA) mechanism: Aromatic rings grow by hydrogen abstraction, which activates the aromatic molecules, and acetylene addition, which propagates molecular growth by cyclisation [89]. Fig. 2-13 shows the formation of naphthalene and phenanthrene from benzene and biphenyl through HACA mechanism, respectively.

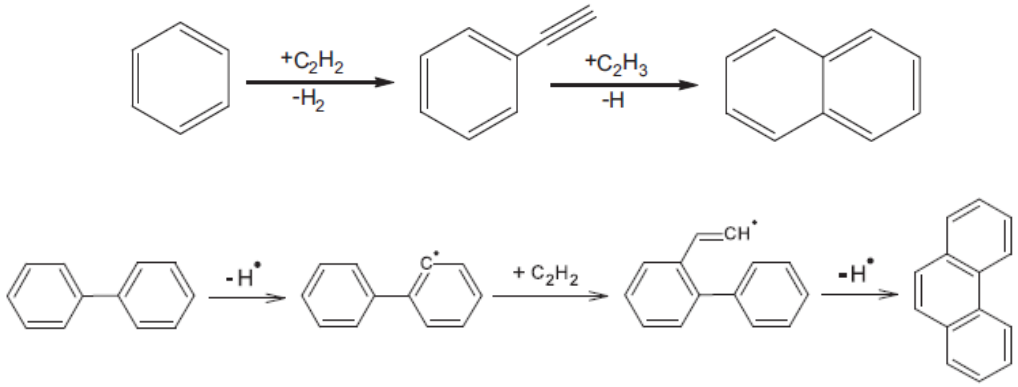

Fig. 2-13. Reactions of cyclisation.

In all three reaction pathways, it is suggested that the radical reaction plays a vital role in the tar formation [90]. The main steps in the radical reaction are (1) radical forming reactions by the breaking of chemical bonds, (2) propagation reactions through the formation of new chemical bonds, and (3) hydrogen transfer.

2.3.4. Tar removal technologies

Extensive studies have been reported on developing technologies for tar reduction and removal which can be classified into two categories: primary methods and secondary methods [91].The primary methods for reducing the tar content in the producer gas during the gasification process and the methods include optimisation of the gasifier design and the gasification operation conditions and addition of catalytic bed materials. It has been reported that catalytic cracking and thermal cracking in high-temperature gasification exhibit effective tar reduction. The secondary methods are those applied in the downstream of gasification including cyclone and filters separation of particulate with tar on them, wet scrubber and high temperature cracking column [92].

Thermal cracking of tar is a process in which tar is converted and cracked into lighter gaseous species at high temperature in which the operation temperature has the most significant effect [93]. This principle applies to both the primary and the secondary tar removal methods. In biomass gasification, higher temperatures lead to a lower of tar concentration in the producer gas [94]. In steam biomass gasification, the effect of operation temperature on tar concentration reduction in the producer gas is a non-linear trend as reported by Hernández et al. [95]. From this report, the reduction of tar content was significant when increasing the temperature from 750°C to 1050°C whereas the reduction of tar content was less noticeable with a further increase in the gasification temperature above 1050°C.

The use of catalytic bed materials during biomass gasification can facilitate tar reduction reactions in the gasifier [96]. These catalytic bed materials include Ni-based catalysts, limestone/dolomite, olivine and iron catalysts. Most of these catalysts are relatively inexpensive and readily available. It is found that the use of catalytic bed materials not only reduces the tar yield but also influences the gas composition [97]. Calcium rich catalytic bed materials such as limestone and dolomite promote the exothermic water gas shift reaction, which increases the hydrogen and carbon dioxide content of the producer gas while the carbon monoxide content is decreased [98]. Saw and Pang [99] reported that the loading of calcite as the bed material in a dual fluidised bed gasifier decreased the tar concentration by 91%. Similar results have also been reported in other studies [100]. Alarcón et al. [101] investigated the catalytic activity of CaO and MgO for steam gasification of naphthalene in a laboratory scale reactor. From this study, catalytic synergy was found with CaO and MgO blends. The highest carbon conversion of 79% was achieved by using a mixture of 10% CaO and 90% MgO, compared to pure MgO and CaO with which the carbon conversion was 54% and 62%, respectively.

An alternative catalytic bed material which is naturally occurring olivine sand, which is a mineral containing magnesium, iron oxide and silica. Olivine is advantageous due to its higher attrition resistance than that of dolomite/limestone. The catalytic effect of olivine on the tar reduction has been studied [102-104]. In the study of Naqvi et al. [105], the total tar content was reduced by 40% in the dual bed steam gasification with pre-treated olivine. Tursun et al. [106] reported that lower tar concentration (7.8g/Nm^3)

with olivine sand were achieved in comparison to that with non-catalytic silica sand as bed material (25.3g/Nm^3).

Wet scrubbing technology uses water or another solvent to absorb tar compounds from the producer gas. Although wet scrubbing method is effective in removing tar, post treatment of tar-contaminating solvent is complicated and may expose environmental issues. However, recent studies using bio-diesel and another organic solvent (rapeseed oil) have shown promising results. By using bio-diesel and an organic solvent, tar laden bio-diesel or organic solvent can be utilised as fuel or recycled. Phuphuakrat et al. [107] investigated the tar removal performance of various solvents including water, vegetable oil, fossil fuel derived oils (engine oil and diesel) and the efficiency of the tar removal are in the order of vegetable oil > engine oil > water > diesel fuel. The successful oil based gas cleaning system developed at ECN is OLGA [108, 109].

2.4. Conclusion

2.4.1. Summary of literature review

Biomass as a renewable energy resource can be processed through various pathways including physical, thermal and biological conversion for future generation of heat, power, gaseous and liquid fuels and chemical feedstock. Among these conversion technologies, gasification is one of the promising thermochemical processes. Biomass gasification converts biomass into a producer gas at high temperatures (700-1100°C) and in the presence of a gasification agent. Biomass gasification is a complicated process, which mainly contains three stages: drying, initial devolatilization and gasification reaction. The product yields and compositions from biomass gasification depend on many factors, which include various physical and chemical characterizations of biomass sources, gasification agent type (air or steam), gasifier design and operating conditions. In order to obtain a hydrogen-rich producer gas, a 100kW dual fluidised bed (DFB) steam gasifier has been designed, constructed and tested in past 10 years. However, during the biomass gasification, tar formation and presence in the producer gas are the major technical issues, which causes operational problems by blocking downstream equipment. Therefore, it is important to investigate and understand the complex tar formation and evolution during biomass gasification.

2.4.2. Knowledge gap and research motivation

Up to now, tar production (composition and yield) from biomass gasification have been investigated and reported in many studies. However, there is still a lack of knowledge on tar production and tar conversion.

Firstly, only a few studies reported tar production in initial devolatilization stage of the gasification process, especially the aromatic tar formation mechanism, which is useful to understand the tar conversion and transformation during biomass gasification. Furthermore, no relation between initial devolatilization and final gasification on the tar and gas production has been previously established.

Secondly, despite the numerous studies on tar formation in the biomass gasification [85, 110, 111], they have selected only one or two tar compounds as the model tar, which were converted in a readily controlled reactor (TGA or bench scale reactor), allowing for tracking the decomposition process and determination of the conversion kinetics. This method is simple and accurate, but the interaction among the different tar compounds is neglected. Therefore, it is necessary to test the production and conversion of tar compounds generated from complete biomass decomposition, which enables determination of more realistic tar formation and conversion during the whole process.

Finally, the DFB technology is highly qualified for scale-up and commercialisation of biomass gasification. Up to now, few studies on the tar production and formation in the DFB gasifier have been found [112, 113]. Gathering the experimental data relating the operating variations to the concentration and composition of the tar compounds in the producer gas in the 100kW DFB gasifier in CAPE can highly support the scale-up of the gasifier and provide the useful information for the development of downstream gas cleaning system.

In order to fill these gaps, biomass devolatilization will independently be conducted on in the 100kW DFB gasifier, where N_2 instead of steam was used as fluidisation agent, to investigate the tar and gas production. The results contribute to better assess the correlation between initial devolatilization and final gasification on the tar and gas production.

At the same time, examining the operating conditions and biomass species in the DFB gasifier on the tar formation and conversions can provide the necessary knowledge to relate the experimental variations to the reduction of tar content in the producer gas. Finally, the catalytic effects of bed materials used on tar cracking in the DFB gasifier will also be tested.

2.5. Reference

[1] A. C. Chang, H.-F. Chang, F.-J. Lin, K.-H. Lin, and C.-H. Chen, "Biomass gasification for hydrogen production," *International Journal of Hydrogen Energy,* vol. 36, pp. 14252-14260, 2011.

[2] A. V. Bridgwater, "Renewable fuels and chemicals by thermal processing of biomass," *Chemical Engineering Journal,* vol. 91, pp. 87-102, 2003.

[3] A. Demirbas, "Biomass resource facilities and biomass conversion processing for fuels and chemicals," *Energy Conversion and Management,* vol. 42, pp. 1357-1378, 2001.

[4] M. F. Demirbas, M. Balat, and H. Balat, "Potential contribution of biomass to the sustainable energy development," *Energy Conversion and Management,* vol. 50, pp. 1746-1760, 2009.

[5] H. B. Goyal, D. Seal, and R. C. Saxena, "Bio-fuels from thermochemical conversion of renewable resources: A review," *Renewable and Sustainable Energy Reviews,* vol. 12, pp. 504-517, 2008.

[6] S. V. Vassilev, D. Baxter, L. K. Andersen, and C. G. Vassileva, "An overview of the chemical composition of biomass," *Fuel,* vol. 89, pp. 913-933, 2009.

[7] T. Hanaoka, S. Inoue, S. Uno, T. Ogi, and T. Minowa, "Effect of woody biomass components on air-steam gasification," *Biomass and Bioenergy,* vol. 28, pp. 69-76, 2005.

[8] S. Luo, B. Xiao, Z. Hu, S. Liu, X. Guo, and M. He, "Hydrogen-rich gas from catalytic steam gasification of biomass in a fixed bed reactor: Influence of temperature and steam on gasification performance," *International Journal of Hydrogen Energy,* vol. 34, pp. 2191-2194, 2009.

[9] R. C. Brown, Q. Liu, and G. Norton, "Catalytic effects observed during the co-gasification of coal and switchgrass," *Biomass and Bioenergy,* vol. 18, pp. 499-506, 2000.

[10] A. J. Byrd, S. Kumar, L. Kong, H. Ramsurn, and R. B. Gupta, "Hydrogen production from catalytic gasification of switchgrass biocrude in supercritical water," *International Journal of Hydrogen Energy,* vol. 36, pp. 3426-3433, 2011.

[11] K. Li, R. Zhang, and J. Bi, "Experimental study on syngas production by co-gasification of coal and biomass in a fluidized bed," *International Journal of Hydrogen Energy,* vol. 35, pp. 2722-2726, 2009.

[12] R. N. André, F. Pinto, C. Franco, M. Dias, I. Gulyurtlu, M. A. A. Matos, and I. Cabrita, "Fluidised bed co-gasification of coal and olive oil industry wastes," *Fuel,* vol. 84, pp. 1635-1644, 2005.

[13] S. Priyadarsan, K. Annamalai, J. M. Sweeten, M. T. Holtzapple, and S. Mukhtar, "Co-gasification of blended coal with feedlot and chicken litter biomass," *Proceedings of the Combustion Institute,* vol. 30, pp. 2973-2980, 2005.

[14] A. International, "ASTM E870-82(2013), Standard Test Methods for Analysis of Wood Fuels," West Conshohocken, PA, 2013.

[15] D. L. Klass, *Biomass for renewable energy, fuels, and chemicals*. San Diego: Academic Press, 1998.

[16] Y. J. Lu, H. Jin, L. J. Guo, X. M. Zhang, C. Q. Cao, and X. Guo, "Hydrogen production by biomass gasification in supercritical water with a fluidized bed reactor," *International Journal of Hydrogen Energy,* vol. 33, pp. 6066-6075, 2008.

[17] H. Jin, E. D. Larson, and F. E. Celik, "Performance and cost analysis of future, commercially mature gasification-based electric power generation from switchgrass," *Biofuels, Bioproducts and Biorefining,* vol. 3, pp. 142-173, 2009.

[18] W. L. Saw and S. Pang, "Co-gasification of blended lignite and wood pellets in a 100kW dual fluidised bed steam gasifier: The influence of lignite ratio on producer gas composition and tar content," *Fuel,* vol. 112, pp. 117-124, 2013.

[19] A. Demirbas, "Sustainable cofiring of biomass with coal," *Energy Conversion and Management,* vol. 44, pp. 1465-1479, 2003.

[20] E. Kastanaki, D. Vamvuka, P. Grammelis, and E. Kakaras, "Thermogravimetric studies of the behavior of lignite-biomass blends during devolatilization," *Fuel Processing Technology,* vol. 77-78, pp. 159-166, 2002.

[21] T. Ganga Devi and M. P. Kannan, "Calcium catalysis in air gasification of cellulosic chars," *Fuel,* vol. 77, pp. 1825-1830, 1998.

[22] L. Zhang, S. Xu, W. Zhao, and S. Liu, "Co-pyrolysis of biomass and coal in a free fall reactor," *Fuel,* vol. 86, pp. 353-359, 2007.

[23] S. Wang, X. Guo, K. Wang, and Z. Luo, "Influence of the interaction of components on the pyrolysis behavior of biomass," *Journal of Analytical and Applied Pyrolysis,* vol. 91, pp. 183-189, 2011.

[24] P. McKendry, "Energy production from biomass Part 1: overview of biomass," *Bioresource Technology,* vol. 83, pp. 37-46, 2002.

[25] K. Raveendran, A. Ganesh, and K. C. Khilar, "Pyrolysis characteristics of biomass and biomass components," *Fuel,* vol. 75, pp. 987-998, 1996.

[26] L. Burhenne, J. Messmer, T. Aicher, and M.-P. Laborie, "The effect of the biomass components lignin, cellulose and hemicellulose on TGA and fixed bed pyrolysis," *Journal of Analytical and Applied Pyrolysis,* 2013.

[27] P. Giudicianni, G. Cardone, and R. Ragucci, "Cellulose, hemicellulose and lignin slow steam pyrolysis: Thermal decomposition of biomass components mixtures," *Journal of Analytical and Applied Pyrolysis,* vol. 100, pp. 213-222, 2013.

[28] C. Fushimi, S. Katayama, and A. Tsutsumi, "Elucidation of interaction among cellulose, lignin and xylan during tar and gas evolution in steam gasification," *Journal of Analytical and Applied Pyrolysis,* vol. 86, pp. 82-89, 9// 2009.

[29] Y. Qin, A. Campen, T. Wiltowski, J. Feng, and W. Li, "The influence of different chemical compositions in biomass on gasification tar formation," *Biomass and Bioenergy,* vol. 83, pp. 77-84, 2015.

[30] "About Lignin."

[31] J. Diebold and A. Bridgwater, "Overview of fast pyrolysis of biomass for the production of liquid fuels," in *Developments in thermochemical biomass conversion*: Springer, 1997, pp. 5-23.

[32] R. Alén, E. Kuoppala, and P. Oesch, "Formation of the main degradation compound groups from wood and its components during pyrolysis," *Journal of Analytical and Applied Pyrolysis,* vol. 36, pp. 137-148, 1996.

[33] T. Hosoya, H. Kawamoto, and S. Saka, "Secondary reactions of lignin-derived primary tar components," *Journal of Analytical and Applied Pyrolysis,* vol. 83, pp. 78-87, 2008.

[34] D. Shen, R. Xiao, S. Gu, and K. Luo, "The pyrolytic behavior of cellulose in lignocellulosic biomass: a review," *RSC Advances,* pp. 1641-1660, 2011.

[35] F.-X. Collard and J. Blin, "A review on pyrolysis of biomass constituents: Mechanisms and composition of the products obtained from the conversion of cellulose, hemicelluloses and lignin," *Renewable and Sustainable Energy Reviews,* vol. 38, pp. 594-608, 2014.

[36] T. Faravelli, A. Frassoldati, G. Migliavacca, and E. Ranzi, "Detailed kinetic modeling of the thermal degradation of lignins," *Biomass and Bioenergy,* vol. 34, pp. 290-301, 2010.

[37] A. Gani and I. Naruse, "Effect of cellulose and lignin content on pyrolysis and combustion characteristics for several types of biomass," *Renewable Energy,* vol. 32, pp. 649-661, 2007.

[38] H. Yang, R. Yan, H. Chen, D. H. Lee, and C. Zheng, "Characteristics of hemicellulose, cellulose and lignin pyrolysis," *Fuel,* vol. 86, pp. 1781-1788, 2007.

[39] T. Haensel, A. Comouth, P. Lorenz, S. I. U. Ahmed, S. Krischok, N. Zydziak, A. Kauffmann, and J. A. Schaefer, "Pyrolysis of cellulose and lignin," *Applied Surface Science,* vol. 255, pp. 8183-8189, 2009.

[40] A. A. Peterson, F. Vogel, R. P. Lachance, M. Froling, M. J. Antal, and J. W. Tester, "Thermochemical biofuel production in hydrothermal media: A review of sub- and supercritical water technologies," *Energy & Environmental Science,* vol. 1, pp. 32-65, 2008.

[41] J. Ahrenfeldt and H. Knoef, *Handbook biomass gasification* Enschede, The Netherlands: BTG Biomass Technology Group, 2005.

[42] M. M. Küçük and A. Demirbas, "Biomass conversion processes," *Energy Conversion and Management,* vol. 38, pp. 151-165, 1997.

[43] F. Yan, S.-y. Luo, Z.-q. Hu, B. Xiao, and G. Cheng, "Hydrogen-rich gas production by steam gasification of char from biomass fast pyrolysis in a fixed-bed reactor: Influence of temperature and steam on hydrogen yield and syngas composition," *Bioresource Technology,* vol. 101, pp. 5633-5637, 2010.

[44] K. Umeki, Y.-i. Son, T. Namioka, and K. Yoshikawa, "Basic Study on Hydrogen-Rich Gas Production by High Temperature Steam Gasification of Solid Wastes," *Journal of Environment and Engineering,* vol. 4, pp. 211-221, 2009.

[45] A. Abuadala, I. Dincer, and G. F. Naterer, "Exergy analysis of hydrogen production from biomass gasification," *International Journal of Hydrogen Energy*, vol. 35, pp. 4981-4990, 2010.

[46] A. V. Bridgwater, "The technical and economic feasibility of biomass gasification for power generation," *Fuel*, vol. 74, pp. 631-653, 1995.

[47] M. L. d. Souza-Santos, *Solid fuels combustion and gasification : modeling, simulation, and equipment operations*, 2nd ed. Boca Raton: Taylor & Francis, 2010.

[48] T. Murakami, G. Xu, T. Suda, Y. Matsuzawa, H. Tani, and T. Fujimori, "Some process fundamentals of biomass gasification in dual fluidized bed," *Fuel*, vol. 86, pp. 244-255, 2007.

[49] M. L. Mastellone, L. Zaccariello, and U. Arena, "Co-gasification of coal, plastic waste and wood in a bubbling fluidized bed reactor," *Fuel*, vol. 89, pp. 2991-3000, 2010.

[50] Z. A. B. Z. Alauddin, P. Lahijani, M. Mohammadi, and A. R. Mohamed, "Gasification of lignocellulosic biomass in fluidized beds for renewable energy development: A review," *Renewable and Sustainable Energy Reviews*, vol. 14, pp. 2852-2862, 2010.

[51] M. Puig-Arnavat, J. C. Bruno, and A. Coronas, "Review and analysis of biomass gasification models," *Renewable and Sustainable Energy Reviews*, vol. 14, pp. 2841-2851, 2010.

[52] K. Göransson, U. Söderlind, J. He, and W. Zhang, "Review of syngas production via biomass DFBGs," *Renewable and Sustainable Energy Reviews*, vol. 15, pp. 482-492, 2011.

[53] M. D. Baker, *Gasification: Chemistry, Processes and Applications*. Hauppauge, US: Nova Science Publishers, Inc., 2011.

[54] L. Emami Taba, M. F. Irfan, W. A. M. Wan Daud, and M. H. Chakrabarti, "The effect of temperature on various parameters in coal, biomass and CO-gasification: A review," *Renewable and Sustainable Energy Reviews*, vol. 16, pp. 5584-5596, 2012.

[55] T. A. Milne, N. Abatzoglou, and R. J. Evans, "Biomass gasifier" tars": their nature, formation, and conversion," National Renewable Energy Laboratory, Golden, Colorado, USA, 1998.

[56] L. Devi, K. J. Ptasinski, F. J. J. G. Janssen, S. V. B. van Paasen, P. C. A. Bergman, and J. H. A. Kiel, "Catalytic decomposition of biomass tars: use of dolomite and untreated olivine," *Renewable Energy,* vol. 30, pp. 565-587, 2005.

[57] K. Maniatis and A. Beenackers, "Tar protocols. IEA bioenergy gasification task," *Biomass and Bioenergy,* vol. 18, pp. 1-4, 2000.

[58] R. J. Evans and T. A. Milne, "Molecular characterization of the pyrolysis of biomass," *Energy & Fuels,* vol. 1, pp. 123-137, 1987.

[59] J. Kiel, S. Van Paasen, J. Neeft, L. Devi, K. Ptasinski, F. Janssen, R. Meijer, R. Berends, H. Temmink, and G. Brem, "Primary measures to reduce tar formation in fluidised-bed biomass gasifiers," Energy research Centre of the Netherlands (ECN) Report, The Netherlands, ECN-C-04-014, 2004.

[60] R. Zwart, A. Van der Drift, A. Bos, H. Visser, M. Cieplik, and H. Könemann, "Oil-based gas washing—Flexible tar removal for high-efficient production of clean heat and power as well as sustainable fuels and chemicals," *Environmental Progress & Sustainable Energy,* vol. 28, pp. 324-335, 2009.

[61] L. P. Rabou, R. W. Zwart, B. J. Vreugdenhil, and L. Bos, "Tar in biomass producer gas, the Energy research Centre of the Netherlands (ECN) experience: an enduring challenge," *Energy & Fuels,* vol. 23, pp. 6189-6198, 2009.

[62] S. Van Paasen, J. Kiel, and H. Veringa, "Tar formation in a fluidised bed gasifier," Energy research Centre of the Netherlands (ECN) Report, The Netherlands, ECN-C-04-013, 2004.

[63] D. Fuentes-Cano, A. Gómez-Barea, S. Nilsson, and P. Ollero, "The influence of temperature and steam on the yields of tar and light hydrocarbon compounds during devolatilization of dried sewage sludge in a fluidized bed," *Fuel,* vol. 108, pp. 341-350, 2013.

[64] P. Morf, P. Hasler, and T. Nussbaumer, "Mechanisms and kinetics of homogeneous secondary reactions of tar from continuous pyrolysis of wood chips," *Fuel,* vol. 81, pp. 843-853, 2002.

[65] R. J. Evans and T. A. Milne, "Chemistry of tar formation and maturation in the thermochemical conversion of biomass," in *Fuel and Energy Abstracts*, 1998.

[66] N. E. Sánchez, Á. Millera, R. Bilbao, and M. U. Alzueta, "Polycyclic aromatic hydrocarbons (PAH), soot and light gases formed in the pyrolysis of acetylene at different temperatures: effect of fuel concentration," *Journal of analytical and applied pyrolysis,* vol. 103, pp. 126-133, 2013.

[67] D. C. Elliott, "Relation of Reaction Time and Temperature to Chemical Composition of Pyrolysis Oils," in *Pyrolysis Oils from Biomass*. vol. 376: American Chemical Society, 1988, pp. 55-65.

[68] G. Guan, M. Kaewpanha, X. Hao, and A. Abudula, "Catalytic steam reforming of biomass tar: Prospects and challenges," *Renewable and Sustainable Energy Reviews,* vol. 58, pp. 450-461, 2016.

[69] C. Font Palma, "Modelling of tar formation and evolution for biomass gasification: A review," *Applied Energy,* vol. 111, pp. 129-141, 2013.

[70] U. Wolfesberger-Schwabl, I. Aigner, and H. Hofbauer, "Mechanism of tar generation during fluidized bed gasification and low temperature pyrolysis," *Industrial & Engineering Chemistry Research,* vol. 51, pp. 13001-13007, 2012.

[71] R. Michel, A. Łamacz, A. Krzton, G. Djéga-Mariadassou, P. Burg, C. Courson, and R. Gruber, "Steam reforming of α-methylnaphthalene as a model tar compound over olivine and olivine supported nickel," *Fuel,* vol. 109, pp. 653-660, 2013.

[72] L. Devi, K. J. Ptasinski, and F. J. J. G. Janssen, "A review of the primary measures for tar elimination in biomass gasification processes," *Biomass and Bioenergy,* vol. 24, pp. 125-140, 2003.

[73] D. Swierczynski, C. Courson, and A. Kiennemann, "Study of steam reforming of toluene used as model compound of tar produced by biomass gasification," *Chemical Engineering and Processing: Process Intensification,* vol. 47, pp. 508-513, 2008.

[74] D. Świerczyński, S. Libs, C. Courson, and A. Kiennemann, "Steam reforming of tar from a biomass gasification process over Ni/olivine catalyst using toluene as a model compound," *Applied Catalysis B: Environmental,* vol. 74, pp. 211-222, 2007.

[75] M. Virginie, C. Courson, and A. Kiennemann, "Toluene steam reforming as tar model molecule produced during biomass gasification with an iron/olivine catalyst," *Comptes Rendus Chimie,* vol. 13, pp. 1319-1325, 2010.

[76] L. Devi, K. J. Ptasinski, and F. J. Janssen, "Pretreated olivine as tar removal catalyst for biomass gasifiers: investigation using naphthalene as model biomass tar," *Fuel Processing Technology,* vol. 86, pp. 707-730, 2005.

[77] H. Noichi, A. Uddin, and E. Sasaoka, "Steam reforming of naphthalene as model biomass tar over iron–aluminum and iron–zirconium oxide catalyst catalysts," *Fuel Processing Technology,* vol. 91, pp. 1609-1616, 2010.

[78] B. Zhao, X. Zhang, L. Chen, R. Qu, G. Meng, X. Yi, and L. Sun, "Steam reforming of toluene as model compound of biomass pyrolysis tar for hydrogen," *Biomass and Bioenergy,* vol. 34, pp. 140-144, 2010.

[79] H. Zhou, C. Wu, J. A. Onwudili, A. Meng, Y. Zhang, and P. T. Williams, "Polycyclic aromatic hydrocarbons (PAH) formation from the pyrolysis of different municipal solid waste fractions," *Waste Management,* vol. 36, pp. 136-146, 2015.

[80] M. Zhai, X. Wang, Y. Zhang, P. Dong, G. Qi, and Y. Huang, "Characteristics of rice husk tar secondary thermal cracking," *Energy,* vol. 93, pp. 1321-1327, 2015.

[81] H. Yu, Z. Zhang, Z. Li, and D. Chen, "Characteristics of tar formation during cellulose, hemicellulose and lignin gasification," *Fuel,* vol. 118, pp. 250-256, 2014.

[82] C. Font Palma, "Model for biomass gasification including tar formation and evolution," *Energy & Fuels,* vol. 27, pp. 2693-2702, 2013.

[83] S. Anis and Z. A. Zainal, "Tar reduction in biomass producer gas via mechanical, catalytic and thermal methods: A review," *Renewable and Sustainable Energy Reviews,* vol. 15, pp. 2355-2377, 2011.

[84] C. Li and K. Suzuki, "Tar property, analysis, reforming mechanism and model for biomass gasification—An overview," *Renewable and Sustainable Energy Reviews,* vol. 13, pp. 594-604, 2009.

[85] A. Jess, "Mechanisms and kinetics of thermal reactions of aromatic hydrocarbons from pyrolysis of solid fuels," *Fuel,* vol. 75, pp. 1441-1448, 1996.

[86] A. Fourcault, F. Marias, and U. Michon, "Modelling of thermal removal of tars in a high temperature stage fed by a plasma torch," *Biomass and Bioenergy,* vol. 34, pp. 1363-1374, 2010.

[87] R. K. Sharma and M. R. Hajaligol, "Effect of pyrolysis conditions on the formation of polycyclic aromatic hydrocarbons (PAHs) from polyphenolic compounds," *Journal of Analytical and Applied Pyrolysis*, vol. 66, pp. 123-144, 2003.

[88] R. Bayard, L. Barna, B. Mahjoub, and R. Gourdon, "Influence of the presence of PAHs and coal tar on naphthalene sorption in soils," *Journal of Contaminant Hydrology*, vol. 46, pp. 61-80, 2000.

[89] B. Shukla and M. Koshi, "A novel route for PAH growth in HACA based mechanisms," *Combustion and Flame*, vol. 159, pp. 3589-3596, 2012.

[90] B. Vreugdenhil, R. Zwart, and J. P. A. Neeft, "Tar formation in pyrolysis and gasification," Energy research Centre of the Netherlands (ECN) Report, The Netherlands, ECN-E--08-087, 2009.

[91] J. Han and H. Kim, "The reduction and control technology of tar during biomass gasification/pyrolysis: An overview," *Renewable and Sustainable Energy Reviews*, vol. 12, pp. 397-416, 2008.

[92] S. Nakamura, S. Kitano, and K. Yoshikawa, "Biomass gasification process with the tar removal technologies utilizing bio-oil scrubber and char bed," *Applied Energy*, vol. 170, pp. 186-192, 2016.

[93] L. Fagbemi, L. Khezami, and R. Capart, "Pyrolysis products from different biomasses: application to the thermal cracking of tar," *Applied Energy*, vol. 69, pp. 293-306, 2001.

[94] Y. Shen and K. Yoshikawa, "Recent progresses in catalytic tar elimination during biomass gasification or pyrolysis—A review," *Renewable and Sustainable Energy Reviews*, vol. 21, pp. 371-392, 2013.

[95] J. J. Hernández, R. Ballesteros, and G. Aranda, "Characterisation of tars from biomass gasification: Effect of the operating conditions," *Energy*, vol. 50, pp. 333-342, 2013.

[96] D. Fuentes-Cano, A. Gómez-Barea, S. Nilsson, and P. Ollero, "Decomposition kinetics of model tar compounds over chars with different internal structure to model hot tar removal in biomass gasification," *Chemical Engineering Journal*, vol. 228, pp. 1223-1233, 2013.

[97] D. A. Constantinou, J. L. G. Fierro, and A. M. Efstathiou, "A comparative study of the steam reforming of phenol towards H2 production over natural

calcite, dolomite and olivine materials," *Applied Catalysis B: Environmental,* vol. 95, pp. 255-269, 2010.

[98] F. Kirnbauer, V. Wilk, H. Kitzler, S. Kern, and H. Hofbauer, "The positive effects of bed material coating on tar reduction in a dual fluidized bed gasifier," *Fuel,* vol. 95, pp. 553-562, 2012.

[99] W. L. Saw and S. Pang, "The influence of calcite loading on producer gas composition and tar concentration of radiata pine pellets in a dual fluidised bed steam gasifier," *Fuel,* vol. 102, pp. 445-452, 2012.

[100] C. Berrueco, D. Montané, B. M. Güell, and G. del Alamo, "Effect of temperature and dolomite on tar formation during gasification of torrefied biomass in a pressurized fluidized bed," *Energy,* vol. 66, pp. 849-859, 2014.

[101] N. Alarcón, X. García, M. A. Centeno, P. Ruiz, and A. Gordon, "New effects during steam gasification of naphthalene: the synergy between CaO and MgO during the catalytic reaction," *Applied Catalysis A: General,* vol. 267, pp. 251-265, 2004.

[102] C. Christodoulou, D. Grimekis, K. D. Panopoulos, E. P. Pachatouridou, E. F. Iliopoulou, and E. Kakaras, "Comparing calcined and un-treated olivine as bed materials for tar reduction in fluidized bed gasification," *Fuel Processing Technology,* vol. 124, pp. 275-285, 2014.

[103] S. Koppatz, C. Pfeifer, and H. Hofbauer, "Comparison of the performance behaviour of silica sand and olivine in a dual fluidised bed reactor system for steam gasification of biomass at pilot plant scale," *Chemical Engineering Journal,* vol. 175, pp. 468-483, 2011.

[104] M. Virginie, J. Adánez, C. Courson, L. F. de Diego, F. García-Labiano, D. Niznansky, A. Kiennemann, P. Gayán, and A. Abad, "Effect of Fe–olivine on the tar content during biomass gasification in a dual fluidized bed," *Applied Catalysis B: Environmental,* vol. 121, pp. 214-222, 2012.

[105] M. Naqvi, J. Yan, M. Danish, U. Farooq, and S. Lu, "An experimental study on hydrogen enriched gas with reduced tar formation using pre-treated olivine in dual bed steam gasification of mixed biomass compost," *International Journal of Hydrogen Energy,* vol. 41, pp. 10608-10618, 2016.

[106] Y. Tursun, S. Xu, G. Wang, C. Wang, and Y. Xiao, "Tar formation during co-gasification of biomass and coal under different gasification condition," *Journal of Analytical and Applied Pyrolysis,* vol. 111, pp. 191-199, 2015.

[107] T. Phuphuakrat, T. Namioka, and K. Yoshikawa, "Absorptive removal of biomass tar using water and oily materials," *Bioresource Technology*, vol. 102, pp. 543-549, 2011.

[108] H. Boerrigter, S. Van Paasen, P. Bergman, J. Könemann, R. Emmen, and A. Wijnands, "OLGA tar removal technology," Energy research Centre of the Netherlands (ECN), ECN-C--05-009, 2005.

[109] P. C. Bergman, S. V. van Paasen, and H. Boerrigter, "The novel “OLGA” technology for complete tar removal from biomass producer gas," in *Pyrolysis and gasification of biomass and waste*, 2002.

[110] M. Kuba, F. Havlik, F. Kirnbauer, and H. Hofbauer, "Influence of bed material coatings on the water-gas-shift reaction and steam reforming of toluene as tar model compound of biomass gasification," *Biomass and Bioenergy*, vol. 89, pp. 40-49, 2016.

[111] G. Taralas, M. G. Kontominas, and X. Kakatsios, "Modeling the thermal destruction of toluene (C7H8) as tar-related species for fuel gas cleanup," *Energy & Fuels*, vol. 17, pp. 329-337, 2003.

[112] F. Kirnbauer, V. Wilk, and H. Hofbauer, "Performance improvement of dual fluidized bed gasifiers by temperature reduction: The behavior of tar species in the product gas," *Fuel*, vol. 108, pp. 534-542, 2013.

[113] J. C. Schmid, U. Wolfesberger, S. Koppatz, C. Pfeifer, and H. Hofbauer, "Variation of feedstock in a dual fluidized bed steam gasifier—influence on product gas, tar content, and composition," *Environmental Progress & Sustainable Energy*, vol. 31, pp. 205-215, 2012.

Chapter 3. Experiment Setup and Methodology

In this chapter, a 100kw dual fluidised bed (DFB) gasifier for steam gasification which was used in this PhD project is described. Methods of gas sampling and tar sampling from this gasifier system and analysis techniques are introduced.

3.1. Introduction

A 100kW dual fluidised bed (DFB) steam gasifier as shown in Fig. 3-1 has been constructed at the University of Canterbury (UoC) [1, 2], and experiments have been conducted by the Bioenergy Research Team in the Department of Chemical and Process Engineering (CAPE) [3-7]. This gasifier consists of a bubbling fluidised bed (BFB) column and a fast fluidised bed (FFB) column. BFB column is the gasification reactor and has an internal diameter of 0.2 m with a height of 2 m. FFB column, which is the combustion reactor has an inner diameter of 0.1 m and length of 3.7 m.

Fig. 3-1. 100kW dual fluidised bed gasifier in CAPE, UoC.

As steam gasification is an endothermic process, heat is provided by circulating bed material which is heated in the FFB column by combustion of chars generated from the biomass gasification in the BFB column [5].

Fig. 3-2 presents the schematic diagram of the 100kW DFB steam gasifier used in the present study. During the gasification experiments, solid fuels (biomass) are fed via a screw auger from the fuel hopper into the BFB bed, approximately 0.13 m above the BFB base. 5 L/min of N_2 as a purge gas is introduced into the fuel hopper to prevent the undesired back flow of the producer gas from BFB into the feeder throughout the experiment, which is corresponded to 1%-2% of the producer gas yield [4].

Steam as the gasification agent and the fluidising agent is injected from the BFB bottom at 350°C and 6 bars (gauge) which is supplied by a boiler and super-heated by the tracing heating elements. Producer gas generated from the steam gasification flows out of BFB column at the top of the column. As some fine particles of char, ash and fine bed materials entrained are entrained in the producer gas; the producer gas flows to the BFB cyclone for separation of these particles [6].

In the BFB column, the solid char generated from the gasification process moves together with the bed material from the BFB column bottom to the FFB column through an inclined chute. In the FFB column, air is introduced from the FFB bottom for char combustion to heat up the bed material. The air to the FFB column is supplied by a 50 HP roots blower and a compressor. The primary air is injected at the base of the FFB and is also used to fluidise the solid material for it to be in good contact with secondary combustion air, which is introduced 0.2 m above the primary air nozzles. In initial heating start-up stages and in most of the gasification experiments supplementary liquefied petroleum gas (LPG) is introduced into the FFB reactor to achieve required gasification temperature, contributing heat of equivalent to 40-50kW [3].

The heated bed material in FFB column is carried upwards by the flue gas and, eventually, the flue gas and the bed materials flow out of the FFB column into the FFB cyclone, where the bed material is separated from the flue gas. Finally, the hot bed material is delivered back to the BFB through a siphon to provide heat for the endothermic gasification reactions. The flue gas flows out of the FFB cyclone and then

through a heat exchanger for heating up of the steam for gasification and air for combustion, it can increase the overall efficiency of DFB gasifier by heat recovery.

Both the chute and the siphon are fluidised with the superheated steam to enhance the bed material flow and to prevent cross-flows of gases between the two reactors.

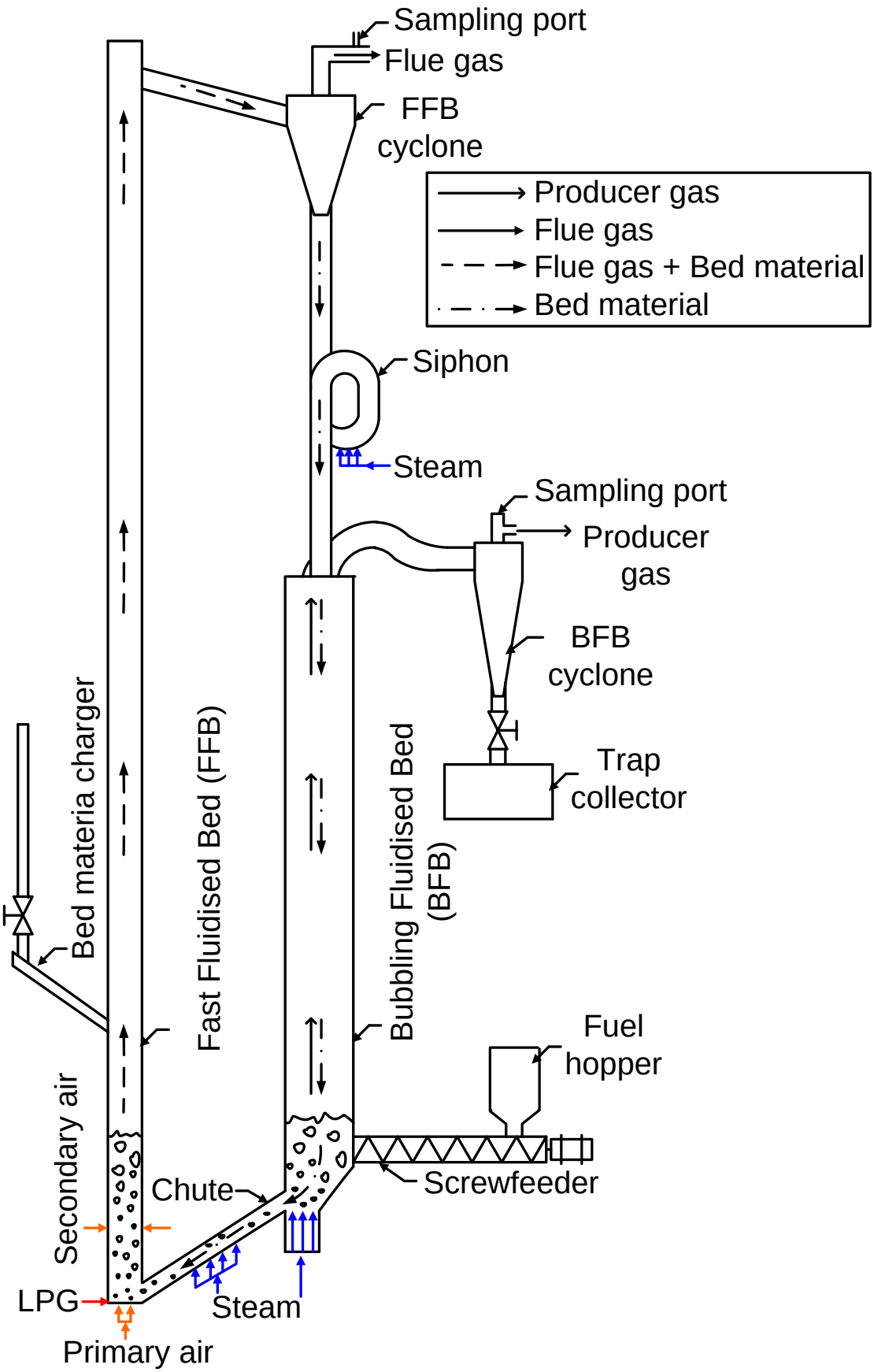

Fig. 3-2. Schematic drawing of the operation of DFB steam gasifier in CAPE [4].

3.2. Operation and parameter setup

3.2.1. Operating procedure

Before each experimental run, the entire gasifier system was cleaned to ensure that there were no blockages in pipes and in the two reactors. Both the BFB base and the FFB base were removed, and any remaining bed material from the previous run was removed and weighed to check the bed material loss in the previous experiment. In addition, chars left in the bed material were separated if the bed material was to be re-used. Connection tubes for pressure sensors were flushed with compressed air to ensure that they were not blocked with foreign material.

If a different type of solid fuel was used, any residual solid fuel in the fuel hopper was removed. The variable speed drive on the feed-hopper auger was calibrated to determine the speed at a specified mass flow rate of the solid feeding fuel. This calibration was done by running the auger at four different speeds for five minutes and measuring the weight of the solid fuel collected at the bottom of the BFB column. The calibration of feeding rate for testing biomass species is shown in Appendix A. The mass flow rate was changed if the steam to biomass ratio was varied during gasification as the steam feeding ratio was fixed.

At the start of the each run, approximately 10 kg of bed material was introduced to the FFB column. Then both columns were heated up by combustion of LPG with air in the FFB column with a circulation of heated bed material. Air as a fluidisation agent was injected, respectively, to the bottom of BFB column, to the chute and to the siphon for the promotion of the bed material circulation between the FFB and BFB columns. After the target temperatures in both columns had been reached, additional 20 kg of bed material was added to the FFB column through the bed material charger. Once the temperature was stabilized, the air supply to the BFB, the chute and the siphon was gradually changed over to steam. The steam feeding rates to these three locations were set at 7.0, 2.0 and 1.5 kg/h, respectively, and these flow rates were maintained constant during the experiments. Steam is supplied by a separated diesel boiler and super-heated by the tracing heating elements to maintain at 350°C and 6 bars (gauge). The screw feeder of the solid fuel was turned on for steam biomass gasification. The feeding rate of solid fuel was varied depending on the pre-set steam to biomass (S/B) ratio and the

moisture content in the fuel. The S/B ratio in the present study for steam was calculated according to Eq. (3-1) in which the steam includes both the fed steam into the system and the water in the fed solid fuel.

$$\mathrm{S/B} = \frac{\dot{m}_{steam} + \dot{m}_{moisture\ in\ biomass}}{\dot{m}_{dry\ biomass}} \quad (3\text{-}1)$$

In the experiments, the flow rate of supplementary LPG supplied to the FFB was adjustable to achieve the required temperature in the BFB column during the gasification. The test conditions were kept constant for 30 minutes to reach a steady state. Then, producer gas samples were taken and analysed during the gasification experiments which details will be present later in this chapter.

When the experiments were completed, the screw feeder of the solid fuel was turned off, while the supplementary LPG to the FFB was also shut down. While the BFB and the FFB columns were cooling down, the steam supply to the BFB, the chute and the siphon, as well as the air supply to the FFB, was gradually turned off. When the temperatures within the two columns were below 600 °C, the DFB gasifier system was allowed to cool down naturally. The full checklist of experiment procedure is shown in Appendix B.

3.2.2. Fluidisation calculations

As described early in Chapter 2, in BFB column, the gas flow rate is selected above the minimum fluidisation velocity but less than the terminal velocity to ensure that the solid fuel and bed material maintain bubbling fluidisation. The gas flow rate must be carefully selected so that the fine solid particles of ash, char and bed material are entrained and carried out of the BFB column by the producer gas. In the FFB column, the gas flow rate should be above the terminal velocity so that bed materials are carried up to the top of the FFB column and then to the FFB cyclone.

Based on the flow regimes and gasifier configuration, the minimum fluidisation velocity and terminal velocity in the both BFB and FFB columns have been calculated as follows [8, 9]:

(a) Terminal velocity, U_t

For a spherical particle of diameter d_p, the terminal velocity (m/s) is calculated by

$$U_t = \sqrt{\frac{4 \times g \times d_p \times (\rho_p - \rho_f)}{3 \times \rho_f \times C_D}} \quad (3\text{-}2)$$

Where

g is the gravity constant with a value of 9.81 m/s^2;

d_p is the diameter of particle, m;

ρ_p is density of particle, kg/m^3;

ρ_f is density of fluid, kg/m^3;

C_D is drag coefficient

To obtain the drag coefficient in Eq (3-2), the Reynolds number is required

$$Re_p = \frac{d_p \times \rho_f \times u}{\mu} \quad (3\text{-}3)$$

Where

u is superficial velocity (m/s), which is gas flow rate (m^3/s) is divided by the cross sectional area of column (m^2);

μ is viscosity of fluid, Pa·s,

Base on the Reynolds number, the drag coefficient is calculated by the following equations from Kunii and Levenspiel [10]

$$C_D = \frac{24}{Re_p} \qquad Re_p < 0.1 \quad (3\text{-}4)$$

$$C_D = \left(\frac{24}{Re_p}\right)\left(1 + 0.14 \times Re_p^{0.7}\right) \qquad 0.1 < Re_p < 1000 \quad (3\text{-}5)$$

(b) Minimum fluidisation velocity, U_{mf}

For a spherical particle of diameter d_p, the minimum fluidisation velocity (m/s) is calculated by

$$U_{mf} = \frac{\mu \times \left[\left(27.2^2 + 0.0408 \times Ar\right)^{0.5} - 27.2\right]}{\rho_f \times d_p} \quad (3\text{-}6)$$

Where

Ar is Archimedes number

The Archimedes number is calculated by:

$$Ar = \frac{g \times d_p^3 \times \rho_f \times (\rho_p - \rho_f)}{\mu^2} \quad (3\text{-}7)$$

Fig. 3-3 adapted from Kunii and Levenspiel [10] presents a fluidisation regime map of a particular gas-solid system. In the figure, it can be seen four type of fluidisation behaviour by referring to the Geldart classification [11], they are cohesive (C), aeratable (A), sand-like (B), and spoutable (D). The curves of the minimum fluidisation velocity and terminal velocity are calculated through Eqs (3-1) to (3-7). Fig. 3-3 also point out the regimes of BFB and FFB for stable operation by dash line and dash-dot line, respectively. The boundaries of regimes depend on the dimensionless gas velocity, u^* (m/s) and dimensionless particle, d_p^* (m), which can be determined by Eqs. (3-8) and (3-9), respectively.

$$u^* = u \left[\frac{\rho_f^2}{\mu(\rho_p - \rho_f)g}\right]^{1/3} \quad (3\text{-}8)$$

$$\mathrm{d}_p^* = d_p \left[\frac{\rho_f(\rho_p - \rho_f)g}{\mu^2}\right]^{1/3} \quad (3\text{-}9)$$

Fig. 3-3 can be used to identify the operating parameters of bed materials in BFB and FFB columns. The fluidisation behaviours (dimensionless gas velocity and dimensionless particle) of silica sand as the bed material has been calculated at the practical conditions. The air flow at the temperature of 800°C in the BFB column and FFB column are given as an example. Three different particle sizes of 100, 300 and 900 μm have been chosen for calculation, which represents the practical range of particle sizes of bed material. The calculated results are shown in Fig. 3-3 in which the rectangular dots and solid circle dots represents the fluidisation behaviours of silica

sand in BFB column and FFB column, respectively. Bed materials with a smaller particle size can be easily carried out from BFB column, while bed materials with larger particle sizes are difficult to be lifted up in the FFB column. The diagram in Fig. 3-3 also shows that the small particles of chars and ash and broken bed materials can be carried out from the BBF column when appropriate gas velocity is chosen (above their ultimate velocity).

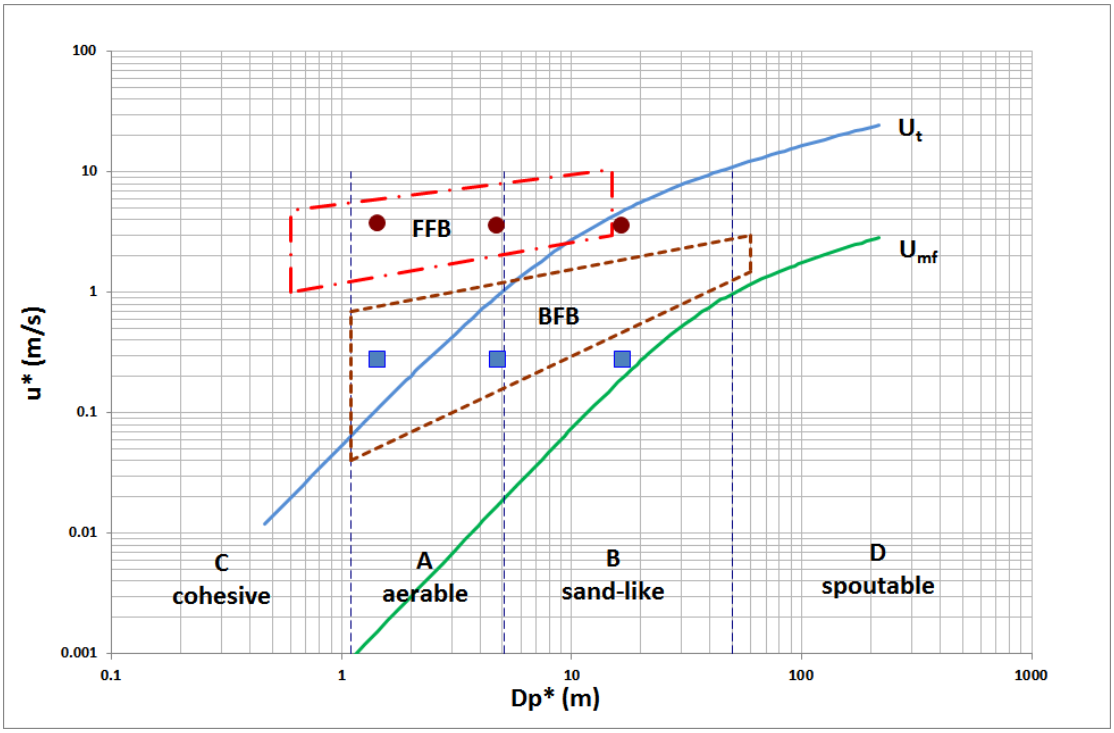

Fig. 3-3. Fluidisation mapping for Silica sand. Adapted from Kunii and Levenspiel [10].

3.3. Sampling and analysis of product gas and tar

3.3.1. Producer gas sampling and analysis

During the gasification runs, producer gas samples were taken using a specially designed device from the sampling port at the top of the BFB column. Tar samples in the producer gas were also extracted from the gas sampling port in two 50-mL aliquots through a 3 mL Supelclean LC-NH_2 solid phase extraction (SPE) column. During the sampling, the tar components in the producer gas were condensed and adsorbed on the silica gel base matrix in the SPE column for later extraction and analysis. This producer gas and tar sampling device were developed by Bull [1] as shown in Fig. 3-4.

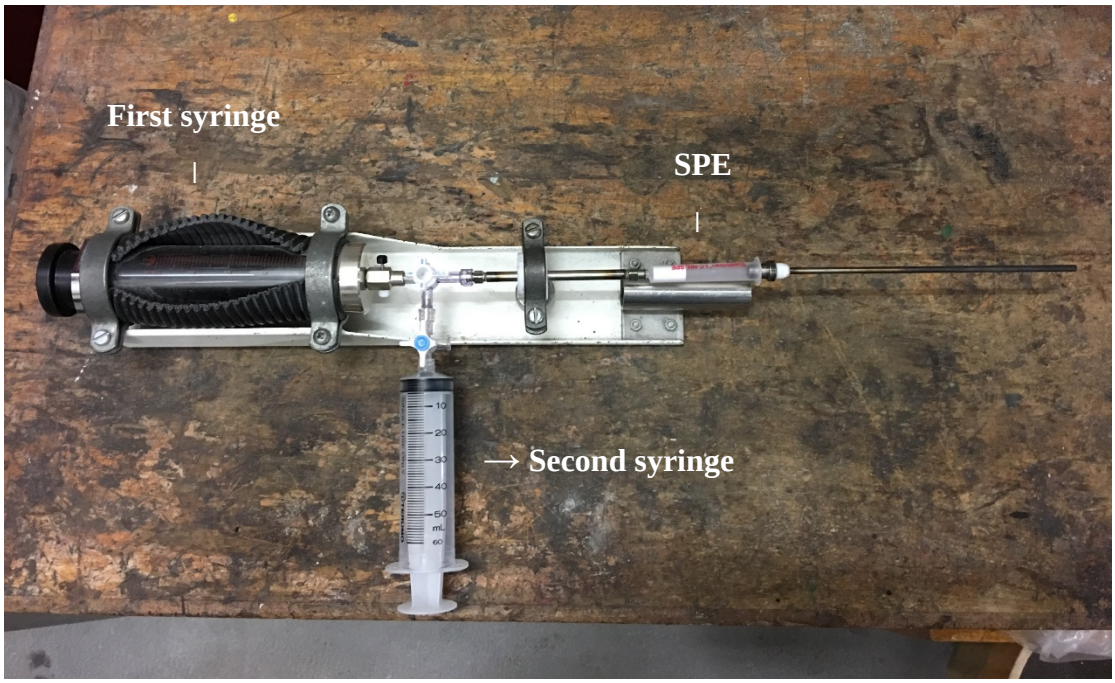

Fig. 3-4. Gas and tar sampling device.

Each SPE column was pre-conditioned with 2 mL dichloromethane (DCM) before use to remove contaminants. The first 50-mL aliquot was extracted from the sampling line using a plastic sample syringe to flush out the air trapped in the syringe, then expelled. The second 50-mL aliquot was extracted in the same way and stored in the sample syringe, which was then sealed, removed from the sampling system and transported to an Agilent 3000 micro gas chromatography (GC) with a thermal conductivity detector (TCD) for producer gas analysis. H_2, CO, CH_4 and N_2 were analysed with a 10 m × 0.32 mm molecular sieve 5A Polt column with Ar as the carrier gas, while CO_2, C_2H_4 and C_2H_6 were analysed by an 8m × 0.32 mm Plot Q column with He as the carrier gas.

3.3.2. tar extraction and analysis

The tar extraction method was adopted from the study of Brage et al. [12]. In a similar way to gas sampling, tar adsorbed in the SPE column was extracted using a 0.1 mL of 400 ppm n-dodecane as an internal standard and eluted with 0.9 mL DCM into a 2 mL vial to obtain aromatic and PAH components. The same SPE column was then eluted again with 0.1 mL of 400 ppm n-dodecane and 0.9 mL mixture of DCM and isopropanol (IPA) (1:1 v/v) to obtain the phenolic portion of the tar into a separate 2 mL vial.

A Varian CP-3800 GC with a flame ionization detector (GC-FID) was used for the tar analysis, in which the tar samples were separated in a 50% phenyl and 50% dimethylpolysiloxane fused silica capillary column. The tar analysis methods were developed by Saw and Pang [6] and used in the present study to analyse determine the different tar species and their concentrations. The tar compound identification and classification used in the present study are shown in Table 3-1 following the work of Kiel et al. [13]. Class 1 tar compounds, which are non-detectable by GC-FID, are not included in this study as they condense at high temperature.

In the tar analysis, the temperature of the injector and the FID was set at 300 °C. The flow rate of the carrier gas, helium, was set at 1 mL/min. Each tar sample of 1 μL was injected into the injector with an auto-sampler. To provide a good separation of the analytes, the column temperature was controlled with the following programme:

(i) 50 °C hold for 1 min,
(ii) 50 to 180 °C with a heating-up rate of 4 °C/min,
(iii) 180 to 245 °C with a heating-up rate of 2.5 °C/min,
(iv) 245 to 270 °C with a heating-up rate of 2 °C/min, and then hold at 270 °C for 10 min,
(v) 270 to 350 °C with a heating-up rate of 8 °C/min and then hold at 350 °C for 5 min.

Before the tar analysis, an IS calibration was conducted with the same column conditions as described above to obtain the response factor for each tar standard relative to the IS of 40 ppm. The Five different concentrations were prepared and analysed, and each concentration was measured three times. Fig. 3-5 shows the peaks of each tar species in 50 ppm tar standard solution with 40 ppm IS. The retention time of each tar species is listed in Table 3-1 following the tar classification system proposed by Kiel et al. [13]. The detailed operation, sample preparation and sample analysis are recorded in Appendix C.

It is noticeable that tar composition, as discussed in Chapter 2.3, strongly depends on the operating conditions of the process where they are produced. Although the tar

mixture in the gas contains a fraction of GC-undetectable tar compounds, such as primary heteroatomic tar compounds, which would condense at ambient temperature. The most of tar compounds produced at temperature between 700 and 1000ºC is aromatic hydrocarbon. Therefore, in this study, at the testing conditions, the impact of GC-undetectable tar is insignificant due to the low concentrations and thus, Class 1 tar compounds are ignored.

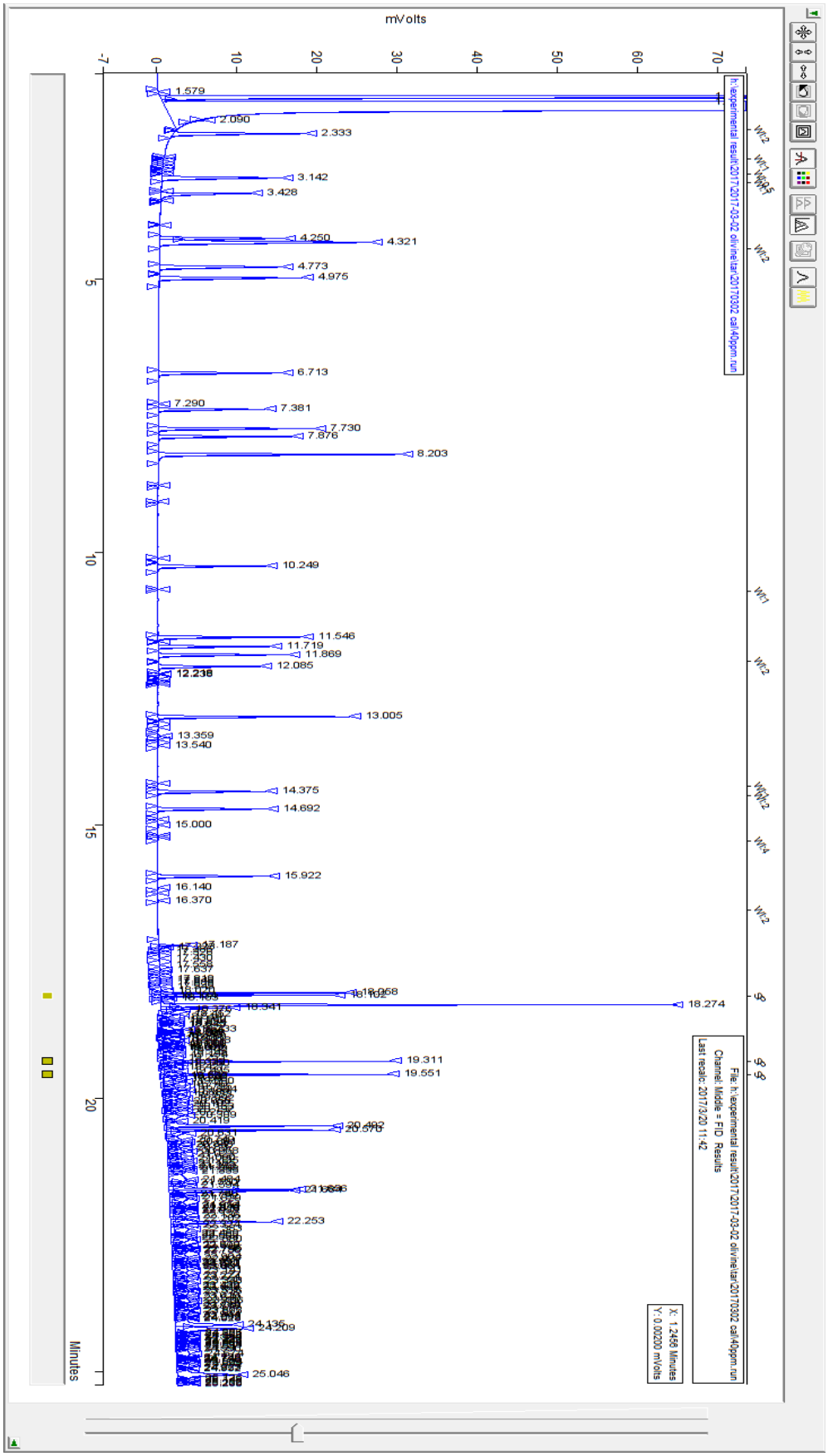

Fig. 3-5. GC results of 40 ppm standard tar sample with 40 ppm IS.

Table 3-1. The classification of tar compounds detected in the present study according to Kiel et al. [13].

Tar class	Class name	Compounds	Retention time (seconds)
Class 1 (C1)	GC-undetectable	Very heavy tar compounds, cannot be detected by GC	
Class 2 (C2)	Heterocyclic	Pyridine	3.44
		Phenol	6.71
		o-cresol	7.87
		m+p-cresol	8.19
		Quinoline	11.54
		Isoquinoline	11.87
Class 3 (C3)	Light aromatic (1 ring)	Toluene	3.14
		p-xylene + Ethylbenzene	4.25
		m-xylene	4.32
		o-xylene	4.77
		Styrene	4.97
Class 4 (C4)	Light PAH compounds (2-3 rings)	Indene	7.73
		Naphthalene	10.25
		2-Methylnaphthalene	11.72
		1-Methylnaphthalene	12.08
		Biphenyl	13.00
		Acenaphthylene	14.37
		Acenaphthene	14.69
		Fluorene	15.92

		Phenanthrene	18.06
		Anthracene	18.10
Class 5 (C5)	Heavy PAH compounds (4-7 rings)	Fluoranthene	19.32
		Pyrene	19.56
		Bens(a)anthracene	20.50
		Chrysene	20.58
		Benzo(b)fluoranthene	21.67
		Benzo(k)fluoranthene	21.70
		Benzo(a)Pyrene	22.26
		Indeno(1,2,3-cd)pyrene	24.15
		Benzo(g,h,i)perylene	24.22
		Dibenzo(a,h)anthracene	25.06

3.4. Analysis of experimental errors

The accuracies of gas and tar measurements are critical for this study. These measurements are determined by many operating parameters (temperature, flow rate of steam, analytic instruments and so on), so that the deviations and fluctuation of the measurements are difficult to avoid. In order to minimise this impact, the results presented in this study are an average value of, at least, three different measurements conducted in the same operating conditions is applied. The uncertainty of measurements are defined by from Eq. (3-10) to Eq. (3-12) [14]:

- Mean = $\frac{\sum_{i=1}^{i=n} x_n}{n}$, where n is the number of measurements made (3-10)
- deviation = $\frac{\sum_{i=1}^{i=n} |x_n - mean|}{n}$ (3-11)
- Error percentage = $\frac{Deviation}{Mean} \times 100\%$ (3-12)

In addition, the error propagation from gasifier system, sampling and analytic instruments on the gas and tar production is also unavoidable, a certain margin of error on the gas and tar production should be allowed. The limitation of error margin has been stated in Table 3.5, which is calculated by the Eq. (3-13) [14]. If the error percentage of measurement in a trial exceeds the limitation, then this trial is rejected.

$$\text{Error propagation} = \sqrt{(a^2 + b^2 + c^2 + \cdots + n^2)} \quad (3\text{-}13)$$

, where a, b, c, n represents error percent of individual item.

Table 3-2. Limitation of error margin for gas measurement and tar measurement

Gas production		
Items	Measurement	Error percentage
1. Bed material inventory	30 ± 0.1kg	0.3%
2. BFB temperature	700 ± 5°C	0.7%
3. Biomass feeding rate	16 ± 0.5 kg/h	3.1%
4. Steam feeding rate	10.5 ± 0.3 kg/h	2.9%
5. Helium flowrate	5 ± 0.1 l/min	2.0%
6. Micro-GC analysis		1.0%
Total uncertainty for gas production		4.9%
Tar production		
Items	Measurement	Error percentage
1. Gas production		4.9%
2. Pipette injection	20 ± 0.01µl	0.2%
3. Vial weight	2.345 ± 0.001g	0.1%
4. Tar extraction		2.0%
5. Syringe sampling	50 ± 2 ml	4.0%
6. GC analysis		1.0%
Total uncertainty for tar production		6.8%

Note: The 100kW DFB gasifier plant have been repaired and modified in 2015 due to the Christchurch Earthquake, but the experimental results before and after the system

modification, which were preform at the same operating conditions, were within the error margin, as shown in Table 3-3.

Table 3-3. Comparison the experimental data before and after the gasifier modification

Gas composition	Experiment in 2013	Experiment in 2016	Error
H2 %	29.9	30.7	1.3%
CO %	36.6	36.3	0.4%
CO2 %	18.0	16.7	3.7%
CH4 %	12.9	12.1	3.2%

3.5. Reference

[1] D. R. Bull, "Performance Improvements to a Fast Internally Circulating Fluidised Bed (FICFB) Biomass Gasifier for Combined Heat and Power Plants," in *Department of Chemical and Process Engineering*: University of Canterbury, 2008.

[2] J. Rutherford, "Heat and power applications of advanced biomass gasifiers in New Zealand's wood industry : a chemical equilibrium model and economic feasibility assessment " in *Department of Chemical and Process Engineering*: University of Canterbury, 2006.

[3] W. Saw, H. McKinnon, I. Gilmour, and S. Pang, "Production of hydrogen-rich syngas from steam gasification of blend of biosolids and wood using a dual fluidised bed gasifier," *Fuel*, vol. 93, pp. 473-478, 2012.

[4] W. L. Saw and S. Pang, "The influence of calcite loading on producer gas composition and tar concentration of radiata pine pellets in a dual fluidised bed steam gasifier," *Fuel*, vol. 102, pp. 445-452, 2012.

[5] W. L. Saw and S. Pang, "Influence of mean gas residence time in the bubbling fluidised bed on the performance of a 100-kW dual fluidised bed steam gasifier," *Biomass Conversion and Biorefinery*, vol. 2, pp. 197-205, 2012.

[6] W. L. Saw and S. Pang, "Co-gasification of blended lignite and wood pellets in a 100kW dual fluidised bed steam gasifier: The influence of lignite ratio on producer gas composition and tar content," *Fuel*, vol. 112, pp. 117-124, 2013.

[7] Z. Zhang and S. Pang, "Experimental investigation of biomass devolatilization in steam gasification in a dual fluidised bed gasifier," *Fuel*, vol. 188, pp. 628-635, 2017.

[8] J. Rezaiyan and N. P. Cheremisinoff, *Gasification technologies : a primer for engineers and scientists*. Boca Raton: Taylor & Francis, 2005.

[9] M. L. d. Souza-Santos, *Solid fuels combustion and gasification : modeling, simulation, and equipment operations*, 2nd ed. Boca Raton: Taylor & Francis, 2010.

[10] D. Kunii and O. Levenspiel, *Fluidization Engineering*, Second Edition ed. Boston: Butterworth-Heinemann, 1991.

[11] D. Geldart, *Gas Fluidization Technology*. Chichester, United Kingdom: John Wiley and Sons Ltd, 1986.

[12] C. Brage, Q. Yu, G. Chen, and K. Sjöström, "Use of amino phase adsorbent for biomass tar sampling and separation," *Fuel*, vol. 76, pp. 137-142, 1997.

[13] J. Kiel, S. Van Paasen, J. Neeft, L. Devi, K. Ptasinski, F. Janssen, R. Meijer, R. Berends, H. Temmink, and G. Brem, "Primary measures to reduce tar formation in fluidised-bed biomass gasifiers," Energy research Centre of the Netherlands (ECN) Report, The Netherlands, ECN-C-04-014, 2004.

[14] J. R. Taylor, *An Introduction to Error Analysis: The Study of Uncertainties in Physical Measurements*: University Science Books, 1997.

Chapter 4. Experimental investigation on tar formation from initial devolatilization to final gasification process

This Chapter is based on a journal paper published in 'Fuel 188 (2017) 628-635'. In this chapter, biomass devolatilization, which is the initial stage of steam gasification stage, was experimentally investigated in a 100kW dual fluidised bed gasifier. In the experiments, pellets of radiata pine wood were used as the feedstock, and silica sand was used as the bed material. The operation temperature was varied from 700 to 800°C, and the bed material inventory was 30kg. N_2 was used as the fluidisation agent. The concentration of each gas component (H_2, CO_2, CO and CH_4) and each tar class in the product gas was measured. The experimental results show that, in the devolatilization, gas yield was increased and tar yield and concentration was decreased with an increase in the operation temperature. Significant correlation was also observed on between the gas composition from the devolatilization stage and the final gasification producer gas. Correlations on tar concentrations and tar classes were also found for gases produced from the devolatilization and the subsequent gasification. The results provide important insight for understanding the mechanism of steam gasification and will guide future improvements to the biomass gasification process.

4.1. Introduction

Steam gasification is a promising process which converts biomass to a hydrogen-rich producer gas with a high calorie value [1-4]. The producer gas can be used for production of heat and electricity or for synthesis of liquid fuel through the Fischer-Tropsch synthesis process [5]. As shown in Fig. 4-1, the steam gasification process can be divided into two stages: 1) biomass devolatilization; 2) gasification reactions [6]. Before the biomass devolatilization, drying may occur when the temperature reaches to 200-300°C if the biomass moisture content is high. With further increase in the temperature to 300-500°C, biomass devolatilization occurs, and the biomass is decomposed into gases, char and tar [7] . In the subsequent gasification process, homogeneous reaction (among gases and steam) and heterogeneous reactions (among char and gases as well as steam) occur simultaneously. The reaction formulae have been given in Table 2-5 from Chapter 2.

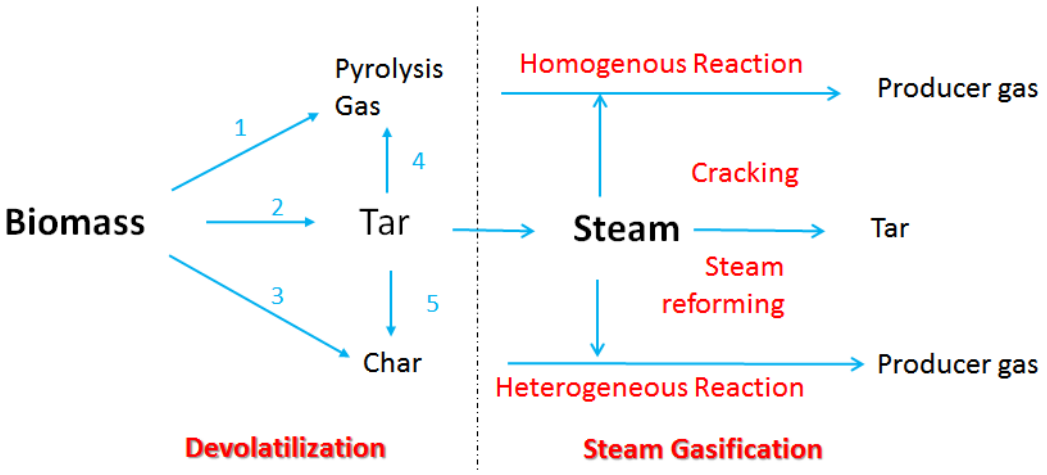

Fig. 4-1. Proposed mechanism from devolatilization to steam gasification.

By examining the above reactions, it is observed that in steam char reaction, water-gas shift reaction and steam reforming reaction, steam is involved as a reactant; therefore, the steam supply as a gasification agent is important. It is also observed that the gaseous products from the initial devolatilization act as the reactants in reactions described by Eqs. (2-4) to (2-7) whereas char is the reactant in reactions of Eqs. (2-2) to (2-5). Therefore, the product yields and gas composition from the initial devolatilization have significant impacts on the yield and composition of the producer gas from the whole gasification process although the steam-char reaction is believed to be dominant in the subsequent gasification process [8-13]. By knowing the correlation between the product yields and composition from the initial devolatilization and the yield and composition of the producer gas from the whole gasification process, the gasification operations (such as temperature, bed material and S/B ratio) can be optimised.

Furthermore, the determination of tar production from devolatilization is also essential, since during the devolatilization, tar compounds may reform, further react by cracking, dealkylation, deoxygenation, aromatisation and polymerisation to form light gas, soot and poly aromatic hydrocarbons [14]. In addition, the steam input and gasification operation conditions also have impacts on the final tar formation and cracking as described in the following reactions [15, 16].

Steam-tar reforming $C_mH_n + mH_2O \leftrightarrow mCO + (m + \frac{n}{2})H_2$ (4-1)

Thermal tar cracking $pC_mH_n \leftrightarrow qC_xH_y + rH_2$ (4-2)

Where C_mH_n represents tar which can be a mixture of several high molecular weight compounds in the tar compound and C_xH_y represents hydrocarbons in the tar compounds with smaller carbon number than C_mH_n.

Previous studies [17-23] have investigated the influence of operating conditions on the final producer gas yield and composition including tar in the DFB gasifier. Meanwhile, several mathematical models on steam gasification of biomass in the DFB gasifier have been developed to predict the final producer gas composition [24-27]. However, the intermediate products from the initial devolatilization were not available in literature, and thus most of the modelling studies assume the products from the initial devolatilization are the same as those from stand-alone fast pyrolysis [23, 27-30]. This may be not valid as the char generated from the initial devolatilization in the BFB initially accumulated over time and then maintains constant once a balance is reached between the char generation and char flow from BFB to CFB. In addition, the reaction temperature in the initial devolatilization is higher than fast pyrolysis.

The objectives of the present study are, therefore to investigate (i) product yields, gas composition and tar formation from the devolatilization (intermediate products) in the DFB gasifier; (ii) to develop correlations between the yield and composition of products from the initial devolatilization and those of the producer gas from the overall gasification process.

Table 4-1. Results of proximate analysis and ultimate analysis of pellet of radiata pine wood used in the present study.

Proximate (%)	Method	
Total moisture	ISO 5068	8.0
Volatile matter	ISO 562	77.4
Fixed carbon	By difference	14.2
Ash	ASTM D1102	0.4
Ultimate (%)		
Carbon	Microanalytical	51.3
Hydrogen	Microanalytical	5.81
Nitrogen	Microanalytical	<0.2
Sulphur	ASTM D4239	<0.1
Oxygen	By difference	42.6
LHV (MJ/kg)	ISO 1928	18.6

4.2. Experimental and materials

In the present study, experiments of devolatilization and gasification were conducted in the 100kW dual fluidised bed steam gasifier, which has been described in Chapter 3. N_2 was introduced into the BFB column as a fluidisation agent instead of steam in order to investigate the devolatilization performance in the DFB gasifier. In experiments, chute and siphon were both fluidised with controlled N_2 to enhance the bed material flow and to prevent cross-flows of gases between the two columns. Wood pellets of radiata pine wood were used as the fuel source for the experiments. The results of proximate analysis and ultimate analysis of the test feedstock are presented in Table 4-1. Silica sand with an average particle size of 245μm was used as the bed material in the study. Detailed descriptions of the experiment operations procedures are given in Chapter 3. The operation conditions of the gasification experiments in the present study are listed in Table 4-2. In this study, the sampling and analysis methods for product gas and tar have also been given in Chapter 3.

Table 4-2. The operating conditions experiments in the present study.

Test		Devolatilization (3 groups)	Steam gasification (3 groups)
Bed Material	(kg)	30	30
Gasifier temperature	(°C)	700 750 800	700 750 800
Combustor temperature	(°C)	750 ~ 850	750 ~ 850
Nitrogen to BFB	(Nm^3/h)	6.19	-
Nitrogen to Chute	(Nm^3/h)	1.57	-
Nitrogen to Siphon	(Nm^3/h)	2.02	-
Steam to BFB	(Kg/h)	-	6
Steam to Chute	(Kg/h)	-	2
Steam to Siphon	(Kg/h)	-	2

4.3. Results and discussion

In steam gasification process, the devolatilization occurs immediately after the biomass is heated to a temperature above 300°C. In this stage, product gas is released rapidly which are largely the volatile matters from biomass. Product gas and tar contents from the devolatilization exhibit a range of characteristics depending on the reaction temperatures. These products from the devolatilization stage will be involved in subsequent gasification reactions as described by Eqs. (2-4) to (2-7). In this section, the product gas and tar generated from the devolatilization stage will be presented and discussed. In addition, the correlations between the products of initial devolatilization and the gas composition and tar content in the final producer gas will also be examined.

4.3.1. Product yields, gas composition and tar concentration from the biomass devolatilization

Fig. 4-2 shows the composition (N_2 free) of gas produced from the biomass devolatilization as a function of reaction temperature. From the results, it is found that when the temperature increased from 700 to 800°C, the H_2 content in the product gas increased slightly from 22% to 25% and that of CO increased from 40% to 42% whereas the CO_2 content decreased from 18% to 13%. In addition, the CH_4 content maintained relativity constant at 14%.

The influence of reaction temperature on gas yield (kg/kg_{daf}), total tar concentration in the gas product and the tar yield (g/kg_{daf}) from the devolatilization are presented in Fig. 4-3. The gas yield was calculated as the mass production of specific gas species (H_2, CO_2, CO and CH_4) of the gas product (Nm^3/h) over a period of time divided by the feeding dry biomass (kg_{daf}/h). It is found that when the reaction temperature increased from 700 to 800°C, the gas yield increased significantly from 0.54 kg/kg_{daf} to 0.59 kg/kg_{daf}. The results presented in Fig. 4-3 included all classes of tar compounds from Class 2 to Class 5 detected by GC-FID. The tar yield was defined as the total tar concentration in the product gas (g/Nm^3) divided by the gas yield per unit mass of dry fuel (Nm^3/kg_{daf}). As a result, as the reaction temperature was increased, the tar concentration decreased by 17% from 12.7 g/Nm^3 at 700°C to 10.5 g/Nm^3 at 800°C. In a similar manner, the tar yield decreased slightly by 5% from 13.8 g/kg_{daf} at 700°C to 13.1 g/kg_{daf} at 800°C.

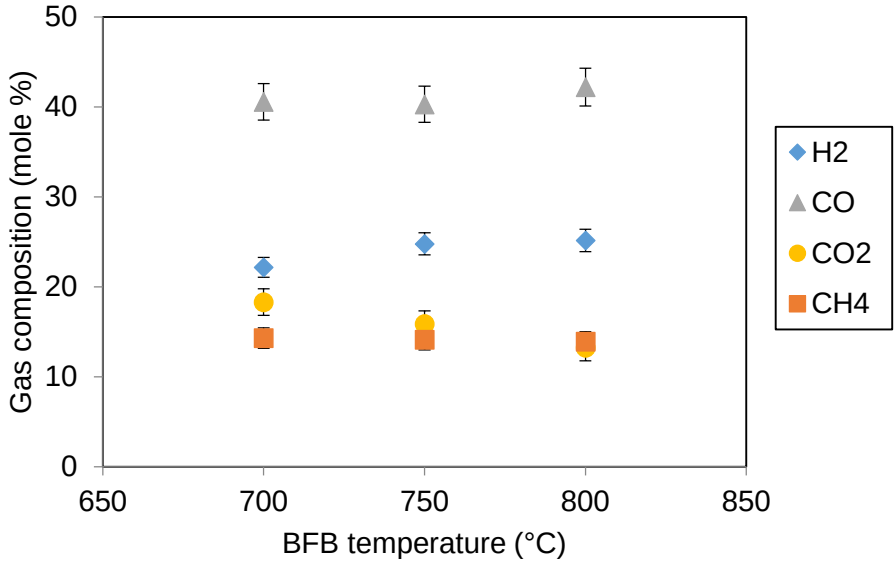

Fig. 4-2. The variation of product gas composition (H_2, CO, CO_2 and CH_4) with BFB temperature in the devolatilization.

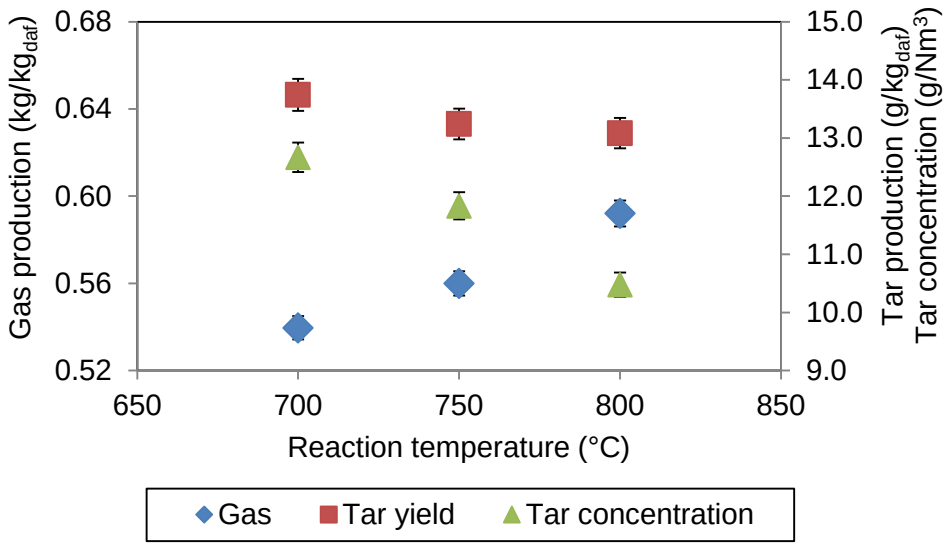

Fig. 4-3. The gas yield, tar yield and tar concentration in the product gas varying with the BFB temperature in the devolatilization.

During the devolatilization process, the gas product and tar are largely the volatiles released from biomass decomposition. The high temperature clearly favours the stripping of more volatile matter from biomass. However, biomass decomposition is a complex process, in general, it can be divided into three individual stages: cellulose decomposition, hemicellulose decomposition and lignin decomposition [31].

The different inherent chemical structures of cellulose, hemicellulose and lignin attribute to different gas and tar production in terms of temperature. Cellulose contains higher carbonyl and carboxyl function groups to contribute more CO production. Hemicellulose with higher carboxyl content and COOH, the cracking and reforming of these two groups accounted for the releasing of CO_2 yield [32, 33]. The lignin contains higher contents of aromatic ring and O-CH_3 functional groups, the cracking and deformation of lignin released out much more H_2 and tar with the aromatic rings [16, 34].

Furthermore, the thermal stability of these three components is different. When the wood temperature increased, the hemicellulose component is first degraded to release more CO_2 in the product gas, since hemicellulose is thermally the least stable component of biomass [34]. Then the cellulose component is degraded to generate the more CO in the product gas. Lignin is the most complex component, which is mainly

present in woody biomass. Lignin is more thermally stable than cellulose and hemicellulose and thus requires a higher temperature to complete the decomposition. Tars with the aromatic rings are largely released from the decomposition of lignin.

Therefore, during the biomass devolatilization, the variation of gas composition in the product gas with the increase of reaction temperature can be explained by the following reasons: (1) the generation of CO_2 mainly attributed to the cracking of hemicellulose, which degraded at low temperature, thus as the reaction temperature increased, the composition of CO_2 was decreased. (2) The releasing of CO mainly came from the decomposition of cellulose and (3) lignin is decomposed at high temperature. Hence the H_2 content in the product gas increased with the reaction temperature.

The effects of temperature on each tar class have also been examined, and the results are shown in Fig. 4-4. The tar compounds were classified following the method described in Chapter 3. From Fig. 4-4, it was found that with increase in temperature from 700 to 800°C, the concentration of the Class 2 tar (heterocyclic) compounds decreased significantly by 42%, from 5.87 to 3.38 g/Nm^3. The Class 2 tar compounds were highly reactive tar compounds formed from the heteroatoms group in the wood (N and O), which were decomposed at lower temperatures, as proposed by Vreugendhil [35]. Therefore, this class of tar compounds was cracked significantly with increase in the reaction temperature. Similar to the Class 2 tar compounds, in the same range of temperature increase, the concentration of Class 3 tar was reduced by 54%, from 1.95 to 0.89 g/Nm^3. Furthermore, the reduction of both Class 2 and Class 3 tar concentrations in the product gas is also contributed to dealkylation (Eq. 4-3) and dimerization (Eq. 4-4). However, most of PAH tar (Class 4 and Class 5 tars) compounds increased with the reaction temperatures. With the same temperatures increase from 700 to 800°C, the concentration of Class 4 tar increased by 28%, from 4.41 to 5.65 g/Nm^3, while that of Class 5 tar increased by 27%, from 0.44 to 0.56 g/Nm^3. It suggests that the high temperature favours the formation of Class 4 and Class 5 tar compounds. These trends can be explained by (1) direct combination of two aromatic species producing a dimer; (2) addition of light unsaturated hydrocarbon to aromatic rings for PAH formation and growth [36]. These two mechanisms increased the molecular weight of the tar components, which means more heavy tar compounds (Class 4 and Class 5 tars) are produced [37, 38].

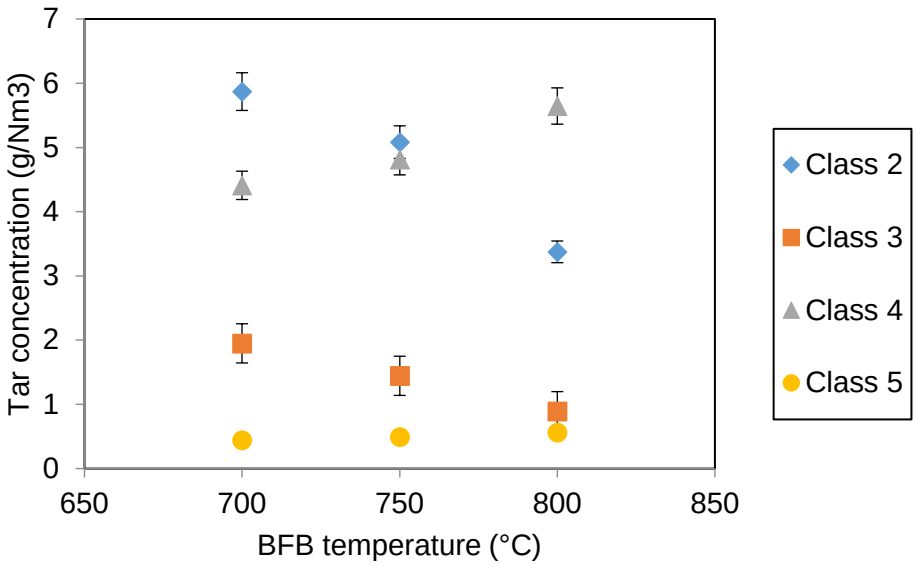

Fig. 4-4. The influence of the BFB temperature on the tars concentration.

4.3.2. Correlations between the products of initial devolatilization and the gas composition and tar content in the final producer gas

In the steam biomass gasification process, after the initial devolatilization, the subsequent homogeneous reactions (among gases and steam) and heterogeneous reactions (among char and gases as well as steam) occur simultaneously. Hence, the intermedia products (gas, tar and char) from the initial devolatilization are involved in the gasification reactions and thus also influence the final producer gas. The correlation between the gas yield of devolatilization and final producer gas yield as a function of reaction temperature is shown in Fig.4-5. In the figure, each point represents an average value of three repeatable measurements. Fig.4-5 indicates that the final producer gas yield also increased with reaction temperature, in the same trend as the product gas from devolatilization, but was higher than the gas yield of devolatilization at all reaction temperatures. At 700°C, the final producer gas yield was 5% higher, increasing from 0.51 in the initial devolatilization to 0.54 kg/kg_{daf} in the final gasification. This increase was 7% for 750°C, from 0.55 to 0.59 kg/kg_{daf}; and 12% for 800°C, from 0.60 to 0.66 kg/kg_{daf}. It is believed that the introduction of steam enhances the heterogeneous char-steam reaction, the homogeneous water-gas shift reaction and steam methane reforming to produce more gas.

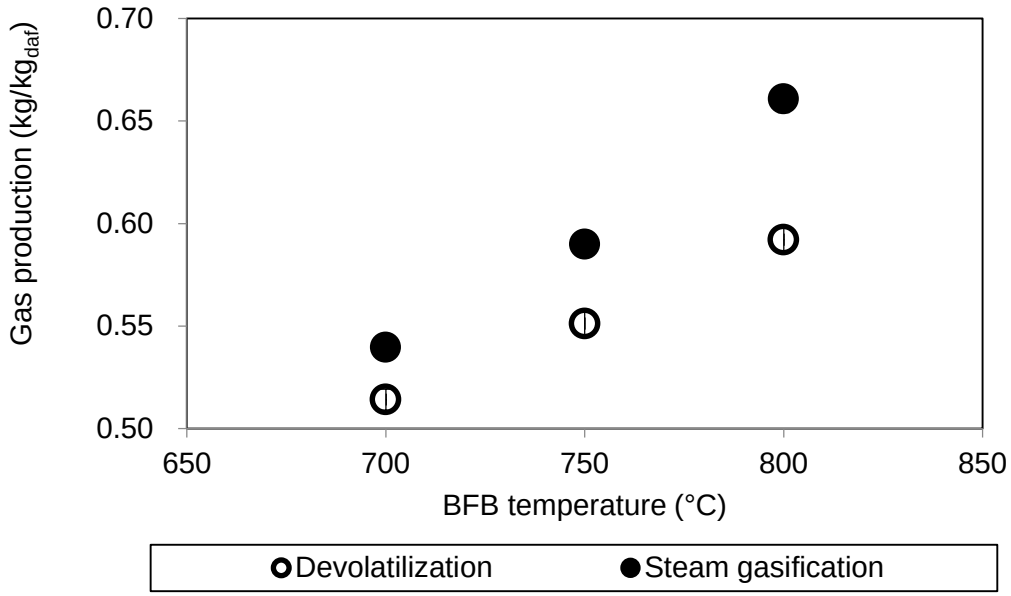

Fig. 4-5. The variation of gas productions with BFB temperature in the devolatilization (hollow point) and final gasification (solid point).

The correlation on the cumulative gas yield between the initial devolatilization (hollow point) and the final gasification (solid point) as a function of reaction temperature are shown, respectively, in Fig. 4-6(a) for H_2 yield, Fig. 4-6(b) for CO yield, Fig. 4-6(c) for CO_2 yield and Fig. 4-6(d) for CH_4 yield. The results in Fig. 4-6 exhibited a complicated process with homogeneous reactions among gases and heterogeneous reactions among chars and gases. It is also demonstrated that these reactions may play different roles when the reaction temperature varies.

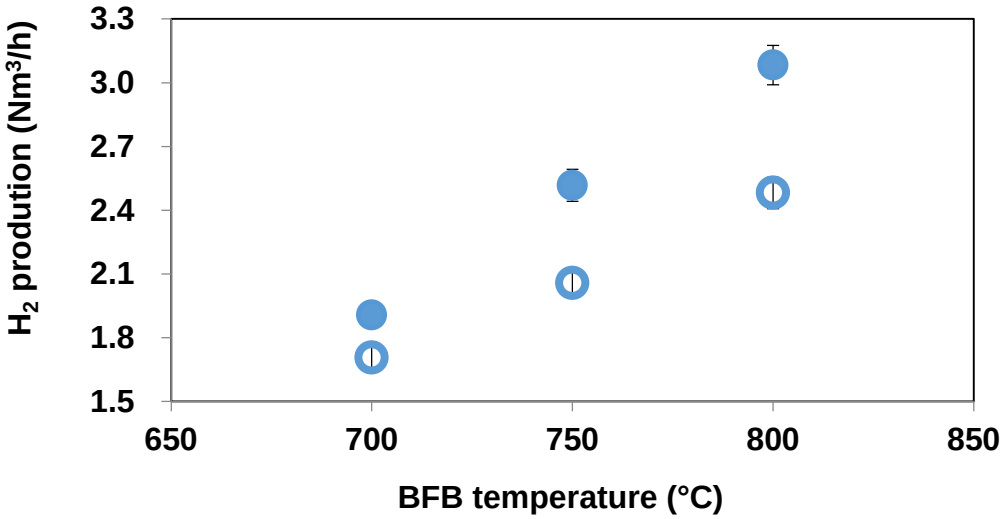
3.3
3.0
2.7
2.4
2.1
1.8
1.5
H2 prodution (Nm3/h)
650
700
750
800
850
BFB temperature (°C)

(a)

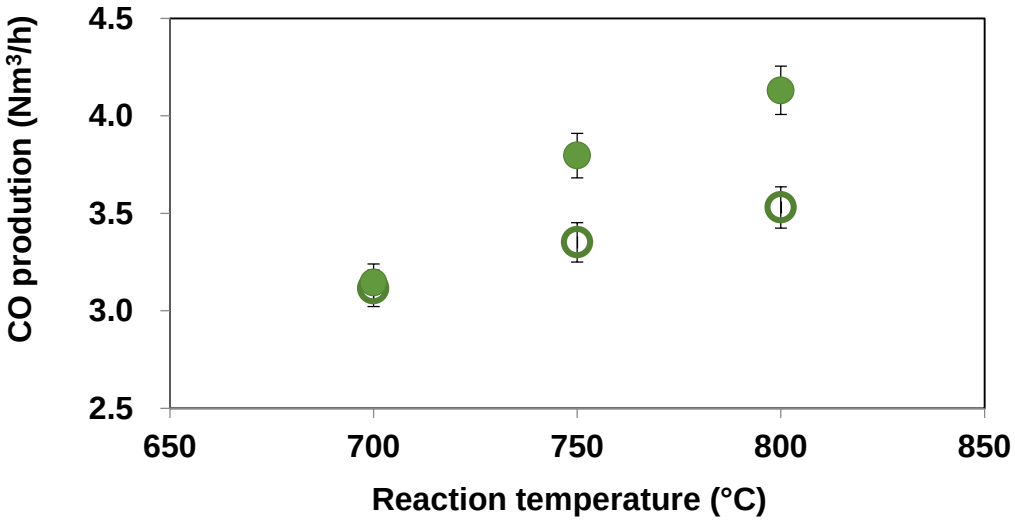
4.5
4.0
3.5
3.0
2.5
CO prodution (Nm3/h)
650
700
750
800
850
Reaction temperature (°C)

(b)

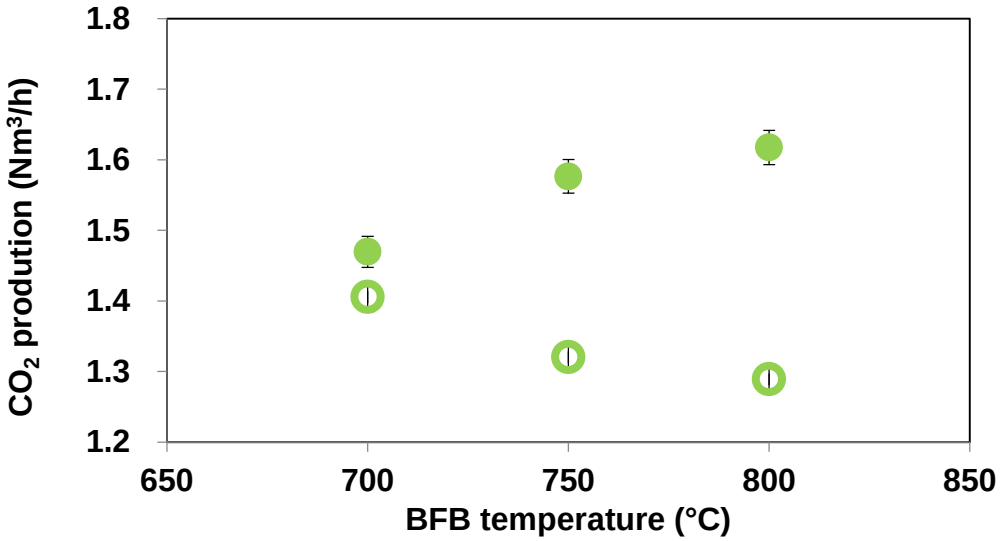
1.8
1.7
1.6
1.5
1.4
1.3
1.2
CO2 prodution (Nm3/h)
650
700
750
800
850
BFB temperature (°C)

(c)

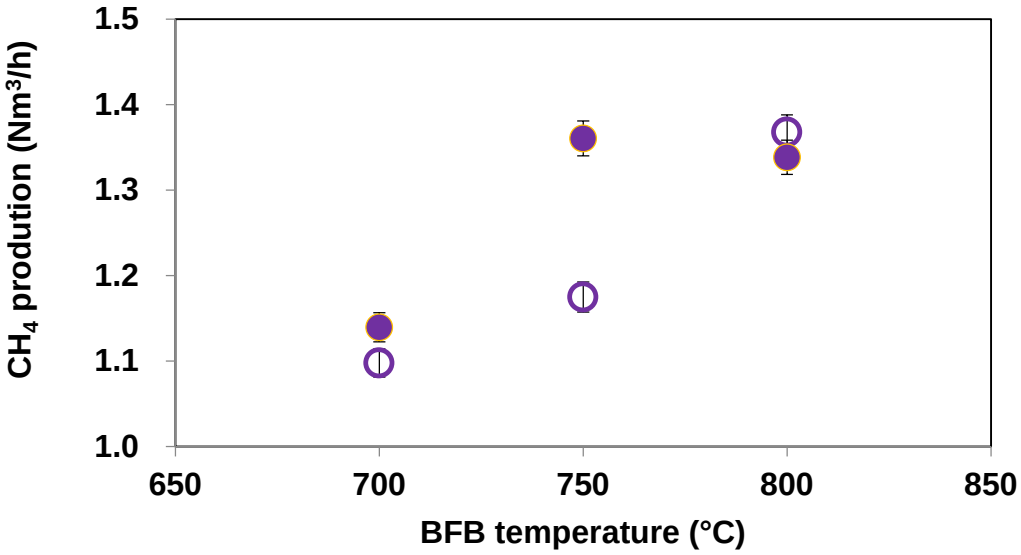

(d)

Fig. 4-6. The variation of gas yields of H_2 (a), CO (b), CO_2 (c) and CH_4 (d) with BFB temperature in the devolatilization (hollow point) and final gasification (solid point).

From Fig. 4-6(a), it is found that at 700°C, the H_2 yield in the gasification process increased by 12%, from 1.7 Nm^3/h in the initial devolatilization to 1.9 Nm^3/h in the final gasification. This increase in H_2 yield rose to 22% for reaction temperature of 750°C, from 2.0 to 2.5 Nm^3/h, and to 24% for 800°C, from 2.5 to 3.1 Nm^3/h. Fig. 4-6(c) presented the change of CO_2 yield between in the initial devolatilization and final gasification at the three temperatures of 700, 750 and 800°C. Comparing to devolatilization, the CO_2 yields in the gasification process at these three temperatures increased, respectively, by 5%, (from 1.4 to 1.5 Nm^3/h), 19% (from 1.32 to 1.58 Nm^3/h) and 25% (from 1.29 to 1.62 Nm^3/h).

The increase in the gas yields for H_2 and CO_2 yield from devolatilization to final gasification can be attributed to the addition of steam and the rate of steam-related reactions (steam-char reaction and water-gas shift reaction). These two reactions produce H_2 and CO_2 at the expenses of char and steam and are promoted with increasing temperature.

Fig. 4-6(b) shows the change of CO yield which has a similar trend to that of H_2 yield. At 700°C, the increase in the CO yield from the initial devolatilization to the final gasification was 1% (from 3.12 to 3.15 Nm^3/h); that at 750°C was 13%, (from 3.3 to

3.8 Nm^3/h). Finally, at 800°C, the CO yield increased by 17% from 3.5 to 4.1 Nm^3/h. As the reaction temperature increased, the exothermic steam-char reaction is enhanced for producing CO. Furthermore, high temperature promotes both exothermic Boudouard reaction and steam methane reforming reaction and inhibits the endothermic water gas shift reaction; these mechanisms contribute the formation of CO.

However, the change of CH_4 yield varied with the reaction temperature as shown in Fig. 4-6(d). The CH_4 yield increased by 4% at reaction temperature of 700°C, from 1.1 Nm^3/h in the initial devolatilization to 1.14 Nm^3/h in the final gasification; and the corresponding increase was 16% at 750°C (from 1.17 to 1.36 Nm^3/h); but at 800°C, the CH_4 yield decreased by 2% from 1.37 to 1.34 Nm^3/h. Base on the chemical equilibrium, the endothermic hydro-reaction was more active at low temperature; meanwhile, the exothermic steam methane reforming reaction was enhanced at high temperatures. Therefore, when the temperature is below 800°C, the hydro-reaction is more dominant to produce CH_4; in contrast, when the temperature is above 800°C, more CH_4 is reformed via the steam methane reforming reaction. The same trends are presented in the other studies [39-41].

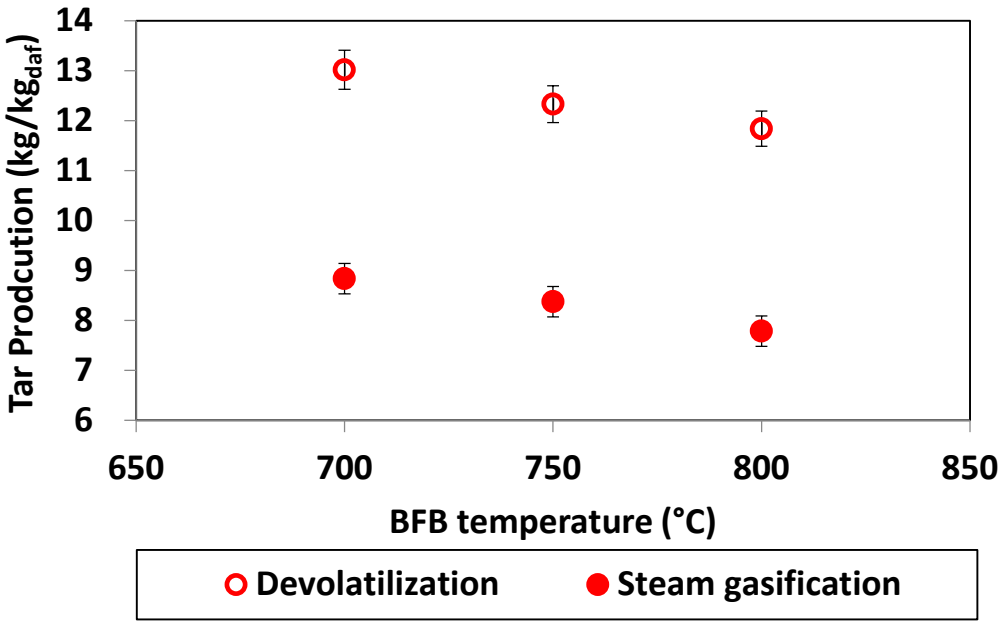

Fig. 4-7. The influence of BFB temperature on the tar production in the devolatilization (hollow point) and final gasification (solid point).

The influence of reaction temperature on total tar yield was shown in Fig 4-7. Each data point on the tar concentration represents an average of three repeated measurements. The results in Fig. 4-7 exhibit that, with increasing reaction temperature from 700 to 800°C, the tar yield decreased not only in the devolatilization but also in the steam char gasification stage. At all three tested temperatures, the total tar yields were decreased by 32% to 34% from the devolatilization to the final gasification. The decrease in the tar yield was due to the steam-tar reforming reaction for cracking the tar compounds produced in devolatilization [6, 42, 43].

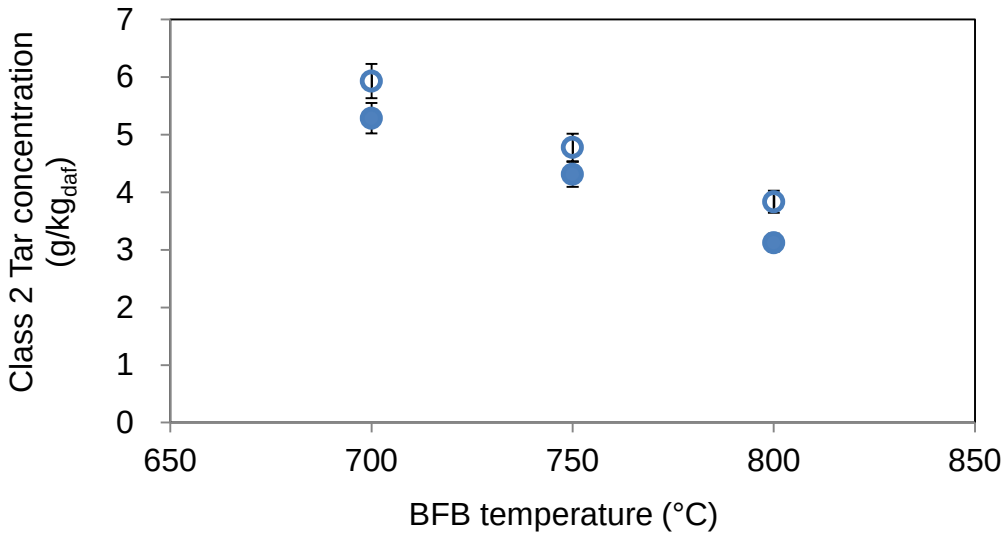

(a)

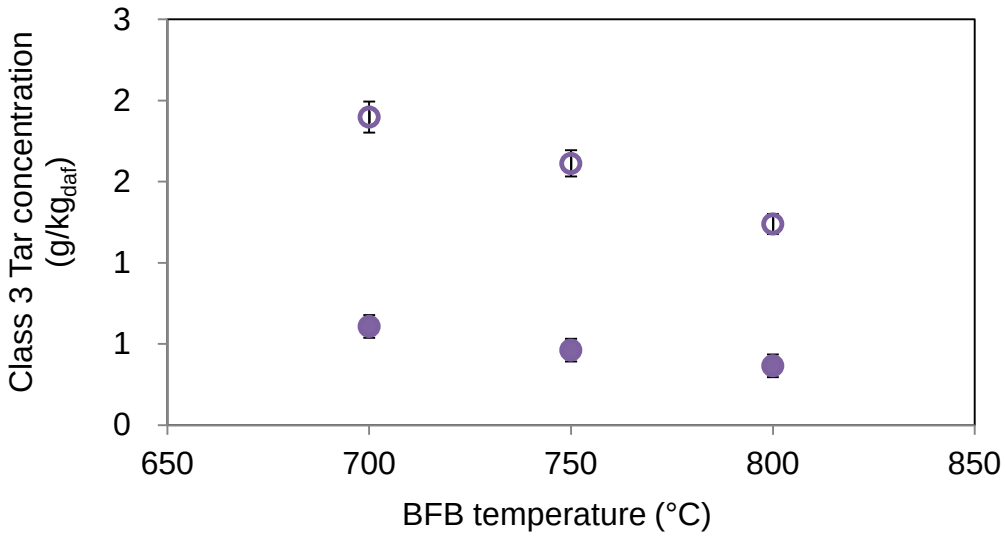

(b)

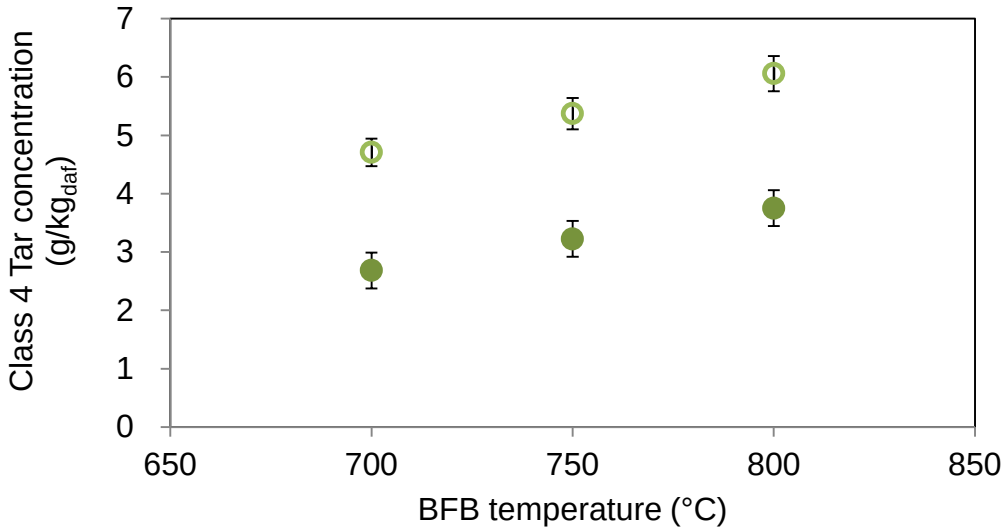

(c)

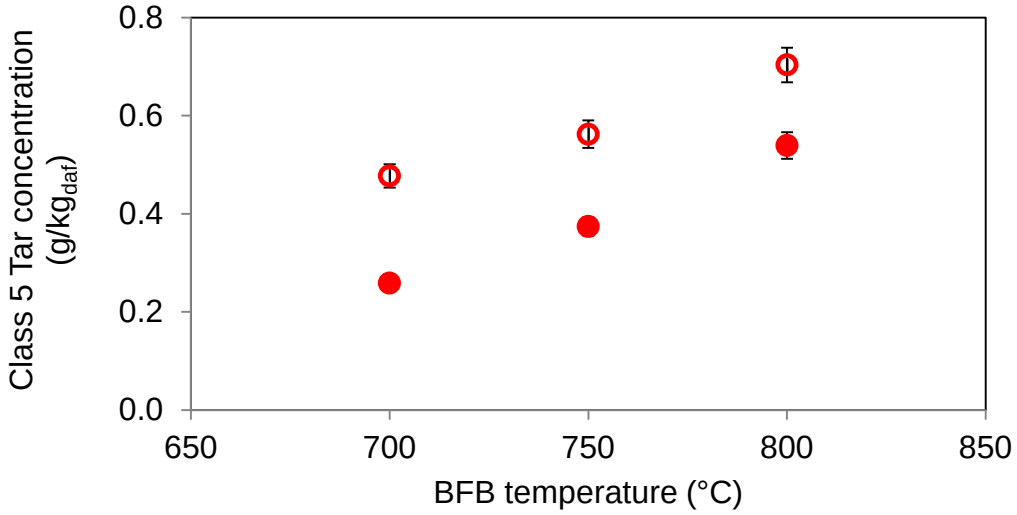

(d)

Fig. 4-8. The variation of concentration of tars both in the product gas from devolatilization (hollow point) and in the final producer gas from gasification (solid point) for different classes, Class 2 tar (a), Class 3 tar (b), Class 4 tar (c) and Class 5 tar (d).

Although the total tar yield was reduced from devolatilization to final gasification, the evolution of each tar class at different reaction temperatures was different. The tar concentrations were measured by the GC-FID, and the tar compounds were classified following the method described in Chapter 3.

The tar concentrations in the gas between the initial devolatilization (hollow point) and final gasification (solid point) as a function of reaction temperature are shown,

respectively, in Fig. 4-8(a) for Class 2 tar, Fig. 4-8(b) for Class 3 tar, Fig. 4-8(c) for Class 4 tar and Fig. 4-8(d) Class 5 tar.

From Fig. 4-8(a), the concentration of Class 2 tar in the product gas from devolatilization was reduced by 10% to 18% in final gasification producer gas while the greatest decrease was found at reaction temperature of 800°C. At this temperature, the concentration of Class 2 tar in final producer gas from gasification was also found to be the minimum with a value of 3.13 g/kg_{daf} compared to 5.29 g/ kg_{daf} at 700°C.

From Fig. 4-8(b), it is found that the concentrations of Class 3 tar in the product gas from devolatilization were significantly reduced in the gasification process by 68% to 71%. The significant reduction of Class 3 tar, which is the light hydrocarbons with a single ring, indicates that the injection of steam favours the reaction of dimerization (Eq. 4-4) to generate the PAH tars. This dimerization reaction also contributed to a reduction in the concentration of Class 4 tar in the product gas from devolatilization which decreased by 30% to 43% as shown in Fig. 4-8(c)

The evolution of Class 5 tar from devolatilization to final gasification is shown in Fig. 4-8(d). It is found that as the BFB temperature was increased, the reduction rate of Class 5 tar concentration was decreased from 46% at 700°C to 23% at 800°C, which means the formation heavy PAH tar is enhanced in the steam gasification with high temperature.

The formation of poly-aromatic tar and the reactions has been reported in literature [35, 44-47], and the above phenomena can be explained by the fact that injection of steam and high temperature can increase the concentration of radical, such as H^+. Firstly, the increase of radical enhanced the reactions of dealkylation (Eq. 4-3) of phenolic tar (Class 2 tar) readily; therefore, the alkyl groups attached in the Class 2 tar compounds were removed. In this way, a large number of tar compounds with single aromatic ring (Class 3 tar) were formed, leading an increase of the aromaticity of tar mixtures. Secondly, the reactions of dimerization (Eq. 4-4) and H_2-abstraction-C_2H_2-addition sequence (Eq. 4-5) were promoted by the increase of the radical and aromaticity of tar, causing the mono-aromatic tars and di-aromatic tar compounds (Class 4 tar) to be reformed to ploy-aromatic tar compounds (Class 5 tar).

Reactions of dealkylation (4-3):

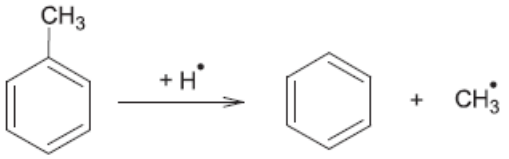

Reaction of dimerization (4-4):

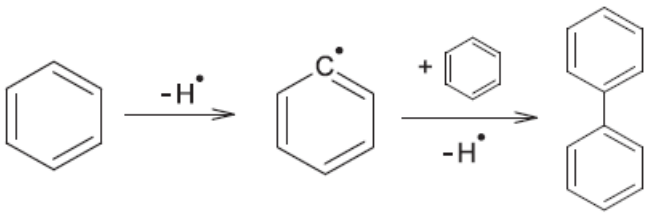

Reaction of H_2-abstraction-C_2H_2-addition sequence (4-5):

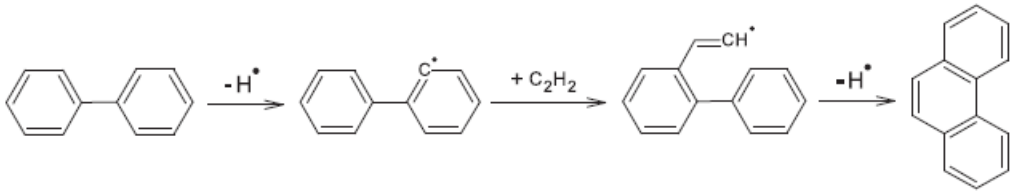

4.3.3. Interrelation between light gas and tar compounds

In the devolatilization, gas production is mainly controlled by primary and secondary, alkyl tertiary tar conversion [48]. Dufour and Brage [49, 50] reported the methods to estimate the tar production from light gas measurements in biomass pyrolysis, which is easier to be quantified than tar. A simple scheme of CH_4, C_2H_4 and tar formation was also proposed from above studies as shown in Figure 4-9. However, the interaction of tar and light gas during devolatilization depends on the fuel, reactor configuration and operating conditions, hence, it is expected that some relations exist between tar composition and light gas.

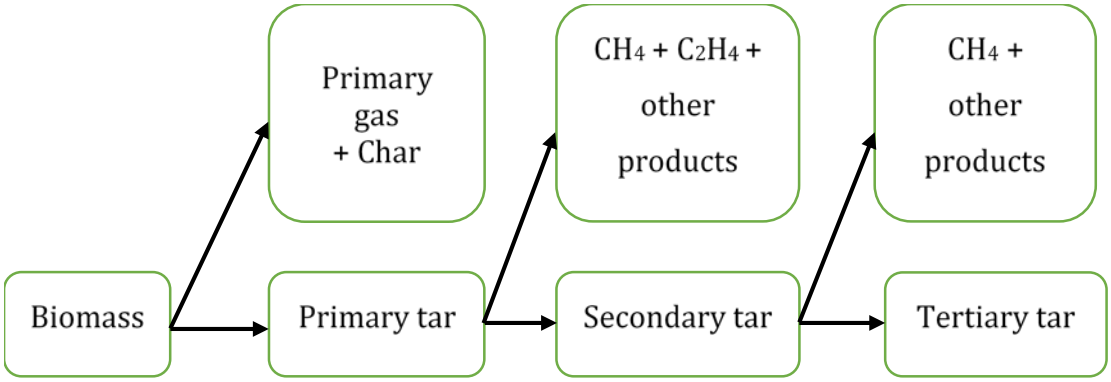

Fig. 4-9. Simplified scheme of methane, ethylene and tar formation in devolatilization adapted from Dufour et al. [50]

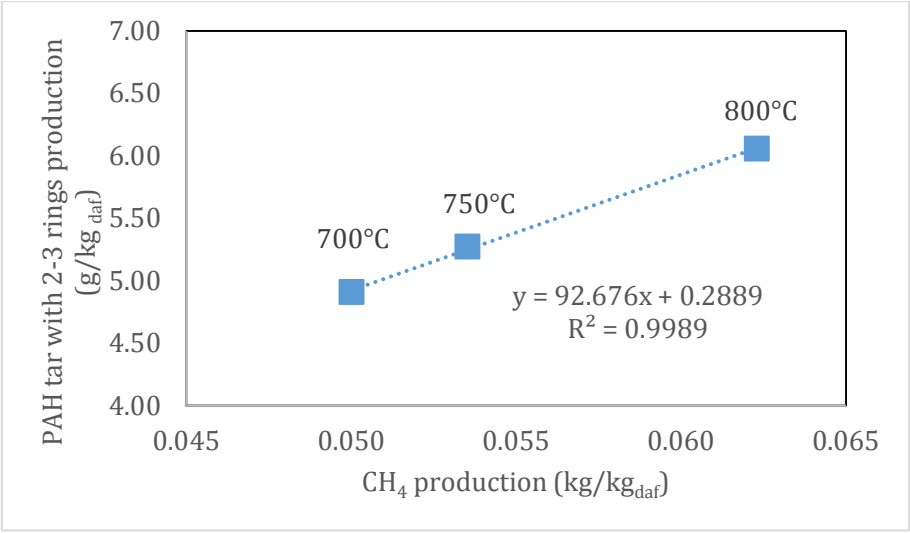

(a)

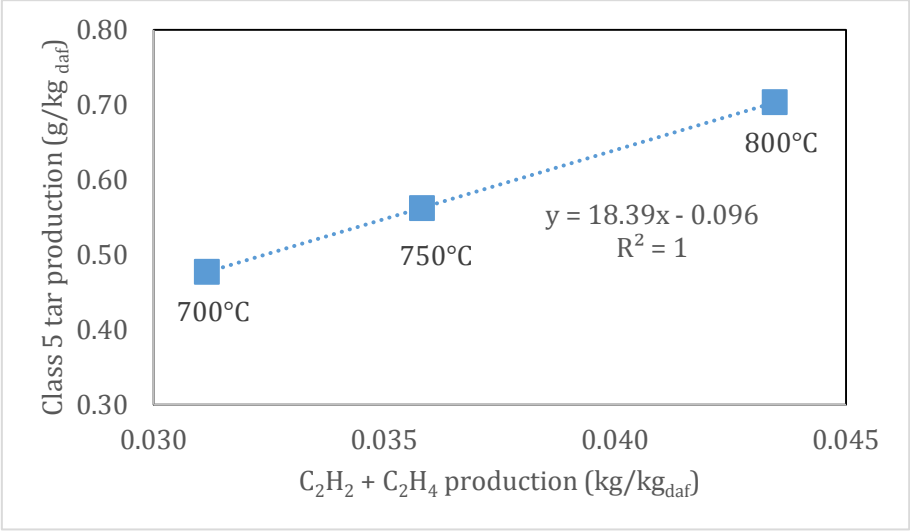

(b)

Fig. 4-10. Relations (a) between PAH tar with 2 and 3 rings and CH_4 production and (b) between Class 5 tar and C_2H_2 + C_2H_4 production in devolatilization

The correlation on mass production between the light gas and the tar in the devolatilization are shown, respectively, in Fig. 4-10(a) for PAH tar with 2 and 3 rings and CH_4 production, Fig. 4-10(b) for Class 5 tar and C_2H_2 + C_2H_4 production. Fig 4-10(a) presents linear relations between the mass production of PAH tar with 2 or 3 rings (which is all Class 4 tar without methylnaphthalene) and CH_4. Both quantities are clearly correlated within the whole temperature range tested (700-800°C). The scheme in Fig. 4-9 could explain the relation measured between the CH_4 production and PAH tar production. CH_4 is produced from conversion of the secondary and tertiary tar compounds, which mostly are the methylated tar compounds (such as toluene, xylenes, cresols, and methylnaphthalene), through de-alkylation reactions [49]. For instance, Phenols is mainly decomposed to benzene, indene, and naphthalene via cyclopentadienyl radicals. Toluene is competitively formed from cresols and converted to benzene and methane by demethylation. The conversion of phenol and toluene in the different biomass species will be further discussed in Chapter 6.

Fig 4-10 (b) shows a linear relation between the total Class 5 tars and C_2 light gas (C_2H_4 + C_2H_6) in the range of devolatilization temperature from 700 to 800 °C. It is believed that the formation of Class 5 tar compounds is strongly related with the presence of C_2 light gas in the reacting gas due to the H_2-abstraction-C_2H_2-addition (HACA) mechanism.

Overall, the relations found indicate that, under the conditions tested, is possible to correlate the yields of certain light hydrocarbons with different tar properties or yields in the devolatilization stage. When steam is introduced for the subsequent gasification reaction, which has chemical effects on the tar and gas production. It is also expected that some relations exist between tar composition and light gas in the subsequent gasification.

The correlation on mass production between the light gas and the tar in the steam gasification are shown, respectively, in Fig. 4-11(a) for PAH tar with 2 and 3 rings and CH_4 production, and Fig. 4-11(b) for Class 5 tar and C_2H_2 + C_2H_4 production. As shown in Fig 4-11(a), within the range of gasification temperature, relations on the CH_4 and light PAH tar production did not perfectly match a line. It is believed that CH_4 produced

in steam gasification is related to the combination of the steam methane reforming reaction and conversion of methylated tar compounds.

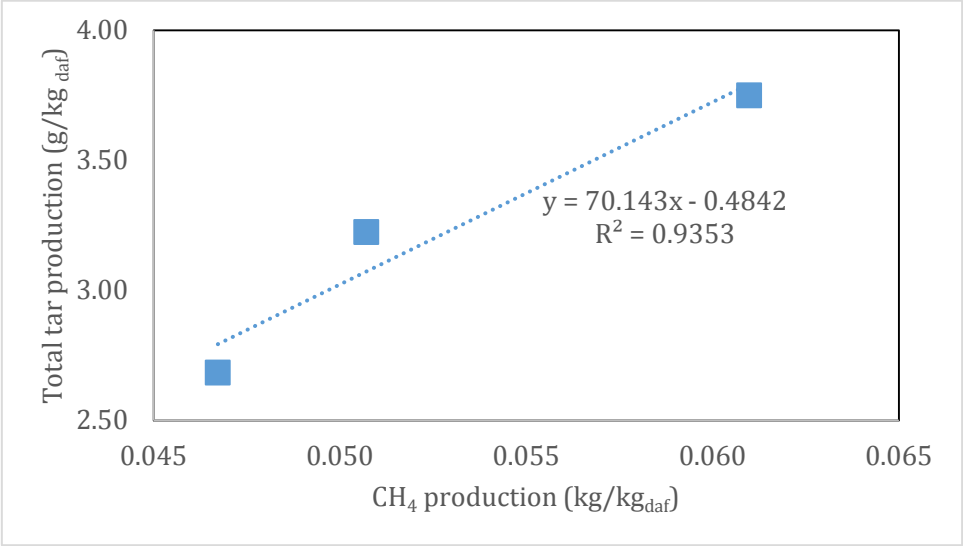

(a)

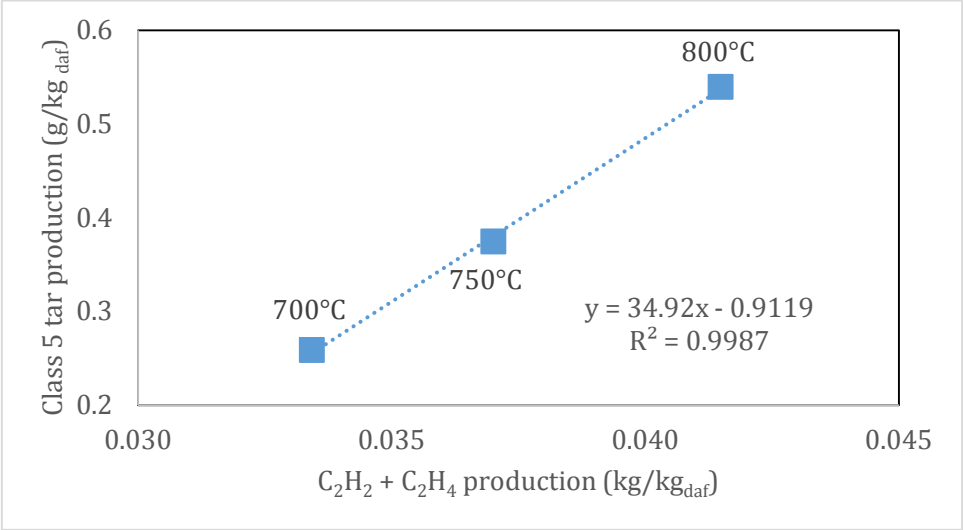

(b)

Fig. 4-11. Correlations (a) between PAH tar with 2 and 3 rings and CH_4 production and (b) between Class 5 tar and C_2H_2 + C_2H_4 production in steam gasification

However, from Fig 4-11(b), a linear relationship between the total Class 5 tars and C_2 light gas (C_2H_4 + C_2H_6) was obtained. It demonstrated that the injection of steam had few effects on the relative production of heavy PAH tar and C_2 light gas. It is possible to obtain a good estimation of the Class 5 tar production by measuring the C_2 light gas yield in biomass gasification under the conditions tested.

These relations are expected to depend on the fuel used and probably on other operating conditions. This makes it necessary to validate these correlations for other process conditions. The influence of the operating conditions (residence time and steam to biomass ratio) and biomass selection further discussed in Chapter 5 and Chapter 6, respectively.

4.4. Conclusions

This study has investigated the product yield and composition in the initial devolatilization during biomass steam gasification in a dual fluidised bed gasifier. Correlation on yield and composition between the product gas from devolatilization and the final producer gas from overall gasification are established. Influence of reaction temperature has been examined.

Key findings from the present studies are:

- In the initial biomass devolatilization stage, gas yield increases and tar yield decreases with reaction temperature. In the gas product, the concentration of H_2 and CO increase with increase in the reaction temperature but the CO_2 concentration decreases while CH_4 remains relatively constant.

- The reaction temperature has different impact on the concentrations of different classes of tar compounds in the product gas from biomass devolatilization. With increase in the reaction temperature, the concentrations of Class 2 and Class 3 tar compounds decrease while those of Class 4 and Class 5 tar compounds increase.

- The products from the initial devolatilization are actively involved in the subsequent steam gasification reaction. Consequently, the total gas yield is increased whereas the total tar yield is reduced. With steam injection for the gasification process, more gas is produced from heterogeneous char-gas reaction and the homogeneous reactions among gases and steam.

- Reactions temperature also has significant impact on the yield and composition of the producer gas from the gasification. With increase in the reaction temperature,

water-gas shift reaction and steam methane reforming reaction are enhanced while tar is cracked. In addition, the steam-char reforming reaction is hindered with the increase in reaction temperature.

- The reaction temperature has different impacts on changes in the concentration of different classes of tar compounds from the product gas in devolatilization to the final producer gas in the gasification. With increase in the reaction temperature, the concentration of Class 2 and Class 3 tar compounds are decreased while those of Class 4 and Class 5 tar compounds are increased. The most significant changes are for Class 2 and Class 3 tar compounds.

- The interrelations between PAH tar and light gas production enabled to estimate the yield of PAH tars production during biomass gasification. Besides, the analysis of the observed relations provides understanding of the mechanisms of tar conversion from initial devolatilization to subsequent gasification in the DFB gasifier.

The results from the present study can be used for better understanding of the biomass steam gasification process and for operation optimisation. Further studies are being undertaken to investigate the effect of operating condition, gas residence time and steam to biomass ratio, on the performance of a DFB gasifier in Chapter 5.

4.5. Reference

[1] H. B. Goyal, D. Seal, and R. C. Saxena, "Bio-fuels from thermochemical conversion of renewable resources: A review," *Renewable and Sustainable Energy Reviews*, vol. 12, pp. 504-517, 2008.

[2] M. M. Küçük and A. Demirbas, "Biomass conversion processes," *Energy Conversion and Management*, vol. 38, pp. 151-165, 1997.

[3] D. L. Klass, *Biomass for renewable energy, fuels, and chemicals*. San Diego: Academic Press, 1998.

[4] J. Rezaiyan and N. P. Cheremisinoff, *Gasification technologies : a primer for engineers and scientists*. Boca Raton: Taylor & Francis, 2005.

[5] A. C. Chang, H.-F. Chang, F.-J. Lin, K.-H. Lin, and C.-H. Chen, "Biomass gasification for hydrogen production," *International Journal of Hydrogen Energy*, vol. 36, pp. 14252-14260, 2011.

[6] J. Moon, J. Lee, U. Lee, and J. Hwang, "Transient behavior of devolatilization and char reaction during steam gasification of biomass," *Bioresource Technology*, vol. 133, pp. 429-436, 2013.

[7] A. V. Bridgwater, "Renewable fuels and chemicals by thermal processing of biomass," *Chemical Engineering Journal*, vol. 91, pp. 87-102, 2003.

[8] K. Umeki, T. Namioka, and K. Yoshikawa, "The effect of steam on pyrolysis and char reactions behavior during rice straw gasification," *Fuel Processing Technology*, vol. 94, pp. 53-60, 2012.

[9] M. Asadullah, S. Zhang, Z. Min, P. Yimsiri, and C.-Z. Li, "Effects of biomass char structure on its gasification reactivity," *Bioresource Technology*, vol. 101, pp. 7935-7943, 2010.

[10] A. Tremel and H. Spliethoff, "Gasification kinetics during entrained flow gasification – Part I: Devolatilisation and char deactivation," *Fuel*, vol. 103, pp. 663-671, 2013.

[11] W. Klose and M. Wölki, "On the intrinsic reaction rate of biomass char gasification with carbon dioxide and steam," *Fuel*, vol. 84, pp. 885-892, 2005.

[12] Q. Xu, S. Pang, and T. Levi, "Reaction kinetics and producer gas compositions of steam gasification of coal and biomass blend chars, part 1: Experimental investigation," *Chemical Engineering Science*, 2011.

[13] H. Haykiri-Acma, S. Yaman, and S. Kucukbayrak, "Gasification of biomass chars in steam-nitrogen mixture," *Energy Conversion and Management,* vol. 47, pp. 1004-1013, 2006.

[14] F. Miccio, S. Russo, and N. Silvestri, "Assessment of the devolatilization behavior of fuel pellets in fluidized bed," *Fuel Processing Technology,* vol. 115, pp. 122-129, 2013.

[15] L. Fagbemi, L. Khezami, and R. Capart, "Pyrolysis products from different biomasses: application to the thermal cracking of tar," *Applied Energy,* vol. 69, pp. 293-306, 2001.

[16] C. Font Palma, "Model for biomass gasification including tar formation and evolution," *Energy & Fuels,* vol. 27, pp. 2693-2702, 2013.

[17] I. Aigner, C. Pfeifer, and H. Hofbauer, "Co-gasification of coal and wood in a dual fluidized bed gasifier," *Fuel,* vol. 90, pp. 2404-2412, 2011.

[18] F. Kirnbauer, V. Wilk, and H. Hofbauer, "Performance improvement of dual fluidized bed gasifiers by temperature reduction: The behavior of tar species in the product gas," *Fuel,* vol. 108, pp. 534-542, 2013.

[19] T. Murakami, G. Xu, T. Suda, Y. Matsuzawa, H. Tani, and T. Fujimori, "Some process fundamentals of biomass gasification in dual fluidized bed," *Fuel,* vol. 86, pp. 244-255, 2007.

[20] C. Pfeifer, S. Koppatz, and H. Hofbauer, "Steam gasification of various feedstocks at a dual fluidised bed gasifier: Impacts of operation conditions and bed materials," *Biomass Conversion and Biorefinery,* vol. 1, pp. 39-53, 2011.

[21] J. C. Schmid, U. Wolfesberger, S. Koppatz, C. Pfeifer, and H. Hofbauer, "Variation of feedstock in a dual fluidized bed steam gasifier—influence on product gas, tar content, and composition," *Environmental Progress & Sustainable Energy,* vol. 31, pp. 205-215, 2012.

[22] J. Kiel, S. Van Paasen, J. Neeft, L. Devi, K. Ptasinski, F. Janssen, R. Meijer, R. Berends, H. Temmink, and G. Brem, "Primary measures to reduce tar formation in fluidised-bed biomass gasifiers," Energy research Centre of the Netherlands (ECN) Report, The Netherlands, ECN-C-04-014, 2004.

[23] H. Liu, M. Kaneko, C. Luo, S. Kato, and T. Kojima, "Effect of pyrolysis time on the gasification reactivity of char with CO2 at elevated temperatures," *Fuel,* vol. 83, pp. 1055-1061, 2004.

[24] P. Kaushal, T. Pröll, and H. Hofbauer, "Model development and validation: Co-combustion of residual char, gases and volatile fuels in the fast fluidized combustion chamber of a dual fluidized bed biomass gasifier," *Fuel*, vol. 86, pp. 2687-2695, 2007.

[25] C. Loha, S. Gu, J. De Wilde, P. Mahanta, and P. K. Chatterjee, "Advances in mathematical modeling of fluidized bed gasification," *Renewable and Sustainable Energy Reviews*, vol. 40, pp. 688-715, 2014.

[26] M. Narobe, J. Golob, D. Klinar, V. Francetič, and B. Likozar, "Co-gasification of biomass and plastics: Pyrolysis kinetics studies, experiments on 100kW dual fluidized bed pilot plant and development of thermodynamic equilibrium model and balances," *Bioresource Technology*, vol. 162, pp. 21-29, 2014.

[27] T. D. B. Nguyen, S. I. Ngo, Y.-I. Lim, J. W. Lee, U.-D. Lee, and B.-H. Song, "Three-stage steady-state model for biomass gasification in a dual circulating fluidized-bed," *Energy Conversion and Management*, vol. 54, pp. 100-112, 2012.

[28] M. Barrio, B. Gøbel, H. Risnes, U. B. Henriksen, J. Hustad, and L. Sørensen, "Steam gasification of wood char and the effect of hydrogen inhibition on the chemical kinetics," in *Conference on Progress in Thermochemical Biomass Conversion*, 2000.

[29] S. Rapagnà and G. Mazziotti di Celso, "Devolatilization of wood particles in a hot fluidized bed: Product yields and conversion rates," *Biomass and Bioenergy*, vol. 32, pp. 1123-1129, 2008.

[30] A. Gomez-Barea, S. Nilsson, F. Vidal Barrero, and M. Campoy, "Devolatilization of wood and wastes in fluidized bed," *Fuel Processing Technology*, vol. 91, pp. 1624-1633, 2010.

[31] H. Yang, R. Yan, H. Chen, D. H. Lee, and C. Zheng, "Characteristics of hemicellulose, cellulose and lignin pyrolysis," *Fuel*, vol. 86, pp. 1781-1788, 2007.

[32] L. Burhenne, J. Messmer, T. Aicher, and M.-P. Laborie, "The effect of the biomass components lignin, cellulose and hemicellulose on TGA and fixed bed pyrolysis," *Journal of Analytical and Applied Pyrolysis*, 2013.

[33] K. Raveendran, A. Ganesh, and K. C. Khilar, "Pyrolysis characteristics of biomass and biomass components," *Fuel*, vol. 75, pp. 987-998, 1996.

[34] C. Font Palma, "Modelling of tar formation and evolution for biomass gasification: A review," *Applied Energy*, vol. 111, pp. 129-141, 2013.

[35] B. Vreugdenhil, R. Zwart, and J. P. A. Neeft, *Tar formation in pyrolysis and gasification*: ECN, 2009.

[36] S. Van Paasen, J. Kiel, and H. Veringa, "Tar formation in a fluidised bed gasifier," Energy research Centre of the Netherlands (ECN) Report, The Netherlands, ECN-C-04-013, 2004.

[37] R. J. Evans and T. A. Milne, "Molecular characterization of the pyrolysis of biomass," *Energy & Fuels*, vol. 1, pp. 123-137, 1987.

[38] D. C. Elliott, "Relation of Reaction Time and Temperature to Chemical Composition of Pyrolysis Oils," in *Pyrolysis Oils from Biomass*. vol. 376: American Chemical Society, 1988, pp. 55-65.

[39] R. N. André, F. Pinto, C. Franco, M. Dias, I. Gulyurtlu, M. A. A. Matos, and I. Cabrita, "Fluidised bed co-gasification of coal and olive oil industry wastes," *Fuel*, vol. 84, pp. 1635-1644, 2005.

[40] F. Pinto, C. Franco, R. N. André, C. Tavares, M. Dias, I. Gulyurtlu, and I. Cabrita, "Effect of experimental conditions on co-gasification of coal, biomass and plastics wastes with air/steam mixtures in a fluidized bed system," *Fuel*, vol. 82, pp. 1967-1976, 2003.

[41] A. Smolinski, K. Stanczyk, and N. Howaniec, "Steam gasification of selected energy crops in a fixed bed reactor," *Renewable Energy*, vol. 35, pp. 397-404, 2010.

[42] C. Li and K. Suzuki, "Tar property, analysis, reforming mechanism and model for biomass gasification—An overview," *Renewable and Sustainable Energy Reviews*, vol. 13, pp. 594-604, 2009.

[43] X. Xiao, X. Meng, D. D. Le, and T. Takarada, "Two-stage steam gasification of waste biomass in fluidized bed at low temperature: parametric investigations and performance optimization," *Bioresource Technology*, vol. 102, pp. 1975-1981, 2011.

[44] A. Gani and I. Naruse, "Effect of cellulose and lignin content on pyrolysis and combustion characteristics for several types of biomass," *Renewable Energy*, vol. 32, pp. 649-661, 2007.

[45] C. Kinoshita, Y. Wang, and J. Zhou, "Tar formation under different biomass gasification conditions," *Journal of Analytical and Applied Pyrolysis*, vol. 29, pp. 169-181, 1994.

[46] P. Morf, P. Hasler, and T. Nussbaumer, "Mechanisms and kinetics of homogeneous secondary reactions of tar from continuous pyrolysis of wood chips," *Fuel*, vol. 81, pp. 843-853, 2002.

[47] D. Fuentes-Cano, A. Gómez-Barea, S. Nilsson, and P. Ollero, "The influence of temperature and steam on the yields of tar and light hydrocarbon compounds during devolatilization of dried sewage sludge in a fluidized bed," *Fuel*, vol. 108, pp. 341-350, 2013.

[48] M. J. Antal, "Effects of reactor severity on the gas-phase pyrolysis of cellulose- and kraft lignin-derived volatile matter," *Industrial & Engineering Chemistry Product Research and Development*, vol. 22, pp. 366-375, 1983.

[49] C. Brage, Q. Yu, and K. Sjöström, "Characteristics of evolution of tar from wood pyrolysis in a fixed-bed reactor," *Fuel*, vol. 75, pp. 213-219, 1996.

[50] A. Dufour, E. Masson, P. Girods, Y. Rogaume, and A. Zoulalian, "Evolution of Aromatic Tar Composition in Relation to Methane and Ethylene from Biomass Pyrolysis-Gasification," *Energy & Fuels*, vol. 25, pp. 4182-4189, 2011.

Chapter 5. Influence of gas residence time and steam to biomass ratio on gasification performance and tar yield in steam gasification of biomass

In the chapter, effects of mean gas residence time and steam to biomass ratio on gasification performance and tar yield in steam gasification were experimentally investigated on a 100kW dual fluidised bed (DFB) gasifier. Pellets of radiata pine wood were used as the feedstock, and silica sand was used as the bed material. The gasification temperature was controlled at 800°C. In the first part of this study, in order to change the gas residence time, three bed material inventories of 20, 25 and 30 kg were tested which corresponding gas residence times were 0.19, 0.22 and 0.25s, respectively. In the second part, the steam flow rate was kept constant at 10.5 kg/h to maintain a constant gas residence time in the bubbling fluidised bed gasifier, and then the biomass feeding rate was changed from 7.1 to 21.0 kg/h, which corresponding steam to biomass (S/B) ratio varied from 0.63 to 1.51.

From the experimental results, it is found that with increase in bed material inventory and thus increase in gas residence time, the change of gas composition in initial devolatilization stage was not significant, but the producer gas composition was significantly affected. With increase of gas residence time, the concentrations of H_2, CO_2 and CH_4 were increased while the CO concentration was reduced. As the gas residence time increased from 0.19 to 0.25s, the total tar yield was reduced from 17.3 to 11.8 g/kg$_{daf}$ in the initial devolatilization, while that in the final gasification was decreased from 11.9 to 7.7 g/kg$_{daf}$. The effect of gas residence time on the distribution of classes of tar compounds was inconsistent. With increase of steam to biomass ratio, the H_2 and CO_2 contents in the producer gas were increased, whereas the CO and CH_4 contents were reduced. For the tar compounds, with increasing S/B from 0.63 to 1.51, the total tar yield was reduced from 9.5 to 5.1 g/kg$_{daf}$. In the meantime, the concentrations of Class 2, Class 3 and Class 4 tar compounds were decreased while that of Class 5 tar compounds was increased.

5.1. Introduction

Effects of different operating conditions on the gasification performance have been extensively studied and reported in literature [1-7]. Gas residence time in fluidised bed gasifier is defined as the time for product gas passes through the bed material [8], and it is an important parameter for mixing and entrainment of bed material. The gas residence time can be calculated based on the volumetric flow rate of fluidisation gas, inventories of bed material and dimension of gasifier [9]. It is reported that the gas residence affects char conversion during the gasification since the contact time between char and gasification agent determines the approach to the equilibrium state of heterogeneous reactions in the gasification. Some studies have been found in literature [10, 11] on the effect of gas residence time during the biomass conversion. However, these results may not be comparable due to the different gasifier system. In addition, there is an apparent lack of information on the influence of gas residence time on gas and tar products from devolatilization to final gasification in a pilot scale fluidised bed.

As mentioned in Chapter 2, the injection of steam affects the producer gas composition through the water-gas shift reaction, steam-char reaction and methane steam reforming reaction. Meanwhile, the tar compounds in the producer gas can be reduced by the steam tar reforming. However, the literature reports about the effect of steam on the tar composition are inconsistent. In the study of Jess [12], it was found that steam had only slight influence on the conversion of the aromatic tar at the temperature below 1100°C. A similar result was shown in the study of Fuentes-Cano et al. [13], who demonstrated that steam had negligible influence on the yields of aromatic tar compounds and light hydrocarbon compounds in producer gas from devolatilization of dried sewage sludge in a fluidised bed. However, a separate study by Herguido et al. [14] found a significant reduction in tar yield with steam-to-biomass ratio increasing from 0.5 to 2.5 and this was attributed to the promotion of tar-reforming reaction by steam. In addition, Wang et al. [15] reported that the tar compounds were much reduced by increasing the steam to biomass ratio from 0.5 to 1.0 for gasification of wood chips.

The aims of the present study are to investigate (1) the influences of gas residence time on the yields and composition of producer gas and tar in initial devolatilization stage of

biomass gasification and correlation to those in the final stage of steam gasification process, and (2) the effect of steam to biomass ratio in the steam gasification.

5.2. Experimental Setup

5.2.1. Experimental conditions

Experiments were conducted on devolatilization and gasification of woody biomass (pellets of radiata pine) in a 100kW dual fluidised bed (DFB) gasifier, which has been described in Chapter 3. The experimental conditions tested are summarised in Table 5-1. Before the experiments, the pellets of radiata pine wood were analysed, and the results of proximate analysis and ultimate analysis are given in Table 4-2 from Chapter 4. Silica sand was used as the bed material in the experiments. Detailed descriptions of the experiment operations procedures and methods of gas and tar sampling and analysis are given in Chapter 3. The steam to biomass (S/B) ratio is calculated by using the Eq. (3-1).

Table 5-1. The operating conditions experiments in the present study.

Test for steam to biomass ratio		Devolatilization	Steam gasification
Bed Material	(kg)	30	
Gasifier temperature	(°C)	800	
Combustor temperature	(°C)	800 ~ 850	
Fuel	kg	7.1, 10.2, 14.2, 21.0	
Steam	kg	0	10.5
S/B ratio		0	0.63, 0.89, 1.21, 151
Test for mean gas residence time		Devolatilization	Steam gasification
Bed Material	(kg)	20, 25, 30	
Gasifier temperature	(°C)	800	
Combustor temperature	(°C)	800 ~ 850	
Fuel	kg	14.2	
Steam	kg	0	10.5
S/B ratio		0	0.89

5.2.2. Calculation of mean gas residence time of the producer gas

The mean gas residence time of the producer gas in the BFB, τ_f, in the present study was calculated following the approaches in the studies of Saw and Pang [8]. The results of mean gas residence time of the producer gas in the BFB based on the bed material inventory are given in Table 5-2.

The mean gas residence time of producer gas, τ_f,

$$\tau_f = \frac{L_f \times \varepsilon_f}{U_{pg}} \quad (5\text{-}1)$$

Where

L_f is expansion bed height, m, which consists of bubble phase and emulsion phase in the bubbling fluidised bed (BFB). This is calculated by Eq. (5-2).

ε_f is voidage of the BFB and is determined by Eq. (5-4).

U_{pg} is superficial velocity of producer gas, m/s.

$$\frac{L_f - L_{mf}}{L_f} = \frac{Q_b}{A \times U_{bm}} = \varepsilon_b \quad (5\text{-}2)$$

Where

L_{mf} is bed height at the minimum fluidisation, m. Its value is estimated to be 5% higher than that of initial bed height, L_0, which is calculated by Eq. (5-3).

Q_b is volumetric flow rate for bubbling phase, m^3/s, and determined by using Eq. (5-6)

A is cross section area of BFB, m^2.

U_{bm} is mean rise velocity of a bubble through the BFB, m/s. It is related to the rise velocity of a bubble, U_b by using Eq. (5-7).

ε_b is voidage of the bubble phase.

$$L_0 = \frac{M}{A \times \rho_{bulk}} \quad (5\text{-}3)$$

where

M is mass of the bed material in BFB, kg.

ρ_{bulk} is the bulk particle density of the particle (sand), kg/m^3.

$$\varepsilon_f = 1 - (1 - \varepsilon_b - \varepsilon_{mf}) \quad (5\text{-}4)$$

Where

ε_{mf} is voidage at minimum fluidisation. Its value is estimated to be 5% higher than that of voidage of the fixed bed ε_0, which is determined by Eq. (5-5).

$$\varepsilon_0 = 1 - \frac{\rho_{bulk}}{\rho_p} \quad (5\text{-}5)$$

Where

ρ_p is the particle density of bed material, kg/m^3.

$$Q_b = Y \times A \times (U_m - U_{mf}) \quad (5\text{-}6)$$

Where

Y is correction factor for two phase theory, as shown in Fig. 5-1 adapted from Geldart [16].

U_m is mean superficial gas velocity, m/s.

U_{mf} is minimum fluidisation gas velocity, m/s. The calculation method was described in Chapter 3.

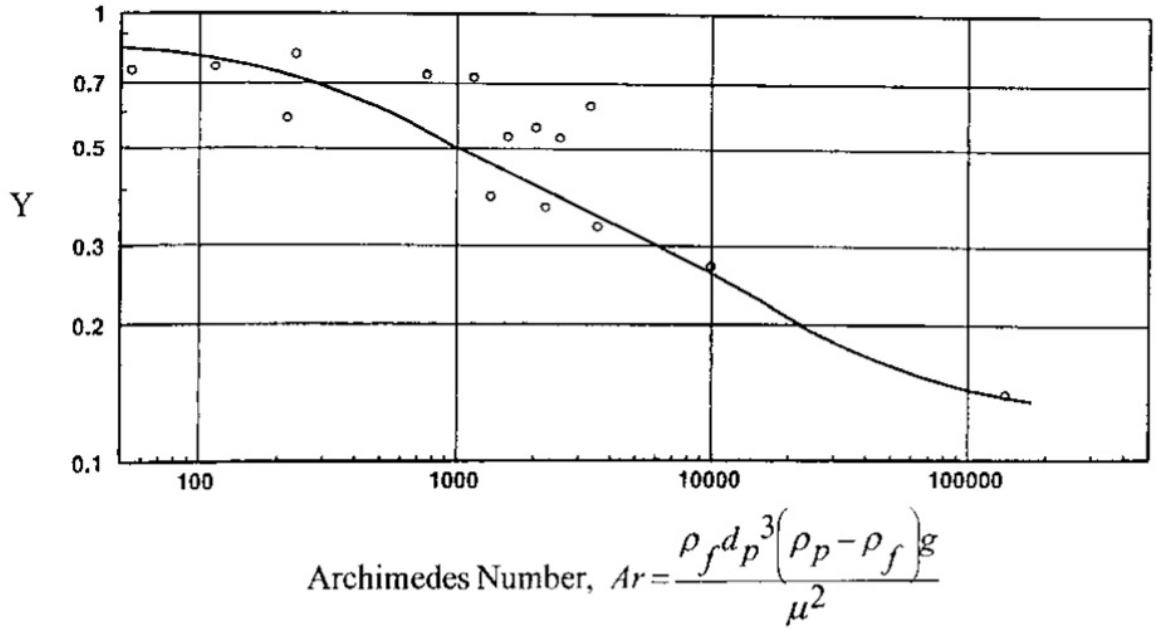

Fig. 5-1. Correction for deviation from the two phase theory (adapted from Geldart [16]).

$$U_b = (U_m - U_{mf}) + U_{bf} \quad (5\text{-}7)$$

U_b is the rise velocity of a bubble through the BFB, m/s.

U_{bf} is the rise velocity of a bubble with respect to the emulsion phase, m/s, which can be determined by using Eq. (5-8).

$$U_{bf} = 0.711 \times (g \times d_{bv})^{0.5} \quad (5\text{-}8)$$

Where

g is the gravity constant with a value of 9.81 m/s^2.

d_{bv} is effective bubble diameter, m, by using Eq. (5-9).

$$d_{bv} = \frac{0.54}{g^2}(U - U_{mf})^{0.4}(L_d + 4 \times N^{-0.5})^{0.8} \quad (5\text{-}9)$$

Where

L_d is distance above the distributor, m.

N is number of holes per unit area in the distributor (1/m^2).

Table 5-2. The calculated values of L_f, L_{mf}, ε_f and τ_f based on the bed material properties.

Bed material	Silica sand		
Bulk particle density of the sand, ρ_{bulk} (kg/m^3)	1550		
Particle density of the sand, ρ_p (kg/m^3)	2600		
Average particle size of the sand, d_p (μm)	215		
Minimum fluidisation velocity, U_{mf} (m/s)	0.018		
Superficial velocity of producer gas, U_{pg}, (m/s)	0.694 ~ 0.733		
Total inventory of bed material (kg)	30	25	20
Residual bed material in BFB(kg)	19.77	17.52	15.12
L_f (m)	0.575	0.506	0.457
L_{mf} (m)	0.398	0.342	0.304
ε_f	0.601	0.611	0.617

τ_f (s)	0.249	0.215	0.192

5.3. Results and discussion

5.3.1. Effect of mean gas residence time

Fig. 5-2 presents the results of composition of producer gas at different means gas residence time, τ_f in initial devolatilization. From the figure, it can be seen that the influence of τ_f on the compositions of gas from initial devolatilization were not obvious. With τ_f increasing from 0.19 to 0.25, the concentrations of H_2, CO and CO_2 were found to be virtually constant at approximately 25%, 43% and 13%, respectively. The concentration of CH_4 was slightly increased from 13% to 15%. In the devolatilization stage, the primary decomposition of biomass releases the volatile matter from biomass to produce both condensable vapours and non-condensable gas [17]. The non-condensable gas including the light species like H_2, CO, CO_2 and CH_4 is the main gas product in the devolatilization [18]. The yield and composition of non-condensable gas depend on the reaction temperature and biomass properties. The condensable vapours, which consist of heavier molecules species, can condense to form tar compounds if being cooled down. However, if these compounds are held in contact with biomass within the reactor, they undergo secondary cracking reactions, which may be reformed to char, secondary tar compounds, and non-condensable gases [19]. Therefore, a longer residence time favour secondary cracking reaction, affecting the yield and composition of tar in the initial devolatilization which will be discussed later.

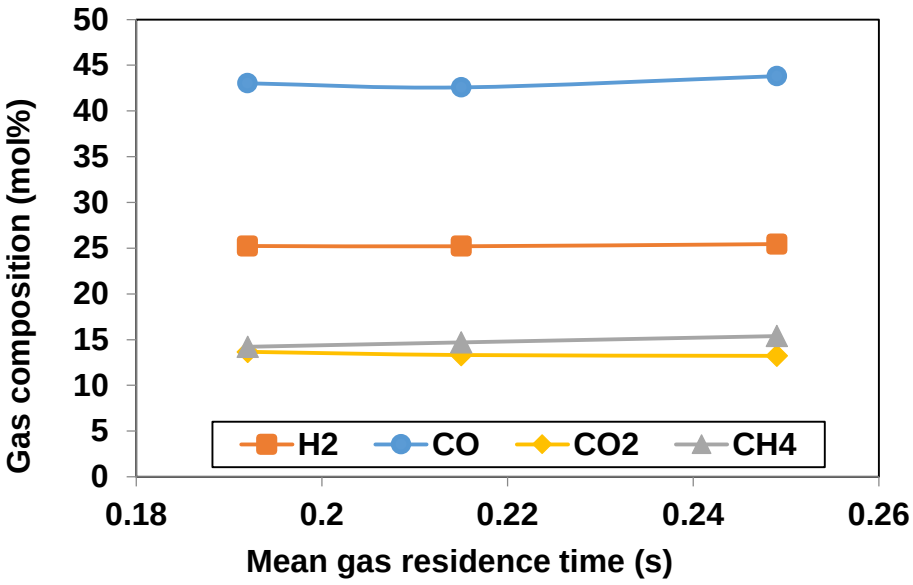

Fig. 5-2. The effect of gas residence time on gas composition in devolatilization.

The influence of τ_f on the final producer gas composition is shown in Fig. 5-3. It is found that with τ_f increasing from 0.19 to 0.25 s, the concentration of H_2 was increased from 27% to 30% and those of CO_2 and CH_4 were increased from 15% to 18% and from 12% to 14%, respectively. However, the concentration of CO was decreased from 39% to 36%. During the steam gasification, the gas formation is related to the reactions among gas, char, tar and steam [16, 20, 21]. In particular, the contact time and position between char and tar with steam in the reactor are important factors on reaction rates and state towards the equilibrium. For example, when the biomass is fed at the bottom of the reactor, the devolatilization is rapid and releases volatiles in the bottom zone of the bed while the char particles circulate within the bed which can thus have longer contacting time with steam for char steam reaction. The 100kW dual fluidised gasifier in the present study has an in-bed feeding system where the feeding position is approximately 0.13m above the BFB base. As shown in Table 5-2, the expansion bed height was 0.58, 0.51 and 0.46m with an initial sand loading (inventory) of 30, 25 and 20kg, respectively. Therefore, a long residence time promoted the char-related reaction, such steam-char reaction, Boudouard reaction and Methanation reaction. In addition, the increase in τ_f promoted the water-gas shift reaction toward the production of H_2 and CO_2 [22], leading to the increase in the concentrations of H_2, CO_2 and CH_4 in the producer gas.

Fig. 5-4 presents the results of carbon conversion in devolatilization and final gasification as a function of τ_f. The carbon conversion was defined as the total carbon content in the gas products (CO, CO_2, CH_4, C_2H_4 and C_2H_6) divided by the total carbon content found in the wood pellets with a dry and ash free (daf) basis. In Fig.5-4, it was found that with τ_f increasing from 0.19 to 0.21, the carbon conversion in devolatilization was slightly increased from 55% to 61%, while that in final gasification stage was significantly increased from 62% to 77%. The conversion of char in the final stage of gasification is affected by the heterogeneous char-gas reactions, which are much slower at a given temperature that the homogenous gas-gas reaction [23]. Therefore, char conversion may be limited unless the residence time is sufficiently long.

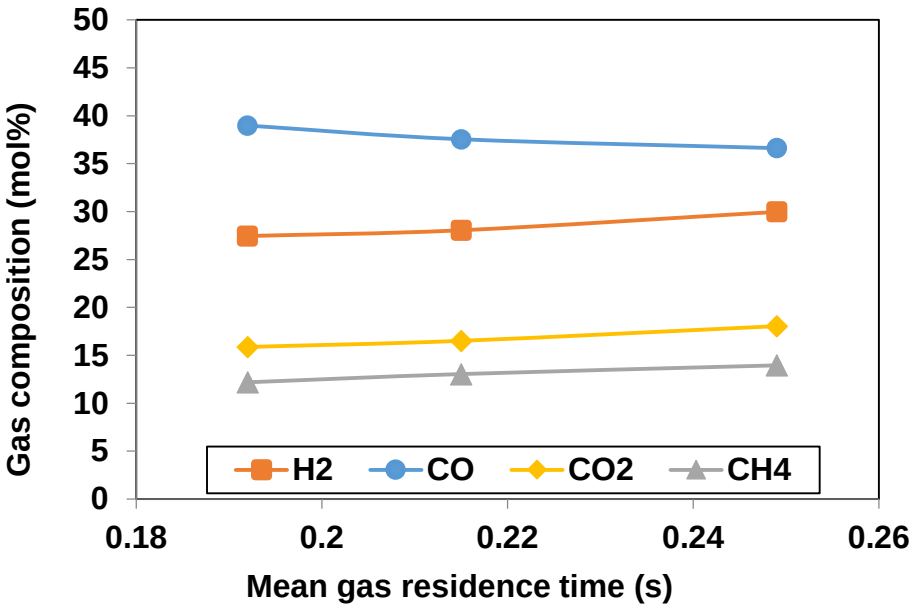

Fig. 5-3. The effect of gas residence time on gas composition in final gasification.

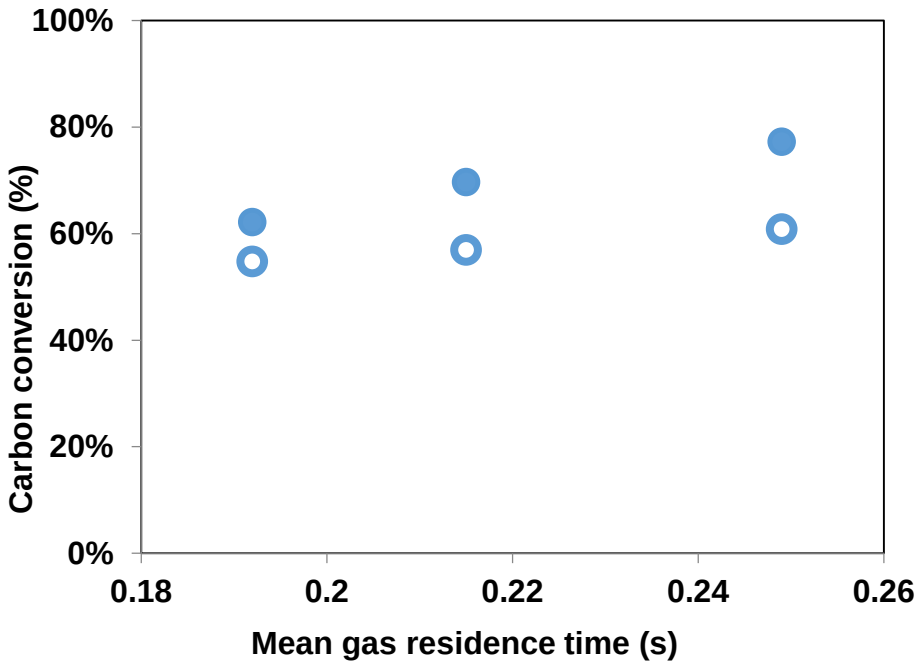

Fig. 5-4. The comparison of carbon conversion with mean gas residence time in the devolatilization (hollow point) and final gasification (solid point).

The correlation on tar yield between the initial devolatilization stage and the final steam gasification process as a function of mean gas residence time, τ_f can be established from the experimental results, which is shown in Fig.5-5. The tar concentrations were measured by the GC-FID and the tar compounds were classified following the method described in Chapter 3. From Fig. 5-5, it can be seen that the tar yield in the final steam gasification was decreased as τ_f was increased from 0.19 to 0.25s, in the same trend as the tar yield from devolatilization, but was lower than the tar yield from devolatilization at all of the gas residence times. At τ_f of 0.19s, the total tar yield was reduced by 31% from 17.3 g/kg_{daf} in the initial devolatilization to 11.9 g/kg_{daf} in the final gasification. This corresponding reduction was 34% for 0.22s, from 13.8 to 9.1 g/kg_{daf}; and 36% for 0.25s, from 11.8 to 7.7 g/kg_{daf}. It is believed that a longer residence time promotes steam tar reforming reaction thus the tar compounds were reduced in the producer gas.

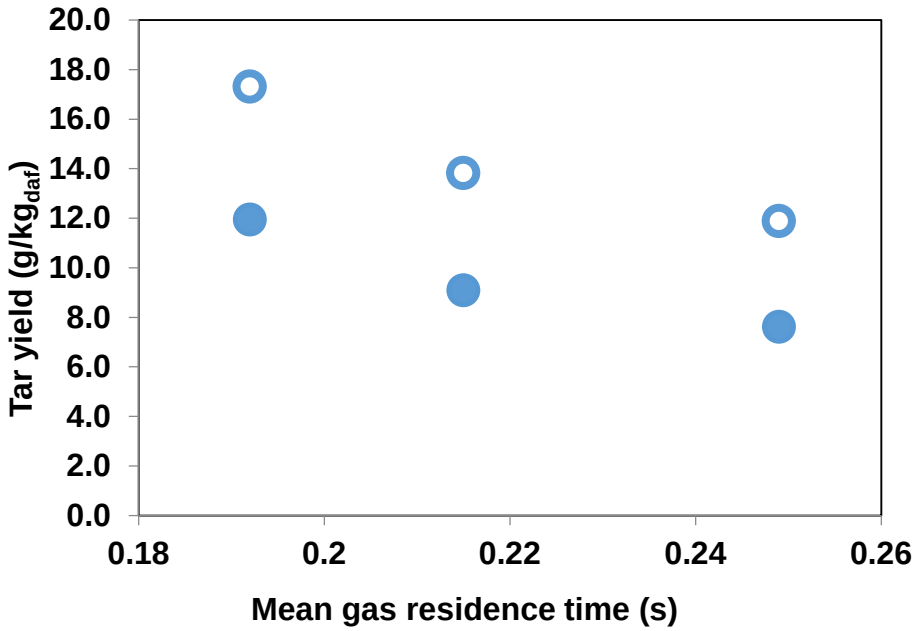

Fig. 5-5. The comparison of tar yield with mean gas residence time in the devolatilization (hollow point) and final gasification (solid point).

In order to quantify the changes of tar yield and composition from the initial devolatilization to final steam gasification. 11 different tar compounds were detected and classified into 5 classes. The tar compounds include phenols, toluene, styrene, xylene, cresol, indene, naphthalene, methylnaphthalene, biphenyl, PAH with 3 aromatic rings and PAH with 4 and more aromatic rings. The yield proportions of each tar compound to the total tar yield in devolatilization stage are shown in Fig. 5-6 for the three gas residence times tested. From Fig. 5-6, it is found that the yield proportions of tar compounds with single aromatic ring were reduced as τ_f increased from 0.19 to 0.25s. For example, the yield proportion of toluene was deceased from 14% to 6%, while that of phenols decreased from 23% to 17%. The yield proportion of PAHs with 2 aromatic rings, such as indene, naphthalene and methylnaphthalene were found to be virtually constant at approximately 12%, 18% and 6%, respectively. However, the yield proportion of PAH with 3 aromatic rings was slightly increased from 14% to 18%, and a similar trend was also obtained for PAHs with 4 and more aromatic rings, which overall yield proportion was increased from 3% to 7%. In the devolatilization, after the primary decomposition, the secondary cracking reactions further converted the primary products from biomass to secondary and tertiary tar, char and non-condensable gas [24].

The secondary cracking reactions involved two pathways, one was dehydration and decarboxylation to remove alkyl groups attached to the aromatic rings, the other was depolymerisation to form the PAH tar compounds [25]. Therefore, a longer residence time would promote the reduction of secondary tar yield, while the formation of heavy PAH is favoured.

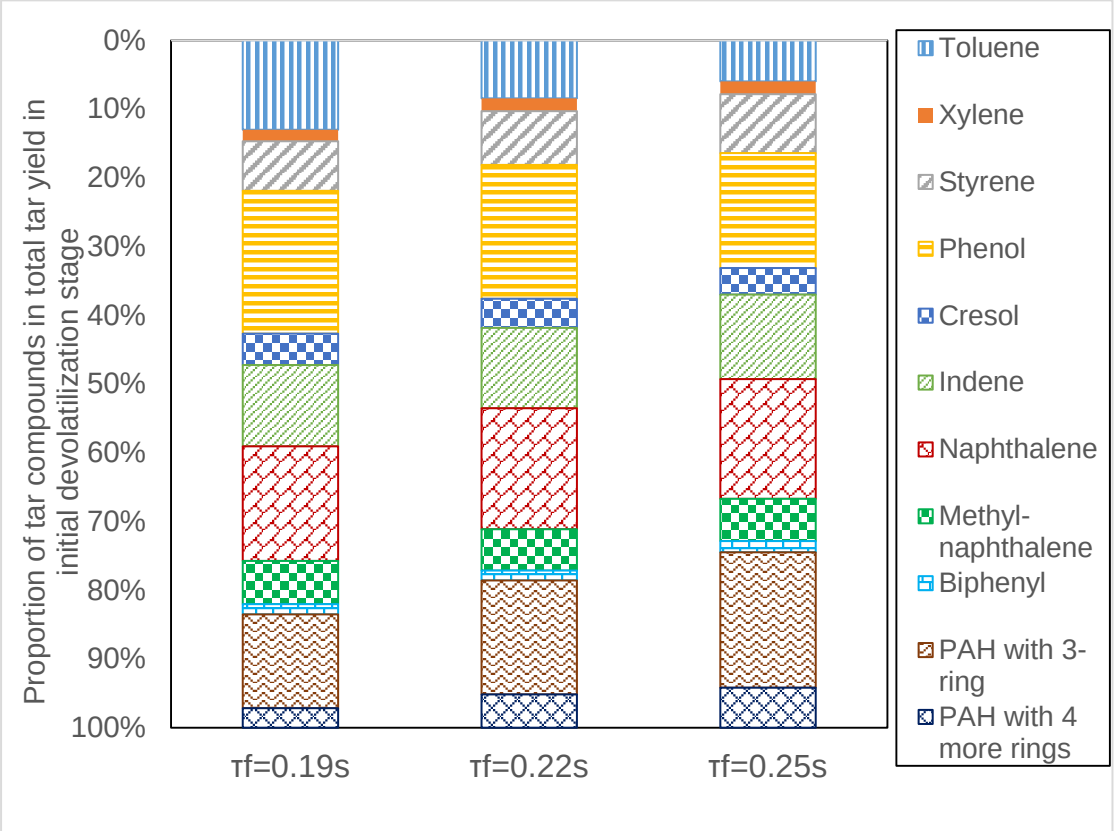

Fig. 5-6. Proportions of yields of different tar compound to the total tar yield in the initial devolatilization stage in biomass gasification with different gas residence times.

Fig. 5-7 presents the changes in yield of each type of tar compound from the initial devolatilization stage to the final gasification process at different gas residence times. It is found that the yields of light tar compounds such as toluene, styrene and phenols were significantly reduced. At τ_f of 0.19s, the yield proportion of toluene was decreased from 14% in the devolatilization to 3% in the final gasification, while that of phenols was decreased from 23% to 15%. Similar trends were also observed at the other two residence times. However, the yields of PAH compounds were all increased. For example, at τ_f of 0.25s, the yield proportion of naphthalene was increased from 17%

to 25%, while that of PAHs with 4 and more aromatic rings was significantly increased from 6% to 10%. It is believed that the injection of steam favoured the steam-tar reforming reactions to reduce the heterotic tar and enhanced the formation of PAH tar.

The results from Fig. 5-7 also illustrate the effect of τ_f on the tar compound distribution in the producer gas from final gasification stage. With the increase of τ_f from 0.19 to 0.25, the proportions of all light tar compounds such as toluene, xylene, styrene and phenols were slight decreased. The proportions of PAHs with 2 aromatic rings, such as naphthalene and methylnaphthalene were found to be virtually constant at approximately 25% and 7%, respectively. However, the proportions of heavy PAH compounds were increased. These results were consistent with those of Kinoshita et al. [26] who found that with increasing residence time, the yields of oxygenated tar compound and 1- and 2- ring tar components were decreased, but those of 3- and 4-ring tar components were increased. Hence, in the producer gas from final steam gasification, the tar contains a larger fraction of PAH tars at a longer residence time.

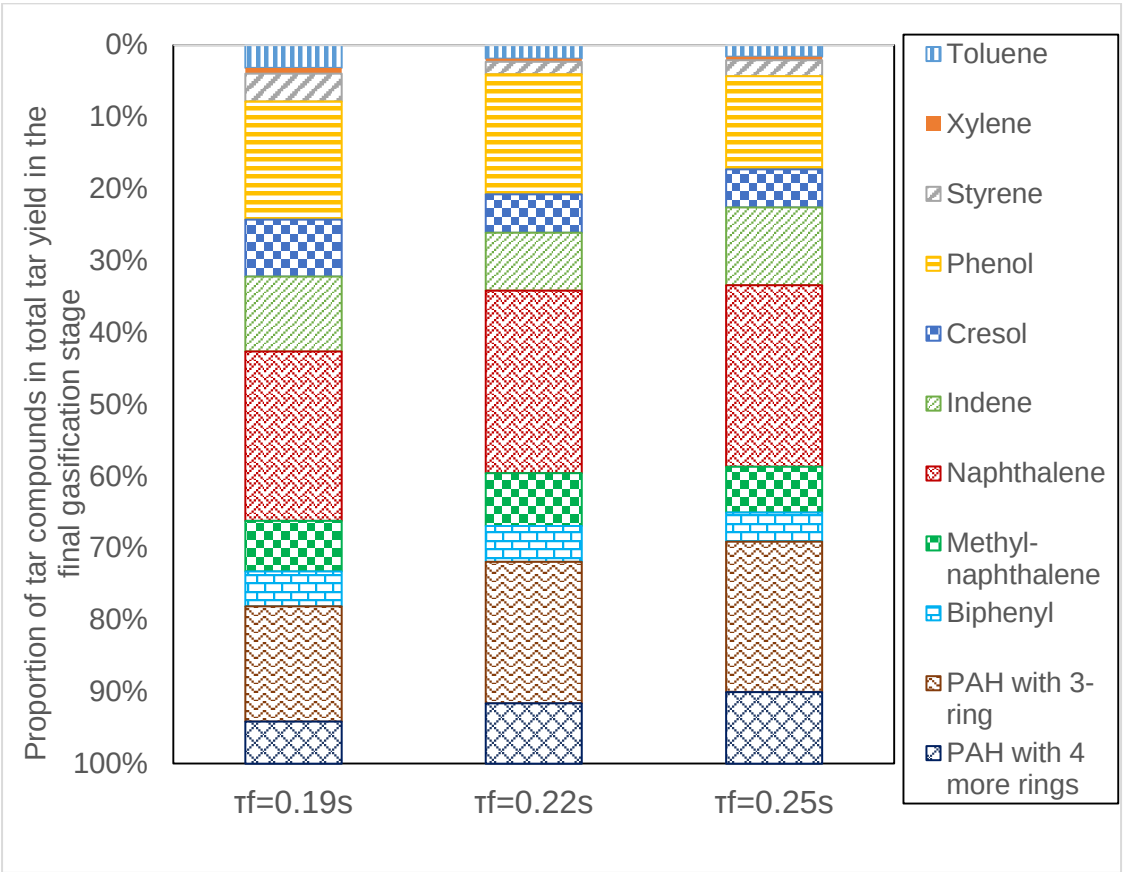

Fig. 5-7. Proportions of yields of different tar compounds to the total tar yield in the final gasification stage with different gas residence times.

The above phenomena can be explained by tar compounds thermal transformation and cracking from which more stable tar compounds were formed. This process was enhanced with a longer residence time in contact with the bed material. Therefore, as τ_f increased, Class 2 tar compounds were reduced due to the highly reactive of the heteroatoms group (N and O) attached in aromatic ring. The significant decomposition of Class 2 tar compounds provided more single aromatic ring units, which are the precursors for the formation of PAH tar compounds with multiple aromatic rings [27]. In addition, these light PAH tar compounds would be either converted into light gases by steam reforming or reformed into heavy tar compounds by dimerization and cyclisation, leading the increase in Class 4 and Class 5 tar yields [28].

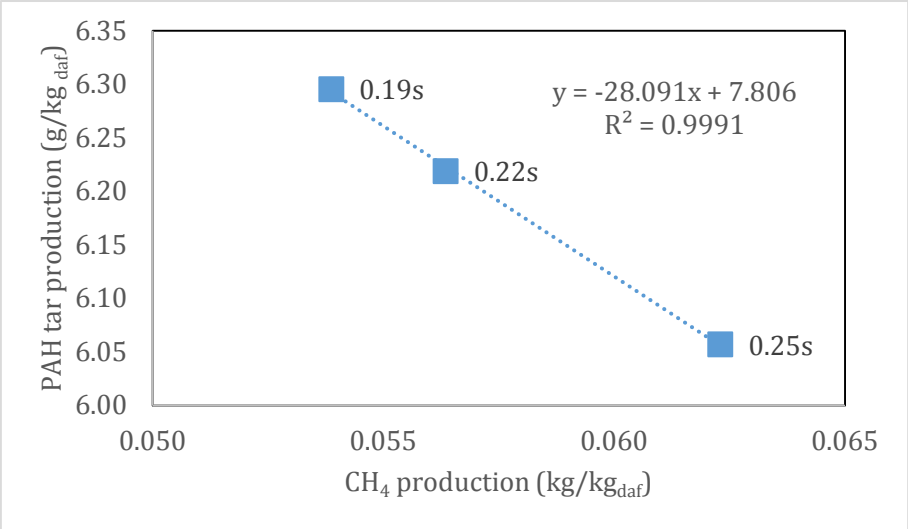

(a)

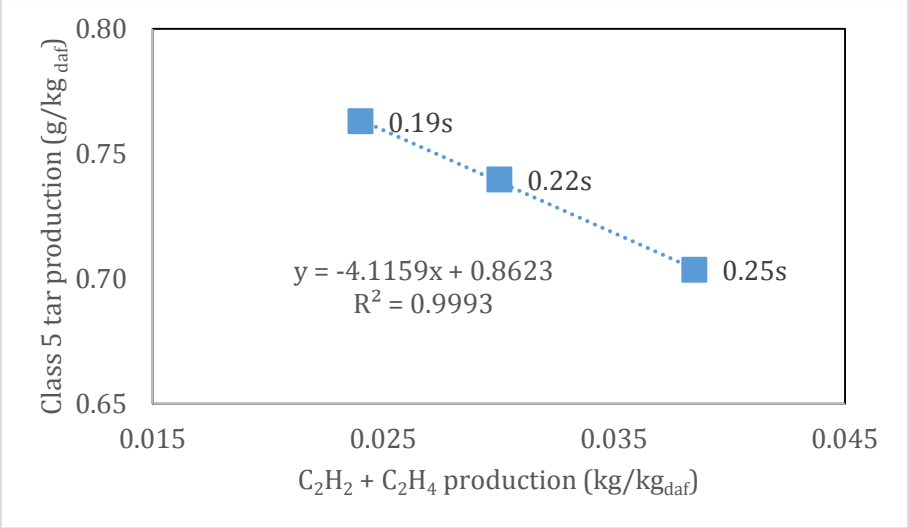

(b)

Fig. 5-8. Correlations (a) between PAH tar with 2 and 3 rings and CH_4 production and (b) between Class 5 tar and C_2H_2 + C_2H_4 production in devolatilization

In the initial devolatilization, the yields of PAH tar and light gas are clearly correlated with the tested residence time (from 0.19 to 0.25s) as shown in Fig. 5-8. Linear relations between the mass production of light PAH tar and CH_4 and between Class 5 tar and C_2 light gas were found with a good regression factor. Consequently, CH_4 and C_2 light gas could also be used as indicators of tar production and speciation under the range of investigated residence time.

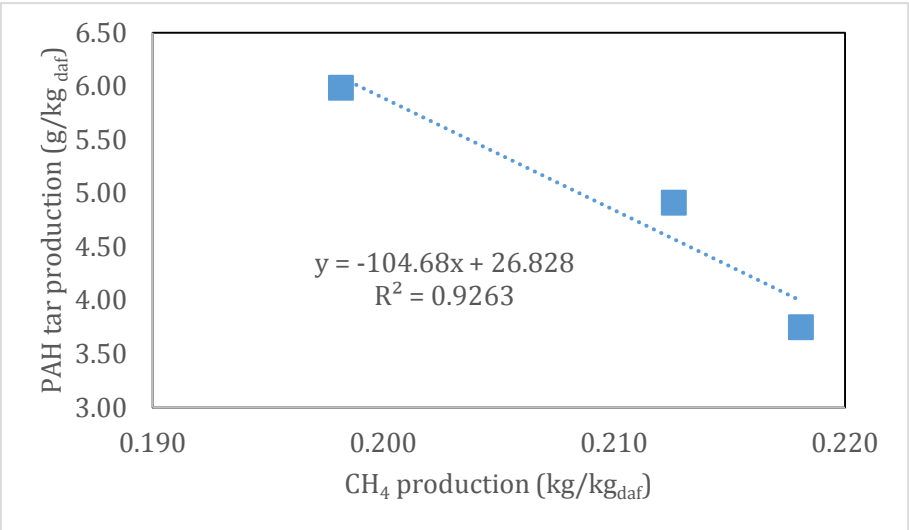

(a)

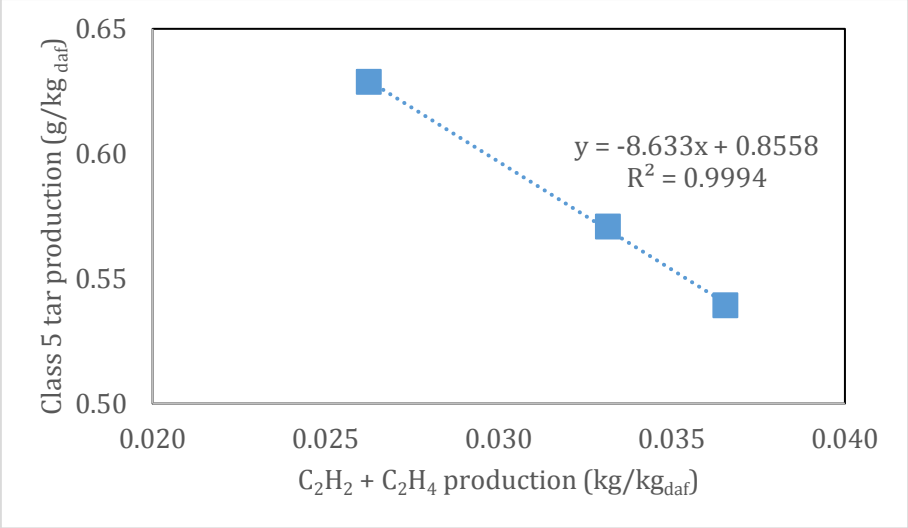

(b)

Fig. 5-9. Correlations (a) between PAH tar with 2 and 3 rings and CH_4 production and (b) between Class 5 tar and C_2H_2 + C_2H_4 production in steam gasification

The correlation on mass production between the light gas and the tar in the devolatilization are shown, respectively, in Fig. 5-8 (a) for PAH tar with 2 and 3 rings and CH_4 production, and Fig. 5-8(b) for Class 5 tar and C_2H_2 + C_2H_4 production. The linear relation on Class 5 tar – C_2 light gas can be used as a simple method for the estimation of the Class 5 tar production by measuring the C_2 light gas. However, the injection of steam affects the reactions of tar and CH_4 reforming, leading that the relation on light PAH tar – CH4 did not perfectly match a linear relationship.

5.3.2. Effect of steam to biomass (S/B) ratio

Steam to biomass (S/B) ratio is the mass flow rate of injected steam plus the moisture in the biomass to the mass flow rate of oven dry biomass into the gasifier. S/B is another important parameter in steam gasification, as the steam is crucial for heterogeneous char-steam gasification, Methanation reaction, water–gas shift reaction, steam methane reforming and tar-steam reforming reactions. The S/B ratio can be varied either by changing the biomass feeding rate while keeping the steam flow constant or vice versa. In this study, the steam flow rate was kept constant, and the S/B ratio was controlled by changing the biomass feeding rate. In this way, the residence time in the BFB gasification reactor was maintained at the pre-set values.

Fig. 5-8 presents the total gas yield from devolatilization and that from final steam gasification with different S/B ratios at the same operation temperature of 800°C. The gas yield was calculated as the production rate of gas product (kg/h) divided by the feeding rate of oven dry biomass (kg_{daf}/h). From Fig. 5-8, it is seen that the gas yield from the devolatilization was 0.59 kg/kg_{daf}. When steam was introduced for steam gasification, the gas yield in the final gasification was significantly increased to 0.66 kg/kg_{daf} at S/B ratio of 0.63. The producer gas yield was further increased with increase in the S/B ratio, to 0.75 kg/kg_{daf} at S/B ratio of 0.89, to 0.88 kg/kg_{daf} at S/B ratio of 1.21 and to 0.98 kg/kg_{daf} at S/B ratio of 1.51. This confirms that the presence of steam has promoted the char gasification, thus increasing the gas production [29].

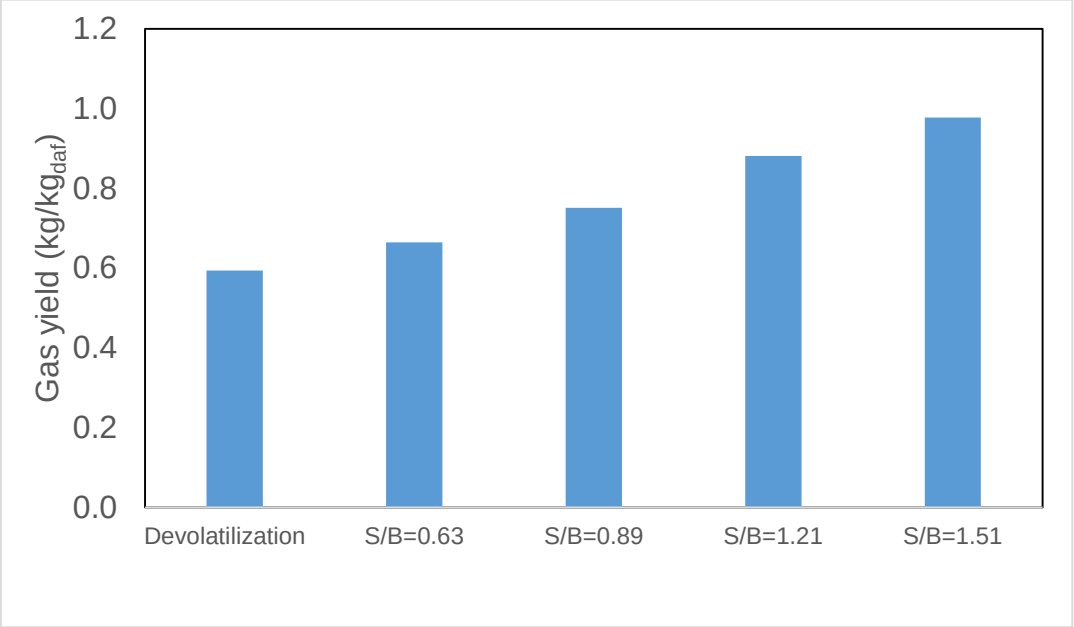

Fig. 5-10. Yields of producer gas from the devolatilization stage and the final steam gasification stage with different S/B ratios at 800°C.

The effect of S/B ratio on the concentration of each gas species (H_2, CO, CO and CH_4) are shown in Fig. 5-9. It is observed that, with S/B ratio increasing from 0.63 to 1.51, the H_2 concentration was significantly increased from 29.5% to 34.8% and the CO_2 concentration was increased from 16.7% to 22.1%. On the contrary, the CO concentration was decreased from 38.8% to 28.2% while the CH_4 concentration was slightly dropped from 14.1% to 10.5%. Similar observations on the gas composition changes with S/B ratio were reported in the literature [30]. It is believed that the increase

of S/B ratio promoted the char-steam reaction and water–gas shift reaction towards H_2 formation direction [31], and enhanced steam-methane reforming reaction [32].

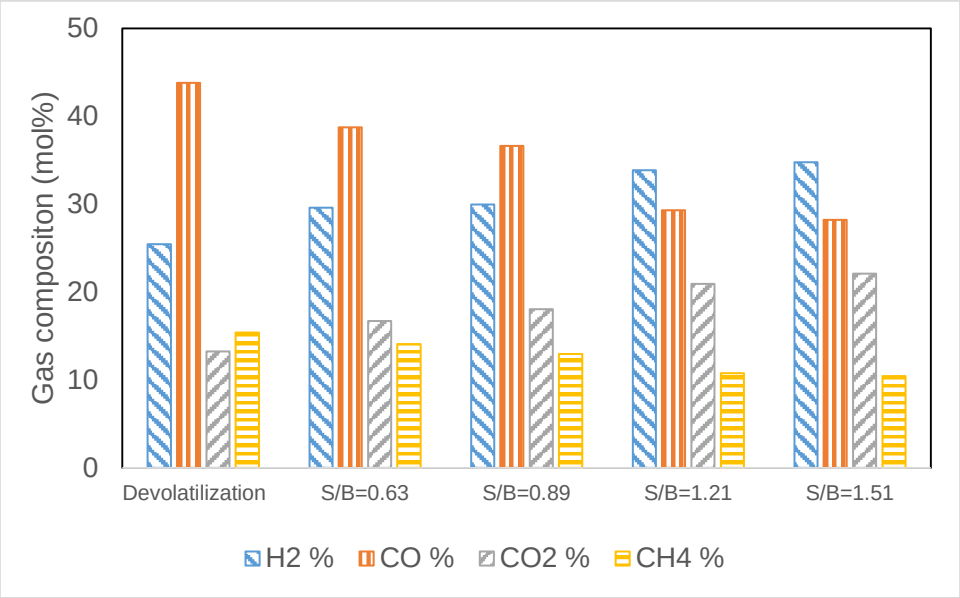

Fig. 5-11. Concentrations of gas species in the producer gas from the devolatilization stage and the final steam gasification stage with different S/B ratios at 800°C.

The effects of S/B ratio on the tar compounds have also been examined in the experiments, and the results are illustrated in Fig. 5-10. It can be clearly seen that the tar yield was significantly reduced in the gasification stage and this was further reduced with increment of S/B. With increasing S/B from 0.63 to 1.51, the total tar yield decreased from 9.5 to 5.1 g/kg_{daf}. This can be expected since high S/B ratio favours the reforming of hydrocarbons, leading to a reduction of the tar yields [33, 34]. Fig. 5-10 also shows the yield of different class of tar compounds from which it is found that with increase of S/B ratio in the above range, the yield of Class 2 tar compounds was decreased from 4.5 to 2.1 g/kg_{daf} while that of Class 3 and Class 4 tar compounds were reduced. However, with the increase of S/B ratio in the above range, the yield of Class 5 tar compounds was increased from 0.72 to 0.99 g/kg_{daf}. These results are in consistent with those from Tursun et al. [35].

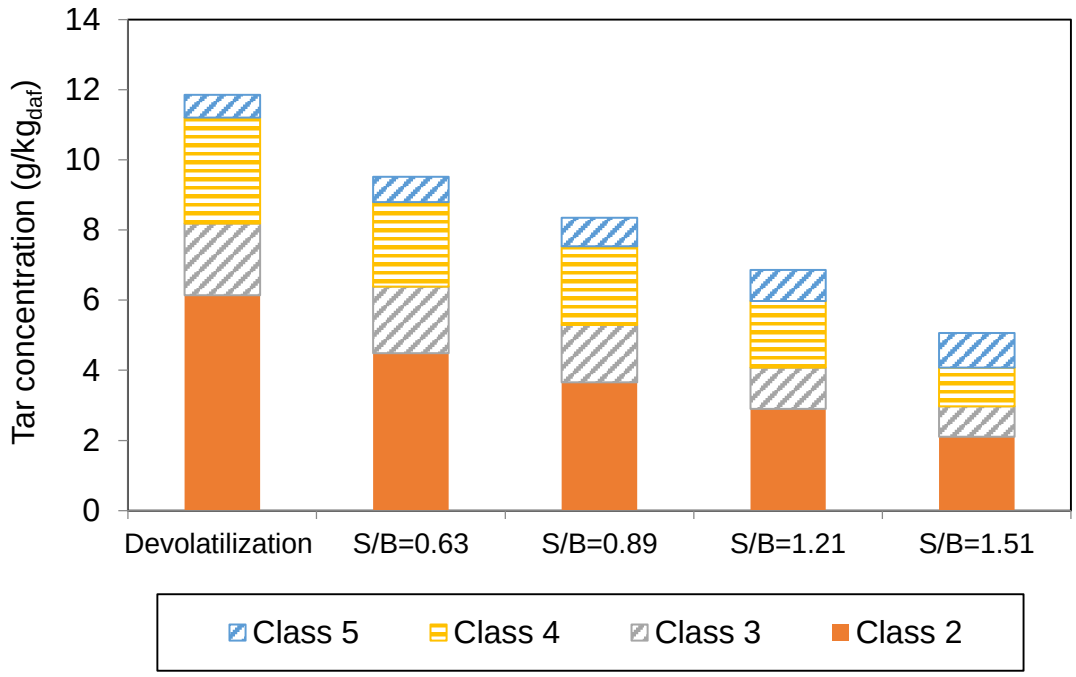

Fig. 5-12. Tar yields from the devolatilization stage and the final steam gasification stage with different S/B ratios at 800°C.

Fig. 5-11 presents the effect of S/B on the proportion of each type of tar compounds. With increase of S/B ratio, the proportion of oxygen containing tar compounds such as phenols and cresols were decreased. The phenomena can be explained by the high S/B ratio increases the concentration of H^+ radical from steam and H_2, which enhances the dealkylation and decarboxylation of heterocyclic tar compounds [36]. The proportion of naphthalene was decreased from 20% to 15% with increasing S/B from 0.63 to 1.51. This result indicates that increased steam enhanced decomposition of naphthalene [35]. The similar trends were obtained for the other 2-ring PAH compounds of indene and biphenyl. It is interesting to notice that the proportion of PAH compounds with three and more aromatic rings was increased when the S/B was increased from 0.63 to 1.51. It can be proposed that the increase of S/B ratio also promoted the reactions of dimerization and cyclisation (H_2-abstraction-C_2H_2-addition sequence) due to an increase of the H^+ radical and intact aromaticity of tar from heterocyclic tar decomposition, leading to the formation of ploy-aromatic tar compounds [37].

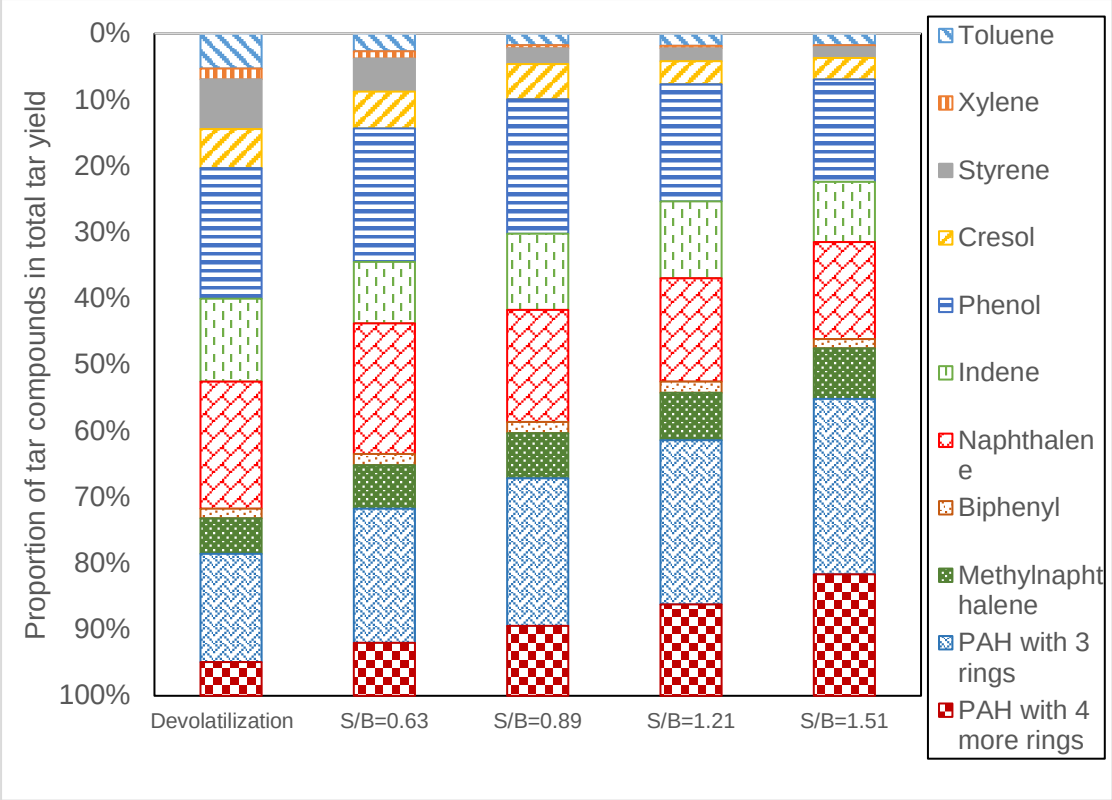

Fig. 5-13. Proportions of yields of different tar compounds to the total tar yield from the devolatilization stage and the final steam gasification stage with different S/B ratios at 800°C.

5.4 Conclusion

The influence of gas residence time and steam to biomass ratio on the performance of a DFB steam gasifier has been experimentally examined. This study also establishes the correlation on yield and composition of the producer gas and tar compounds between the initial devolatilization stage and the final steam gasification.

Key findings from the present studies are:

- The effect of mean gas residence time (τ_f) on the gas composition in initial devolatilization stage was not significant, but the gas residence time had significant effect in the final gasification. With increase of τ_f, the concentrations of H_2, CO_2 and CH_4 in the producer gas were increased while the CO concentration was reduced. It is believed that the τ_f promoted the char-related reaction during the steam gasification.

- As τ_f increased from 0.19 to 0.25s, the total tar yield was reduced from 17.3 to 11.8 g/kg_{daf} in the initial devolatilization, while that in the final gasification was decreased from 11.9 to 7.7 g/kg_{daf}. Gas residence time also affected tar composition. With increase in τ_f, the proportions of tar compounds with single aromatic ring such as toluene and phenols were reduced. The proportion of PAH with 2 aromatic rings, such as indene, naphthalene and methylnaphthalene were found to be virtually constant. However, the proportion of PAH with 3 and more aromatic rings was slightly increased.

- With increase of steam to biomass ratio, gas production was increased and the tar yield was reduced in steam gasification since the char-steam reaction and tar steam reforming reaction were enhanced with increase in the steam input. The steam to biomass ratio affected the equilibrium state of water-gas shift reaction and methane steam reforming, therefore, with increase of steam to biomass ratio, the H_2 and CO_2 contents in the producer gas were increased, but CO and CH_4 contents were reduced.

- The steam to biomass (S/B) ratio had a different impact on different tar compounds although the total tar yield was reduced with increase in the S/B ratio. With the increase in S/B ratio, the concentrations of Class 2, Class 3 and Class 4 tar compounds were decreased while that of Class 5 tar compounds was increased.

5.5. Reference

[1] I. Aigner, C. Pfeifer, and H. Hofbauer, "Co-gasification of coal and wood in a dual fluidized bed gasifier," *Fuel*, vol. 90, pp. 2404-2412, 2011.

[2] F. Kirnbauer, V. Wilk, and H. Hofbauer, "Performance improvement of dual fluidized bed gasifiers by temperature reduction: The behavior of tar species in the product gas," *Fuel*, vol. 108, pp. 534-542, 2013.

[3] T. Murakami, G. Xu, T. Suda, Y. Matsuzawa, H. Tani, and T. Fujimori, "Some process fundamentals of biomass gasification in dual fluidized bed," *Fuel*, vol. 86, pp. 244-255, 2007.

[4] C. Pfeifer, S. Koppatz, and H. Hofbauer, "Steam gasification of various feedstocks at a dual fluidised bed gasifier: Impacts of operation conditions and bed materials," *Biomass Conversion and Biorefinery*, vol. 1, pp. 39-53, 2011.

[5] J. C. Schmid, U. Wolfesberger, S. Koppatz, C. Pfeifer, and H. Hofbauer, "Variation of feedstock in a dual fluidized bed steam gasifier—influence on product gas, tar content, and composition," *Environmental Progress & Sustainable Energy*, vol. 31, pp. 205-215, 2012.

[6] J. Kiel, S. Van Paasen, J. Neeft, L. Devi, K. Ptasinski, F. Janssen, R. Meijer, R. Berends, H. Temmink, and G. Brem, "Primary measures to reduce tar formation in fluidised-bed biomass gasifiers," Energy research Centre of the Netherlands (ECN) Report, The Netherlands, ECN-C-04-014, 2004.

[7] H. Liu, M. Kaneko, C. Luo, S. Kato, and T. Kojima, "Effect of pyrolysis time on the gasification reactivity of char with CO2 at elevated temperatures," *Fuel*, vol. 83, pp. 1055-1061, 2004.

[8] W. L. Saw and S. Pang, "Influence of mean gas residence time in the bubbling fluidised bed on the performance of a 100-kW dual fluidised bed steam gasifier," *Biomass Conversion and Biorefinery*, vol. 2, pp. 197-205, 2012.

[9] A. Gómez-Barea and B. Leckner, "Modeling of biomass gasification in fluidized bed," *Progress in Energy and Combustion Science*, vol. 36, pp. 444-509, 2010.

[10] J. J. Manyà, J. L. Sánchez, J. Ábrego, A. Gonzalo, and J. Arauzo, "Influence of gas residence time and air ratio on the air gasification of dried sewage sludge in a bubbling fluidised bed," *Fuel*, vol. 85, pp. 2027-2033, 2006.

[11] J. J. Hernández, G. Aranda-Almansa, and A. Bula, "Gasification of biomass wastes in an entrained flow gasifier: Effect of the particle size and the residence time," *Fuel Processing Technology,* vol. 91, pp. 681-692, 2010.

[12] A. Jess, "Mechanisms and kinetics of thermal reactions of aromatic hydrocarbons from pyrolysis of solid fuels," *Fuel,* vol. 75, pp. 1441-1448, 1996.

[13] D. Fuentes-Cano, A. Gómez-Barea, S. Nilsson, and P. Ollero, "The influence of temperature and steam on the yields of tar and light hydrocarbon compounds during devolatilization of dried sewage sludge in a fluidized bed," *Fuel,* vol. 108, pp. 341-350, 2013.

[14] J. Herguido, J. Corella, and J. Gonzalez-Saiz, "Steam gasification of lignocellulosic residues in a fluidized bed at a small pilot scale. Effect of the type of feedstock," *Industrial & Engineering Chemistry Research,* vol. 31, pp. 1274-1282, 1992.

[15] Y. Wang, T. Namioka, and K. Yoshikawa, "Effects of the reforming reagents and fuel species on tar reforming reaction," *Bioresource Technology,* vol. 100, pp. 6610-6614, 2009.

[16] D. Geldart, *Gas Fluidization Technology*. Chichester, United Kingdom: John Wiley and Sons Ltd, 1986.

[17] A. Tremel and H. Spliethoff, "Gasification kinetics during entrained flow gasification – Part I: Devolatilisation and char deactivation," *Fuel,* vol. 103, pp. 663-671, 2013.

[18] E. Granada, P. Eguía, J. A. Comesaña, D. Patiño, J. Porteiro, and J. L. Miguez, "Devolatilization behaviour and pyrolysis kinetic modelling of Spanish biomass fuels," *Journal of Thermal Analysis and Calorimetry,* vol. 113, pp. 569-578, 2013.

[19] P. Basu, *Biomass gasification and pyrolysis : practical design and theory*. Burlington, MA: Academic Press, 2010.

[20] A. Gómez-Barea, P. Ollero, and B. Leckner, "Optimization of char and tar conversion in fluidized bed biomass gasifiers," *Fuel,* vol. 103, pp. 42-52, 2013.

[21] D. Kunii and O. Levenspiel, *Fluidization Engineering*, Second Edition ed. Boston: Butterworth-Heinemann, 1991.

[22] J. Corella, M. P. Aznar, J. Delgado, and E. Aldea, "Steam gasification of cellulosic wastes in a fluidized bed with downstream vessels," *Industrial & engineering chemistry research,* vol. 30, pp. 2252-2262, 1991.

[23] M. L. d. Souza-Santos, *Solid fuels combustion and gasification : modeling, simulation, and equipment operations,* 2nd ed. Boca Raton: Taylor & Francis, 2010.

[24] T. Hosoya, H. Kawamoto, and S. Saka, "Secondary reactions of lignin-derived primary tar components," *Journal of Analytical and Applied Pyrolysis,* vol. 83, pp. 78-87, 2008.

[25] M. Zhai, X. Wang, Y. Zhang, P. Dong, G. Qi, and Y. Huang, "Characteristics of rice husk tar secondary thermal cracking," *Energy,* vol. 93, pp. 1321-1327, 2015.

[26] C. Kinoshita, Y. Wang, and J. Zhou, "Tar formation under different biomass gasification conditions," *Journal of Analytical and Applied Pyrolysis,* vol. 29, pp. 169-181, 1994.

[27] A. Sharma, V. Pareek, and D. Zhang, "Biomass pyrolysis—A review of modelling, process parameters and catalytic studies," *Renewable and Sustainable Energy Reviews,* vol. 50, pp. 1081-1096, 2015.

[28] S. Van Paasen, J. Kiel, and H. Veringa, "Tar formation in a fluidised bed gasifier," Energy research Centre of the Netherlands (ECN) Report, The Netherlands, ECN-C-04-013, 2004.

[29] X. Xiao, X. Meng, D. D. Le, and T. Takarada, "Two-stage steam gasification of waste biomass in fluidized bed at low temperature: parametric investigations and performance optimization," *Bioresource Technology,* vol. 102, pp. 1975-1981, 2011.

[30] K. Umeki, K. Yamamoto, T. Namioka, and K. Yoshikawa, "High temperature steam-only gasification of woody biomass," *Applied Energy,* vol. 87, pp. 791-798, 2009.

[31] L. Wei, S. Xu, L. Zhang, C. Liu, H. Zhu, and S. Liu, "Steam gasification of biomass for hydrogen-rich gas in a free-fall reactor," *International Journal of Hydrogen Energy,* vol. 32, pp. 24-31, 2007.

[32] Z. A. B. Z. Alauddin, P. Lahijani, M. Mohammadi, and A. R. Mohamed, "Gasification of lignocellulosic biomass in fluidized beds for renewable

energy development: A review," *Renewable and Sustainable Energy Reviews*, vol. 14, pp. 2852-2862, 2010.

[33] C. Li and K. Suzuki, "Tar property, analysis, reforming mechanism and model for biomass gasification—An overview," *Renewable and Sustainable Energy Reviews*, vol. 13, pp. 594-604, 2009.

[34] J. Moon, J. Lee, U. Lee, and J. Hwang, "Transient behavior of devolatilization and char reaction during steam gasification of biomass," *Bioresource Technology*, vol. 133, pp. 429-436, 2013.

[35] Y. Tursun, S. Xu, G. Wang, C. Wang, and Y. Xiao, "Tar formation during co-gasification of biomass and coal under different gasification condition," *Journal of Analytical and Applied Pyrolysis*, vol. 111, pp. 191-199, 2015.

[36] A. Gani and I. Naruse, "Effect of cellulose and lignin content on pyrolysis and combustion characteristics for several types of biomass," *Renewable Energy*, vol. 32, pp. 649-661, 2007.

[37] B. Vreugdenhil, R. Zwart, and J. P. A. Neeft, "Tar formation in pyrolysis and gasification," Energy research Centre of the Netherlands (ECN) Report, The Netherlands, ECN-E--08-087, 2009.

Chapter 6. Effect of Biomass Species on Tar Formation in Biomass Steam Gasification

This chapter is based on a journal paper submitted to 'Renewable Energy'. In this study, various types of biomass including corn stover, radiata pine wood and rice husk in the form of pellets were gasified with steam as gasification agent in a 100kW dual fluidised bed gasifier. Tar formation in the initial devolatilization stage and its effect on the final tar concentration in the producer gas were investigated. In addition, the yields and composition of the producer gas for each type of biomass were also examined. In the gasification experiments, operation temperature was controlled, respectively, at 700°C and 800°C. Silica sand was used as the bed material with an inventory of 30kg. For simulation of the initial devolatilization stage in the steam gasification, N_2 was used as fluidisation agent.

From this study, it is found that there was a positive correlation between tar contents in the devolatilization product gas and tar contents in the final producer gas from gasification. In the devolatilization stage, radiata pine wood yielded more toluene, while corn stover generated more phenol and rice husk was between these two types of biomass. From these results, the tar formation mechanism was proposed which confirms that more naphthalene was present in the producer gas from gasification of radiata pine wood while gasification of corn stover had more biphenyl. The experimental results also showed that at gasification temperature of 700°C, the producer gas yield was the highest for corn stover followed by rice husk and then radiata pine wood. However, for gasification at 800°C, the trend was reversed with radiata pine wood having the highest yield followed by risk husk and the corn stover. At both 700 and 800℃, the radiata pine wood produced a producer gas with higher contents of H_2 and CH_4 while the producer gas from rice husk had higher content of CO and that from corn stover had higher content of CO_2, C_2H_4 and C_2H_6. Chemical composition of each biomass was analysed which shows that, among the three types of biomass, radiata pine wood had higher content of lignin (32.0 wt.%), rice husk had higher content of hemicellulose (25.3 wt.%) while corn stover was rich in cellulose (69.9 wt.%).

6.1. Introduction

Recently, extensive research has been conducted to optimise and commercialize biomass gasification technology for production of hydrogen-rich syngas [1-3]. The biomass is widely available [4] and a key renewable feedstock for the future energy production [5]. The key advantage of gasification technology is the high efficiency (70-80%) of converting a solid fuel into a gas which provides flexibility for it to be used for various energy products [6]. However, during the gasification process, part of the fuel is transformed into condensable tar compounds [7-9] which is one of most problematic by-product in biomass gasification processes. The tar compounds exist in the vapour phase in the gasifier but condense into liquid droplets while being cooled in gas transportation and in downstream processing. Once condensed, the tar may block the pipes and valves, and contaminates the processing equipment. Therefore, tar is one of the technical issues that hindered the commercialization of biomass gasification technology [10].

To avoid tar formation and eliminate tar components during biomass gasification, some tar removal technologies have been developed [11-14] which can be characterized by two approaches: (i) primary method – tar reduction inside the gasifiers, and (ii) secondary method – post-gasifier tar removal [15]. Although tar elimination after gasification is necessary to achieve the gas purity required by the downstream processing, it increases operating costs and reduces the overall efficiency of the gasification process [16]. The objective of this project was to understand and reduce tar formation (convert tars into lighter gases) during biomass gasification.

Tar formation is the result of a series of complex chemical reactions and molecular structure change. Tar concentration and composition in the gas product are dependent on the operational conditions, gasifier type, bed material used and biomass type. It has been reported that tar-cracking reactions are endothermic [16-21]. Therefore, increasing operation temperature is expected to promote the racking reactions thus decreasing tar concentration in the producer gas. Meanwhile, using steam as gasification agent has been observed to favour the tar reforming reactions [20]. Feedstock properties have noticeable effects on the tar formation. Different biomass materials can have different chemical compositions for cellulose, hemicellulose and

lignin. The difference in chemical composition and nature of these three components can also significantly affect tar characteristics [22]. Fundamental studies have been conducted on tar formation in gasification of both biomass and individual components of the biomass [23-26]. From these studies, it has been found that cellulose, hemicellulose and lignin have different thermal stability upon heating thus behave differently during gasification. Cellulose starts to decompose between 300°C and 400°C [27]. Hemicellulose is decomposed at relatively lower temperatures between 250°C and 350°C due to its lower thermal stability than cellulose. Hemicellulose yields more non-condensable gases and fewer tar compounds than the cellulose [24]. Lignin is thermally more stable than both the cellulose and the hemicellulose and it is not completely decomposed until 700°C [28, 29]. In Basu's report [30], pyrolysis of lignin produces about 55% char, 15% tar, 20% aqueous components and about 12% gases. The above differences can be tracked to the chemical structures of these three main components. Cellulose contains more OH and C-O chemical groups, hemicellulose has a higher proportion of C=O compounds [31, 32], while lignin was reported to be rich in methoxyl-O-CH_3, C-O-C and C=C chemical groups [33].

Most of previous studies were conducted for individual components of the biomass and using thermo-gravimetric analyser (TGA) and bench-scale batch gasification reactor [25, 26, 34, 35]. This approach is useful to understand and describe the gasification kinetics and tar formation. However, the results from these studies may be quite different from those in gasification of biomass at large scale continuous reactors. In gasification of biomass at a large scale reactor, the interaction of the three biomass components and combination of the tar compounds from the individual components would result in different tar yield and composition in the producer gas. In order to investigate the effect of potential interaction of cellulose and lignin, studies were reported on pyrolysis and gasification of both individual and combined cellulose, hemicellulose and lignin [36, 37]. However, limited research has been reported on the tar formation and tar composition from gasification of biomass in a pilot-scaled continuous gasification reactor.

In this part of study, experiments were conducted on gasification of three types of biomass in a pilot scaled system, a 100kW dual fluidised bed steam gasifier. Effects of biomass type have been investigated on tar yields and tar composition during the

gasification process. Chemical compositions of the biomass have also been analysed which results can be linked to the tar formation and tar composition.

6.2. Experimental and materials

6.2.1. Materials and chemical analysis

In the present study, three types of biomass, including rice husk, corn stover, and radiata pine wood (pine), were used as the feeding fuel for the experiments. The biomass was in the form of pellets of 10-15 mm long and 6 mm in diameter. Pellets of rice husk were provided by a company in Indonesia. Corn stover was supplied by a local farm in New Zealand which was processed to pellets in our laboratory. Pellets of pine were purchased from a local retailer in Christchurch, New Zealand.

Before the gasification experiments, samples of each type of biomass were sent to a commercial lab for proximate analysis and ultimate analysis, and the results are presented in Table 6-1. In addition, chemical composition of each biomass was also determined. The lignin content was measured based on TAPPI Standard methods, and the holocellulose (cellulose and hemicellulose) was tested by the modified method from Pettersen [38]. The results on the composition of these three feedstocks are shown in Fig. 6-1. By comparing these three types of biomass, it is found that corn stover is rich in cellulose (69.9 wt.%), pine has the highest content of lignin (32.0 wt.%), and rice husk has the highest content of hemicellulose (25.3 wt.%).

6.2.2. Equipment and procedures

Experiments were conducted on a 100kWth dual fluidised bed (DFB) gasifier with steam as gasification agent. The details of DFB gasifier and the operating procedures have been described in Chapter 3. N_2 was introduced into the BFB column as a fluidisation agent instead of steam in order to investigate the devolatilization performance in the DFB gasifier. In experiments, chute and siphon were both fluidised with controlled N_2 to enhance the bed material flow and to prevent cross-flows of gases between the two columns. The operation conditions of the gasification experiments in the present study are given in Table 6-2. In this study, the sampling and analysis methods for product gas and tar have also been given in Chapter 3.

Table 6-1. Results of proximate and ultimate analysis of the three types of biomass species.

		Corn stover	Rice husk	Pine
Proximate (%) (received basis)	Method			
Total moisture	ISO5068	10.4	8.9	8
Volatile matter	ISO 562	73.3	52.5	77.4
Fixed carbon	By difference	12.2	20.6	14.2
Ash	ASTM D1102	4.1	18	0.4
Ultimate (%) (Dry basis)				
Carbon	Microanalytical	48.5	38.5	51.3
Hydrogen	Microanalytical	6.2	5.2	5.8
Nitrogen	Microanalytical	1.1	0.5	<0.2
Sulphur	ASTM D4239	0.03	<0.1	<0.1
Oxygen	By difference	44	34.7	42.6
LHV (MJ/kg) (dry basis)	ISO1928	18.2	13.2	14.4

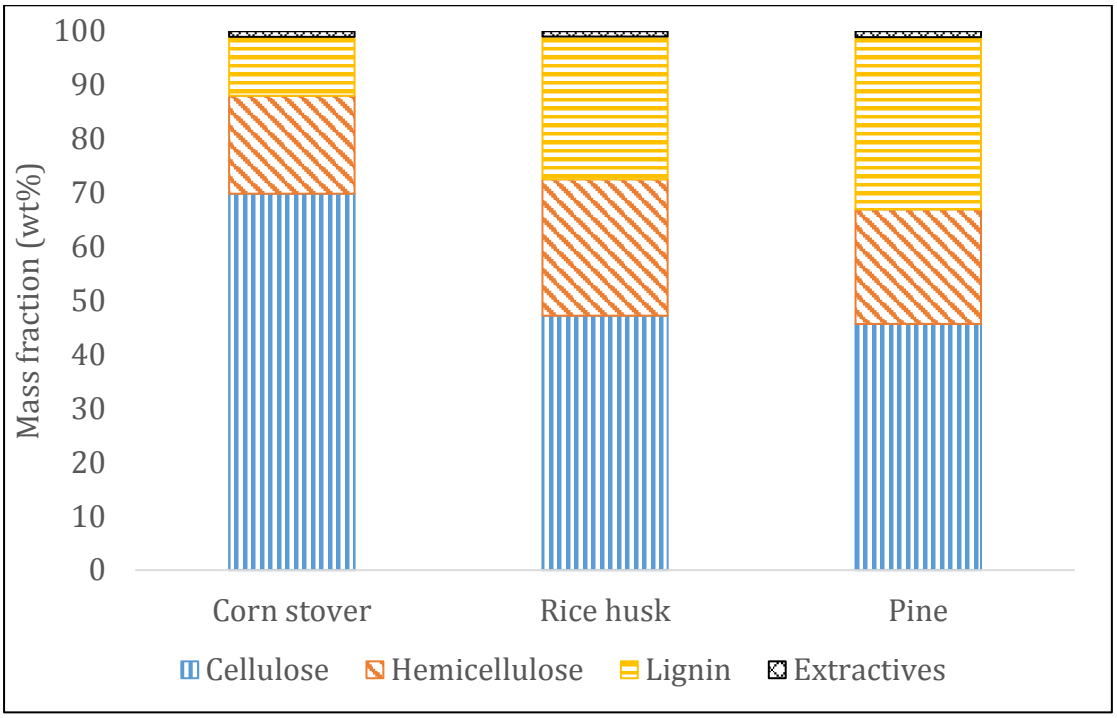

Fig. 6-1. Cellulose, hemicellulose and lignin contents in three types of biomass.

Table 6-2. The operating conditions of the present study on the DFB gasifier.

Test		Devolatilization	Gasification
Bed Material	(kg)	30	
Gasifier temperature	(°C)	700, 800	
Combustor temperature	(°C)	750-850	
Nitrogen to BFB	(Nm^3/h)	6.2	-
Nitrogen to Chute	(Nm^3/h)	1.6	-
Nitrogen to Siphon	(Nm^3/h)	2.1	-
Steam to BFB	(kg/h)	-	7.0
Steam to Chute	(kg/h)	-	2.0
Steam to Siphon	(kg/h)	-	1.5
S/B ratio		-	0.89
Corn stover	(kg/h)	15.8	
Rice husk	(kg/h)	18.5	
Pine	(kg/h)	14.2	

6.3. Results and discussion

6.3.1. Gas product

For comparing the difference between biomass types, the producer gas yield was determined as the mass yield of the producer gas per kg of dry and ash-free biomass, which was determined as sum of volumetric yields of all gas species (H_2, CO_2, CO and CH_4) times their corresponding standard densities in the producer gas. The results for the three types of biomass at the gasification temperatures of 700°C and 800°C are shown in Fig. 6-3. From this figure, it can be seen that at 700°C, the producer gas yield was 0.58 kg/kg$_{daf}$ for corn stover, 0.55 kg/kg$_{daf}$ for rice husk and 0.54 kg/kg$_{daf}$ for pine. However, at 800°C, the producer gas yields were increased for all of the biomass species, and the pine had the highest gas yield (0.81 kg/kg$_{daf}$) followed by rice husk (0.78 kg/kg$_{daf}$). The gas yield for corn stover was the lowest at 0.63 kg/kg$_{daf}$. It is known that high temperature favours the producer gas generation. However, effects of the gasification temperature varied with biomass species which can be attributed to differences in biomass chemical composition (cellulose, hemicellulose and lignin) as measured in this study.

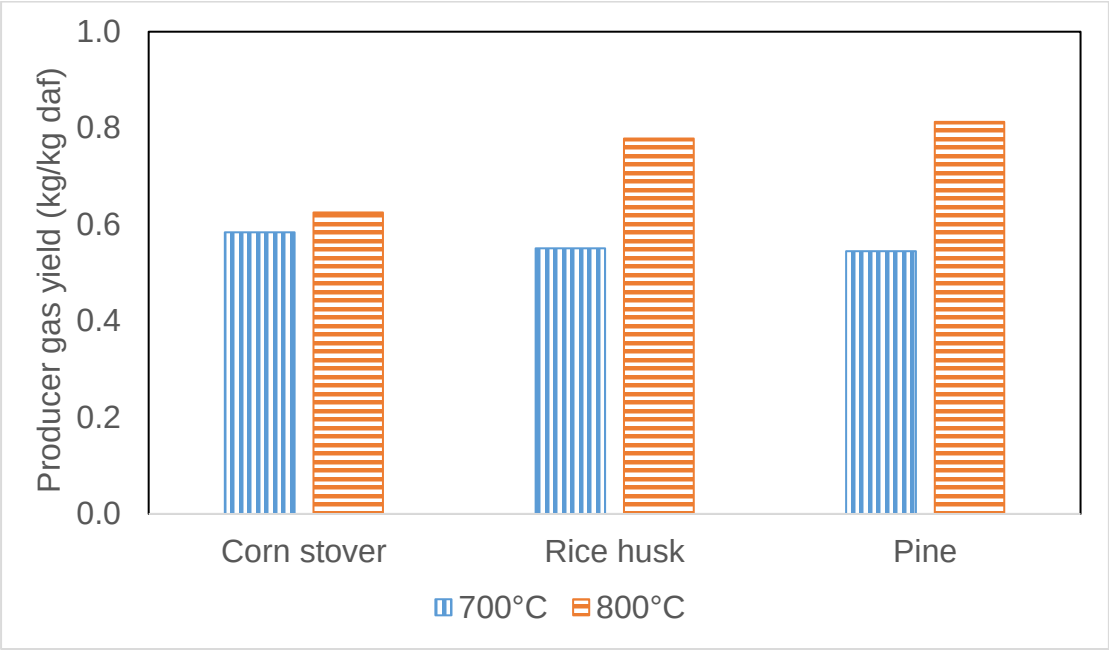

Fig. 6-2. Yields of producer gas in the gasification of corn stover, rice husk and pine at 700 and 800°C.

From these findings, it indicated that the cellulose and lignin content in the biomass play a different role for gasification characteristics since their thermal stability and cracking characterises are different. Cellulose and hemicellulose start to decompose at the temperature of 250-400°C [39]. Therefore, the corn stover, which contained 88% of combined cellulose and hemicellulose, would have released most of the volatiles at 700°C, thus further increasing the gasification temperature had only marginal impact on the gas yield. On the other hand, lignin is more difficult to decompose and needs much higher temperature for complete decomposition. Therefore, the gasification temperature had a significant effect of the lignin-rich pine (31.96% lignin) and rice husk (26.5% lignin). It was also reported that the lignin-rich biomass would generate more char in the gasification [30].

Table 6-3 presents result of composition and lower heating value (LHV) of the producer gas from gasification of three biomass species at the temperature of 700 and 800°C. From Table 6-3, it is seen that the CO_2, C_2H_4 and C_2H_6 contents in the producer gas in the gasification of corn stover were significantly higher than those from gasification of both pine and rice husk. In contrast, the contents of H_2 and CH_4 from pine gasification were higher than those from gasification of corn stover and rice husk. Meanwhile, in the rice husk gasification, CO content in producer gas was the highest.

The results of gas composition in this study are consistent with those reported in literature. Yang et al. [37] have reported that cellulose and hemicellulose with higher carboxyl content had higher yields of CO and CO_2 as well as higher presence of aromatic ring and methoxyl in the volatile gas during pyrolysis which is the process of the early stage of gasification. Cracking and deformation of lignin at high temperatures released a volatile with high contents of H_2 and CH_4. A separate report also found that in the gasification process, the derivatives from cellulose decomposition were readily cracked into gases of light hydrocarbons such as C_2H_4 and C_2H_6 [33].

Table 6-3. Composition of producer gas from the gasification of three types of biomass at gasification temperatures of 700 and 800°C.

	700°C			800°C		
	Corn stover	Rice husk	Pine	Corn stover	Rice husk	Pine
Gas composition (mol%)						
H_2	22.7	22.4	25.0	25.9	28.1	30.7
CO	28.1	36.8	35.2	28.9	37.1	36.3
CO_2	29.8	23.9	22.3	26.3	18.3	16.2
CH_4	11.1	12.0	12.8	10.1	11.3	12.1
C_2H_4	6.9	3.8	3.7	8.1	4.6	4.2
C_2H_6	1.4	1.0	1.0	0.7	0.5	0.6
Lower Heating value (MJ/Nm^3)						
	13.4	12.9	13.2	13.7	13.4	13.6
Cold gas efficiency (%)						
	64	61	62	65	67	69

Table 6-3 also gives results of cold gas efficiency of the gasifier system and the lower heating values (LHV) of the producer gas which are important parameters to assess the gasifier performance and producer gas quality. The cold gas efficiency was defined as the chemical energy content in the producer gas divided by the total input energy, including the energy in the biomass feedstock, the supplied steam and supplementary LPG to the FFB column. At 700°C, the gasification of corn stover presents a higher cold gas efficiency (64%) because the producer gas had a high content of C_2H_4 and C_2H_6 and, consequently, a higher LHV. However, for gasification at 800°C, the LHVs of producer gas from the three types of biomass were similar (13.4 to 13.7 MJ/Nm3), and the pine biomass showed the highest cold gas efficiency (69%) whereas the corn stover had the lowest (65%). In the gasification, the pine biomass with high content of lignin generated more char than other biomass [24]. Therefore, more char particles were transferred to the FFB through the chute for combustion, which required less supplementary LPG to maintain the gasification temperature [40].

At 700°C, the gasification of corn stover presents a higher cold gas efficiency, because the producer gas with a high content of C_2H_4 and C_2H_6 showed a relatively high LHV. At 800°C, although the LHV of producer gas corn stover gasification was still the highest, its cold gas efficiency was the lowest. The cold gas efficiency of pine gasification was the largest. Since at the high temperature, lignin starts to decompose, it yields more char than cellulose and hemicellulose. The increase in char yield improved the cold gas efficiency of the gasification system as more char particles were transferred to the FFB through the chute for combustion, which required less supplementary LPG to maintain the gasification temperature.

6.3.2. Tar formation and analysis

Fig. 6-4. shows the tar yields and tar classes in producer gas from gasification of three types of biomass at two temperatures (700 and 800°C). The tar yield (g/kg_{daf}) was defined as the total tar concentration in the producer gas (g/Nm^3) divided by the product gas yield per unit mass of dry and ash free fuel (Nm^3/kg_{daf}). The tar classification has been described in Section 2.3 of this paper. From Fig. 6-4, it can be found that yield at gasification temperature of 700°C the total tar was 7.77 g/kg_{daf} for corn stover, 7.32 g/kg_{daf} for rice husk and 7.56 g/kg_{daf} for pine. With increase of gasification temperature from 700 to 800°C, the total tar yield for all of the biomass species was decreased by 16% to 6.4 g/kg_{daf} for corn stover, by 10% to 6.61 g/kg_{daf} for rice husk, and by 12% to 6.67 g/kg_{daf} for pine. These results confirm that tar decomposition reactions (cracking and reforming) are endothermic and, therefore, favoured by increasing the temperature. However, the changes of each class tar compounds with increase in gasification temperature were different for each type of biomass due to the differences in molecular structure and proportion of the cellulose, hemicellulose and lignin in the biomass.

At gasification temperature of 700°C, the yields of Class 2 tar compounds were the highest for all biomass species, 4.09 g/kg_{daf} for corn stover, 2.95 g/kg_{daf} for rice husk and 3.04 g/kg_{daf} for pine. However, in corn stover gasification, the yield of Class 3 compounds was the second highest (2.09 g/kg_{daf}) followed by Class 4 (1.4 g/kg_{daf}) while the yield of Class 5 tar compounds was the least at 0.19 g/kg_{daf}. Interestingly rice husk and pine had a similar order of yields of tar class compounds with Class 2 being the second highest (2.35 g/kg_{daf} for rice husk, 2.19 g/kg_{daf} for pine) followed by Class 4 tar

compounds (1.66 g/kg$_{daf}$ for rice husk, 1.87 g/kg$_{daf}$ for pine). The yields of Class 5 tar compounds were again the least for these two biomass species (0.36 g/kg$_{daf}$ for rice husk and 0.46 g/kg$_{daf}$ for pine). At 800°C, the yields of Class 4 tar compounds became the highest for all of the three biomass species, followed by Class 2 tar compounds. In this case, the yields of Class 3 tar compounds were at the same level as those of Class 5 tar compounds.

Tar formation in gasification is a complex process. The gasification can be divided into two stages including the initial devolatilization and the subsequent gasification reactions. In the initial devolatilization stage with temperature ranging from 300 to 500°C, the so-called "primary tar" is produced which is a complex mix of heteroatoms. When the temperature is further increased to 600°C or higher, the primary tar compounds decompose into lighter vapours, lower molecular weight hydrocarbons and substitution aromatic compounds that are more stable at the high temperature than aliphatic chains. At the same time, the secondary tar compounds are formed which consist of various molecules from mono aromatic to poly aromatic hydrocarbons (PAH) through polymerisation reactions [41].

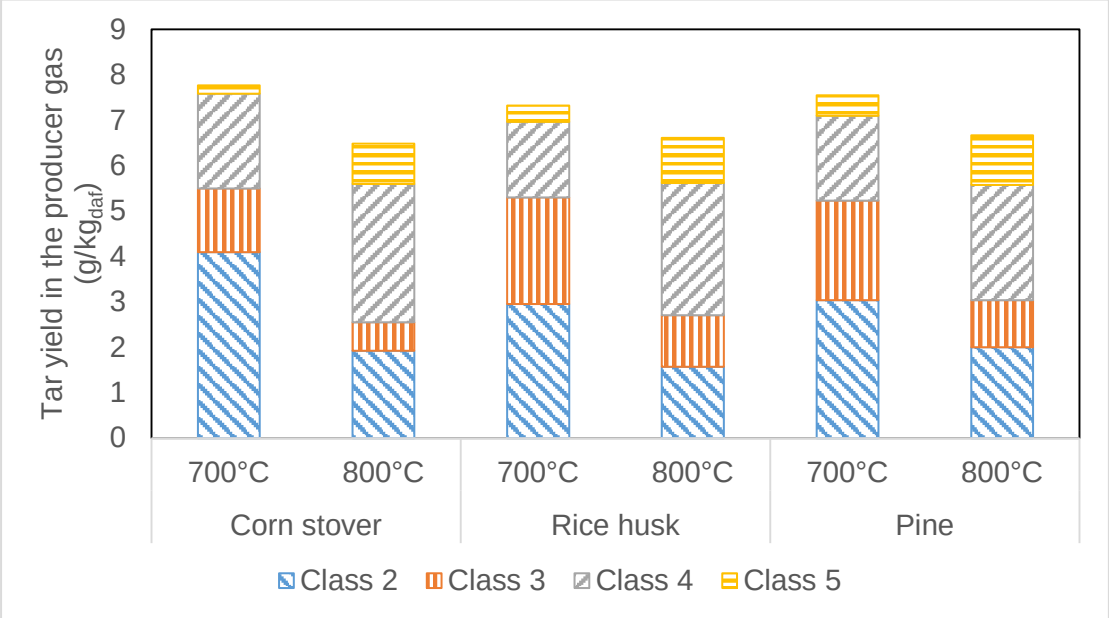

Fig. 6-3. The effect of temperature on the total tar yields and yields of each class tar compounds in gasification of three biomass species.

Based on the above analysis and chemical composition of the biomass, tar formation can be considered as three stages. The first stage is the formation of primary tar compounds in which cellulose, hemicellulose and lignin are decomposed into heterocyclic tar compounds and aromatic tar compounds, such as phenol, benzene and toluene [23]. The second stage of tar formation is the purification and conversion of aromatics products formed from the first stage to intact aromatic rings by cleavage of heterocyclic groups through dehydrogenation and dealkylation and decarboxylation [42]. The final stage is the growth of large PAH in which the combination of intact aromatic rings activates the mono-aromatic molecules to successively form the PAH tar compounds with more ring numbers, such as the reaction of H_2-abstraction-C_2H_2 addition [43].

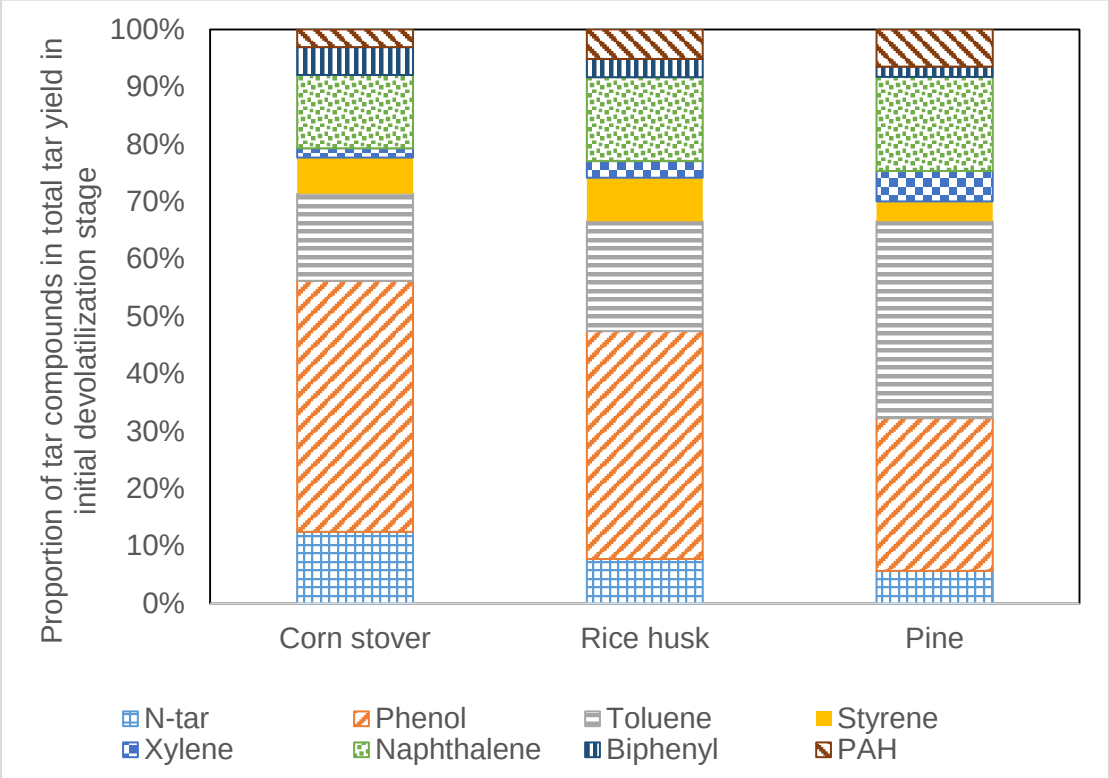

Fig. 6-4. Proportions of various tar compound yield to total tar yield in the initial devolatilization at 700°C.

In order to quantify tar formation in the first stage, tar samples were collected from the initial devolatilization in the biomass gasification and analysed using GC-FID. From the tar analysis, eight types of tar compounds were detected including N-based compounds (pyridine and quinoline), phenol, toluene, styrene, xylene, naphthalene,

biphenyl and PAH (3 and more aromatic rings). The total yields of tart compounds from the biomass devolatilization at 700°C were, respectively, 9.22 g/kg$_{daf}$ for corn stover, 9.85 g/kg$_{daf}$ for rice husk and 12.19 g/kg$_{daf}$ for pine. It is found that the yields of N-tar compounds were 1.15, 0.68 and 0.63 g/kg$_{daf}$, respectively, for corn stover, rice husk and pine. These results confirm that high yield of N-tar compounds from devolatilization of biomass is directly related to the N content in the biomass. Corn stover had higher nitrogen content than pine as presented in Table 5-1. The phenol yields in the devolatilization of corn stove, rice husk and pine were 4.03, 3.50 and 2.91 g/kg$_{daf}$, respectively, which were the major contributor to tar compounds for corn stover and rice husk. However, the yield of toluene was the major contributor for pine which was 3.76 g/kg$_{daf}$. The corresponding yields for corn stover and rice husk were 1.40, 1.69 g/kg$_{daf}$. The other key contributor to the tar compounds was naphthalene which yield was 1.18 g/kg$_{daf}$ for corn stover, 1.69 g/kg$_{daf}$ for rice husk and 1.80 g/kg$_{daf}$ for pine. The yields of other tar compounds were variable from 0.15 to 0.67 g/kg$_{daf}$ depending on the type of biomass. The proportions of each type of tar compounds to the total tar yield in devolatilization at 700°C are shown in Fig. 6-4 for the three species of biomass.

The differences in the tar yields and tar compound distribution among these biomass species are largely attributed to the differences in monomer structure and proportion of cellulose, hemicellulose, and lignin of the biomass. Yu et al. [22], reported that lignin contains a high proportion of aromatic and methyl functional groups. Therefore, more PAH compounds and methyl groups (such as toluene and xylene) were formed in gasification of lignin-rich pine biomass. On the other hand, the monomer of cellulose and hemicellulose contains a larger number of hydroxyl and carboxyl groups. Therefore, more tar compounds containing -OH groups (such as phenols) were generated in the gasification of cellulose-rich biomass (corn stover).

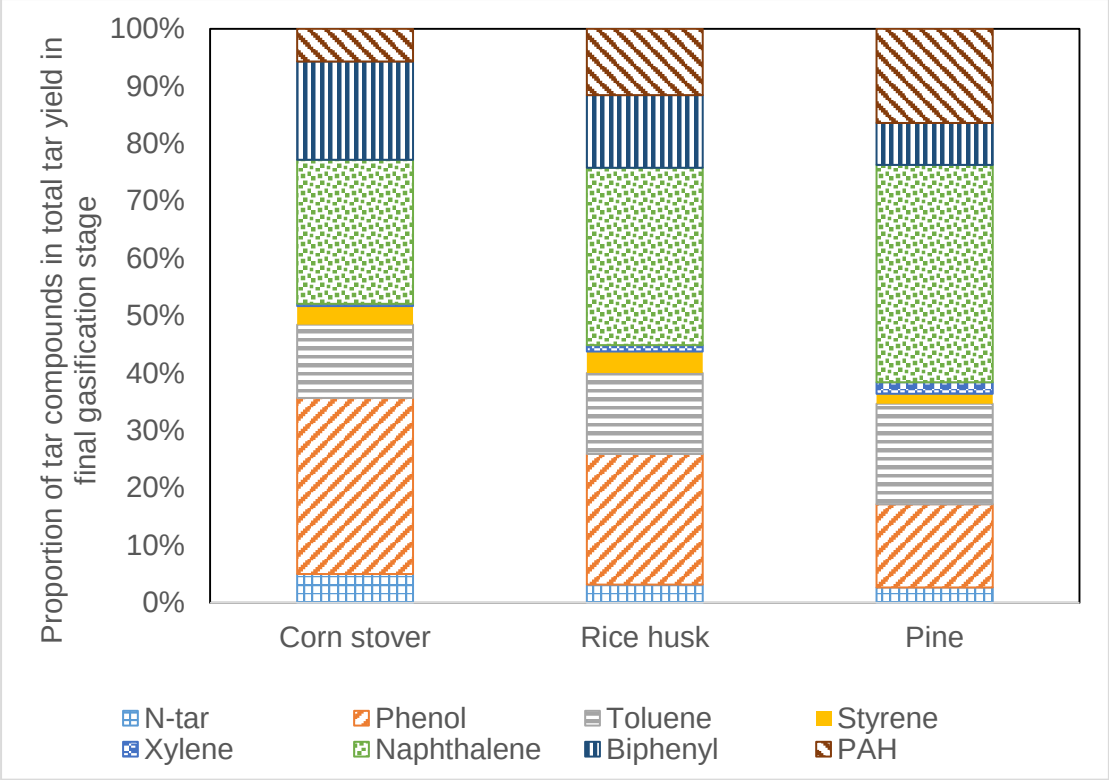

Fig. 6-5. Proportions of various tar compound yield to total tar yield in the final gasification stage at 700°C.

The intermediate tar compounds generated from the initial devolatilization were logical precursors for the cracking of existing tar compounds and the formation of new tar compounds in the subsequent gasification process. From the results of gasification experiments at 700°C, it is observed that the yields of N-based tar compounds, phenols, toluene and styrene were reduced while the yields of other tar compounds were increased. However, the total tar yields were all reduced at different levels, by 21% to 7.26 g/kg$_{daf}$ for corn stover, by 25% to 7.35 g/kg$_{daf}$ for rice husk and by 37% 7.66 g/kg$_{daf}$ for pine. Fig. 6-5. shows the changes in yield of each type of tar compounds through the final gasification process following the initial devolatilization at the same temperature of 700°C.

The PAH compounds in pine gasification were increased from 0.71 to 1.26 g/kg$_{daf}$ which could be formed from toluene as precursor. While, in the gasification of corn stover, phenol, which was reduced from 4.03 to 2.23 g/kg$_{daf}$, could be the precursor to form new PAH compounds, which was increased from 0.28 to 0.41 g/kg$_{daf}$. From Fig. 6-5, it is believed that the single-aromatic tar compounds (such as N-tar, phenol and

toluene) in were consumed as the precursor for the formation of PAH, biphenyl and naphthalene. This supports the observation that the yield of naphthalene was significantly increased (from 1.8 to 2.9 g/kg_{daf}) for lignin-rich pine while the yield of biphenyl was the highest for cellulose-rich corn stover, increasing from 0.45 to 1.25 g/kg_{daf} through gasification.

Based on the above finding, tar formation mechanism can be considered as two pathways with the different precursor as shown in Fig. 6-6 for precursor of toluene and in Fig. 6-7 for precursor of phenols. In Fig. 6-6, benzene (C_6H_6) is formed by the cleavage of alkyl groups (CH_3^+) attached on toluene (C_7H_8) via dealkylation reaction. Then, phenyl (C_6H_5) is generated by losing the H^+ radical from the benzene. After this, a combination of two phenyls ring leads to biphenyl ($C_{12}H_{10}$). Finally, phenanthrene grows by the H_2-abstraction-C_2H_2-addition sequence from biphenyl, in which H-abstraction activates the aromatic molecules, and acetylene addition propagates molecular growth by cyclisation [42].

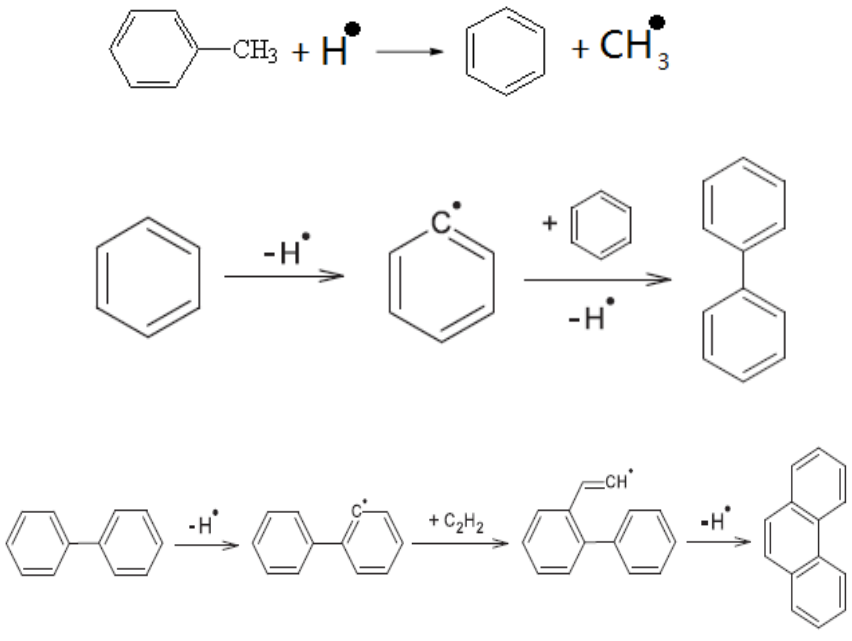

Fig. 6-6. The mechanisms of tar formation with a precursor of toluene.

Fig. 6-8 elucidate s the formation of PAH tar compounds with phenols as precursor. In the pathway, phenol is cracking by losing CO to form cyclopentadiene (C_5H_6). Then,

cyclopentadienyl (C_5H_5) produces through losing H radicals from cyclopentadiene. After this, naphthalene ($C_{10}H_{10}$) is formed by the combinations of two cyclopentadienyls. Naphthalene loses H radical and carbon into indenyl (C_9H_8) under the reaction ($C + H_2O \rightarrow CO + H_2$). Finally, phenanthrene ($C_{14}H_{10}$) is formed when indenyl reacts with cyclopentadiene. [44].

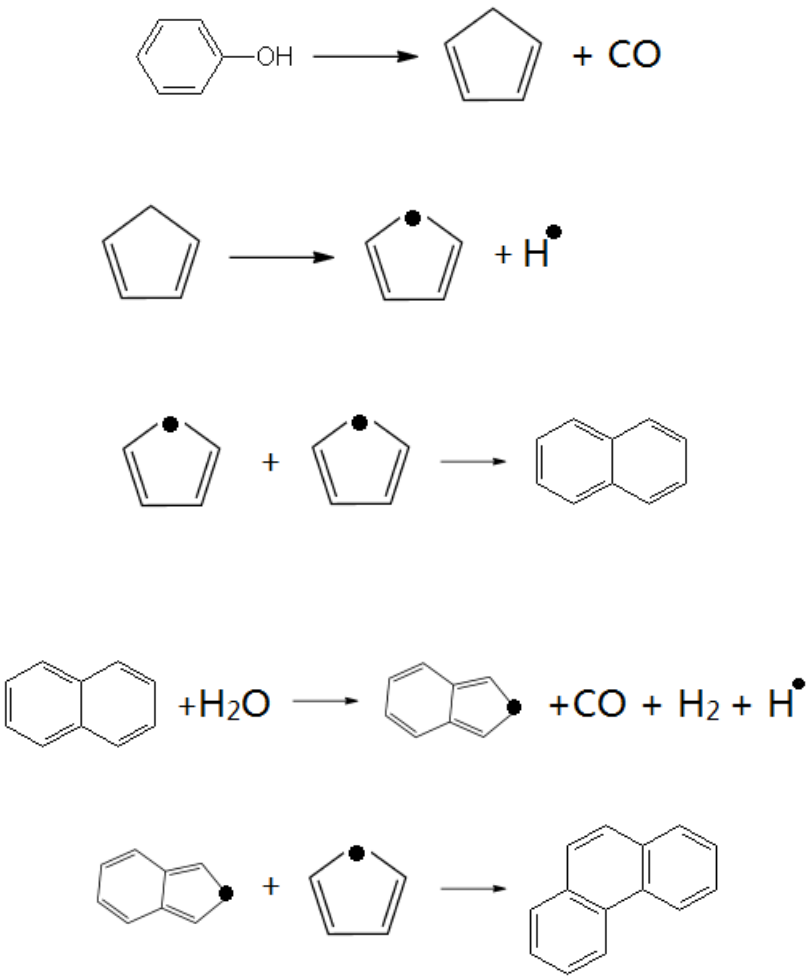

Fig. 6-7. The mechanisms of tar formation with a precursor of phenols.

6.4. Conclusions

In this paper, three biomass species of corn stove, rice husk and radiata pine wood have been tested on a 100 kWth dual fluidised bed gasifier with steam as gasification agent. Effects of biomass species on producer gas yields, gas composition and tar yields have been investigated. Chemical composition of each biomass has been analysed, and the results are used for fundamental understanding of the tar formation process. It is found

that corn stove is rich in cellulose, rice husk contains a high content of hemicellulose and pine wood has a high content of lignin. These differences are the key contributors to the differences in producer gas yield, gas composition and the yields of tar compounds. Changes of tar compounds from initial devolatilization to the final gasification have been examined, and mechanisms of tar formation are proposed.

Key findings from the present studies are:

- As reaction temperature increased, the producer gas yields were increased for all three biomass species. At 700°C, the yield of producer gas is the highest for corn stover followed by rice husk and pine wood has the lowest gas yield. In contrast, at 800°C, the gas yield for pine wood is the highest followed by rice husk and then corn stover. By comparing the producer gases from gasification of the three biomass species at both 700 and 800°C, the contents of H_2 and CH_4 are higher from gasification of pine wood, the content of CO is higher from gasification of rice husk while contents of CO_2, C_2H_4 and C_2H_6 are higher from gasification of corn stover.

- Tar formation is a complex process and can be divided into three stages: (1). Formation of primary tar compounds, (2). tar reforming, and (3). tar polymerisation. Eight types of tar compounds have been detected both in the devolatilization and final gasification, which are N-based compounds (pyridine and quinoline), phenol, toluene, styrene, xylene, naphthalene, biphenyl and PAH (3 and more aromatic rings). During the initial devolatilization stage of gasification, pine wood generates more toluene while both corn stover and rice husk produce more phenols. In the final gasification process, the yields of N-based tar compounds, phenols, toluene and styrene are reduced while the yields of other tar compounds are increased. Two reaction pathways are proposed including, one with toluene as precursor and the other with phenols as precursor. The total tar yields for all of the biomass species are significantly reduced through the final gasification process.

- Tar yields are reduced with increase in gasification temperature for all of the biomass species tested.

6.5. Reference

[1] B. Pathak, S. Chaudhari, and M. Fulekar, "Biomass–resource for sustainable development," *International Journal of Advancements in Research & Technology*, vol. 2, pp. 2278-7763, 2013.

[2] K. Umeki, Y.-i. Son, T. Namioka, and K. Yoshikawa, "Basic Study on Hydrogen-Rich Gas Production by High Temperature Steam Gasification of Solid Wastes," *Journal of Environment and Engineering*, vol. 4, pp. 211-221, 2009.

[3] L. q. Wang, Y. h. Dun, X. n. Xiang, Z. j. Jiao, and T. q. Zhang, "Thermodynamics research on hydrogen production from biomass and coal co-gasification with catalyst," *International Journal of Hydrogen Energy*, vol. 36, pp. 11676-11683, 2011.

[4] A. V. Bridgwater, "Renewable fuels and chemicals by thermal processing of biomass," *Chemical Engineering Journal*, vol. 91, pp. 87-102, 2003.

[5] S. K. Sansaniwal, K. Pal, M. A. Rosen, and S. K. Tyagi, "Recent advances in the development of biomass gasification technology: A comprehensive review," *Renewable and Sustainable Energy Reviews*, vol. 72, pp. 363-384, 2017.

[6] M. M. Küçük and A. Demirbas, "Biomass conversion processes," *Energy Conversion and Management*, vol. 38, pp. 151-165, 1997.

[7] J. Rezaiyan and N. P. Cheremisinoff, *Gasification technologies : a primer for engineers and scientists*. Boca Raton: Taylor & Francis, 2005.

[8] S. Heidenreich and P. U. Foscolo, "New concepts in biomass gasification," *Progress in Energy and Combustion Science*, vol. 46, pp. 72-95, 2015.

[9] A. C. Chang, H.-F. Chang, F.-J. Lin, K.-H. Lin, and C.-H. Chen, "Biomass gasification for hydrogen production," *International Journal of Hydrogen Energy*, vol. 36, pp. 14252-14260, 2011.

[10] Y.-H. Qin, J. Feng, and W.-Y. Li, "Formation of tar and its characterization during air–steam gasification of sawdust in a fluidized bed reactor," *Fuel*, vol. 89, pp. 1344-1347, 2010.

[11] S. Nakamura, S. Kitano, and K. Yoshikawa, "Biomass gasification process with the tar removal technologies utilizing bio-oil scrubber and char bed," *Applied Energy*, vol. 170, pp. 186-192, 2016.

[12] S. Nakamura, U. Siriwat, K. Yoshikawa, and S. Kitano, "Development of Tar Removal Technologies for Biomass Gasification using the By-products," *Energy Procedia,* vol. 75, pp. 208-213, 2015.

[13] A. S. Al-Rahbi and P. T. Williams, "Hydrogen-rich syngas production and tar removal from biomass gasification using sacrificial tyre pyrolysis char," *Applied Energy,* vol. 190, pp. 501-509, 2017.

[14] H. Boerrigter, S. Van Paasen, P. Bergman, J. Könemann, R. Emmen, and A. Wijnands, "OLGA tar removal technology," Energy research Centre of the Netherlands (ECN), ECN-C--05-009, 2005.

[15] L. Devi, K. J. Ptasinski, and F. J. J. G. Janssen, "A review of the primary measures for tar elimination in biomass gasification processes," *Biomass and Bioenergy,* vol. 24, pp. 125-140, 2003.

[16] Y. Tursun, S. Xu, G. Wang, C. Wang, and Y. Xiao, "Tar formation during co-gasification of biomass and coal under different gasification condition," *Journal of Analytical and Applied Pyrolysis,* vol. 111, pp. 191-199, 2015.

[17] J. J. Hernández, R. Ballesteros, and G. Aranda, "Characterisation of tars from biomass gasification: Effect of the operating conditions," *Energy,* vol. 50, pp. 333-342, 2013.

[18] C. Berrueco, D. Montané, B. M. Güell, and G. del Alamo, "Effect of temperature and dolomite on tar formation during gasification of torrefied biomass in a pressurized fluidized bed," *Energy,* vol. 66, pp. 849-859, 2014.

[19] M. Mayerhofer, S. Fendt, H. Spliethoff, and M. Gaderer, "Fluidized bed gasification of biomass – In bed investigation of gas and tar formation," *Fuel,* vol. 117, pp. 1248-1255, 2014.

[20] J. M. de Andrés, E. Roche, A. Narros, and M. E. Rodríguez, "Characterisation of tar from sewage sludge gasification. Influence of gasifying conditions: Temperature, throughput, steam and use of primary catalysts," *Fuel,* vol. 180, pp. 116-126, 2016.

[21] C. Kinoshita, Y. Wang, and J. Zhou, "Tar formation under different biomass gasification conditions," *Journal of Analytical and Applied Pyrolysis,* vol. 29, pp. 169-181, 1994.

[22] H. Yu, Z. Zhang, Z. Li, and D. Chen, "Characteristics of tar formation during cellulose, hemicellulose and lignin gasification," *Fuel,* vol. 118, pp. 250-256, 2014.

[23] A. Gani and I. Naruse, "Effect of cellulose and lignin content on pyrolysis and combustion characteristics for several types of biomass," *Renewable Energy,* vol. 32, pp. 649-661, 2007.

[24] V. Pasangulapati, K. D. Ramachandriya, A. Kumar, M. R. Wilkins, C. L. Jones, and R. L. Huhnke, "Effects of cellulose, hemicellulose and lignin on thermochemical conversion characteristics of the selected biomass," *Bioresource Technology,* vol. 114, pp. 663-669, 2012.

[25] L. Burhenne, J. Messmer, T. Aicher, and M.-P. Laborie, "The effect of the biomass components lignin, cellulose and hemicellulose on TGA and fixed bed pyrolysis," *Journal of Analytical and Applied Pyrolysis,* 2013.

[26] G. Chen and D. Y. C. Leung, "Experimental Investigation of Biomass Waste, (Rice Straw, Cotton Stalk, and Pine Sawdust), Pyrolysis Characteristics," *Energy Sources,* vol. 25, pp. 331-337, 2003.

[27] M. Van de Velden, J. Baeyens, A. Brems, B. Janssens, and R. Dewil, "Fundamentals, kinetics and endothermicity of the biomass pyrolysis reaction," *Renewable Energy,* vol. 35, pp. 232-242, 2010.

[28] F. Kirnbauer, V. Wilk, and H. Hofbauer, "Performance improvement of dual fluidized bed gasifiers by temperature reduction: The behavior of tar species in the product gas," *Fuel,* vol. 108, pp. 534-542, 2013.

[29] K. Umeki, T. Namioka, and K. Yoshikawa, "The effect of steam on pyrolysis and char reactions behavior during rice straw gasification," *Fuel Processing Technology,* vol. 94, pp. 53-60, 2012.

[30] P. Basu, *Biomass gasification and pyrolysis : practical design and theory.* Burlington, MA: Academic Press, 2010.

[31] C. Font Palma, "Modelling of tar formation and evolution for biomass gasification: A review," *Applied Energy,* vol. 111, pp. 129-141, 2013.

[32] C. Font Palma, "Model for biomass gasification including tar formation and evolution," *Energy & Fuels,* vol. 27, pp. 2693-2702, 2013.

[33] C. Wu, Z. Wang, J. Huang, and P. T. Williams, "Pyrolysis/gasification of cellulose, hemicellulose and lignin for hydrogen production in the presence of various nickel-based catalysts," *Fuel,* vol. 106, pp. 697-706, 2013.

[34] T. Hosoya, H. Kawamoto, and S. Saka, "Secondary reactions of lignin-derived primary tar components," *Journal of Analytical and Applied Pyrolysis,* vol. 83, pp. 78-87, 2008.

[35] T. Hosoya, H. Kawamoto, and S. Saka, "Pyrolysis gasification reactivities of primary tar and char fractions from cellulose and lignin as studied with a closed ampoule reactor," *Journal of Analytical and Applied Pyrolysis*, vol. 83, pp. 71-77, 2008.

[36] D. Lv, M. Xu, X. Liu, Z. Zhan, Z. Li, and H. Yao, "Effect of cellulose, lignin, alkali and alkaline earth metallic species on biomass pyrolysis and gasification," *Fuel Processing Technology*, vol. 91, pp. 903-909, 2010.

[37] H. Yang, R. Yan, H. Chen, D. H. Lee, and C. Zheng, "Characteristics of hemicellulose, cellulose and lignin pyrolysis," *Fuel*, vol. 86, pp. 1781-1788, 2007.

[38] R. C. Pettersen, "Wood sugar analysis by anion chromatography," *Journal of Wood Chemistry and Technology*, vol. 11, pp. 495-501, 1991.

[39] T. Haensel, A. Comouth, P. Lorenz, S. I. U. Ahmed, S. Krischok, N. Zydziak, A. Kauffmann, and J. A. Schaefer, "Pyrolysis of cellulose and lignin," *Applied Surface Science*, vol. 255, pp. 8183-8189, 2009.

[40] W. L. Saw and S. Pang, "Co-gasification of blended lignite and wood pellets in a 100kW dual fluidised bed steam gasifier: The influence of lignite ratio on producer gas composition and tar content," *Fuel*, vol. 112, pp. 117-124, 2013.

[41] T. A. Milne, N. Abatzoglou, and R. J. Evans, "Biomass gasifier" tars": their nature, formation, and conversion," National Renewable Energy Laboratory, Golden, Colorado, USA, 1998.

[42] P. Morf, P. Hasler, and T. Nussbaumer, "Mechanisms and kinetics of homogeneous secondary reactions of tar from continuous pyrolysis of wood chips," *Fuel*, vol. 81, pp. 843-853, 2002.

[43] S. Umemoto, S. Kajitani, K. Miura, H. Watanabe, and M. Kawase, "Extension of the chemical percolation devolatilization model for predicting formation of tar compounds as soot precursor in coal gasification," *Fuel Processing Technology*, vol. 159, pp. 256-265, 2017.

[44] A. Sharma, V. Pareek, and D. Zhang, "Biomass pyrolysis—A review of modelling, process parameters and catalytic studies," *Renewable and Sustainable Energy Reviews*, vol. 50, pp. 1081-1096, 2015.

Chapter 7. Effect of Catalytic Bed Materials on Tar Formation and Gas Yields in Steam Gasification of Biomass

This chapter presents experimental studies on the effect of bed materials in steam gasification of woody biomass in a pilot scale a dual fluidised bed (DFB) gasifier. The selected bed materials were silica sand, calcined olivine, Woodhill sand and limestone-silica blends (50-50 wt.%). Experiments were conducted at operation temperatures of 700, 750 and 800°C. Radiata pine wood pellets were used as the biomass feedstock, and the steam to biomass ratio maintained constant at 0.89. The bed material inventory was 30kg.

The results of this study show that all of the bed materials except for silica promoted H_2 production in biomass gasification. At 700°C, the H_2 concentration was 19% in the producer gas with silica sand, and this was increased to 25% with calcined olivine, 26% for Woodhill and 44% for limestone-silica blends. The increased H_2 concentration is believed to be due to the favoured water-shift reaction towards the hydrogen production. Catalytic effects of the bed materials on tar decomposition were also investigated. It was found that, in comparison with silica sand, the tar content was reduced by 24%, 28% and 43% with calcined olivine, Woodhill sand and limestone-silica blends, respectively.

7.1. Introduction

In dual fluidised bed (DFB) gasification of biomass, selection of bed material is important as, in addition to the function of heat transfer medium, it can also provide catalytic effects on the gasification reactions [1]. The natural minerals containing oxides of Ca, Fe, Al and Mg are considered as the potential catalytic bed materials in the biomass steam gasification [2], which can promote steam-char gasification, water-gas-shift and steam reforming reactions and enhance tar cracking and reforming [3].

Among these potential catalytic bed materials, the natural iron mineral such as olivine has the chemical structure of $((Mg, Fe)_2\ SiO_4)$ and thus has been applied for biomass

gasification [4]. Since iron is potentially effective in different oxidation states in the gasifier, metallic iron is known to be an active species for aromatic hydrocarbon destruction through the C–C and C–H bond breaking [5]. Some studies [6-8] have found that the olivine sand has apparent catalytic activity on cracking and reforming of tar and enhanced steam and dry reforming of hydrocarbons. In a separate study, Göransson et al. [9] applied the olivine sand as the bed material in biomass gasification and investigated its reactivity during recycling. It was found that in the environment of combustion, olivine reacts with oxygen and decomposes to iron oxide (Fe_2O_3), magnesium silicate and silica oxide, as shown in Eq. (7-1). In the gasifier, Fe_2O_3 converted from olivine reacts with hydrocarbons and is then reduced to FeO as described by Eq. (7-2). When FeO is transferred from the gasifier to the combustor in the DFB gasification system, it is oxidized back to Fe_2O_3 as shown in Eq. (7-3). In addition, those iron species take place in the redox equations of the water gas shift reaction [10]. This iron reintegration can be described as Eq. (7-4) and Eq. (7-5). Therefore, olivine can be pre-treated by calcination to increase the Fe^{3+} concentration on the olivine surface for increasing better catalytic activity.

$$((Mg, Fe)_2\ SiO_4) + O_2 \rightarrow Fe_2O_3 + SiO_2 + Mg_2SiO_4 \quad (7\text{-}1)$$

$$Fe_2O_3 + C_xH_y \rightarrow FeO + CO_2 + H_2O \quad (7\text{-}2)$$

$$FeO + O_2 \rightarrow Fe_2O_3 \quad (7\text{-}3)$$

$$Fe_2O_3 + CO \leftrightarrow FeO + CO_2 \quad (7\text{-}4)$$

$$FeO + H_2O \leftrightarrow Fe_2O_3 + H_2 \quad (7\text{-}5)$$

In DFB gasification of biomass, limestone is another promising catalytic bed material as well as an excellent in situ CO_2 removal sorbent through a cycling of carbonation and calcination. Reported studies [11-13] have demonstrated that the limestone undergoes two steps: (1) carbonation in the gasification reactor where CaO and CO_2 react to form $CaCO_3$ as described by Eq. (7-6); and (2) calcination in the high temperatures combustor where $CaCO_3$ decomposes to CaO and CO_2. Therefore, in effect CO_2 is transferred from the gasification reactor to the combustor. In addition, with a CO_2 reduction in the gasification reactor, water–gas shift reaction is promoted thus more H_2 is generated. This is confirmed in previous experimental studies in which

H_2 contents of up to 75% in the producer gas were achieved while the tar concentration was reduced to 2 g/Nm^3 [14-16].

$$CaO + CO_2 \leftrightarrow CaCO_3 \quad (7\text{-}6)$$

The objectives of this part of study were to investigate the catalytic effects of three types of bed materials using a pilot scale DFB gasifier for biomass steam gasification and to compare the results with those by using inert silica sand. Producer gas composition and tar content in the producer gas have been measured and analysed.

7.2. Experiment Setup and Materials

7.2.1 Bed material characterization and fuel properties

Four types of naturally occurring sands were selected as bed materials, which were silica sand, calcined olivine sand, Woodhill iron sand and limestone-silica sand blends. As an inert bed material, silica sand was used as the control. All of the bed materials, except for the olivine sand, were purchased from a New Zealand supplier. The chemical composition and mechanical properties of these bed materials are given in Table 7-1 and Table 7-2.

The olivine sand, sourced from Austria, is characterised by its high content of (Fe Mg) SiO_4 and once received, it was pretreated by calcination at 1100°C for 4 hours to increase the free iron (III) concentration. Woodhill iron sand has the similar chemical composition compared to the olivine sand, but it contains more Ca and Al. Limestone sand is CaO based material. Considering that the limestone has high attrition rate, resulting in high bed material loss, it was blended with silica sand at a mass ratio of 50%-50%.

Table 7-1. XRF analysis results of the major elements (wt.%) present in the tested bed materials.

	Silica sand	Calcined Olivine sand	Woodhill iron sand	Limestone
SiO_2	99.29	38.19	56.57	0.73
TiO_2	0.07	0.01	1.81	0.01
Al_2O_3	<0.2	0.26	9.45	0.2
Fe_2O_3	0.05	9.21	11.78	0.12
MnO	<0.1	0.15	0.3	0.01
MgO	<0.005	50.4	6.86	0.22
CaO	0.003	0.71	9.07	55.11
Na_2O	<0.1	0.14	1.89	0.1
K_2O	0.001	<0.01	0.9	0.02
P_2O_5	<0.01	0.01	0.12	0.01
LOI*	0.6	0.1	1.25	44.5

**: Loss on Ignition (LOI) represents the volatile components such as hydrated water, carbonate and carbon present in those sands.*

Table 7-2. Physical properties of the bed materials used in this study.

		Silica Sand	Calcined Olivine sand	Woodhill Iron Sand	Limestone
Particle Density	(g/cm^3)	≈2.9	≈2.6	≈3.2	≈2.5
BET Surface Area	(m^2/g)	0.29	0.24	2.14	0.23
BJH Pore Volume	(cm^3/g)	500	300	2650	200
Particle Size	(μm)	200~300	200~300	200~300	500~700

Pellets of radiata pine wood were purchased from a New Zealand supplier and used as the biomass feedstock for the experiments. The pellets are cylindrically shaped with a diameter of 6 mm and lengths of 12-20 mm. The moisture content of the wood pellets was 8%. Before experiments, proximate and ultimate analyses were performed on the wood pellets, and the results have been given in Table 4-2 from Chapters 4.

7.2.2 Experiment setup, operation conditions and sampling methods

In the present study, experiments were conducted in the 100kW dual fluidised bed steam gasifier, which has been described in Chapter 3. The steam feeding rates to BFB, chute and siphon were set at constant values of 7.0, 2.0 and 1.5 kg/h, respectively. The wood pellet was fed at a constant feeding rate of 14.2 kg/h. Therefore, the steam to biomass ratio maintained at a constant of 0.89 while the steam also includes the moisture in wood pellets. The operation conditions of the gasification experiments are given in Table 7-3 which were the same for all of the experiments. The sampling and analysis methods for producer gas and tar have also been given in Chapter 3.

Table 7-3. Operation parameters and conditions for the experiments.

Parameter	Unit	
Feeding rate of wood pellet	kg/h	14.2
Steam	Kg/h	10.5
Steam/Biomass ratio		0.89
BFB temperature	°C	700, 750, 800
CFB temperature	°C	750 ~ 850
Pressure	kPa	101
Bed material inventory	kg	30

7.3. Results and discussion

Experiments were conducted for steam gasification of wood pellets of radiata pine in the 100kW DFB gasifier using various types of bed materials at operation temperatures of 700, 750 and 800 °C, respectively. The bed materials included olivine sand, Woodhill

sand and blends of limestone and silica sand as well as silica sand as a control. It is well known that the producer gas composition and tar concentration in the producer gas are influenced by gasification temperature through a series of chemical reactions. These chemical reactions during the gasification process have been described in Chapter 2.

7.3.1. Producer gas composition and yield

The variations in the producer gas yield as a function of bed material with a temperature range of 700 to 800°C are shown in Fig. 7-1. It can be seen from Fig. 7-1 that the producer gas yield was increased with an increased temperature for all four tested bed material. As observed, silica sand had the lowest yield of producer gas of 7.4 Nm^3/h at 700°C, 9.2 Nm^3/h at 750°C and 12.1 Nm^3/h at 800°C. For other three catalytic bed material, Woodhill sand gave the highest gas yield of 10.8 Nm^3/h at 700°C, but the limestone-silica blends presented the highest gas yield 13.9 Nm^3/h at 750°C while the highest gas yield at 800°C (16.8 Nm^3/h) was achieved in the gasification with olivine sand.

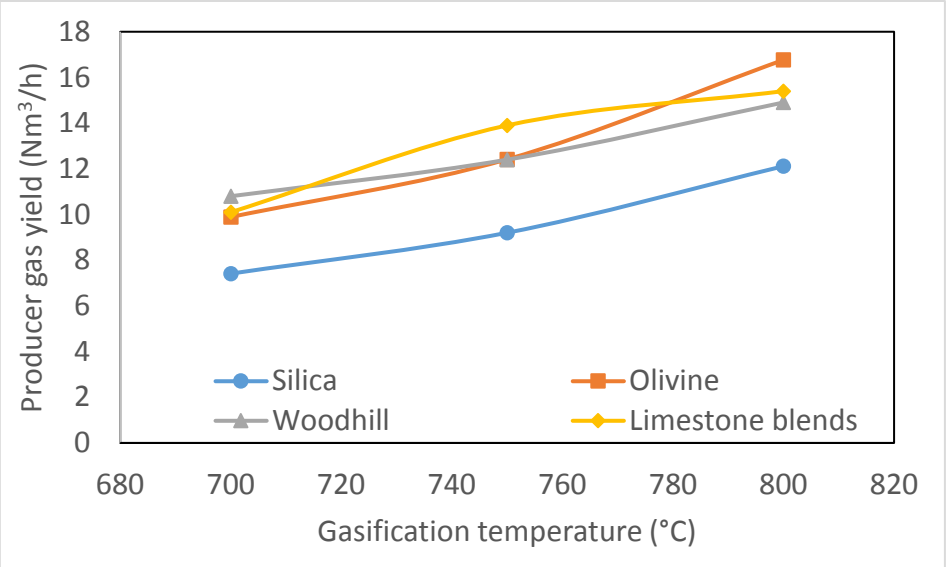

Fig. 7-1. The producer gas yield at different gasification temperatures for four different bed materials.

Fig 7-2 illustrates the effect of temperature on the concentrations of H_2 (Fig. 7-2a), CO (Fig. 7-2b), CO_2 (Fig. 7-2c) and CH_4 (Fig. 7-2d) in the producer gas by using different bed materials. To present comparable data, the concentrations of gas species were

calculated based on the gas compositions from micro-GC. For the silica sand and iron-rich sand, the concentrations of H_2 and CO in the producer gas were increased with temperature, while the concentrations of CO_2 and CH_4 were reduced. It is believed that high temperature enhances both steam-char reaction and tar reforming reaction to release H_2 production. In addition, Franco et al. [17] indicated that the presence of steam favoured that water gas shift (WGS) reaction, leading to an increase in H_2 production. However, WGS reaction is exothermic, the rise in temperature favours the reaction toward the reverse direction for CO formation. Furthermore, the endothermic Boudouard reaction favours the CO formation with an increased temperature. Therefore, CO concentration increased with the temperature. In the meantime, the CO_2 concentration decreased with increase in temperature for all bed materials except for the limestone-silica blends. The decreasing CH_4 concentration with increasing temperature could be due to the effect of the Methanation reaction coupled with the steam methane reforming. Methanation is an exothermic reaction which favours the backward reaction with increasing temperature. Meanwhile, high temperatures promote steam methane reforming, and thus both mechanisms decrease methane formation. These results in the present study were found to be similar those of reports in the literature [18, 19].

However, limestone-silica blends exhibited the different trends in the concentration of H_2, CO and CO_2. As the gasification temperature increased, the concentration of H_2 in the producer gas was firstly increased from 44.1 % to 46.7 %, and then dropped to 45.2%. The CO concentration was increased from 14.2 % to 18.6 %, a similar trend on CO_2 was also observed, which rose from 14.6 % to 17.6 %. It can be explained by the CO_2 capture through the carbonation reaction in BFB, the increased gasification temperature in BFB inhibits the forward the CO_2 absorption [20]. Accordingly, the increasing CO_2 content coupled with high temperature resulted in the reversible WGS reaction toward the direction of CO formation. This result is in agreement with the work of Weerachanchai et al. [21].

As observed, the type of bed material had a strong influence on the concentration of each gas species in the producer gas during the gasification process. From Fig. 7-1(a), silica sand provided a lowest H_2 concentration of 19.0% at 700°C, 23.8% at 750°C and 28.9 at 800°C. On the contrary, the largest H_2 concentration was obtained from the

gasification by using limestone-silica blends as the bed material, which was 44.1% at 700°C, 46.7% at 750°C and 45.2% at 800°C. Fig. 7-2(b) shows the influence of bed materials on CO concentration. The highest CO concentration was generated from the gasification by using silica sand, which was 25.1% at 700°C, 27.5% at 750°C and 28.2 at 800°C. By using iron-rich sand and limestone-silica blends, a lower CO concentration was obtained, for example at 800°C it was 25.3% for olivine, 24.1% for Woodhill sand and 18.6% for limestone-silica blends, respectively.

From Fig. 7-2(c), it can be seen that the CO_2 concentrations in the use of olivine sand and Woodhill sand were different from those using limestone-silica blends as the bed material. At 700°C, the CO_2 concentration in the producer gas for silica sand was 20.4%. When iron-rich sands were used, the CO_2 concentration increased to 23.5% and 23.1%, respectively, for using olivine sand and Woodhill sand. Due to the CO_2 capture by using limestone bed material, the lowest CO_2 concentration was obtained at all three tested temperatures, which was 14.6% at 700°C, 15.0% at 750°C and 17.6% at 800°C. Fig. 7-2 (d) presents the variation of CH_4 concentration as a function of temperature for using different bed materials. The CH_4 concentration for silica sand at 700°C was 12.9%. However, this was reduced to 11.6% for olivine sand, to 12.2% for Woodhill sand and to 9.9% for limestone-silica blends. Similar trends were also obtained at 750 and 800°C.

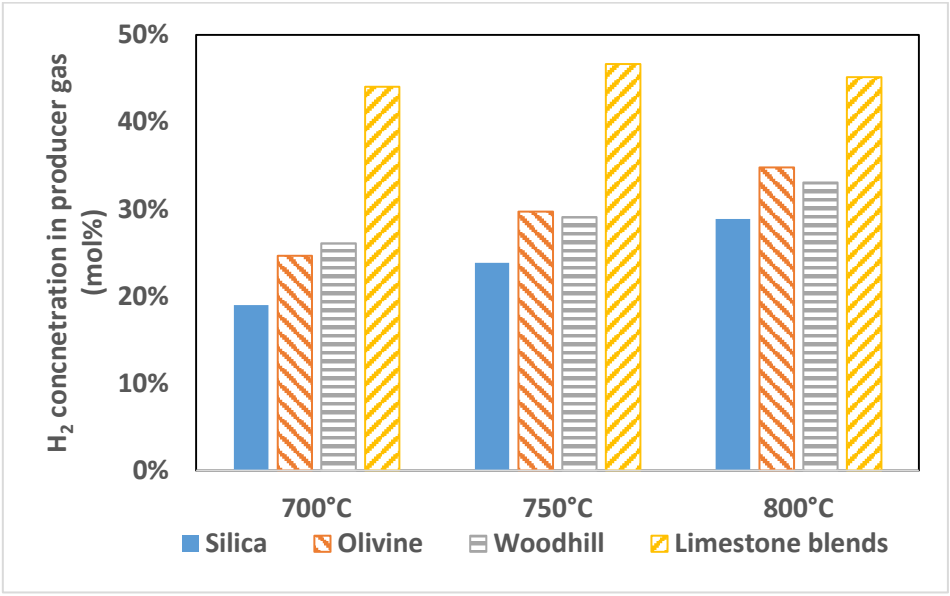

(a)

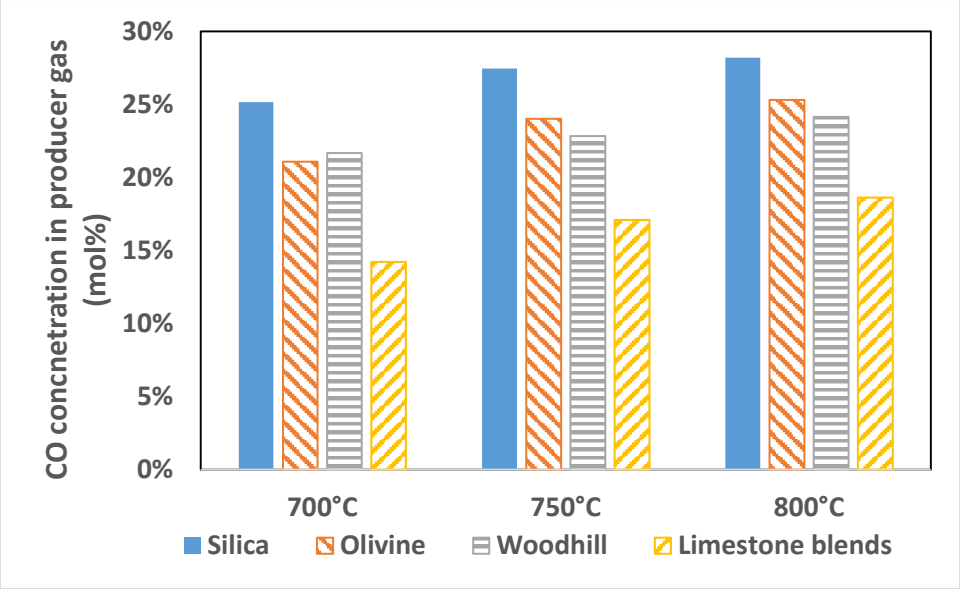
CO concnetration in producer gas (mol%)
30%
25%
20%
15%
10%
5%
0%
700°C
750°C
800°C
Silica
Olivine
Woodhill
Limestone blends

(b)

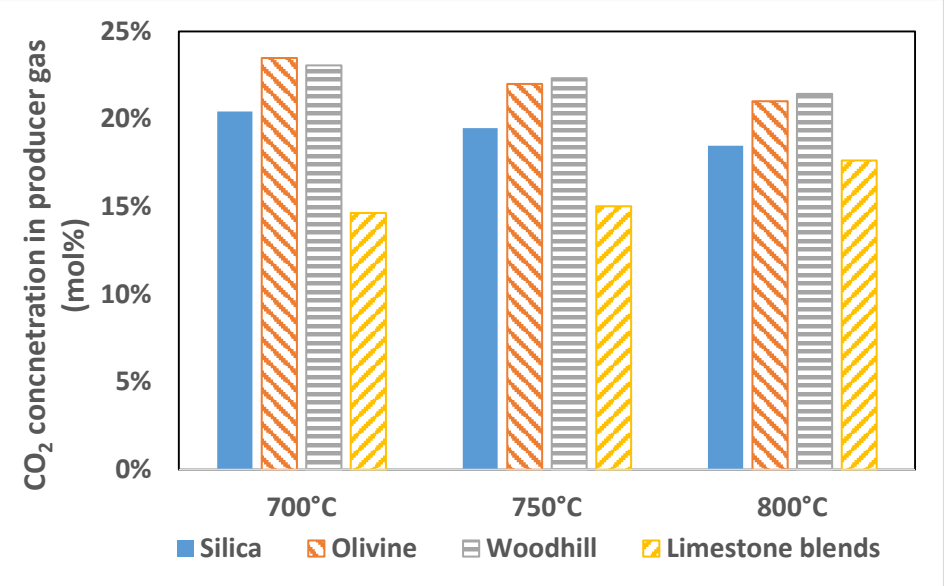
CO_2 concnetration in producer gas (mol%)
25%
20%
15%
10%
5%
0%
700°C
750°C
800°C
Silica
Olivine
Woodhill
Limestone blends

(c)

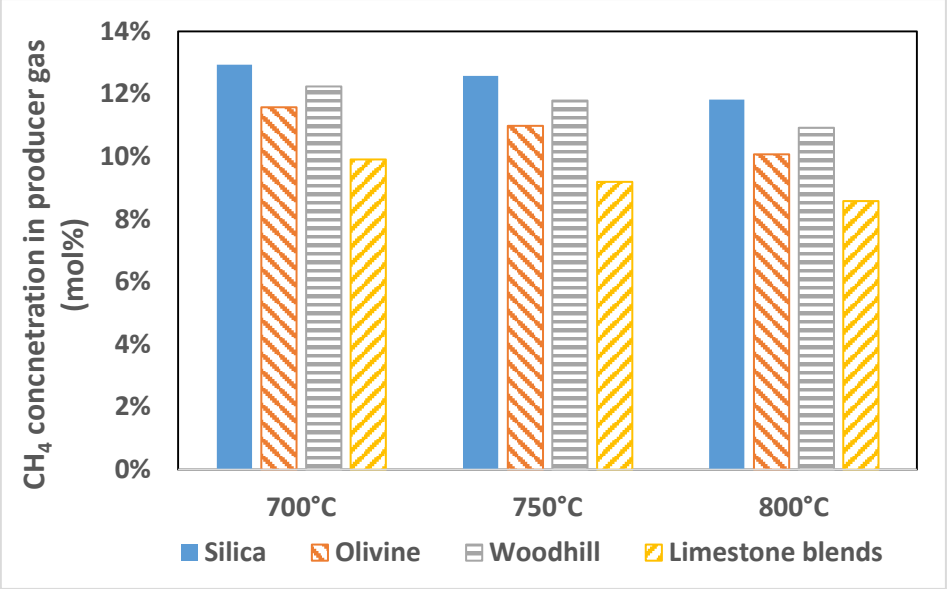

(d)

Fig. 7-2. The variation of gas composition of H_2 (a), CO (b), CO_2 (c) and CH_4 (d) with two gasification temperature for four different bed materials.

The results as shown in Fig. 7-2 are re-organised as concentration ratios of H_2/CO, H_2/CO_2 and CO/CO_2 (mol/mol), and the results are illustrated, respectively, in Figs. 7-3(a) to 7-3(c). From these figures, it was found that the H_2/CO, H_2/CO_2 and CO/CO_2 ratios for silica sand and iron-rich sand increased with an increase in gasification temperature. These results are in agreement with those reported by other researchers [6, 22]. However, in the case of limestone-silica blends, the effects of temperature on these three ratios were different. As the temperature increased, the H_2/CO ratio was reduced, while both the H_2/CO_2 and CO/CO_2 ratios were increased first and then dropped significantly.

These results demonstrated that these bed materials have different catalytic effects on the WGS reaction, which is considered to contribute most significantly to the changes in specific gas composition [23]. The fact that the highest H_2 content in the producer gas for using limestone-silica blends exhibits the largest ratio of H_2/CO and H_2/CO_2 at the same temperature. For example, at 700°C, the ratio of H_2/CO_2 is 3.1 for the limestone-silica blends, 1.22 for the Woodhill sand, 1.11 for the olivine sand and 0.75 for the silica sand. These results are in agreement with those reported by Saw and Pang [12], that the change in these ratios was dependent on the CaO loading in the system. It is believed that the increased H_2 concentration was due to the in-situ CO_2 absorption

by CaO in BFB as shown in Eq. (7-6), which favours the forward direction in the WGS reaction [11, 24]. However, the deactivation of CaO sorbent at the high temperatures resulted in reduction of both H_2/CO and H_2/CO_2 ratios.

In the case of iron-rich sands, iron oxide in the bed material is active on the WGS reaction in forwarding direction for generation of hydrogen and carbon dioxide. Therefore, compared to silica sand, a higher H_2/CO ratio and a lower CO/CO_2 ratio were obtained when iron-rich sand was used. In addition, these two ratios by using olivine sand were lower than those by using Woodhill sand at 700°C. However, as the temperature increased, the ratios of H_2/CO and CO/CO_2 by using olivine sand were higher than those by using Woodhill sand. These variations may be attributed to the chemical composition of the bed materials between olivine sand and Woodhill sand. From Table 7-1, it can be seen that Woodhill sand contains more CaO, while olivine sand has more MgO. In a study of Di Felice et al. [25], it is reported that an increased temperature accelerated the reduction rate of $Fe^{3+} \rightarrow Fe^{2+}$ in the Fe-CaO substrate rather than that in the Fe-MgO substrate. Therefore, the CO_2 production from olivine sand was higher than that in Woodhill sand at high temperatures.

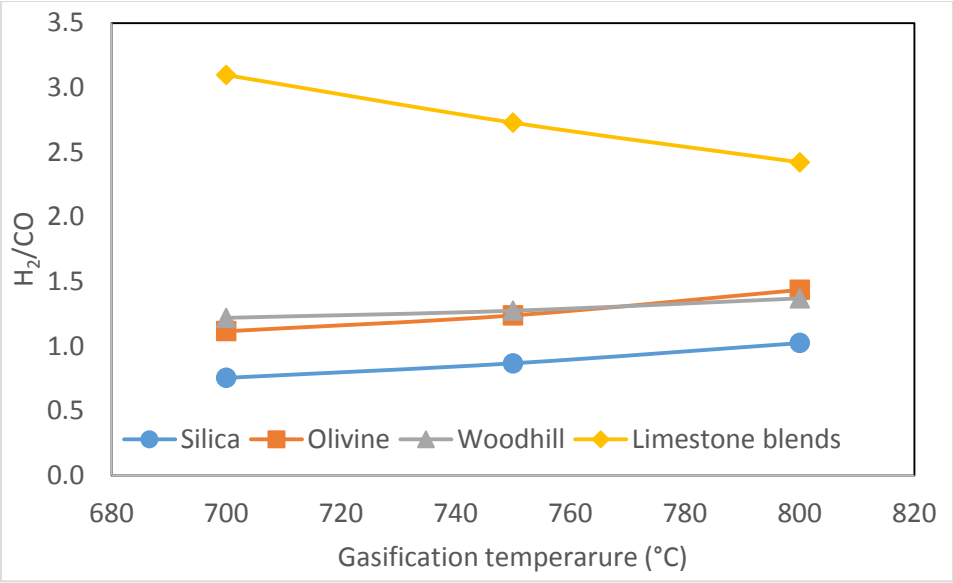

(a)

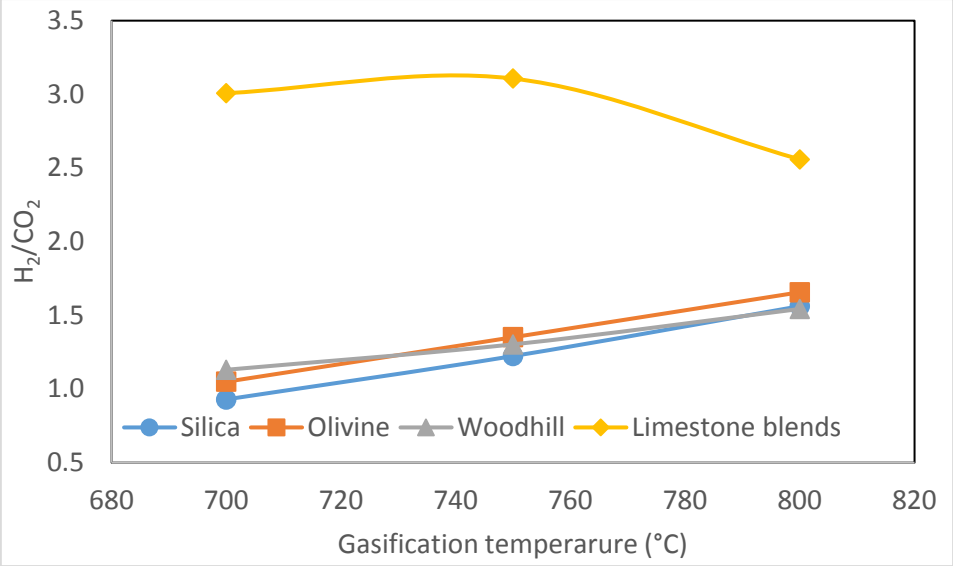

(b)

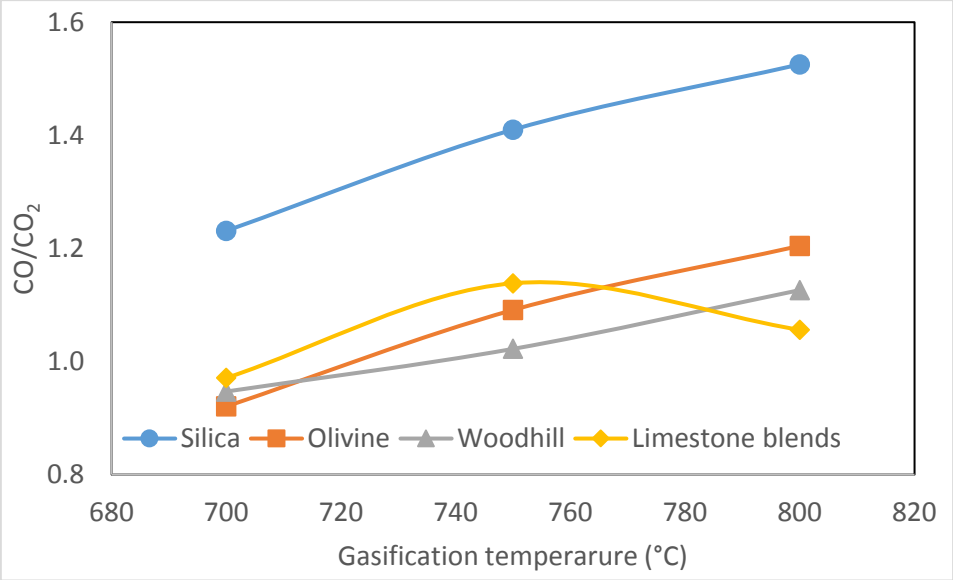

(c)

Fig. 7-3. The influence of bed material and temperature on the ratios of H_2/CO (a), H_2/CO_2 (b), CO/CO_2 (c) in the producer gas.

7.3.2. Tar composition and concentration

The influence of bed material and temperature on tar yield and tar composition is shown in Fig. 7-4(a) for gasification temperature of 700°C, in Fig. 7-4(b) for 750°C and in Fig.7-4(c) for 800°C. The tar compounds presented in Fig. 7-4 include all of the tar classes from light to heavy measured by the GC-FID. Each data presented here was the average value of three repeated measurements. From Fig. 7-4, it is found that the temperature has significant influence on the tar yield and tar composition. The total tar concentration decreased when the temperature was increased from 700 to 800°C for the

all tested bed materials. With the temperature increase from 700 to 800°C, total tar concentration reduced by 21% from 15.8 g/Nm^3 to 12.4 g/Nm^3 for silica sand, by 34% from 11.7 g/Nm^3 to 7.7 g/Nm^3 for olivine sand, by 27% from 10.9 g/Nm^3 to 8.0 g/Nm^3 for Woodhill sand, finally by 38% from 8.1 g/Nm^3 to 5.0 g/Nm^3 for limestone-silica blends.

It is observed that at the gasification temperature of 700°C with comparison with the silica sand, the use of limestone-silica blends reduced the total tar concentration by 49%. While two iron-rich sand showed similar behaviours, the reduction of total tar concentration was 26% for olivine sand and 31% for Woodhill sand, respectively. Apparently, limestone is more reactive than iron-rich sand with respect to tar decomposition due to the steam reforming of tars in the presence of CaO [26]. This phenomenon is in agreement with the other published works [27, 28]. Woodhill sand also shows a greater effect on tar decomposition than olivine sand, since it contained a high proportion of CaO as shown in Table 7-1.

At the gasification temperature of 800°C, the reduction of total tar concentration was 38% for olivine sand, 36% for Woodhill sand and 55% for limestone-silica blends as compared with silica sand. It is believed that the tar decomposing activity of iron-rich sand is increased at the high temperatures. In fact, the iron oxide content in iron-rich sand favours the tar reforming reaction as shown in Eq (7-2), which is enhanced by the rising temperature [29, 30].

The results in Fig. 7-4 also show the effects of catalytic bed material on tar composition (each tar class) at different temperatures which will be discussed in more details in the following sections.

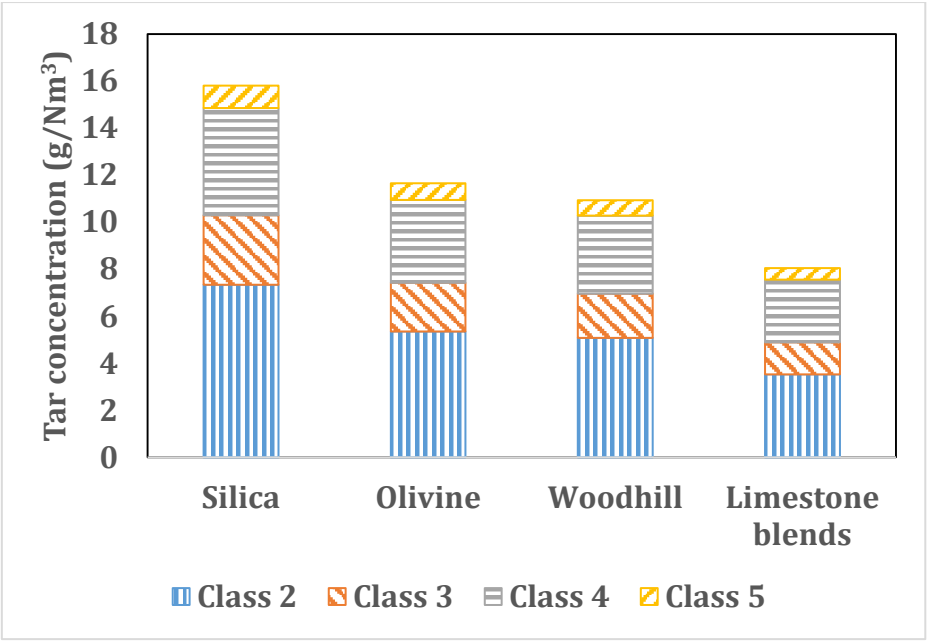
Tar concentration (g/Nm3)
18
16
14
12
10
8
6
4
2
0
Silica
Olivine
Woodhill
Limestone blends
Class 2
Class 3
Class 4
Class 5

(a)

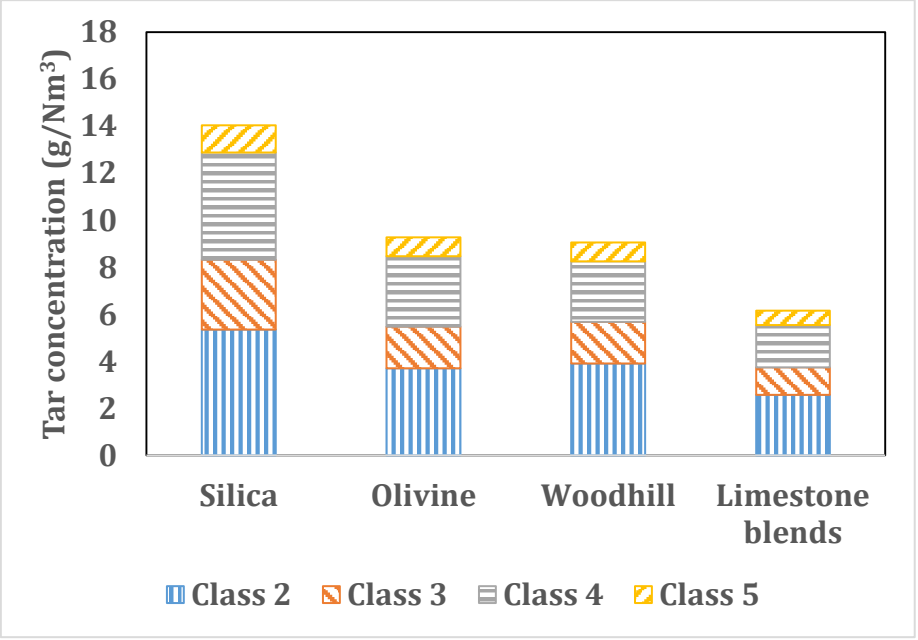
Tar concentration (g/Nm3)
18
16
14
12
10
8
6
4
2
0
Silica
Olivine
Woodhill
Limestone blends
Class 2
Class 3
Class 4
Class 5

(b)

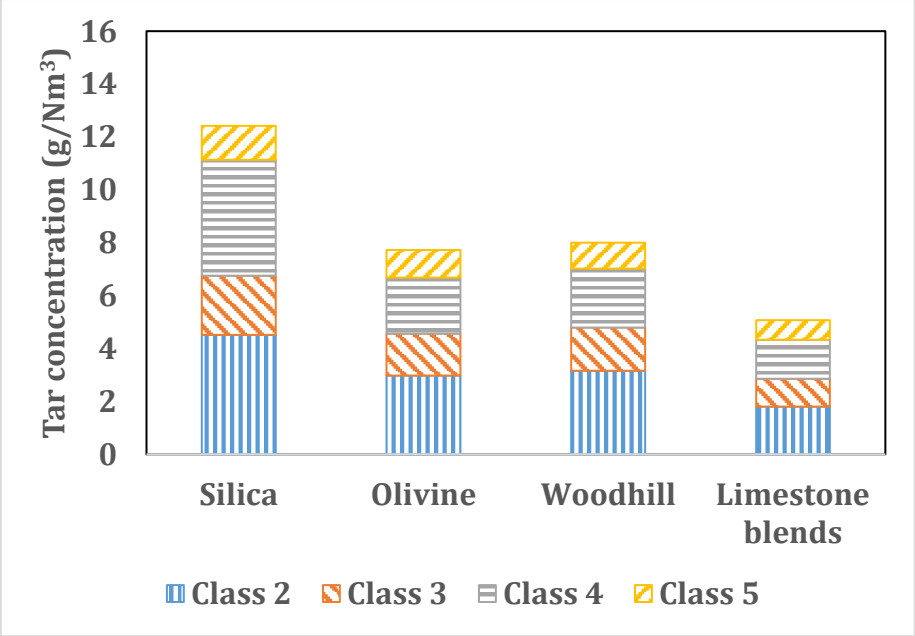

(b)

Fig. 7-4. The variation of tar concentration with four different bed materials at two different gasification temperatures of (a) 700°C, (b) 750°C and (c) 800°C.

7.3.2.1. Class 2 tar compounds

The concentrations of major tar compounds in Class 2 tar are shown in Fig. 7-5 for gasification temperature of 700°C. In the figure, the influence of bed material on the concentrations of phenols, m-cresol and o-cresol are presented. The results in Fig. 7-5 showed that with use of catalytic bed materials, the phenols could be effectively decomposed into gas and other lighter tar compounds. The limestone is the most effective bed material to crack other compounds as well. For example, in comparison with silica sand, the concentration of phenols was reduced from 4.2 g/Nm^3 to 2.6 g/Nm^3 by using the olivine sand, to 2.3 g/Nm^3 for Woodhill sand and to 1.9 g/Nm^3 for limestone-silica blends. Moreover, it is remarkable that by application of the limestone-silica blends, the concentrations of m-cresol and o-cresol were reduced approximately by 50%. However, the reduction rates of m-cresol and o-cresols concentrations for using iron-rich sand were less significant.

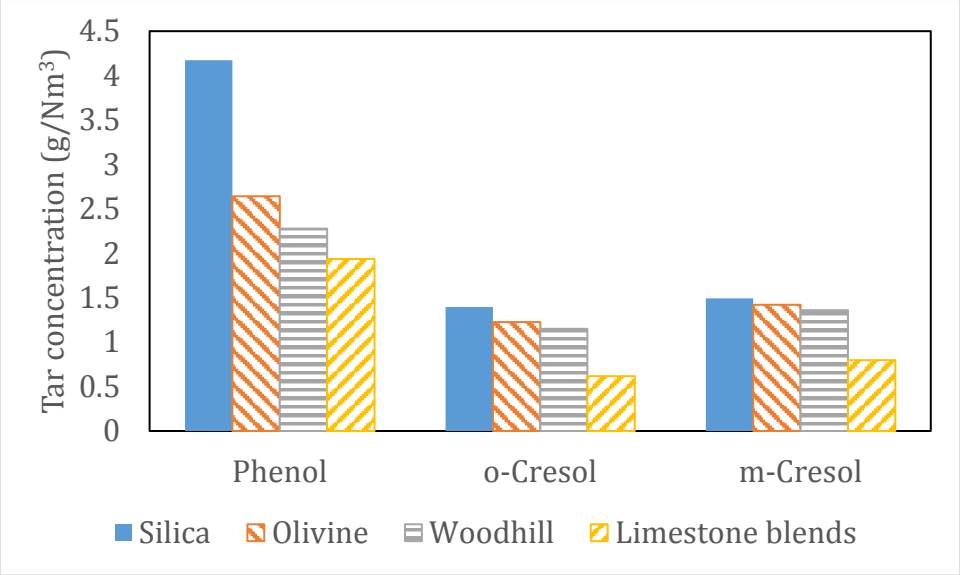

Fig. 7-5. The influence of catalytic bed material on major Class 2 tar compounds in the producer gas at the gasification temperature of 700°C.

7.3.2.2. Class 3 tar compounds

Fig. 7-6 shows the effect of bed materials on major Class 3 tar compounds (toluene, styrene and xylene) at gasification temperature of 700 °C. In the case of silica sand as the bed material, the concentrations of toluene, styrene and xylene were 1.5 g/Nm^3, 0.6 g/Nm^3 and 0.7 g/Nm^3, respectively. By using the limestone-silica blends, the concentrations of these compounds were decreased by 55% to 0.68 g/Nm^3 for toluene, 46% to 0.31 g/Nm^3 for styrene and 58% to 0.28 g/Nm^3 for xylene. The reduction rates of major Class 3 tar compounds for using iron-rich sands as the bed material were less than those using limestone-silica blends. For example, using olivine and Woodhill sands, the toluene concentrations were reduced by 28% to 1.08 g/Nm^3 and by 38% to 0.92 g/Nm^3, respectively. It is anticipated that the formation of Class 3 tar compounds is complex, which can be produced from devolatilization of biomass in the initial gasification stage and from the decomposition of Class 2 tar compounds [31]. In the same time, Class 3 tar compound may also act as precursors for the Class 4 tar compounds through polymerisation [32].

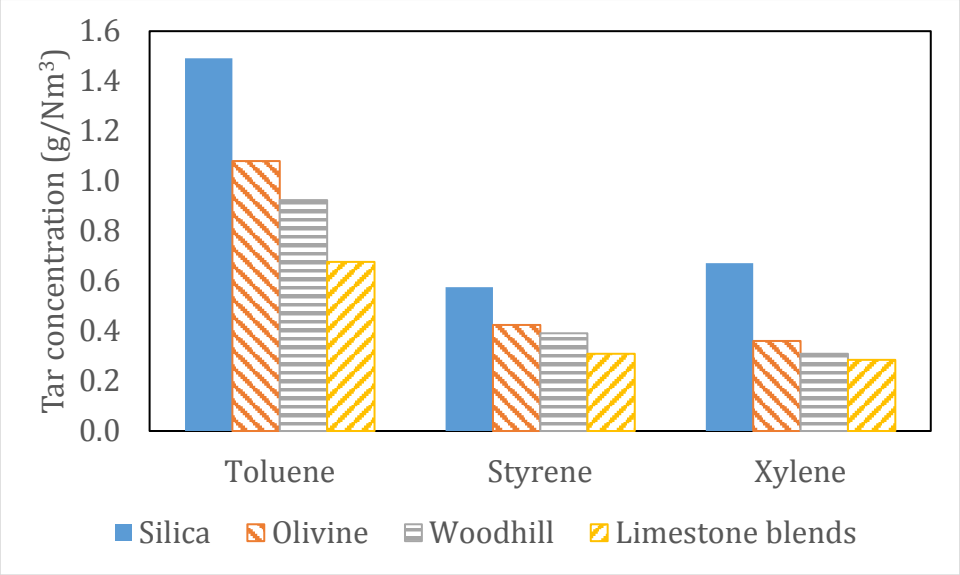

Fig. 7-6. The influence of catalytic bed material on major Class 3 tar compounds in the producer gas at the gasification temperature of 700°C.

7.3.2.3. Class 4 tar compounds

Fig. 7-7 presents the concentrations of major Class 4 tar compounds (naphthalene, biphenyl, 1- and 2-methylnaphthalene, and acenaphthylene) with different bed materials. Among all the major C4 tar compounds, naphthalene was the major compound contributing to almost 50%, and it is a very stable compound. From Fig. 7-7, it is observed that in comparison with silica sand, the concentration of naphthalene was reduced by 23% (from 2.11 to 1.62 g/Nm^3) for using olivine sand, by 26% (to 1.56 g/Nm^3) for using Woodhill sand and by 37% (to 1.33 g/Nm^3) for limestone-silica blends as bed material. Similar trends were also observed from Fig. 7-7 on the reduction of concentrations of other major Class 4 compounds using catalytic bed materials and these compounds include biphenyl, 1- and 2-methylnaphthalene, and acenaphthylene.

From the experimental results, the overall Class 4 tar concentration was 4.15 g/Nm^3 using silica sand as bed material. This was reduced to 3.23 g/Nm^3 using olivine sand, to 2.98 g/Nm^3 using Woodhill sand and to 2.14 g/Nm^3 using limestone-silica blend as the bed material. It is interesting to find that although the overall concentration of major Class 4 tar compounds was reduced by using the catalytic bed materials. The proportion of naphthalene in the overall Class 4 tar compounds increased from 45% for silica sand to 50% for olivine sand, to 52% for Woodhill sand and to 58% for limestone-silica blends. This means that the naphthalene is relatively stable and the potential

naphthalene-steam reaction was inhibited by the increase of H_2 content in the producer gas [33]. In addition, the decomposition of larger PAH components may produce naphthalene.

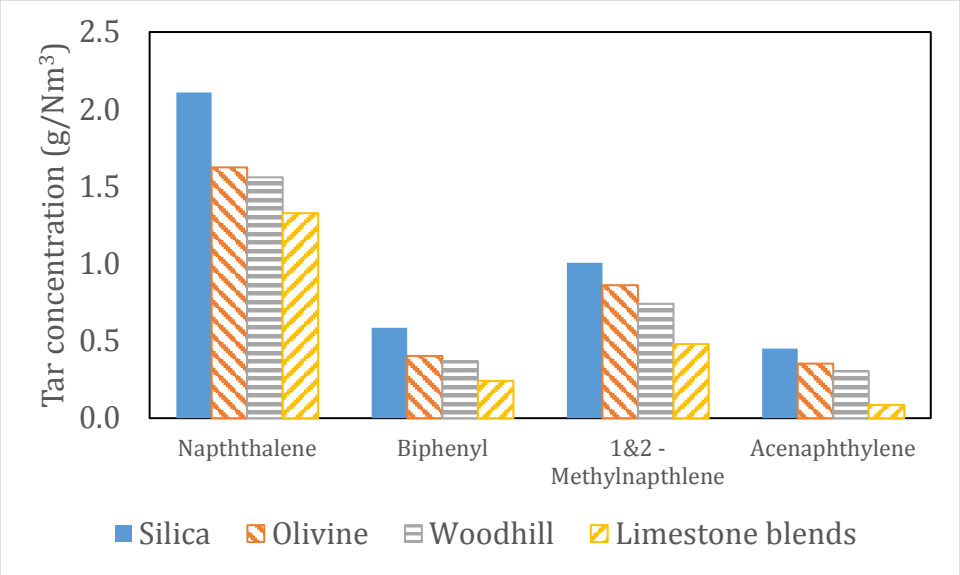

Fig. 7-7. The influence of catalytic bed material on major Class 4 tar compounds in the producer gas at the gasification temperature of 700°C.

7.3.2.4. Class 5 tar compounds

The Class 5 tar is the most important as they have the highest tar dew point at low concentration and thus will condense first while the producer gas cools down. Fluoranthene, pyrene and benzo(a)anthracene are the major Class 5 tar compounds. The comparison of four different bed materials on the Class 5 tar compounds is illustrated in Fig. 7-8 for gasification temperature of 700°C. In a similar trend to other class tar compounds, the concentrations of the major Class 5 tar compounds were also decreased with use of the catalytic bed materials as compared to silica sand. By using olivine sand and Woodhill sand, the fluoranthene concentration was reduced by 29% (from 0.27 to 0.19 g/Nm^3) and by 53% (to 0.13 g/Nm^3), respectively. The use of limestone-silica sand reduced the fluoranthene concentration by 78% to 0.06 g/Nm^3 at the same gasification temperature.

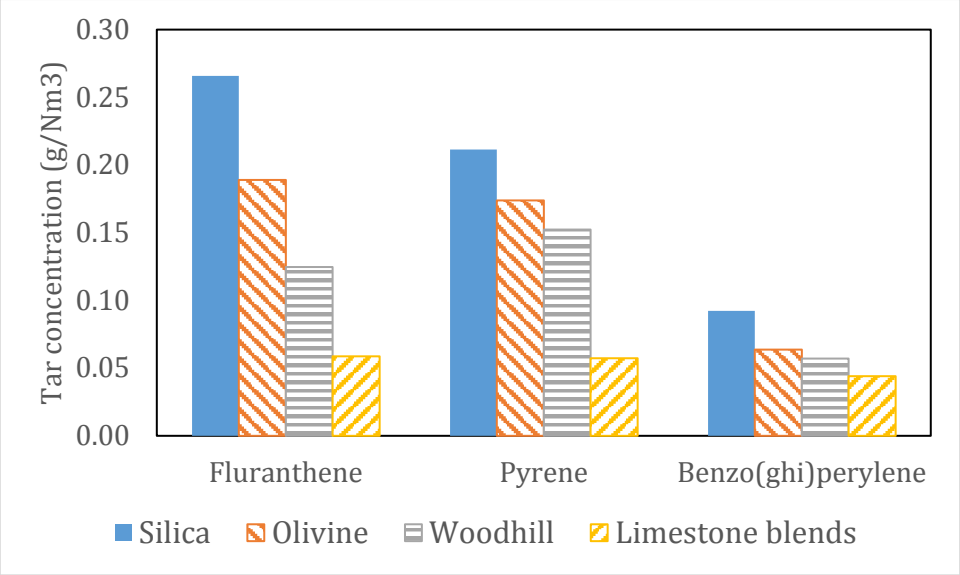

Fig. 7-8. The influence of catalytic bed material on major Class 5 tar compounds in the producer gas at the gasification temperature of 700°C.

7.3.3. Attrition and agglomeration of bed materials

The attrition rate in a commercial scale gasification plant can induce significant costs for the lost bed materials. Hence, it is important to investigate the attrition rate of the bed material in a demonstration plant. In this part of study, the fine particles of bed materials were collected both from the FFB and the BFB reactors and weighed over a pre-set period of time when the gasifier was in normal operation. The attrition rate was determined as the total mass of fine particles of bed materials entrained by gases both from the FFB and the BFB reactors per unit time. The results for the four types of bed materials are shown in Fig. 7-9 for gasification temperature of 700°C. As expected, silica sand showed the best mechanical resistance with the lowest attrition rate of 0.59 kg/h. The attrition rate of iron-rich sand was slightly higher than the silica sand, which was 0.81 kg/h for olivine sand and 0.79 kg/h for Woodhill sand. Limestone-silica blends had the highest attrition rate of 3.08 kg/h, which was nearly 5 times greater than silica sand, confirming the significant impact damage of the limestone with low mechanical strength. In addition, the formation of $Ca(OH)_2$ under steam environment would further aggravate the calcite attrition [14].

Compared to olivine sand and Woodhill sand, limestone favoured the hydrogen production in the producer gas and showed a high efficiency in tar removal, however, limestone would become very friable after a number of calcination/carbonation cycles

which would lead to higher consumption of the bed material and increased costs. Furthermore, the limestone powder from attrition may result in blockage of pipe and filter [34]. Considering the overall performance and potential costs, the olivine sand and Woodhill sand with high resistance to attrition are preferred choice for the fluidised bed gasifier unless high hydrogen content in the producer gas is the primary target for the biomass gasification.

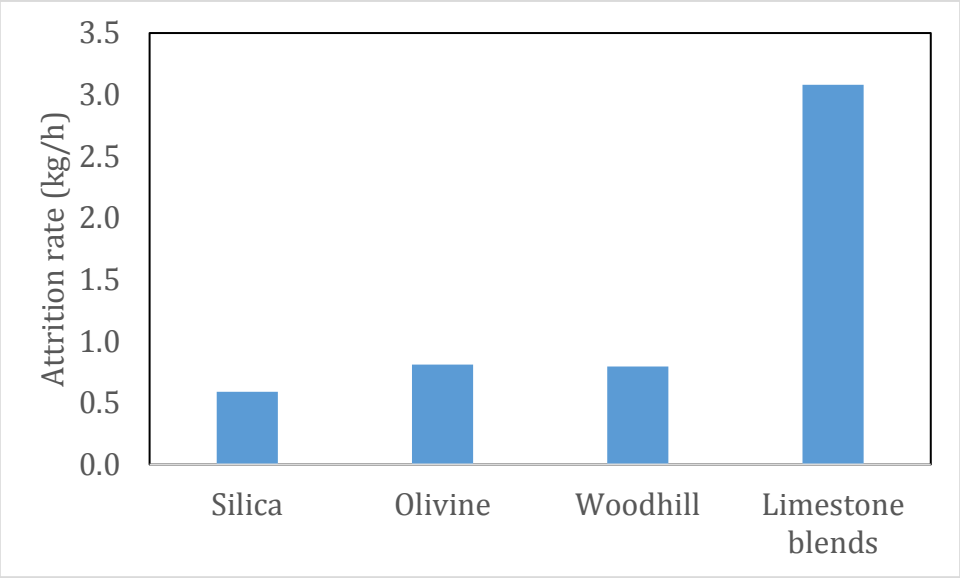

Fig. 7-9. The attrition rate of the bed materials in the steam biomass gasification at gasification temperature of 700°C.

7.4. Conclusion

In this part of study, effects of catalytic bed materials on the performance of steam biomass gasification were experimentally investigated in a 100kW dual fluidised bed gasifier at three different gasification temperatures. These bed materials include including calcined olivine sand, Woodhill sand and limestone-silica blends while silica sand was used as control. From this study, the following conclusions can be derived:

(a) The catalytic bed material overall enhanced producer gas yield although the extent of enhancement varied with gasification temperature. At gasification temperature of 700°C, Woodhill sand gave the highest gas yield of 10.8 Nm^3/h, however, at 750°C, limestone-silica blends showed the highest gas yield of 13.9 Nm^3/h, and at

800°C, the largest gas yield of 16.8 Nm^3/h was found by using olivine sand. The corresponding gas yields for silica sand at these three gasification temperatures were, respectively, 7.4, 9.2 and 12.1 Nm^3/h.

(b) The catalytic bed materials also affect the producer gas composition although the gasification temperature is a key parameter influencing the producer gas composition. For iron-rich sands (olivine sand and Woodhill sand) and silica sand, as the gasification temperature increased, the H_2 and CO concentrations increased while CO_2 and CH_4 concentrations decreased. However, by using limestone-silica blends as the bed material, the H_2 concentration was increased from 700 to 750°C and then slightly decreased with further increase in the gasification temperature. In the meantime, the CO and CO_2 concentrations were increased with increasing temperature. It is believed that water gas shift reaction was promoted for the forward direction by the catalytic bed material promoted. The limestone produced the producer gas with the highest H_2 content due to the CO_2 capture through the carbonation/calcination cycles.

(c) The application of catalytic bed materials enhanced the decomposition of tar compounds. Limestone was more reactive than iron-rich sands with respect to tar decomposition. It is observed that at 700°C, the total tar concentration was reduced by 26% for olivine sand, by 31% for Woodhill sand and by 49% for limestone-silica blends. In addition, the high temperature can promote the reactive of iron-rich sands for tar reforming and cracking.

(d) Due to a higher attrition resistance of the iron-rich sands, it is expected that olivine sand and Woodhill sand are preferred choice as bed materials in steam gasification of biomass in a fluidised-bed biomass gasifier. However, if high hydrogen content in the producer gas is the primary target in biomass gasification, limestone is most promising although strengthening of limestone needs to be investigated for reducing its attrition rate.

7.5. Reference

[1] K. Göransson, U. Söderlind, J. He, and W. Zhang, "Review of syngas production via biomass DFBGs," *Renewable and Sustainable Energy Reviews,* vol. 15, pp. 482-492, 2011.

[2] Y. Shen and K. Yoshikawa, "Recent progresses in catalytic tar elimination during biomass gasification or pyrolysis—A review," *Renewable and Sustainable Energy Reviews,* vol. 21, pp. 371-392, 2013.

[3] M. Shahbaz, S. yusup, A. Inayat, D. O. Patrick, and M. Ammar, "The influence of catalysts in biomass steam gasification and catalytic potential of coal bottom ash in biomass steam gasification: A review," *Renewable and Sustainable Energy Reviews,* vol. 73, pp. 468-476, 2017.

[4] S. Koppatz, C. Pfeifer, and H. Hofbauer, "Comparison of the performance behaviour of silica sand and olivine in a dual fluidised bed reactor system for steam gasification of biomass at pilot plant scale," *Chemical Engineering Journal,* vol. 175, pp. 468-483, 2011.

[5] M. Virginie, C. Courson, D. Niznansky, N. Chaoui, and A. Kiennemann, "Characterization and reactivity in toluene reforming of a Fe/olivine catalyst designed for gas cleanup in biomass gasification," *Applied Catalysis B: Environmental,* vol. 101, pp. 90-100, 2010.

[6] C. Christodoulou, D. Grimekis, K. D. Panopoulos, E. P. Pachatouridou, E. F. Iliopoulou, and E. Kakaras, "Comparing calcined and un-treated olivine as bed materials for tar reduction in fluidized bed gasification," *Fuel Processing Technology,* vol. 124, pp. 275-285, 2014.

[7] L. Devi, K. J. Ptasinski, and F. J. Janssen, "Pretreated olivine as tar removal catalyst for biomass gasifiers: investigation using naphthalene as model biomass tar," *Fuel Processing Technology,* vol. 86, pp. 707-730, 2005.

[8] M. Naqvi, J. Yan, M. Danish, U. Farooq, and S. Lu, "An experimental study on hydrogen enriched gas with reduced tar formation using pre-treated olivine in dual bed steam gasification of mixed biomass compost," *International Journal of Hydrogen Energy,* vol. 41, pp. 10608-10618, 2016.

[9] K. Göransson, U. Söderlind, P. Engstrand, and W. Zhang, "An experimental study on catalytic bed materials in a biomass dual fluidised bed gasifier," *Renewable Energy,* vol. 81, pp. 251-261, 2015.

[10] K. Matsuoka, T. Shimbori, K. Kuramoto, H. Hatano, and Y. Suzuki, "Steam Reforming of Woody Biomass in a Fluidized Bed of Iron Oxide-Impregnated Porous Alumina," *Energy & Fuels,* vol. 20, pp. 2727-2731, 2006.

[11] G. Soukup, C. Pfeifer, A. Kreuzeder, and H. Hofbauer, "In situ CO2 capture in a dual fluidized bed biomass steam gasifier–bed material and fuel variation," *Chemical engineering & technology,* vol. 32, pp. 348-354, 2009.

[12] W. L. Saw and S. Pang, "The influence of calcite loading on producer gas composition and tar concentration of radiata pine pellets in a dual fluidised bed steam gasifier," *Fuel,* vol. 102, pp. 445-452, 2012.

[13] N. H. Florin and A. T. Harris, "Enhanced hydrogen production from biomass with in situ carbon dioxide capture using calcium oxide sorbents," *Chemical Engineering Science,* vol. 63, pp. 287-316, 2008.

[14] L. Han, Q. Wang, Y. Yang, C. Yu, M. Fang, and Z. Luo, "Hydrogen production via CaO sorption enhanced anaerobic gasification of sawdust in a bubbling fluidized bed," *International Journal of Hydrogen Energy,* vol. 36, pp. 4820-4829, 2011.

[15] C. Pfeifer, B. Puchner, and H. Hofbauer, "Comparison of dual fluidized bed steam gasification of biomass with and without selective transport of CO 2," *Chemical Engineering Science,* vol. 64, pp. 5073-5083, 2009.

[16] C. Pfeifer, B. Puchner, and H. Hofbauer, "In-situ CO2-absorption in a dual fluidized bed biomass steam gasifier to produce a hydrogen rich syngas," *International Journal of Chemical Reactor Engineering,* vol. 5, 2007.

[17] C. Franco, F. Pinto, I. Gulyurtlu, and I. Cabrita, "The study of reactions influencing the biomass steam gasification process," *Fuel,* vol. 82, pp. 835-842, 2003.

[18] M. Lapuerta, J. J. Hernández, A. Pazo, and J. López, "Gasification and co-gasification of biomass wastes: Effect of the biomass origin and the gasifier operating conditions," *Fuel Processing Technology,* vol. 89, pp. 828-837, 2008.

[19] M. Detournay, M. Hemati, and R. Andreux, "Biomass steam gasification in fluidized bed of inert or catalytic particles: Comparison between experimental results and thermodynamic equilibrium predictions," *Powder Technology,* vol. 208, pp. 558-567, 2011.

[20] Z.-s. Li, F. Fang, X.-y. Tang, and N.-s. Cai, "Effect of Temperature on the Carbonation Reaction of CaO with CO2," *Energy & Fuels,* vol. 26, pp. 2473-2482, 2012.

[21] P. Weerachanchai, M. Horio, and C. Tangsathitkulchai, "Effects of gasifying conditions and bed materials on fluidized bed steam gasification of wood biomass," *Bioresource Technology,* vol. 100, pp. 1419-1427, 2009.

[22] D. A. Constantinou, J. L. G. Fierro, and A. M. Efstathiou, "A comparative study of the steam reforming of phenol towards H2 production over natural calcite, dolomite and olivine materials," *Applied Catalysis B: Environmental,* vol. 95, pp. 255-269, 2010.

[23] M. Kuba, F. Havlik, F. Kirnbauer, and H. Hofbauer, "Influence of bed material coatings on the water-gas-shift reaction and steam reforming of toluene as tar model compound of biomass gasification," *Biomass and Bioenergy,* vol. 89, pp. 40-49, 2016.

[24] G. Duelli, A. Charitos, M. E. Diego, E. Stavroulakis, H. Dieter, and G. Scheffknecht, "Investigations at a 100kWth calcium looping dual fluidized bed facility: Limestone calcination and CO2 capture under high CO2 and water vapor atmosphere," *International Journal of Greenhouse Gas Control,* vol. 33, pp. 103-112, 2015.

[25] L. Di Felice, C. Courson, D. Niznansky, P. U. Foscolo, and A. Kiennemann, "Biomass Gasification with Catalytic Tar Reforming: A Model Study into Activity Enhancement of Calcium- and Magnesium-Oxide-Based Catalytic Materials by Incorporation of Iron," *Energy & Fuels,* vol. 24, pp. 4034-4045, 2010.

[26] M. R. Mahishi and D. Y. Goswami, "An experimental study of hydrogen production by gasification of biomass in the presence of a CO2 sorbent," *International Journal of Hydrogen Energy,* vol. 32, pp. 2803-2808, 2007.

[27] T. Hanaoka, T. Yoshida, S. Fujimoto, K. Kamei, M. Harada, Y. Suzuki, H. Hatano, S.-y. Yokoyama, and T. Minowa, "Hydrogen production from woody biomass by steam gasification using a CO2 sorbent," *Biomass and Bioenergy,* vol. 28, pp. 63-68, 2005.

[28] L. Devi, K. J. Ptasinski, F. J. J. G. Janssen, S. V. B. van Paasen, P. C. A. Bergman, and J. H. A. Kiel, "Catalytic decomposition of biomass tars: use of

dolomite and untreated olivine," *Renewable Energy,* vol. 30, pp. 565-587, 2005.

[29] M. Virginie, J. Adánez, C. Courson, L. F. de Diego, F. García-Labiano, D. Niznansky, A. Kiennemann, P. Gayán, and A. Abad, "Effect of Fe–olivine on the tar content during biomass gasification in a dual fluidized bed," *Applied Catalysis B: Environmental,* vol. 121, pp. 214-222, 2012.

[30] M. Virginie, C. Courson, and A. Kiennemann, "Toluene steam reforming as tar model molecule produced during biomass gasification with an iron/olivine catalyst," *Comptes Rendus Chimie,* vol. 13, pp. 1319-1325, 2010.

[31] G. Taralas, M. G. Kontominas, and X. Kakatsios, "Modeling the thermal destruction of toluene (C7H8) as tar-related species for fuel gas cleanup," *Energy & Fuels,* vol. 17, pp. 329-337, 2003.

[32] B. Vreugdenhil, R. Zwart, and J. P. A. Neeft, "Tar formation in pyrolysis and gasification," Energy research Centre of the Netherlands (ECN) Report, The Netherlands, ECN-E--08-087, 2009.

[33] R. Michel, A. Łamacz, A. Krzton, G. Djéga-Mariadassou, P. Burg, C. Courson, and R. Gruber, "Steam reforming of α-methylnaphthalene as a model tar compound over olivine and olivine supported nickel," *Fuel,* vol. 109, pp. 653-660, 2013.

[34] G. Hu, S. Xu, S. Li, C. Xiao, and S. Liu, "Steam gasification of apricot stones with olivine and dolomite as downstream catalysts," *Fuel Processing Technology,* vol. 87, pp. 375-382, 2006.

Chapter 8. Conclusion and Recommendation

8.1. Conclusion

Steam gasification in a fluidised bed reactor is one of the promising biomass conversion technologies. The Bioenergy Research Team at the University of Canterbury has been developed and constructed a 100Kw dual fluidised bed (DFB) gasifier to produce a hydrogen-rich producer gas. However, the presence of tar compounds in the producer gas limits the commercialisation of this technology. The present thesis experimentally investigated the performance of the DFB gasifier to better understand the tar formation and conversion from initial devolatilization to subsequent gasification and reduce the tar concentration in the producer gas. Three main tasks are developed in the present thesis. The first task aims to investigate the effects of operating parameters including temperature, residence time and steam to biomass ratio on the tar formation. The second task deals with the tar conversion over different biomass feedstock. And the final task is to investigate the influence of catalytic bed material on the tar conversion. The results from these three parts are intended to clarify the tar formation and conversion and to optimise the operating conditions reducing the tar production in the DFB gasifier.

To achieve these objectives, a series of the experiments have been conducted on the 100kW DFB gasifier to investigate the tar formation and conversions as well as producer gas yield and composition in biomass gasification under various operating conditions. Gas and tar sampling and analysis methods were conducted in the experiments. The gas composition was analysed through a Micro-GC, while the tar compounds in this study were analysed using the GC-FID and categories into 5 classes based on the method reported in literature.

In first part of this study, tar formation and composition in the initial devolatilization of biomass gasification were found to be closely correlated to the producer gas quality from final stage of gasification. The producer gas quality parameters include tar concentration, tar composition, producer gas yield and gas composition. It is found that the tar concentrations in Class 2 to Class 5 were reduced from the devolatilization stage to the final stage of gasification due to cracking of some compounds. The tar compound distribution was also changed through tar conversion and re-polymerization. The gas

yield was increased and gas composition was changed from the devolatilization to final gasification stage towards the equilibrium of homogeneous reactions among the gas species.

The correlations between tar and light gas compounds (PAH tar with 2 and 3 rings-CH_4 and Class 5 tar-C_2 gas) were investigated. In the initial devolatilization, linear relations on the mass production between of light poly-hydrocarbon (PAH) tar compounds and CH_4, and between heavy PAH tar compounds and C_2 gas (C_2H_2+C_2H_4) were obtained. CH_4 is produced from the conversion of the secondary and tertiary tar compounds. On the other hands, it is believed that the formation of Class 5 tar compounds is strongly related to the C_2 light gas in the product gas due to the mechanism of H_2-abstraction-C_2H_2-addition sequence. Consequently, CH_4, C_2H_2 and C_2H_4 could be used as indicators of tar production and speciation during devolatilization.

In the subsequent gasification, the relation on the mass production between light PAH tar compounds and CH_4 did not perfectly match a line since the effect steam on CH_4 and tar reforming. But a linear correlation between heavy PAH tar compounds and C_2H_2+C_2H_4 were still obtained. These results allow demonstrating of the tar conversion and transformation, which can be used for the estimation of heavy PAH tar compounds production in the DFB gasifier.

From the experimental results, the total tar compounds reduced by 34% and 36%, respectively, with increased in the gasification temperature (in the range of 700-800°C) and residence time (from 0.19 to 0.25 s). However, the effects of these operating conditions on each class of tar compounds were different. With increase in the gasification temperature, the concentrations of Class 2 and Class 3 tar compounds were significantly decreased by 42% and 54%, respectively. The reduction of Class 2 and Class 3 tar compounds were caused either by the enhanced steam-tar reforming reaction or by the removal of the functional groups such as heteroatoms and methyl groups. A large number of aromatic ring units were produced from the dealkylation, and thus the formation of poly-aromatic hydrocarbon (PAH) tar compounds through dimerisation and cyclisation reactions were enhanced. Although some of Class 4 and Class 5 tar compounds were also reduced by steam-tar reforming reaction, the concentrations of Class 4 and Class 5 tar compounds were still increased by 25%. On the other hand, as

the τ increased, the concentrations of Class 2, Class 3 and Class 4 tar compounds decreased while those of Class 5 tar compounds were increased.

For the gas composition, the concentrations of H_2 and CO increased with an increase in the gasification temperature, but the CO_2 concentrations decreased while CH_4 remained relatively constant. With increase in gas residence time, the concentrations of H_2, CO_2 and CH_4 in the producer gas were increased while the CO concentration was reduced.

The experimental results show that the steam to biomass (S/B) ratio had significant effect on tar concentration and composition as well as gas yield and composition. The total tar yield was reduced with increase in the S/B ratio since the steam-tar reforming reaction was promoted. In addition, the yields of Class 2, Class 3 and Class 4 tar compounds were also decreased. However, those of Class 5 tar compounds was increased. In the meantime, the increase of steam supply to the gasification process (with increase in S/B ratio) promoted the water-gas shift reaction and methane steam reforming reaction towards forward direction. Therefore, the H_2 and CO_2 concentrations were increased but the CO and CH_4 concentrations were reduced in the producer gas.

In the second part of this study, various biomass species, including radiata pine wood, corn stover and rice husk, were tested as the feedstock for steam gasification. The chemical composition of each biomass was analysed, and the results were used for fundamental understanding of the tar formation process. It is found that corn stove is rich in cellulose, rice husk has a high content of hemicellulose and pine has a high content of lignin. These differences were the key contributors to the differences in the yields of tar compounds, gas composition and producer gas yield.

Due to the different chemical composition of cellulose, hemicellulose and lignin for various biomass species, overall tar concentrations and distributions of tar compounds in the producer gas were different from gasification of various biomass species. During the initial devolatilization stage of gasification, pine biomass generated more toluene while both corn stover and rice husk produced more phenols. In the final gasification process, the yields of light tar compounds, such as phenols, toluene and styrene were reduced while the yields of PAH tar compounds (naphthalene and biphenyl) were

increased for three tested biomass species. In the final gasification, the producer gas with pine wood had high concentrations of naphthalene, while that with corn stover had high concentration of biphenyl. The concentration of total PAH tar compounds in the producer gas for pine wood was the highest followed by rice husk and then corn stover. Based on these results, the two reaction pathways for tar transformation were proposed, one with toluene as a precursor and the other with phenols as a precursor.

The experimental results also show that yield and composition of producer gas were also affected by biomass species and this effect varied with gasification temperature. At 700°C, the yield of producer gas was the highest for corn stover followed by rice husk and pine wood. In contrast, at 800°C, the gas yield for pine wood was the highest followed by rice husk and then corn stover. However, at both gasification temperatures (700 and 800°C), the concentrations of H_2 and CH_4 in the producer gas were the highest from gasification of pine wood, the concentration of CO was the highest from gasification of rice husk while concentrations of CO_2, C_2H_4 and C_2H_6 were greater from gasification of corn stover than other two species.

Finally, this study has found that use of catalytic bed materials (olivine sand, Woodhill sand and blend of limestone and silica sand) enhanced the tar decomposition although limestone based bed material was the most reactive. At gasification temperature of 700°C, in comparison with silica sand, the total tar concentration was reduced from 15.8 g/Nm^3 to 11.7 g/Nm^3 for olivine sand, to 11.0 g/Nm^3 for Woodhill sand and to 8.2 g/Nm^3 for limestone-silica blends. At gasification temperature of 800°C, the total tar concentration was reduced from 12.4 g/Nm^3 to 7.7 g/Nm^3 for olivine sand, to 8 g/Nm^3 for Woodhill sand and to 5.1 g/Nm^3 for limestone-silica blends as compared with the silica sand.

The catalytic bed materials also affect the producer gas composition. At the same operating conditions (temperature and S/B ratio), the producer gas with the limestone based bed material had the highest H_2 content which was due to the CO_2 capture through the carbonation/calcination cycles as well as water gas shift (WGS) reaction. The WGS reaction was also enhanced with the application of iron-rich sands (olivine sand and Woodhill sand). Therefore, the H_2 concentration in the producer gas from biomass

gasification using these catalytic bed materials was also higher than that by using silica sand.

The results from this study have provided new knowledge on tar formation in the initial devolatilization and transformation through the subsequent gasification process during steam gasification of biomass. Based on the information obtained, gasification operation conditions can be optimised to produce producer gas with low tar concentration (approximately 5.0 g/Nm^3) and high hydrogen content, thus high calorific value. The optimised gasification conditions are higher temperature; longer gas residence time, high S/B rate and the use of catalytic bed materials.

8.2. Recommendations for future work

Although the tar concentration was minimised by using the optimum gasification conditions, the tar content in the producer gas is still much higher than the required concentration for downstream applications such as Fischer-Tropsch (F-T) synthesis (<1 ppm) and gas turbine (0.05 – 5 g/Nm^3). Therefore, downstream gas cleaning is needed, and further studies should develop efficient and cost-effective methods for tar removal following the gasification process.

Further studies are also recommended to optimise the gasification conditions based on target applications of the producer gas. For example, if the producer gas is used for power generation, high calorific values of the producer gas should be targeted. If the producer gas is used for liquid fuel through Fischer-Tropsch (F-T) synthesis, H_2 to CO ratio of 2 should be targeted. However, if the producer gas is used for pure H_2 and fuel cell, as high as a possible H_2 concentration in the producer gas should be targeted.

Appendices

A. Calibration of Feeding Rate for Biomass Species

In this part, the calibration curves on feeding rate for the pellets of radiata pine wood, corn stover and rice husk in 100kW dual fluidised bed gasified are shown in Figs. A-1, A-2 and A-3, respectively. The collect data is presented in Table A-1.

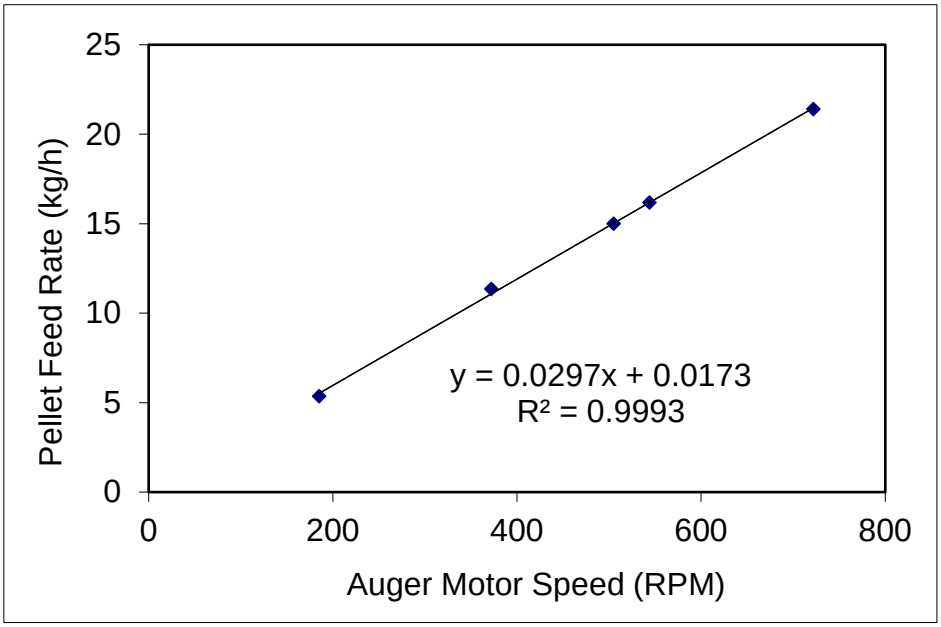

Fig. A-1. Calibration curve of feeding rate for radiata pine wood pellet.

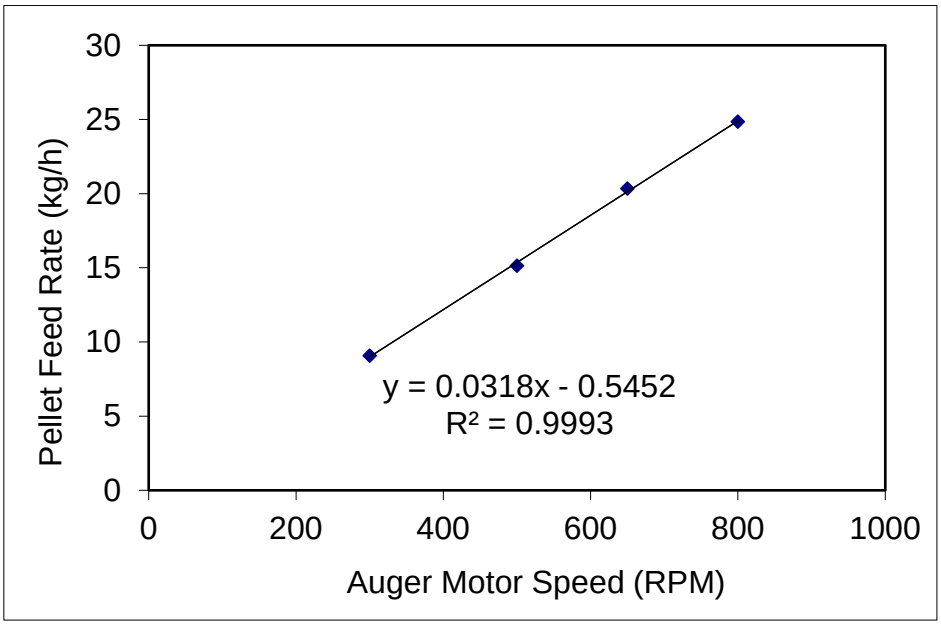

Fig. A-2. Calibration curve of feeding rate for rice husk pellet.

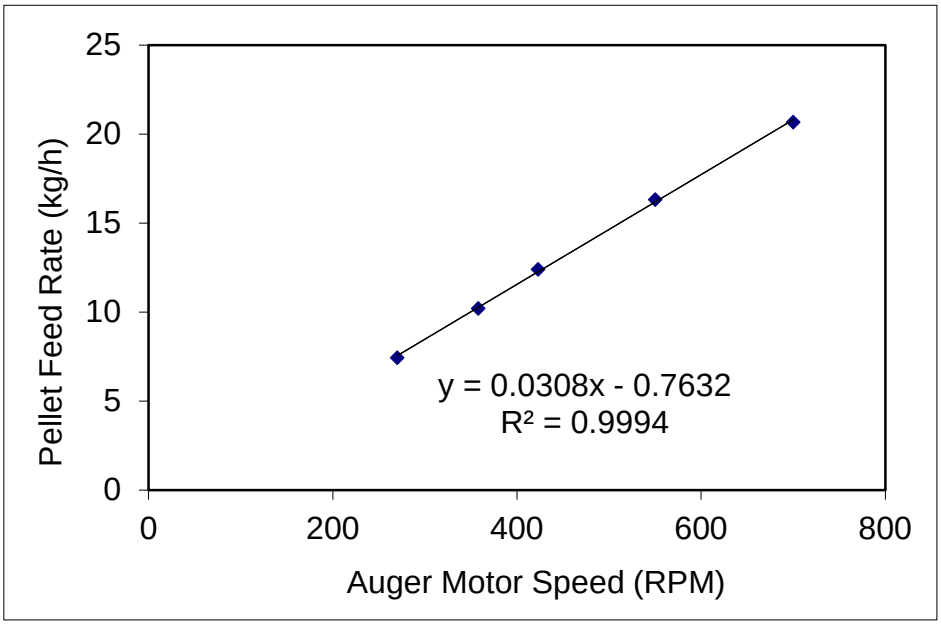

Fig. A-3. Calibration curve of feeding rate for corn stover pellet.

Table A-4. The variance of feeding rate based on the auger motor speed.

Auger Motor Speed	Average feeding rate
(RPM)	(kg/h)
Radiata pine wood	
185	5.35
372	11.34
505	15.00
544	16.18
722	21.40
Rice husk	
300	9.07
500	15.14
800	24.84
650	20.35
Corn stover	

270	7.46
358	10.22
423	12.41
550	16.33
700	20.68

B. Checklist of Gasifier Operation Procedure

In this section, the procedure for operating the 100kW dual fluidised bed gasifier is presented.

Gasifier Operating Procedure

last updated 12/05/2014

Date								

In the Days before Intended Operation

1	Let fire engineering know we need the lab facilities								
2	Check blower availability (Richard Jordan or Garrick)								
3	Check both LPG banks have enough fuel for run								
4	Book use of boiler in workshop logbook								
5	Schedule clear, clashes sorted								
6	Ensure enough SPA columns are available								
7	Email we want to run a test (to operators, technicians & Shusheng)								

After Gasifier run

1	Measure material in flue gas particle trap								
2	Measure material in BFB cyclone particle trap								
3	Remove bases and measure mass of sand left in beds								
4	Check syphon is clear								
5	Check auger head to BFB is clear and no bridging of pellets								
6	Check all viewing ports are clear								
7	Check O_2 Sensor lines are clear of char & ash								
8	Check pressure sensors lines are clear								
9	Check any bolts that have been undone are tightened								
10	H_2, CO and O_2 sensors have current calibration								
11	Start all burners to check system								
12	Wood feeder full								

Pre-run checks

1	Display sign on combustion lab door								
2	Unset alarm and open roller door to particle lab								
3	Screw feeder connected valve closed (V13)								
4	Compressed (red) air valve are open								
5	Open blank pneumatic value for photocell & control valve air (CAV5)								
6	Extractor duct open for gasifier lab extraction system								
7	"Extractor Fan E1 & E2" on								
8	"Fire Hood Fan" on (should read 65% or higher)								
9	Safety glasses on								

Air start-up

1 Start computer temperature reading
2 Vent valve in particle lab D175 1/3 open and hole covered
3 Main red handled blower line valve in lab fully open
4 Check rotameter valves are closed so floats do not hit stoppers
5 BFB & Chute pneumatic hose for rotameters connected & turned on
6 Blower speed 5Hz then set to 20Hz
7 Check the blower temperature ensure below 70°C
8 Turn main power switches on two control cabinet (S5 & S6)
9 Controller in normal mode and faults cleared
10 Wait 10-30 seconds for pneumantic valves to open
11 When control valves open set rotameter flows as shown below
12 Turn trace heating switch 1 on

Initial Rotameter Settings

CFB dist.	Syphon	Prim Air	Chute Air	BFB fluid	A/B Pilot	A/B Main	A/B Dilution
20	18	12	13	11	5.5	6	13.5
5th	1st	4th	3rd	2nd			

LPG Start-up

1 Ensure switches (S2 & S4)are all off
2 LPG on in control room to combustion lab
3 Yellow LPG valve to A/B solenoid open & LPG supply line
4 Check LPG pressure gauge reads 7-15 psig
5 A/B switch S4 on
6 A/B controller set to 1, push blue button
7 Open the cooling air for CFB burner port
8 Check A/B view port for flame
9 Open cold water valve to prevent the pyrolysis in feeding system
10 CFB switch S2 on
11 Open small regular valve, turn cabinet switch to 1 & push blue button
12 Check CFB flame visually and temperature
13 Fill 10kg sand through sand charger into CFB
14 Open air valve (CV09) to CFB view port
15 Turn CFB controller to 2
16 Open yellow CFB valve and needle valves (slowly)
17 Set the CFB LPG flow to 20~30L/min for 2 mins
18 Visual check in CFB and watch O_2 reading decrease
19 Adjust needle until CFB O_2 reads about ~8%
20 Micro GC needs bake out process run before operation

General Heat up

1 All reading monitored constantly and recorded every 30 mins
2 Visual inspection every 30 mins through view ports
3 Check for leaks
4 If temperatures plateau on computer, increase air & LPG for heat-up
7 Turn nitrogen purge on low for heat up (5L/min) once BFB1 > 500°C
8 Check wood pellet level in main hopper

Boiler Start up

1 Check particle lab steam valve is open in room D113
2 Get boiler room key from mechanical workshop & return afterwards
3 Check water level in sight tubes
4 Turn boiler 'burner' switch on in boiler room
5 Fill in boiler use book in boiler room (run times, project, initial)

Wood Feeder Start up

1 Temperature ~800°C
2 Operators only in the lab
3 Turn switch S1 on (interlock will prevent auger operation)
4 Ensure circulation is adequate and no signs of blockages
5 Turn cooling fan on for auger motor
6 Ensure knife gate valve is shut
7 Turn up A/B main air to 6 & A/B dilution air to 14
8 Open main auger circular valve at top of main screw feeder
9 Check auger switches in Fwd. mode (auger will not run unless S1 on)
10 Start feeding wood on a low setting (290rpm)
11 Check feed port is not causing pellets to bridge
12 Set auger RPM depending on feedstock, see white board in gasifier lab for setting

Steam Start up

1 Check BFB distributor, syphon and chute temperatures
2 Ensure large steam line gate valve is shut
3 Check steam on at control panel (switch S1)
4 Empty condensed water into bucket
5 Ensure two checked valves are clear
6 Turn main steam valve on very slowly to clear water into bucket
7 Progressively reduce airflow to BFB & increase steam to 6kg/h
8 Progressively reduce airflow to chute & increase steam to 4kg/h, and then decrease steam to 2kg/h and 1kg/h, depending on pressure measurements P5 & P6
9 Watch BFB #1 probe temperature changes
10 Progressively reduce airflow to Syphon & increase steam to 1kg/h
11 View Syphon, check bed material is circulating

Run hot test experiments!!!!

Adjust LPG rotameter according to the BFB temperature

When steady state conditions have been reached, record all plant data in the spreadsheet

Take gas & tar samples & label both samples with sample number & date

Check pellet level in the main hopper regularly

Stopping Gasification

1 VSD off at wall and zeroed
2 Close circular valve at top of main auger
3 Increase siphon fluidization
4 Monitor A/B O_2 and adjust air accordingly
5 Reduce steam flow, increase air to BFB, chute, syphon
6 Let char burn out for 30 mins
7 Regularly check standpipe view port for char circulation
8 Turn trace heating switch off located near steam meters

LPG Shut down

1 Check main LPG supply valve is shut off on CFB
2 Monitor O_2 then shut off pilot burners at main control panel
3 Leave A/B on for at least 5 min
4 A/B off at control Panel
5 LPG off in control room & keys away

Boiler Shut down

1 Get boiler room key from mechanical workshop and return afterwards
2 Turn off 'burner' switch
3 Write down turn-off time in log book

Plant Shut down

1 Let gasifier circulate on air for 20 mins to help cool down
2 Air flow rates reduced through rotameters
3 Nitrogen purge on to 1L/min until the next day
4 Stop Blower
5 Extraction hood off
6 Extract fans on until the next day
7 Cool Micro GC down below 35°C before turning off
8 Main power switches on control panel off
9 Compressed air on instrument wall until the next day
10 Shut gasifier lab fire-stop doors
11 Put all keys away in the cabinet and lock cabin
12 Cover up warning sign on combustion lab door
13 Put roller door down to particle lab and rest the alarm switch

C. Checklist of Tar Calibration and Extraction

In this section, the procedure for tar calibration and extraction developed in this thesis for the quantification of 25 species of tar compounds is presented.

1. Internal Standard (IS) creation

To create an internal standard to add to tar samples.

1. Rinse a 25mL volumetric flask with DCM. Pipette 0.1mL dodecane into a 25mL volumetric flask using a 1000μL automatic pipette.
2. Fill the 25mL volumetric flask with DCM up to the line. The concentration will be 4000ppm.
3. Pipette 1mL of 4000ppm into a 10mL volumetric flask using a 1mL automatic pipette.
4. Fill the 10mL volumetric flask with DCM up to the line. The concentration will be 400ppm. It is the Internal Standard.
5. Label all flasks with name, date and compound. Place samples in the chemical refrigerator for longevity.

2. Calibration of Internal Standard (IS)

Whenever a new IS solution is made, the GC-FID has to be calibrated using a range of IS concentrations with standard tar solutions including light tar (LT) and heavy tar (HT). The light tar and heavy tar standard solution are purchased from Supelco Analytical and Restek, respectively. The solution certifications are shown in Fig. D-1 and D-2.

- Pipette tips need to be changed every time they use a different chemical
- Pipette tips need to be conditioned with DCM each time they are used
- Label all vials with date, concentration and compounds

The following list indicates a way to get the range of concentrations used in the calibration.

1. 0.1ml LT + 0.1mL HT + 0.8mL DCM =1mL of 100mg/L LT-HT
2. 0.2mL 100mg/L LT-HT + 0.7mL DCM + 0.1mL IS = 1mL of 20mg/L LT-HT-IS
3. 0.1mL 100mg/L LT-HT + 0.8mL DCM + 0.1mL IS = 1mL of 10mg/L LT-HT-IS
4. 0.1mL 100mg/L LT-HT + 0.9mL DCM = 1mL of 10mg/L LT-HT
5. 0.5mL 10mg/L LT-HT + 0.4mL DCM + 0.1mL IS = 1mL of 5mg LT-HT-IS

6. 0.1mL 10mg/L LT-HT + 0.8mL DCM + 0.1mL IS =1mL of 1mg/L LT-HT-IS

3. SPE Column Conditioning

Before Supelclean LC-NH_2 solid phase extraction (SPE) columns are used to take samples from the gasifier they have to be conditioned to remove any contaminants.

1. Pipette 2mL of DCM into SPE column using a 1mL automatic pipette
2. Use a large plastic syringe to force DCM through column into a waste beaker
3. Do for all columns before use
4. Put waste DCM in waste chemical bottle

4. DCM:IPA solution creation

Tar samples need to be treated with a solution of 50:50 vol/vol DCM:IPA to remove some types of tar from the SPE column. The creation of the DCM:IPA solution is done in the following way.

1. Fill 5mL volumetric flask with IPA solution
2. Transfer the 5mL of IPA solution to a 10mL volumetric flask
3. Fill the remainder of the 10mL flask with DCM

5. Tar Extraction Method

Using DCM

1. Weigh an empty GC vial with lid on and record the weight
2. Put vial under used SPE column in retort stand in a fume-hood
3. Pipette 0.1mL of IS into the SPE column using a 1000µL automatic pipette
4. Pipette 0.9mL DCM into the metal sample insert accompanying the SPE column using a 1mL automatic pipette, allowing liquid to fall into SPE column
5. Push liquid through the SPE column with a plastic syringe, slowly to ensure even flow.
6. Weigh vial again, including lid and liquid
7. Label vial with date, sample number and DCM

Using DCMIPA

1. Weigh an empty GC vial with lid on and record the weight

2. Put vial under used SPE column in retort stand in a fume-hood

3. Pipette 0.1mL of IS into the SPE column using a 1000µL automatic pipette

4. Pipette 0.9mL 50:50 vol/vol DCM:IPA into the metal sample insert accompanying the SPE column using a 1mL automatic pipette, allowing liquid to fall into SPE column

5. Push liquid through the SPE column with a plastic syringe, slowly to ensure even flow.

6. Weigh vial again, including lid and liquid

7. Label vial with date, sample number and DCMIPA

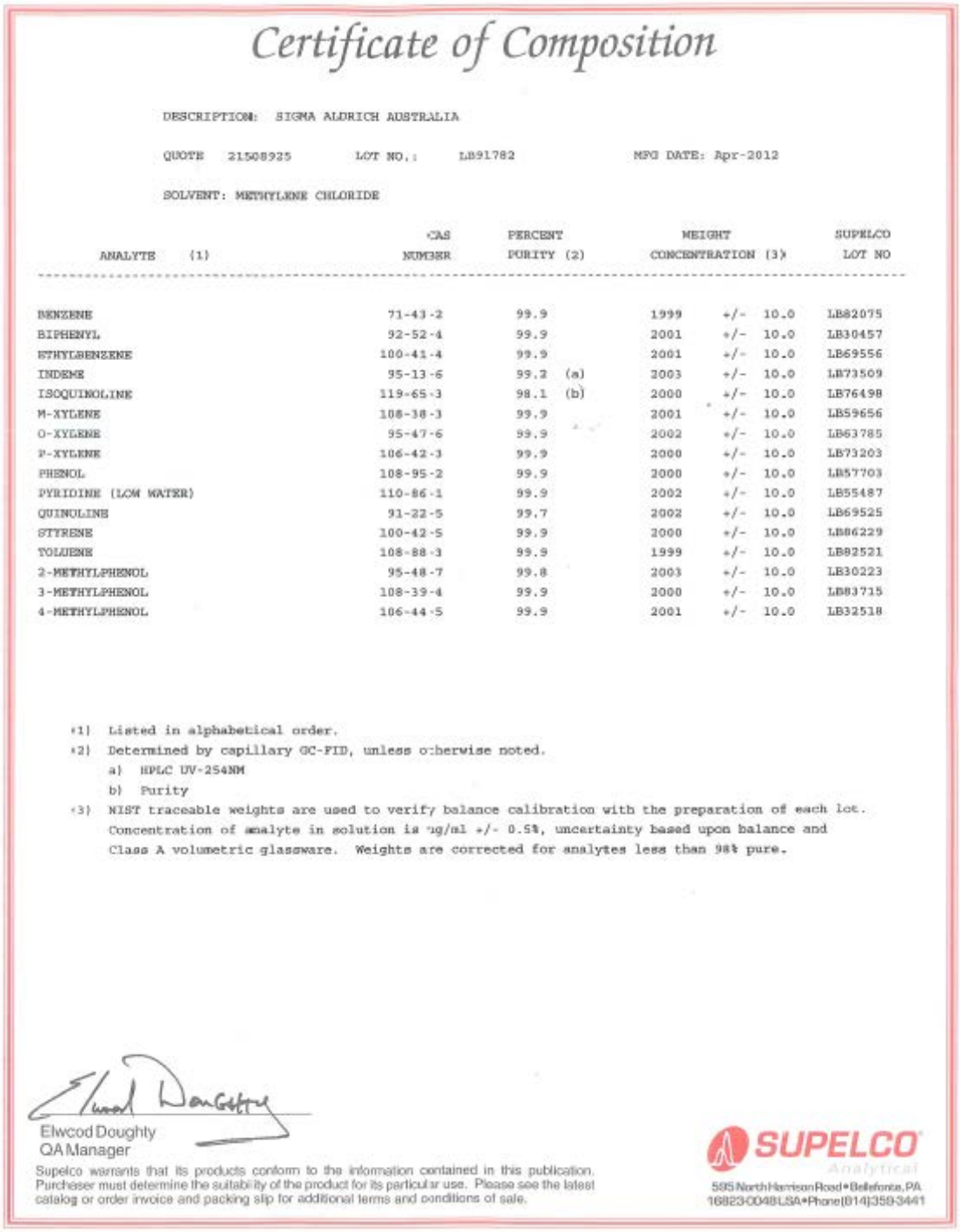

Certificate of Composition

DESCRIPTION: SIGMA ALDRICH AUSTRALIA

QUOTE 21508925 LOT NO.: LB91782 MFG DATE: Apr-2012

SOLVENT: METHYLENE CHLORIDE

ANALYTE (1)	CAS NUMBER	PERCENT PURITY (2)		WEIGHT CONCENTRATION (3)			SUPELCO LOT NO
BENZENE	71-43-2	99.9		1999	+/-	10.0	LB82075
BIPHENYL	92-52-4	99.9		2001	+/-	10.0	LB30457
ETHYLBENZENE	100-41-4	99.9		2001	+/-	10.0	LB69556
INDENE	95-13-6	99.2	(a)	2003	+/-	10.0	LB73509
ISOQUINOLINE	119-65-3	98.1	(b)	2000	+/-	10.0	LB76498
M-XYLENE	108-38-3	99.9		2001	+/-	10.0	LB59656
O-XYLENE	95-47-6	99.9		2002	+/-	10.0	LB63785
P-XYLENE	106-42-3	99.9		2000	+/-	10.0	LB73203
PHENOL	108-95-2	99.9		2000	+/-	10.0	LB57703
PYRIDINE (LOW WATER)	110-86-1	99.9		2002	+/-	10.0	LB55487
QUINOLINE	91-22-5	99.7		2002	+/-	10.0	LB69525
STYRENE	100-42-5	99.9		2000	+/-	10.0	LB86229
TOLUENE	108-88-3	99.9		1999	+/-	10.0	LB82521
2-METHYLPHENOL	95-48-7	99.8		2003	+/-	10.0	LB30223
3-METHYLPHENOL	108-39-4	99.9		2000	+/-	10.0	LB83715
4-METHYLPHENOL	106-44-5	99.9		2001	+/-	10.0	LB32518

(1) Listed in alphabetical order.
(2) Determined by capillary GC-FID, unless otherwise noted.
a) HPLC UV-254NM
b) Purity
(3) NIST traceable weights are used to verify balance calibration with the preparation of each lot. Concentration of analyte in solution is ug/ml +/- 0.5%, uncertainty based upon balance and Class A volumetric glassware. Weights are corrected for analytes less than 98% pure.

Elwood Doughty
QA Manager

Supelco warrants that its products conform to the information contained in this publication. Purchaser must determine the suitability of the product for its particular use. Please see the latest catalog or order invoice and packing slip for additional terms and conditions of sale.

SUPELCO Analytical
595 North Harrison Road • Bellefonte, PA 16823-0048 USA • Phone (814) 359-3441

Fig. C-1. Certification of light tar standard solution purchased from SUPELCO Analytical.

RESTEK
110 Benner Circle
Bellefonte, PA 16823-8812
Tel: (800)356-1688
Fax: (814)353-1309

www.restek.com

CERTIFIED REFERENCE MATERIAL

Certificate of Analysis

FOR LABORATORY USE ONLY-READ SDS PRIOR TO USE.

This Reference Material is intended for Laboratory Use Only as a standard for the qualitative and/or quantitative determination of the analyte(s) listed.

Catalog No. : 31995 **Lot No.:** A0128336

Description : 8270 Calibration Mix #5, Revised

8270 Calibration Mix #5, Revised 2,000µg/mL, Methylene Chloride, 1mL/ampul

Container Size : 2 mL **Pkg Amt:** > 1 mL

Expiration Date : May 31, 2023 **Storage:** 10°C or colder

Handling: Sonication required. Mix is photosensitive.

CERTIFIED VALUES

Elution Order	Compound	Grav. Conc. (weight/volume)	Expanded Uncertainty (95% C.L.; K=2)	
1	Naphthalene CAS # 91-20-3 (Lot MKBW2603V) Purity 99%	2,000.0 µg/mL	+/- 11.7371 µg/mL +/- 90.0953 µg/mL +/- 99.9689 µg/mL	Gravimetric Unstressed Stressed
2	2-Methylnaphthalene CAS # 91-57-6 (Lot STBF0201V) Purity 95%	2,003.6 µg/mL	+/- 11.7580 µg/mL +/- 90.2552 µg/mL +/- 100.1464 µg/mL	Gravimetric Unstressed Stressed
3	1-Methylnaphthalene CAS # 90-12-0 (Lot 523400-9) Purity 98%	2,002.6 µg/mL	+/- 11.7526 µg/mL +/- 90.2138 µg/mL +/- 100.1004 µg/mL	Gravimetric Unstressed Stressed
4	Acenaphthylene CAS # 208-96-8 (Lot L18Q) Purity 98%	2,000.7 µg/mL	+/- 11.7411 µg/mL +/- 90.1255 µg/mL +/- 100.0024 µg/mL	Gravimetric Unstressed Stressed
5	Acenaphthene CAS # 83-32-9 (Lot MKBW9515V) Purity 99%	2,000.5 µg/mL	+/- 11.7401 µg/mL +/- 90.1179 µg/mL +/- 99.9939 µg/mL	Gravimetric Unstressed Stressed
6	Fluorene CAS # 86-73-7 (Lot 10193329) Purity 99%	2,003.0 µg/mL	+/- 11.7547 µg/mL +/- 90.2305 µg/mL +/- 100.1189 µg/mL	Gravimetric Unstressed Stressed
7	Phenanthrene CAS # 85-01-8 (Lot MKCB1762V) Purity 99%	2,004.0 µg/mL	+/- 11.7606 µg/mL +/- 90.2755 µg/mL +/- 100.1689 µg/mL	Gravimetric Unstressed Stressed

8	Anthracene		2,002.0 µg/mL	+/- 11.7489	µg/mL	Gravimetric
	CAS # 120-12-7	(Lot MKBV7759V)		+/- 90.1854	µg/mL	Unstressed
	Purity 99%			+/- 100.0689	µg/mL	Stressed
9	Fluoranthene		2,001.2 µg/mL	+/- 11.7439	µg/mL	Gravimetric
	CAS # 206-44-0	(Lot MKBQ6360V)		+/- 90.1476	µg/mL	Unstressed
	Purity 98%			+/- 100.0269	µg/mL	Stressed
10	Pyrene		2,004.5 µg/mL	+/- 11.7635	µg/mL	Gravimetric
	CAS # 129-00-0	(Lot BCBR9108V)		+/- 90.2980	µg/mL	Unstressed
	Purity 99%			+/- 100.1939	µg/mL	Stressed
11	Benz(a)anthracene		2,000.5 µg/mL	+/- 11.7401	µg/mL	Gravimetric
	CAS # 56-55-3	(Lot ER031412-01)		+/- 90.1179	µg/mL	Unstressed
	Purity 99%			+/- 99.9939	µg/mL	Stressed
12	Chrysene		2,004.5 µg/mL	+/- 11.7635	µg/mL	Gravimetric
	CAS # 218-01-9	(Lot 012015)		+/- 90.2980	µg/mL	Unstressed
	Purity 99%			+/- 100.1939	µg/mL	Stressed
13	Benzo(b)fluoranthene		2,008.5 µg/mL	+/- 11.7870	µg/mL	Gravimetric
	CAS # 205-99-2	(Lot ER022008-02)		+/- 90.4782	µg/mL	Unstressed
	Purity 99%			+/- 100.3938	µg/mL	Stressed
14	Benzo(k)fluoranthene		2,000.0 µg/mL	+/- 11.7371	µg/mL	Gravimetric
	CAS # 207-08-9	(Lot 012012K)		+/- 90.0953	µg/mL	Unstressed
	Purity 99%			+/- 99.9689	µg/mL	Stressed
15	Benzo(a)pyrene		2,005.0 µg/mL	+/- 11.7665	µg/mL	Gravimetric
	CAS # 50-32-8	(Lot ER071309-02)		+/- 90.3206	µg/mL	Unstressed
	Purity 99%			+/- 100.2189	µg/mL	Stressed
16	Indeno(1,2,3-cd)pyrene		2,005.0 µg/mL	+/- 11.7665	µg/mL	Gravimetric
	CAS # 193-39-5	(Lot ER082107-02)		+/- 90.3206	µg/mL	Unstressed
	Purity 99%			+/- 100.2189	µg/mL	Stressed
17	Dibenz(a,h)anthracene		2,000.0 µg/mL	+/- 11.7371	µg/mL	Gravimetric
	CAS # 53-70-3	(Lot ER032211-01)		+/- 90.0953	µg/mL	Unstressed
	Purity 99%			+/- 99.9689	µg/mL	Stressed
18	Benzo(g,h,i)perylene		2,006.0 µg/mL	+/- 11.7723	µg/mL	Gravimetric
	CAS # 191-24-2	(Lot ER05121401)		+/- 90.3656	µg/mL	Unstressed
	Purity 99%			+/- 100.2689	µg/mL	Stressed
Solvent:	Methylene chloride					
	CAS # 75-09-2					
	Purity 99%					

Fig. C-2. Certification of heavy tar standard solution purchased from RESTEK.

D. Properties Analysis of Bed Material and Feedstock

In this section, the fuel properties analysed by local research institutes in New Zealand are presented. Veritec analysed the cellulose, hemicellulose and lignin of solid fuel, while CRL completed the proximate and ultimate analysis. The reports are shown in Fig. D-1 and D-2.

D1. Cellulose, hemicellulose and lignin analysis

VERITEC

Te Papa Tipu Innovation Park
49 Sala Street
Private Bag 3020
Rotorua, New Zealand
Telephone: +64 7 343 5899

ANALYSIS REPORT

16 January 2017

ENCH Chemical and Process Engineering
UC Warehouse
20Kirkwood Ave
Christchurch 8041

Attention: Simon Zhang

Report No: LMS 7146 **Order No.:** 587694

Analysis Requested: Extractive, lignin and carbohydrate analysis
Sample Description: 4 x Biomass samples received 5/12/16

Lab ID	Client ID	DCM Extractives (%w/w od sample)	Lignin (%w/w extracted od sample)	
			Acid-insoluble (Klason)	Acid-Soluble
C00242	Wood pellets	1.06	30.33	0.51
		1.08	30.61	0.48
C00243	Corn Stover	1.08	10.72	2.40
		0.92	10.87	2.83
C00244	50:50 Coal:Biomass pellets	0.69	51.77	0.60
		0.63	53.35	0.53
C00245	80:20 Coal:Biomass pellets	1.11	70.18	0.44
		1.18	70.02	0.44

Method: Samples are extracted using DCM solvent on a Soxtec apparatus, boiling time 1 hour, rinse time 1/2 hour
Acid-insoluble lignin in wood and pulp - modified method based on TAPPI Standard Methods, T 222 om-88
Acid-soluble lignin in wood and pulp -modified TAPPI Useful Method UM 250

Analyst/s: **P Gray / S Jeram**
Lab Technician / Lab Analyst

Checked: **K Martin**
Snr Lab Analyst

Te Papa Tipu Innovation Park
49 Sala Street
Private Bag 3020
Rotorua, New Zealand
Telephone: +64 7 343 5899

ANALYSIS REPORT

27 February 2017

ENCH Chemical and Process Engineering
UC Warehouse
20Kirkwood Ave
Christchurch 8041

Attention: Simon Zhang
Report No: LMS 7146 **Order No.:** 587694

Analysis Requested: Extractive, lignin and carbohydrate analysis
Sample Description: 4 x Biomass samples received 5/12/16

Lab ID	Client ID	Neutral Carbohydrates (%w/w extracted od sample)				
		Arabinan	Galactan	Glucan	Xylan	Mannan
C00242	Wood pellets	1.14	2.80	42.43	5.59	11.36
		1.38	2.74	43.65	6.17	9.37
C00243	Corn Stover	2.46	1.21	70.73	12.75	ND
		2.89	1.25	65.49	11.40	ND
C00244	50:50 Coal:Biomass	0.76	1.76	40.13	3.31	4.19
		1.08	1.92	44.06	3.71	4.49
C00245	80:20 Coal:Biomass	0.49	0.72	14.85	1.86	1.98
		0.52	0.76	15.71	2.13	1.83

Comments : Sugars are reported as anhydrosugar units
ND = none detected

Method: Carbohydrates - modified Wood Sugar Analysis by Anion Chromatography, R.C. Pettersen, V.H. Schwandt, Journal Of Wood Chemistry And Technology, 11(4), 495-501 (1991)

Analyst/s: **K Martin**
Snr Lab Analyst

Checked: **K Newick**
Snr Lab Analyst

Fig. D-1. Analytic report for cellulose, hemicellulose and lignin from VERITEC.

D2. Wood pellet analysis by CRL

INTERIM REPORT OF ANALYSIS

Date Received: 26-Aug-05

Client: Canterbury University

Description: Wood Chip pellets and Husk samples supplied by client.

CRL Energy Ltd Reference:			76/050	76/051	76/052
Customer Reference:			Sample#1 Chips	Sample#2 Pellets	Sample#3 Husks
Analysis - As Received Basis					
Moisture	ISO 5068	%	52.6	8.0	9.9
Ash	ASTM D1102	%	0.2	0.4	2.6
Volatile	ISO 562	%	39.8	77.4	73.8
Fixed Carbon	By Difference	%	7.4	14.2	13.7
Gross Calorific Value	ISO 1928	MJ/kg	9.53	18.63	17.08
Carbon	micro analytical	%	24.3	47.2	43.7
Hydrogen	micro analytical	%	2.87	5.35	5.07
Nitrogen	micro analytical	%	<0.1	<0.2	0.56
Sulphur	ASTM D4239	%	0.01	0.01	0.06
Oxygen	By Difference	%	20.0	38.7	38.1
CHN determined by Chemsearch Otago University					
Analysis - Dry Basis					
Ash	ASTM D 1102	%	0.4	0.4	2.9
Volatile	ISO 562	%	84.0	84.1	81.9
Fixed Carbon	By Difference	%	15.6	15.4	15.2
Gross Calorific Value	ISO 1928	MJ/kg	20.10	20.25	18.95
Carbon	micro analytical	%	51.2	51.3	48.5
Hydrogen	micro analytical	%	6.10	5.81	5.63
Nitrogen	micro analytical	%	<0.2	<0.2	0.62
Sulphur	ASTM D4239	%	0.02	0.01	0.07
Oxygen	By Difference	%	42.3	42.4	42.9

Signature:

Date of Issue: **13-Oct-05**

Grant Murray

Laboratory Supervisor

THIS REPORT MUST NOT BE QUOTED EXCEPT IN FULL

Distribution:

Dept of Chemical and Process Engineering, PB 4800, CHCH ATTN: Ian Gilmour

CRL Energy Ltd, Laboratory

Fig. D-2. Report of proximate and ultimate analysis from CRL